CLICK CHEMISTRY of β-CYCLODEXTRIN AND ITS GUESTS

Design, Synthesis, and Application of Polymersomes and Photo-Active Metal Complexes

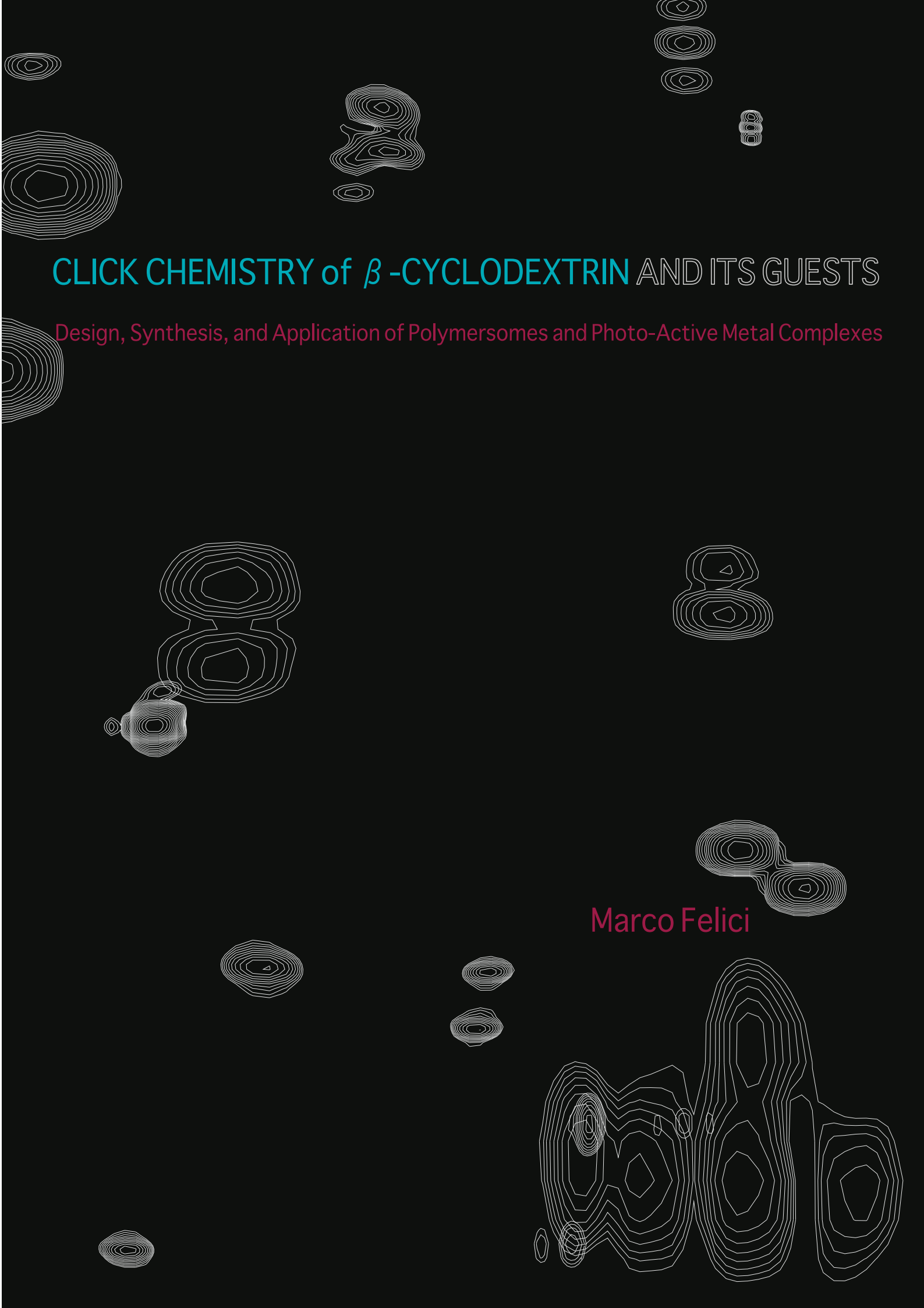

Marco Felici

Click Chemistry of β-Cyclodextrin and its Guests: Design, Synthesis, and Application of Polymersomes and Photo-Active Metal Complexes

Proefschrift

ter verkrijging van de graad van doctor
aan de Radboud Universiteit Nijmegen
op gezag van rector magnificus prof. mr. S.C.J.J. Kortmann,
volgens besluit van het college van decanen
in het openbaar te verdedigen op maandag 28 januari 2013
om 15.30 uur precies

door

Marco Felici
geboren op 24 april 1975
te Colleferro (Italië)

Promotor:
Prof. dr. R.J.M. Nolte

Copromotor:
Dr. M.C. Feiters

Manuscriptcommissie:
Prof. dr. A.E. Rowan
Dr. N.S. Hatzakis (Universiteit van Kopenhagen)
Dr. R.M. Williams (Universiteit van Amsterdam)

Paranimfen:
Guillaume Delaittre
Daniel Gironés Delgado-Ureña

The work described in this thesis has been developed within the framework of the Marie Curie Research and Training Network (RTN) UNI-NANOCUPS. The EU (EU-FP MRTN-CT-2003-504233) is gratefully acknowledged for the financial support that made this work possible.

Financial support for the printing of this thesis was granted by Lead Pharma B.V.

Cover design: Theodora Kotsi
Printed by: Proefschriftmaken.nl, Uitgeverij BOXPress
ISBN: 978-90-8891-563-5

Click Chemistry of β-Cyclodextrin and its Guests: Design, Synthesis, and Application of Polymersomes and Photo-Active Metal Complexes

Doctoral Thesis

to obtain the degree of doctor
from Radboud University Nijmegen
on the authority of the Rector Magnificus prof. dr. S.C.J.J. Kortmann,
according to the decision of the Council of Deans
to be defended in public on Monday, January 28, 2013
at 15.30 hours

by

Marco Felici
born on April 24, 1975
in Colleferro (Italy)

Supervisor:
Prof. dr. R.J.M. Nolte

Co-supervisor:
Dr. M.C. Feiters

Doctoral Thesis Committee:
Prof. dr. A.E. Rowan
Dr. N.S. Hatzakis (University of Copenhagen)
Dr. R.M. Williams (University of Amsterdam)

Defence Assistants:
Guillaume Delaittre
Daniel Gironés Delgado-Ureña

The most exciting phrase to hear in science, the one that heralds new discoveries, is not "Eureka!" (I found it!) but "That's funny ..."

Isaac Asimov

List of Abbreviations

acac	acetylacetonate	ox	oxidation
atm	atmosphere	phen	phenanthroline
calcd	calculated	pic	picolinate
DMF	*N,N*-dimethylformamide	PL	photoluminescence
EDCI	1-ethyl-3-(3-dimethylaminopropyl) carbodiimide)	ppm	parts per million
em	emission	red	reduction
ESI	electrospray ionisation	*mer*	meridional isomer
exc	excitation	SEM	scanning electron microscopy
HRMS	high-resolution mass spectrometry	TEM	transmission electron microscopy
IR	infrared	TFA	trifluoroacetic acid
ITC	isothermal calorimetry	THF	tetrahydrofuran
^{3}LC	ligand-centred triplet state	TLC	thin-layer chromatography
MALDI	matrix-assisted laser desorption ionisation	TMS	trimethylsilyl
max	maximum	TOF	time of flight
^{3}MC	metal-centred triplet state	Ts	4-toluenesulfonyl
^{3}MLCT	metal-to-ligand charge-transfer triplet state	UV-vis	ultraviolet-visible
Mp	melting point	Δ	delta stereoisomer
MWCO	molecular weight cut off	Φ	emission quantum yield
NHS	*N*-hydroxysuccinimide	Λ	lambda stereoisomer
NIR	near infrared spectroscopy	λ	wavelength
NMR	nuclear magnetic resonance	τ	lifetime
OD	optical density	^{1}MLCT	metal-to-ligand charge-transfer singlet state

Table of Contents

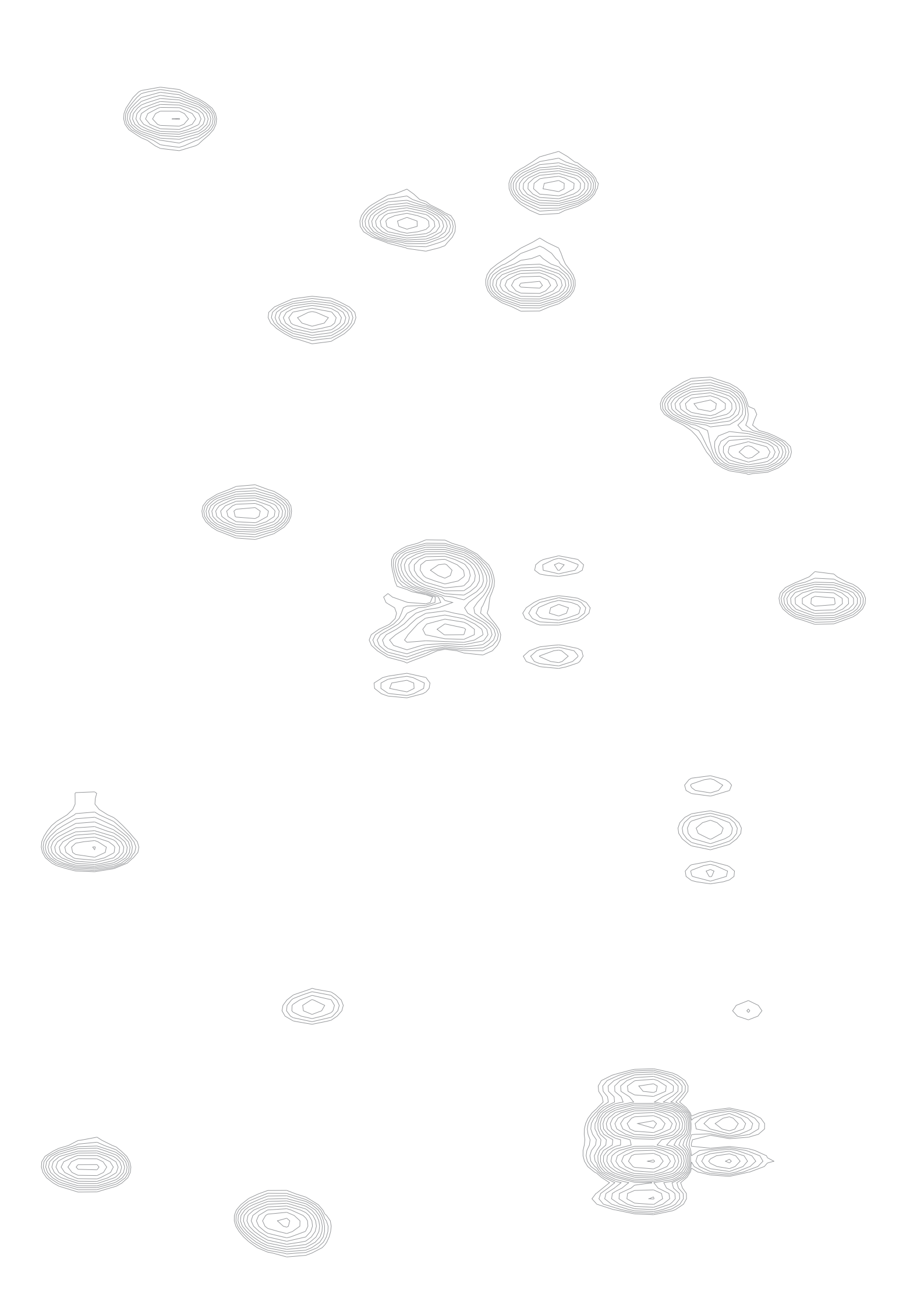

1

Introduction

Abstract

In this chapter an overview of the two major topics discussed in this thesis is given: i) cyclodextrins (CDs) and their ability to form inclusion complexes, and ii) light-induced electronic transitions in coordination compounds. By taking advantage of the binding ability of CDs, it is possible to induce and control the formation of self-assembled nano-systems. The combination of the properties of CDs and coordination compounds is of particular interest. Many examples of CD-appended metal complexes, which have been used as photo- and electro-active molecular functional systems, namely, CD-based phosphorescence sensors and nanowires, are reported. Subsequently, a chronological description of the increasing interest in 1,2,3-triazoles, which were also investigated in this thesis, together with the physical properties of the corresponding coordination compounds is given. The introduction is concluded by a description of the aim and outline of this thesis.

1.1 Cyclodextrin: Structure and properties

Cyclodextrins (CDs) are cyclic glucose oligosaccharides composed of D-glucopyranose units linked through α-(1,4)-glycosidic bonds. They are formed during the enzymatic degradation of a component of starch, amylose, by the enzyme CD glycosyl transferase (CGTase). First starch is liquefied by either heat treatment or using α-amylase then CGTase is added for the enzymatic conversion. CGTases can synthesise various forms of CDs; thus the product of the conversion results in a mixture of the three main types of cyclic molecules. The ratios depend on the enzyme used.

The three most important CDs are α, β, and γ, which contain six, seven, and eight glucose monomers, respectively (Figure 1.1). Higher analogues contain up to 30–60 glucose units, but rather than having a ring shape, these CDs tend to adopt a more elliptic shape and are less suited for complexation of guests. In α-, β-, and γCDs, the glucose units have the $^4C_1$ (chair) conformation. This gives the CD the form of a truncated cone with a wide rim formed by the secondary 2- and 3-hydroxyl groups and a narrow rim formed by the primary 6-hydroxyl groups (Figures 1.1 and 1.2). The diameter of the CD cavity increases with the number of glucose units.

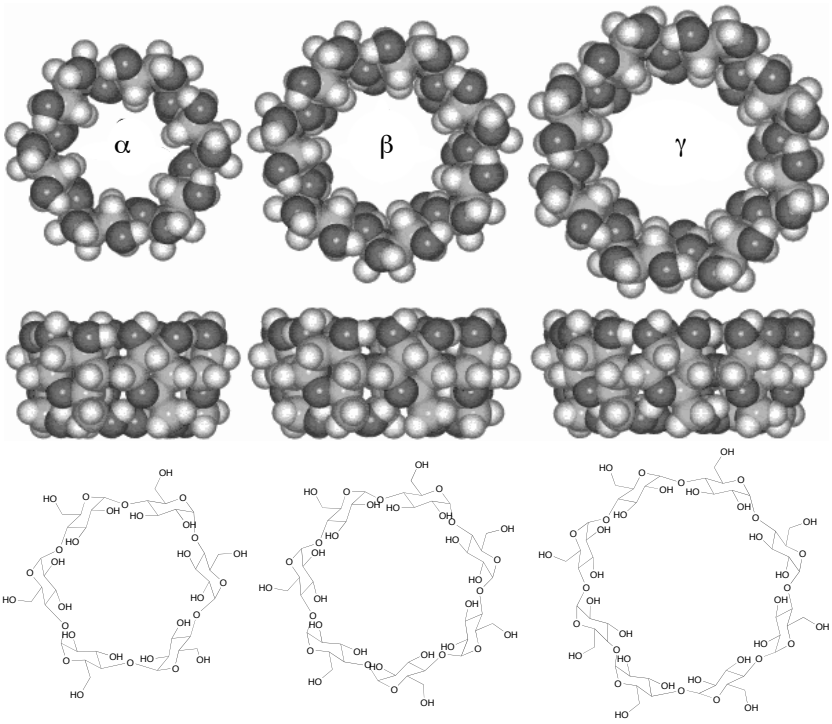

Figure 1.1 *Models of the native α-, β-, and γCDs. The diameter of the ring increases with the number of glucose units (adapted from ref.[1]).*

As a consequence of the exposure of the hydroxyl groups to the solvent, CDs are soluble in water (Table 1.1). The cavity of CD is relatively hydrophobic and is able to form inclusion complexes with various inorganic and organic molecules in aqueous solutions. Furthermore, CDs can exhibit regio- and stereoselectivity in organic reactions.

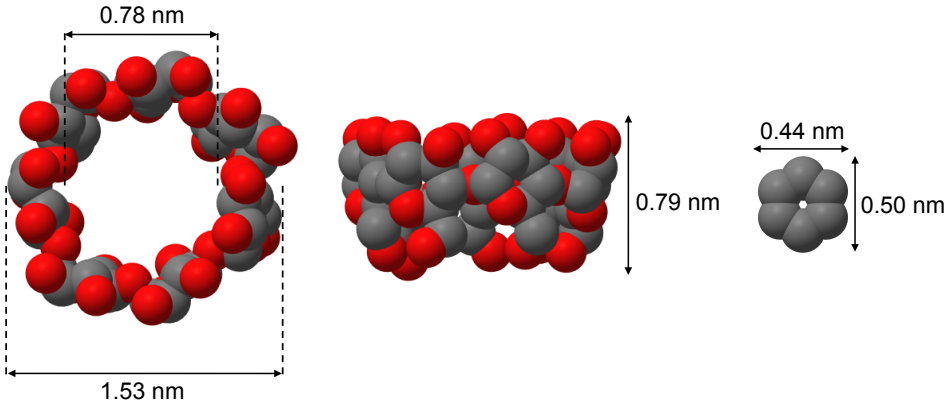

Figure 1.2 *Dimensions of native βCD and benzene.*[2]

Table 1.1 *Solubility of native α-, β-, and γCDs.*[3]

CD	Solubility (g L^{-1})
αCD	145
βCD	18.5
γCD	232

βCD is the most frequently used CD. The dimensions of βCD are such that six-membered ring molecules like cyclohexanes and benzenes are bound best (Figure 1.2). The solubility of βCD in water is lower than that of the other CDs because of the presence of a network of intramolecular hydrogen bonds between the hydroxyl groups at positions 2 and 3 of adjacent glucose units (Scheme 1.1). This makes the structure of βCD rather rigid.[4,5] It was established from variable-temperature NMR spectroscopy experiments that for βCD the hydroxyl at C-3 is the predominant hydrogen donor in this process (Scheme 1.1).[5,6] The 21 hydroxyl groups of βCD can be divided into three groups characterised by different reactivity. The primary OH groups at C-6 are the most nucleophilic OHs. The secondary hydroxyls at C-2 are the most acidic ones, due to both the intramolecular hydrogen bond and the presence of the electron-withdrawing acetal function at C-1. In general the C-3 OH groups are the least reactive. This difference in reactivity is used in the selective functionalisation of βCD which is described in Chapter 2 of this thesis.[7]

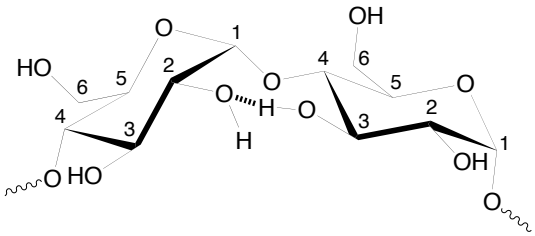

Scheme 1.1 *Hydrogen bond formed between C-3 OH and C-2 OH of two adjacent glucose moieties in βCD.*

The ability of CDs to include guests in their cavity is the reason for the enormous interest in CD applications. The main driving force for the inclusion of apolar guests into the CD cavity in aqueous solutions is believed to originate from i) penetration of the hydrophobic part of the guest molecule into the CD cavity, and ii) dehydration of the organic guest. Usually, the combination of contributions i and ii is referred to as the *hydrophobic effect*.[8] The water molecules surrounding the hydrophobic surfaces of the CD cavity and the guest form highly structured hydration shells. The release of these so-called "high-energy" water molecules from the CD cavity and the induced dehydration of the guest molecule upon complexation give a positive entropic contribution to the binding process (Figure 1.3).[9,10] This increase in entropy is large and compensates for the loss of entropy due to the reduced mobility of the host and guest upon complexation.

Other factors such as electrostatic interactions,[11,12] conformational changes, or strain release of the CD molecule upon complexation have been invoked to play a role as well.[13] Hydrogen bonds[14] or charge stabilisation originating from the interaction of the guest with the large number of OH groups can also contribute to the strength and selectivity of the binding.

In this thesis only permethylated βCDs have been used, in which all hydroxyls are converted into methoxy groups. The only exception are the perthiolated βCDs which are used to functionalise the Pt nanoparticles (Chapter 5). Methylation of the hydroxyl groups breaks the intramolecular network of hydrogen bonds and increases the flexibility and, therefore, the solubility of the βCD in water. The structures of permethylated CDs are somewhat different from those of native CDs because they no longer have a circular rigid shape. At the same time, the permethylated CD becomes soluble in organic solvents and the absence of hydrogen-bond donors makes purification with chromatographic techniques possible. The permethylated CD cavity has the same diameter as the cavity of a native CD but its depth is increased by about 1.5 Å.[15]

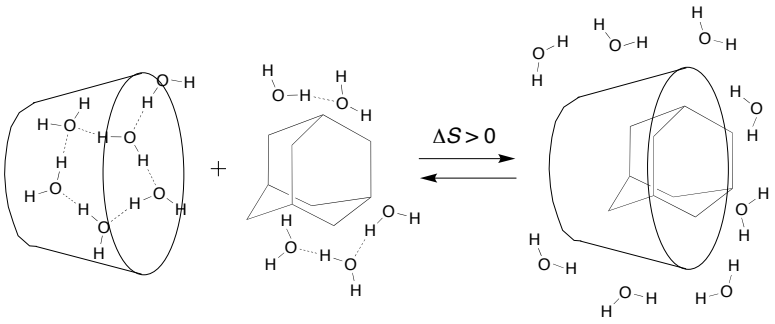

Figure 1.3 *Complexation of a hydrophobic guest in a* CD *cavity is a thermodynamically favourable process. The entropic factor is favoured by the disorder introduced in the solvent molecules otherwise organised around the hydrophobic surfaces of the two components (adapted from ref.[1]).*

1.1.1 Complexation equilibria and binding constants

An important field of research in supramolecular chemistry is host-guest chemistry which involves the study of complexes in which a larger molecule (the host, e.g., CD) and a smaller molecule or ion (the guest, e.g., a small organic molecule) are held together by forces other than covalent bonds. The stoichiometric ratio between the host and the guest depends on the binding mode. In the case of CD complexes, the most common stoichiometric ratio is 1:1. Other ratios are known, the most observed probably being 1:2. More complicated systems containing 2:2 and 2:1 complexes or, for example, a three-component system with molecules such as pyrene, *n*-butyl alcohol, and γCD, have also been observed.[16–19]

Complexes between CDs and organic guests are assumed to be formed in bimolecular processes. If we define CD as the host (H) and a small organic molecule as the guest (G), we can describe the complexation process according to Equilibria (1) and (2):

$$G + H \rightleftharpoons GH \qquad (1)$$

$$GH + G \rightleftharpoons G_2H \qquad (2)$$

Equilibrium (1) describes a 1:1 complex and the binding constant, *K*, is defined by the Equation (3).

$$K = \frac{[GH]}{[G] \cdot [H]} \qquad (3)$$

For the binding of two guests in one host, the process is described by Equilibria (1) and (2), and the binding constant is defined by Equation (4).

$$K_2 = \frac{[G_2H]}{[GH] \cdot [H]} \qquad (4)$$

Some examples of binding constants of complexes between CDs and organic guest molecules are given in Table 1.2.

Table 1.2 *Examples of binding constants for native CDs (except for [a]) and guests at 298 K.*

Host	Guest	Solvent	Log *K*
αCD	octan-1-aminium[b]	H_2O	3.37
	octanoic acid[c]	H_2O	3.26
	adamantane-1-carboxylate[d]	H_2O	2.15
	adamantan-1-aminium[e]	H_2O	1.70
	pyrene[f]	H_2O	2.17
βCD	octan-1-aminium[b]	H_2O	2.62
	octanoic acid[c]	H_2O	2.75
	adamantane-1-carboxylate[g]	H_2O (pH = 8.5)	4.51
	adamantan-1-aminium[h]	H_2O	3.95
	sodium ursodeoxycholate[i]	H_2O	5.89
	sodium cholate[i]	H_2O	3.61
	pyrene[f]	H_2O	2.69
γCD	sodium ursodeoxycholate[j]	H_2O	5.51
	sodium cholate[j]	H_2O	3.75
	pyrene[f]	H_2O	3.05
PMBCD[a]	adamantan-1-aminium[h]	H_2O	1.76

a, The abbreviation PMBCD stands for permethylated βCD, that is, all hydroxyl groups have been converted into methoxy groups; b, see ref.[20]; c, see ref.[21]; d, see ref.[22]; e, see ref.[23]; f, see ref.[24]; g, see ref.[25]; h, see ref.[26]; i, see ref.[27]; j, see ref.[28].

1.1.2 Methods for calculation of the binding constant

There are several physical and chemical methods available to determine or estimate the binding of a guest to a CD host. Possibly the most accurate technique is isothermal titration calorimetry (ITC) because it allows the direct determination of the equilibrium constant of complex formation as well as thermodynamic parameters such as the molar enthalpy of the process.

The most widespread technique, however, is nuclear magnetic resonance (NMR) spectroscopy because of its simplicity and availability. Through relatively simple NMR titration experiments, knowing the concentration of the components, the complexation-induced changes in chemical shifts (complexation-induced shift (CIS)) can be determined and a binding constant can be derived for complex formation. It has to be noted, however, that the CIS method is only easily applicable to CDs that still possess full symmetry, namely, non- or per-functionalised derivatives. When a CD is mono-functionalised the symmetry of the CD ring is disrupted and the proton NMR spectrum becomes extremely complicated to such an extent that high frequencies and two dimensional techniques are needed to study the inclusion of guests.[29]

Inclusion of a substrate in a CD cavity can also be studied by a number of electronic (UV-vis absorption and emission) spectroscopy techniques. In the case of UV-vis absorption spectroscopy, a change in the absorbance and/or absorption wavelength can be the effect of the altered polarity of the cavity microenvironment or of specific interactions upon complexation. Similarly, fluorescence or room-temperature phosphorescence (RTP) have been applied for the evaluation of the binding constants of luminescent molecules. In this case a change in the emission intensity and/or emission wavelength maximum of the guest is observed. One significant limitation of UV-vis and emission spectroscopy techniques is that the guest has to be UV-active or exhibit polarity-sensitive emission. Moreover, these techniques usually give only limited structural information on the geometry and mode of inclusion and they should be used as complementary techniques to NMR spectroscopy or ITC.

1.2 Light-induced electronic transitions in molecules

Compounds can have a specific colour. This colour is the first consequence of the absorption of visible light and associated electronic transitions. A compound will, however, only absorb energy if the incident radiation ($h\nu$) matches the energy gap between the ground state of the constituting molecule and one of its excited states. The absorbed photon leads, therefore, to an electronic transition that brings the molecule into an excited state which differs from the ground state by its energy content, structure, and electron distribution.

If we consider the excited state of a molecule formed by the transition of one electron in a paired electronic ground state into a higher energy state where the electrons are unpaired, we can have excited states of different multiplicity. The most common excited states in organic molecules have singlet multiplicity ($2S + 1 = 1$, where $S = 0$) or, if the electrons in the excited

state have parallel spin, triplet multiplicity ($2S + 1 = 3$, where $S = 1$). Electronic transitions must follow a number of selection rules: transitions between states of the same multiplicity are allowed, whereas transitions between states of different multiplicity are forbidden.[30,31]

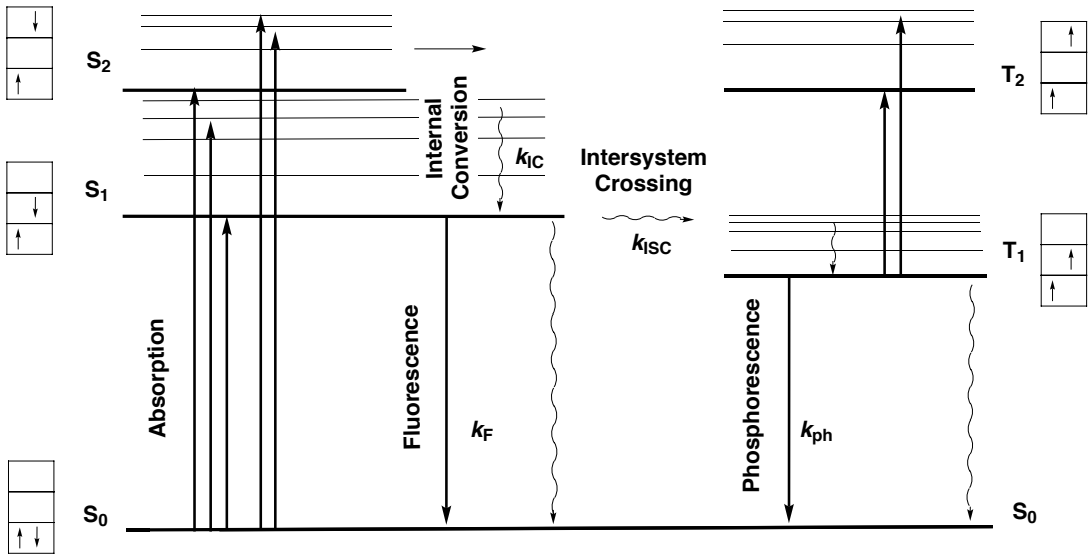

Figure 1.4 *Simplified molecular electronic energy level diagram commonly referred to as Jablonski diagram (adapted from ref.[1]).*

Deactivation of the excited state of a molecule and its return to the ground state can occur by different relaxation mechanisms. The excess of energy is released by either emission of radiative energy (phosphorescence or fluorescence) or molecular interactions with the environment. Possible electronic transitions between different states can be summarised in a molecular energy level diagram, also known as Jablonski diagram (Figure 1.4). Only two emission processes are shown in Figure 1.4, although many different electronic absorption processes may occur. When a molecule is excited, several states can be populated and the highest excited states reached relax to the lowest (despite few exceptions) excited level S_1 through a radiationless process called internal conversion (IC). Fluorescence is the emission of radiative energy from a singlet state and typically occurs on the time scale 10^{-9}–10^{-12} s. Phosphorescence, however, is the process of emission of radiative energy from a triplet state and occurs over a significantly longer time (10^{2}–10^{-9} s). This longer lifetime is due to the improbable forbidden spin reorientation that must accompany a triplet to singlet transition.

The multiplicity rule does not apply when heavy atoms are present in the molecules. The heavy atom induces mixing of the singlet and triplet excited states because of the strong spin-orbit coupling. Such an effect is known as the internal heavy atom effect, and was first observed by McClure.[32,33] The heavy atom effect allows spin-forbidden transitions between

singlet and triplet electronic states; this process is known as intersystem crossing (ISC). The internal heavy atom effect is also responsible for the fact that the luminescent organometallic complexes studied in this thesis are mainly phosphorescent or triplet-state emitters, with a small singlet character, since the ISC in these systems can be considered to have a quantum yield close to 100%.[34]

1.2.1 Polypyridine metal complexes as triplet-state emitters

The electronic transitions of the ruthenium(II) and iridium(III) d^6 octahedral complexes used in this thesis fall in the visible and near UV regions of the electromagnetic spectrum. These complexes have a singlet electronic configuration in the ground state, corresponding to the six d electrons paired among the t_{2g} states. Light emission occurs from the lowest excited state, which is a triplet state. The efficiency of ISC is close to unity, and therefore, the most usual emission observed is phosphorescence, even at room temperature. Due to the strong coupling of singlet and triplet states, the lowest triplet state contains a certain singlet-state character (for ruthenium this calculated to be close to 10%),[35] and therefore, the term luminescence is used to indicate emission from this state. This triplet state has a much shorter excited state lifetime compared to fluorescent organic molecules.

The electronic transition occurring in metal complexes involve the orbitals of the ligands as well as the metal d orbitals. The latter are split into two levels when strongly σ-donating and π-accepting ligands are coordinated in the metal complex in an octahedral fashion. The resulting possible transitions are therefore as follows:

1. *Metal-centred* (MC) d–d transitions between non-bonding π-metal-centred orbitals and anti-bonding σ*-metal-centred orbitals.

2. *Ligand-centred* (LC) strongly allowed transitions in the UV region of the spectrum, between bonding ligand-centred π orbitals and anti-bonding ligand-centred π* orbitals.

3. *Ligand-to-metal charge-transfer* (LMCT) transitions from bonding ligand-centred π orbitals to non-bonding π-metal-centred or anti-bonding σ*-metal-centred orbitals.

4. *Metal-to-ligand charge-transfer* (MLCT) d–π* transitions from non-bonding π-metal-centred or anti-bonding σ*-metal-centred orbitals to ligand-centred anti-bonding π* orbitals.

For complexes with easily reducible ligands (low-lying LUMO), the MLCT levels are observed in the visible region and often possess rather high molar extinction coefficients ($\approx 10^4$ M^{-1} cm^{-1}). The molecules can, thus, be excited into their ^{1}MLCT state. After excitation, ISC populates the ^{3}MLCT state which subsequently decays to the ground state with emission of light, and with a lifetime typically between nano- and milliseconds (phosphorescence).

The excited states of a luminescent complex are deactivated by radiative decays and also by a number of other pathways.[36] Ruthenium complexes, for example, present a ^{3}MC state that becomes thermally accessible at room temperature and will be populated immediately after ^{3}MLCT formation. This state decays non-radiatively to the ground state shortening the lifetime and reducing the emission quantum yield of the complexes,[37] as described in Chapter 2.[7] A compilation of the possible transformations of the excitation energy in a metal complex is depicted in Figure 1.4.

1.2.2 Intra- and intermolecular photo-induced processes

As explained above, there are several pathways that energy can follow after a photon has been absorbed by a molecule. The absorbed photons give rise to varied electronic transitions inside the molecule, placing it in an excited state. Deactivation can then occur through emission of light (radiative decay) or through thermal or other non-radiative depopulation processes. In the presence of a second molecule in close proximity, the excited species can be subjected to other energy or electron transfer processes, leading to the formation of new excited states (energy transfer) or charge-separated states (electron transfer; Figure 1.5).

In energy transfer processes, the excess of energy of the donor in its excited state is transferred to the acceptor, which has an energetically lower excited state (Figure 1.5). As a result, the donor returns to the ground state, while the acceptor reaches its excited state. Often the acceptor is a luminescent species so that the occurrence of energy transfer can be proven by the emission of the acceptor.

In electron transfer processes, the deactivation of the excited state of the donor occurs through transfer of an electron to the acceptor, producing an oxidised radical cation and a reduced radical anion (Figure 1.5). This process, in which an electron is transferred from a donor to an acceptor upon irradiation with light, is called photo-induced electron transfer. The charge-separated species formed are characterised by a high energy content and tend to decay to the ground state to reform uncharged species (back electron transfer). The formation of the charge-separated state can be irreversible if the donor or the acceptor undergoes chemical or physical processes.

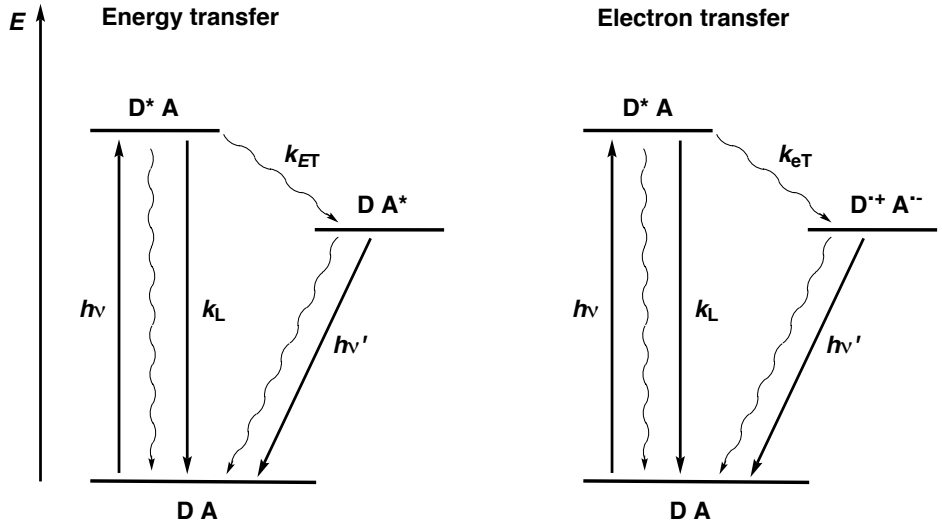

Figure 1.5 *Schematic representation of an energy or electron transfer process between donor (D) and acceptor (A) molecules. In an energy transfer process the excitation energy is transferred to the acceptor promoting it into its excited state (A^*). In an electron transfer process a charge-separated state ($D^{\bullet+}A^{\bullet-}$) is created.*[1]

1.3 Cyclodextrins as components in nano-scaled systems

The preparation of complex multicomponent architectures usually requires multistep covalent reactions to link several building blocks together; such multistep processes generally result in complex synthetic routes and poor yields. An alternative way to create multicomponent architectures is by means of intermolecular, non-covalent bonding, for example, between CDs and a suitable guest. The versatility of the CD molecule (e.g., size and functionalisation) allows the selective binding of guests (size control) and the attachment of photo- and redox-active moieties to its rim. These components (i.e., guest and photo- and redox-active moiety) are the building blocks for systems in which photo-induced processes are possible.

The use of CDs covalently functionalised with organometallic complexes and their interaction with a variety of electro- or photo-active guests have been reported in the literature. For example, Haider et al. described how control over the directionality of energy transfer can be achieved by a simple change of the guest in a self-assembled system.[38,39] This system consisted of a ruthenium bipyridine (bpy) permethylated βCD centre decorated with either iridium or osmium terpyridine (tpy) complexes functionalised with biphenyl and adamantyl moieties (Figure 1.6). Efficient energy transfer was monitored from the iridium bis-tpy derivatives to the ruthenium tris-bpy centre when both units were conveniently

functionalised to act as guest and host, respectively, through CD cavity assembly. When, instead of iridium, an osmium centre was used as the guest the energy transfer was reversed, that is, from the central ruthenium centre to the outer guest metal centre. The authors described a nice and versatile system for communication between the inner metal core and the outer guest unit by triplet energy transfer. The influence of the nature of the guest was also examined, employing species with either biphenyl or adamantyl substituents. Although biphenyl has a lower binding affinity for the βCD cavity, energy transfer is favoured by the conjugated π system of the guest moiety.

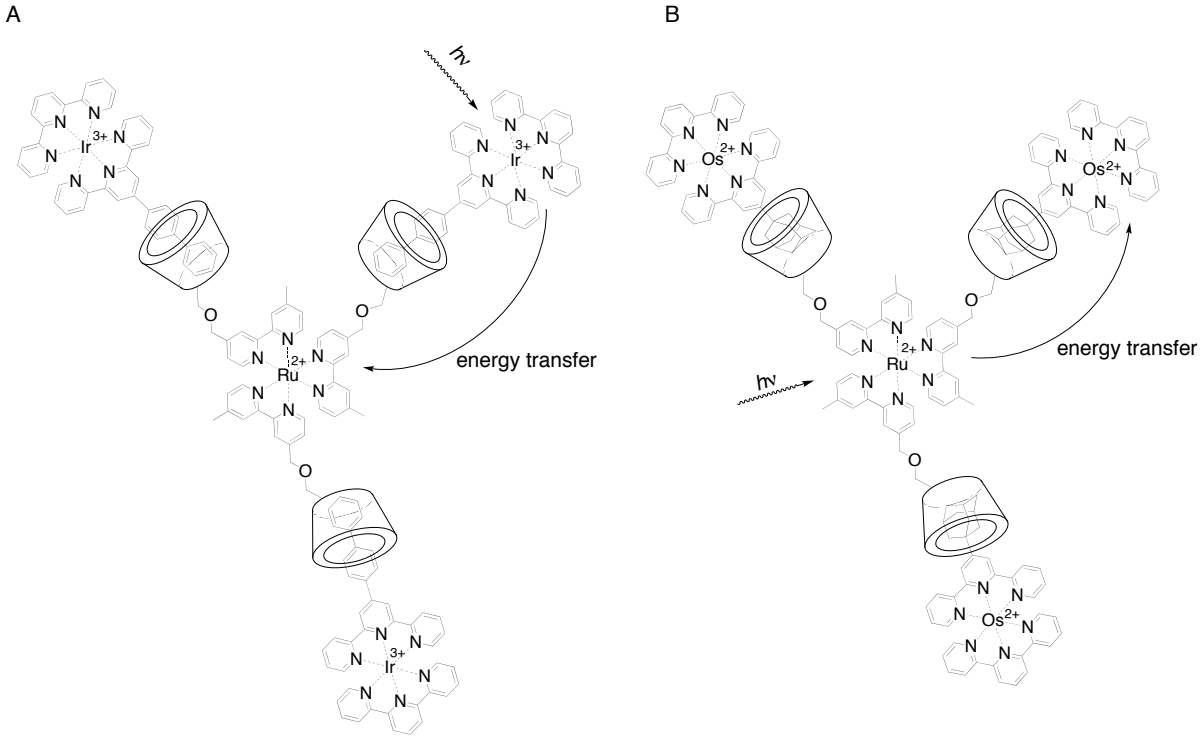

Figure 1.6 *Self-assembled system with permethylated βCD for energy transfer in aqueous medium. Transfer occurs from the iridium guest to the ruthenium host or from the ruthenium host to the osmium guest (A, λ_{exc} = 330 nm; B, λ_{exc} = 324 nm).*[38]

In a more recent paper, Faiz at al. reported a self-assembled triad formed after the binding of three different photo-active components (Figure 1.7).[40] A unidirectional, two-step, photo-induced energy transfer was shown to take place, due to asymmetric functionalisation of the central metal complex with permethylated CDs of two different sizes. Upon excitation of the anthracene moiety in the supramolecular assembly (λ_{exc} = 360 nm), a unidirectional energy-transfer cascade occurred with rates of 1.8×10^{10} (from anthracene to ruthenium) and

0.9×10^9 s^{-1} (from ruthenium to osmium) through the excited state of Ru(II), leading to the population of the lowest excited state localised on the osmium complex.

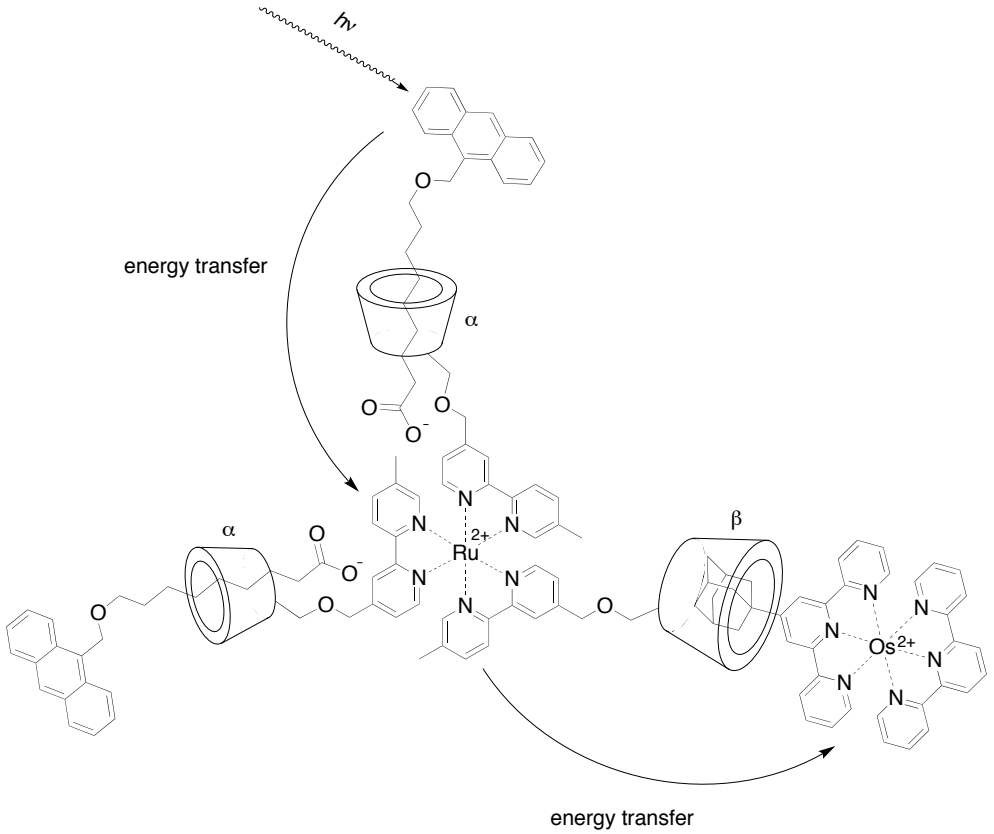

Figure 1.7 *Energy transfer process in a self-assembled triad with permethylated α- and βCD. Energy transfer occurs from anthracene to ruthenium and then to osmium.*[40]

1.3.1 CD-based sensors

The design of luminescent CD sensors, which are able to detect bioactive organic molecules, such as steroids, has attracted much interest in fields related to diagnostics and analytics. These systems take advantage of changes in emission properties that occur when interactions with a molecule of interest takes place.

Nelissen et al. described a luminescent tris(bpy)ruthenium(II) complex with six non-methylated βCDs, in which fluorescence is completely quenched by the introduction of viologen guests into the host cavities (Figure 1.8).[41] Upon addition of steroids, which have a much higher binding affinity for βCD than viologen, luminescence was recovered and this recovery was a function of the steroid concentration. The luminescence/steroid concentration relationship was used to detect the presence of these compounds accurately. Different displacement strengths for various steroids were reported. These observations indicated that

the various members of a steroid family had a variable complementarity with the cavity of the CD. One of the highest reported binding constant was that for ursodeoxycholic acid (at pH = 7 in TRIS-HCl buffer; $K \approx 10^6$ M^{-1}), also known as Ursodiol, which is used in medicine to dissolve a specific type of gall bladder stones.

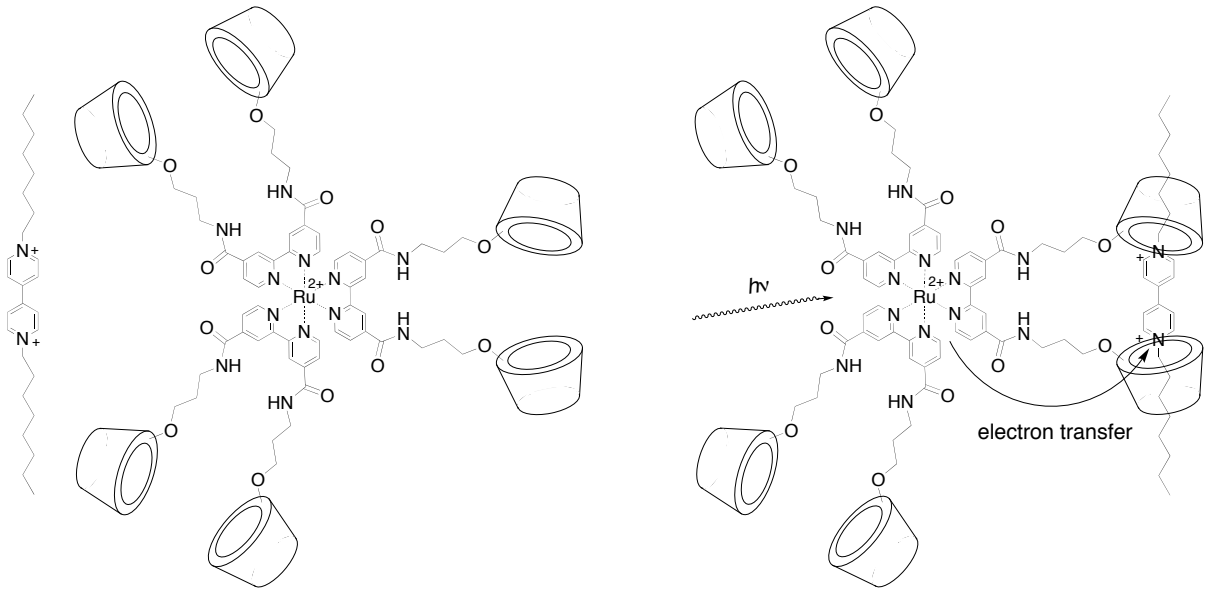

Figure 1.8 *A non-methylated βCD-appended ruthenium complex as luminescent steroid sensor. Electron transfer takes place after binding of a viologen molecule in the CD cavity.*[41]

1.3.2 Linear wires and related systems based on CDs

CDs have been used to construct nano-size self-forming linear wires. These molecular systems are formed by self-assembly of individual photo- or electro-active components in aqueous media, in which complexation in a CD cavity can occur efficiently. Application of an external stimulus to one end of the wire (for example, a laser pulse in the case of photo-active molecules) leads to transmission of the signal to the other end.

Several examples of energy or electron transfer have been reported in systems where only two components (donor and acceptor) are linked by complexation in the CD cavity. Such systems are simpler than a wire, and therefore, easier to investigate. The first electron transfer observed from a ruthenium metal centre towards a guest bound in a covalently attached permethylated-βCD cavity was reported by Armspach et al. in 2000 (Figure 1.9A).[42] Shortly thereafter, Haider et al. reported on similar experiments with analogous organometallic complexes and quinones as electron-accepting guests (Figure 1.9B).[43] The main difference between the two systems presented in Figure 1.9 is the nature of the donating ruthenium

complex. In the first example we have a $[Ru(bpy)_3]^{2+}$ derivative characterised by a relatively long phosphorescence lifetime (≈ 390 ns), which allows this process to occur easily. In the other example (Figure 1.9B) the lifetime of the donor is much shorter (τ = 1.9 ns). However, the authors observed that it was long enough to measure the electron transfer process. If we want to expand these systems by assembling a larger number of Ru-CD building blocks, it is clear that the geometry of the compound presented in Figure 1.9B is more favourable for the assembly of linear wires than the compound in Figure 1.9A, since $[Ru(tpy)_2]^{2+}$ has inherent axial symmetry and does not have the problem of stereoisomerism.

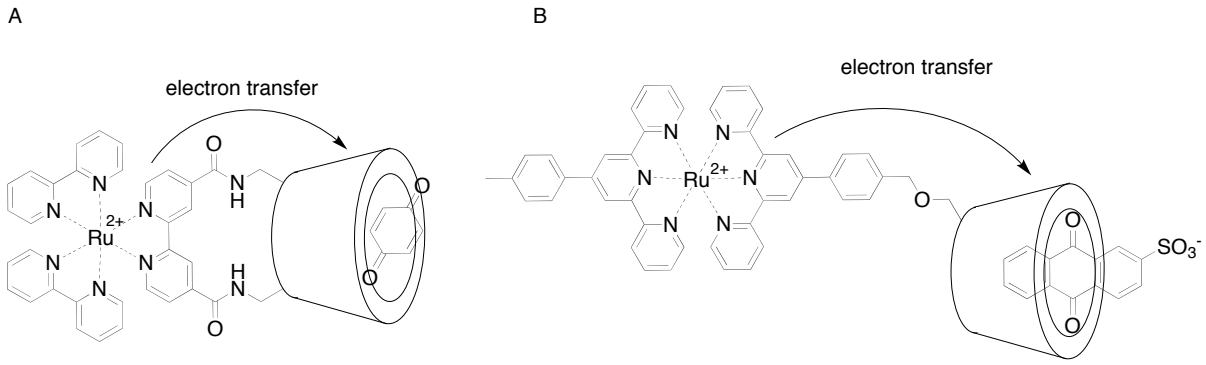

Figure 1.9 *Self-assembled systems with permethylated βCD that display electron transfer from a Ru(II) centre to a quinone in aqueous solution. Electron transfer was induced by excitation of the ruthenium centre. (A, λ_{exc} = 460 nm; B, λ_{exc} = 490 nm)*[42,43]

In the same publication, Haider et al. described the formation of a photo-induced electron transfer process between ruthenium(II) and osmium(III) polypyridine complexes (Figure 1.10).[43,44]

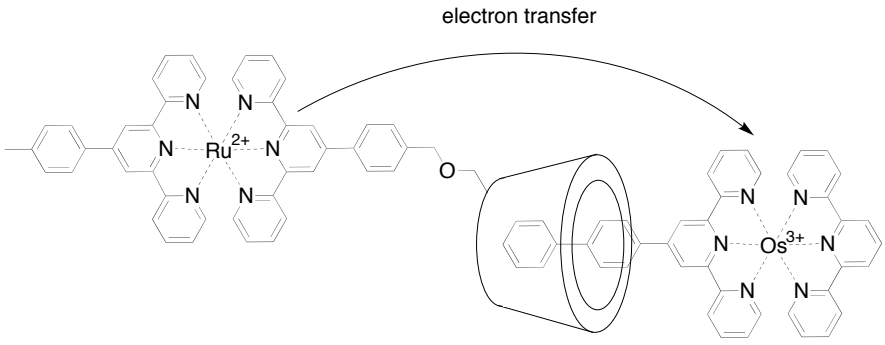

Figure 1.10 *Nano-sized "wire" in which permethylated βCD acts as linker between a ruthenium and an osmium complex. The osmium(III) species is generated by using cerium(IV) as an oxidising agent.*[43]

Encapsulation of a long organic conjugated molecule by several CD cavities has also been described.[45] Cacialli et al. reported an example of a CD-based nanowire that has the form of a polyrotaxane.[45] Inclusion provides chemical and physical stabilisation of the conjugated structure and has been mentioned as being promising for molecular electronics and other various applications.

A nice example of how CD complexation protects an organic conjugated molecule from undesired chemical reactions was given by Stone and Anderson, who described the formation of a relatively simple rotaxane with an anthracene moiety as the thread (Figure 1.11).[46]

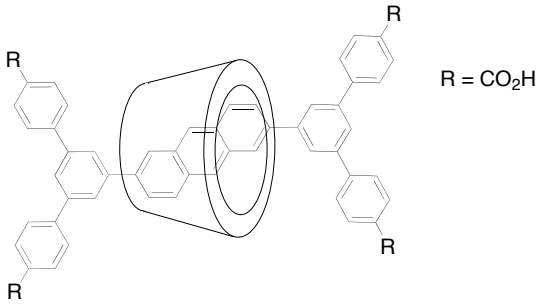

Figure 1.11 *A rotaxane in which an anthracene thread is encapsulated in a native βCD cavity. The stability and luminescence of the anthracene moiety were significantly enhanced.[46]*

It is well known that anthracene is subject to dimerisation after laser excitation or under exposure to UV light due to the formation of highly reactive anthracene triplet-state species. Encapsulation of a single anthracene molecule as the thread in the native βCD prevents these photochemical reactions from occurring. Furthermore, encapsulation also prevents quenching of the anthracene fluorescence.

1.3.3 Cyclodextrins as building blocks for the construction of giant structures and the functionalisation of surfaces

As described above, CDs allow the possibility of derivatisation, especially at their primary side, due to the higher reactivity of the primary hydroxyls relative to the secondary hydroxyls present on the secondary rim. Introduction of long hydrocarbon chains on the primary side combined with the hydrophilicity of the secondary side has led to the formation of amphiphilic molecules that self-assemble in aqueous solution to give nano-sized structures (Chapter 7).[47,48] A pioneering study in this direction was reported by Ravoo et al., who studied the formation of vesicles derived from CDs that were fully substituted with alkyl chains (C12 and C16) on their primary side and functionalised with short poly(ethylene

glycol) chains on their secondary side.[49,50] The resulting amphiphiles self-assembled in water into bilayer vesicular structures. The surfaces of the resulting vesicles were covered by CD moieties that could act as hosts and recognise guest molecules (Figure 1.12).[47] The authors have also described the possibility of triggering the aggregation/adhesion of these host vesicles by using multivalent guests. The aggregation process is reversible and controlled by a change in the conformation of the host moieties; this conformational change can be induced by either metal ion binding[51] or irradiation with light.[52]

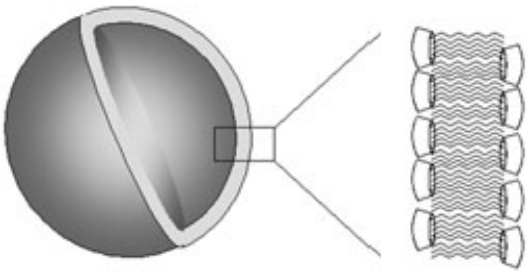

Figure 1.12 *Schematic representation of a CD unilamellar vesicle consisting of bilayers of CDs, in which the hydrophobic tails are directed inwards and the hydrophilic CD head groups are facing the water phase.[50]*

Another example of self-assembled CD architectures was reported by Zhang et al.[53] They prepared a class of porous nanospheres (radius of 25–35 nm) from amphiphilic cholic acid modified βCD **1** using sodium 1-naphthylamino-4-sulfonate (1,4-SNS) as the guest molecule to trigger the assembly process (Figure 1.13). The study revealed that the strong host-guest inclusion interaction, the shape of the guest molecule, and pH were essential factors in the aggregation of amphiphilic compound **1** into nanospheres.

CDs have also been applied to construct monolayers on metal surfaces. In this case, the ideal chemical functions to act as anchor points are either nitrogen atoms, for example, from an attached pyridine group, or attached thiol groups;[54] the latter are the more widely studied species. Thiols provide the strongest attachment to noble-metal surfaces and their reaction can be easily followed by IR spectroscopy through the disappearance of the S–H vibrational mode. One example is the elegant work of Reinhoudt and co-workers, who developed the concept of molecular printboards (Figure 1.14).[55–58]

As already mentioned, the primary side of the CD cavity can be substituted with functionalities as far as synthetic technology allows. This approach has been utilised to introduce alkyl tails ending in vinylidene groups in CDs.[59] The photochemical reaction between a hydrogen-terminated monocrystalline silicon surface (Si–H) and the 1-alkene

chains of the modified CD was used to covalently functionalise semiconductor surfaces, opening the possibility of these systems for applications as recognition devices.[59]

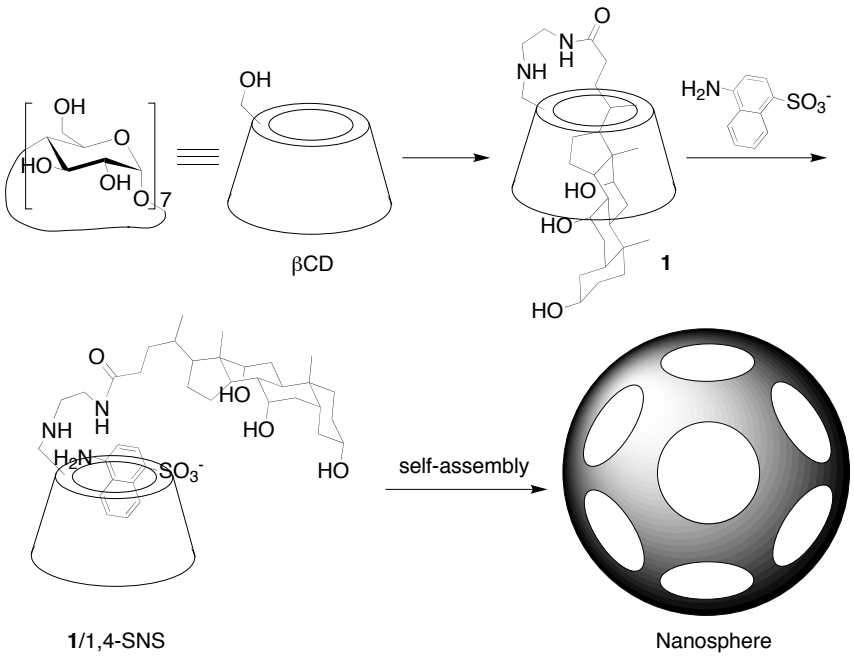

Figure 1.13 *Proposed pathway for the formation of **1**/1,4-SNS nanospheres.*[53]

Figure 1.14 *Formation of a thiol-containing CD monolayer on a gold surface and its use to bind multi-functionalised "ink" molecules (molecular printboard).*[57]

1.3.4 Colloidal particles based on cyclodextrins

Modification of metal and semiconductor nanoparticles with organic monolayers is an active field of research in chemistry.[60–66] An interesting aspect is that the final materials may exhibit the combined properties of their inorganic and organic components.[67]

Several metals have been studied, including gold, palladium, and platinum. In the case of platinum and palladium the most interesting characteristics for study are, of course, their catalytic properties.[68,69] The formation of organic monolayers on the platinum surface normally shields the catalytic centre and as a result leaves an inactive surface. However, this

is not necessarily the case for CD-modified metal particles, the surfaces of which remain accessible to the substrate and retain their catalytic activity.[68–70] Indeed, the presence of CDs stabilises the nanoparticles by preventing their aggregation, affording highly water-compatible and stable colloids; an indispensable requirement for allowing the formation of host-guest complexes in solution (Chapter 5).[71,72] The CDs attached to the particle surface retain their binding abilities towards common CD guests.[70,73,74] For example, Kaifer and co-workers have reported the inclusion of hydrophobic guests into the cavities of thiolated βCDs attached to metal nanoparticles and the subsequent arrangement of the particles into self-assembled structures.[75] In particular, they exploited the well-known host-guest molecular interactions between βCD and ferrocene dimers to form a network of interconnected nanoparticles, in which the ferrocene derivatives act as linkers between the different gold particles, leading to their aggregation (Figure 1.16).[76]

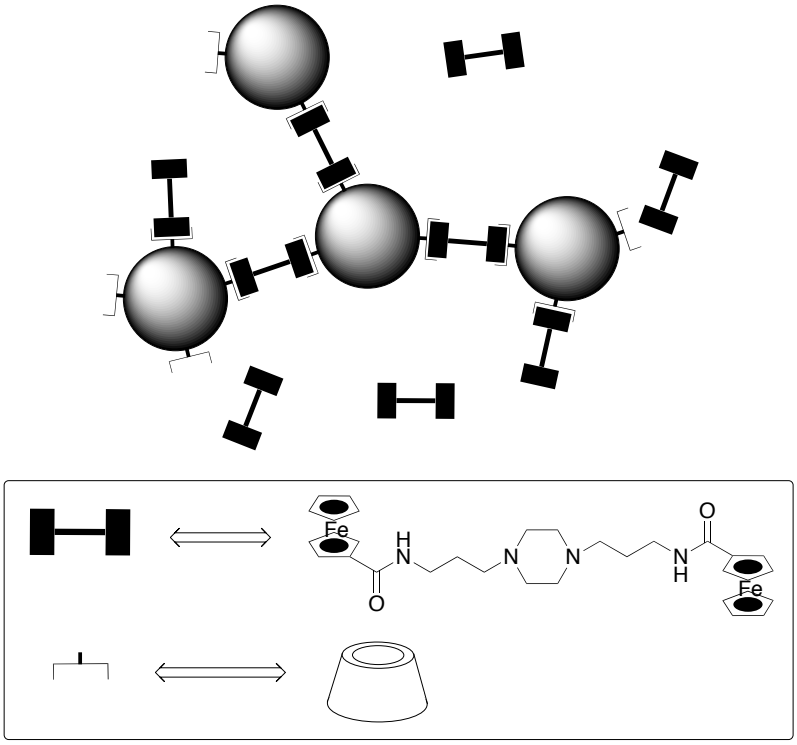

Figure 1.16 *Schematic representation of a nanoparticle-ferrocene dimer composite formed by mixing per-6-thio-βCD with a ferrocene dimer. The inset shows the molecular structures of the βCD and the linker.*[76]

Decoration of a metal colloidal particle with a series of host-guest compounds can be used to grow linear-like wire systems from the surfaces of the particles; in combination with the

catalytic properties of the metal particle, this structural feature is of interest for photocatalytic applications (see Chapter 5).

1.4 Triazole-based chelating ligands and their coordination complexes

1.4.1 Metal complexes as phosphorescent probes

Phosphorescent heavy-metal complexes based on MLCT transitions exhibit important photophysical properties, such as relatively long lifetimes, high chemical and photochemical stability,[77–79] and significant Stokes shifts (which implies easy separation of excitation and emission wavelengths).[78] These features give heavy-metal complexes an advantage over fluorescent organic dyes for application in different fields. In this connection, complexes of ruthenium(II)[80–85] and iridium(III)[86–92] have received particular attention in recent years.

Several families of luminescent transition-metal complexes have been developed, and α,α-diimines such as bpy ligands have been extensively used as chelators.[93–101] These complexes show long-lived photoluminescence in the visible region and their emission energy is largely affected by the nature of the chelators.[102] The photophysical properties (including the quantum efficiency, wavelength of maximum emission, and the redox properties) of these luminescent metal complexes can be modulated by controlling the electronic structure of the α,α-diimine ligands that act as electron acceptors from the metal centre. A popular example is the class of five-membered heterocyclic ligands such as imidazole, pyrazole, and triazole, for which the π-electronic structure can be tuned to a large extent. The introduction of electron-donating or electron-withdrawing groups to the α,α-diimine ligands effectively adjusts the highest occupied molecular orbital (HOMO) and lowest unoccupied molecular orbital (LUMO) levels of the complexes. Since these coordination metal complexes are finding many applications, it is essential that their physical and chemical properties, including their solubility, can be fine-tuned. The synthesis of new versatile chelating ligands, therefore, is the key step for the development of tailor-made luminescent metal complexes; the design of new ligands should take into account important aspects including a straightforward synthetic approach and the possibility to easily introduce functional groups.

Due to their high luminescence quantum yields and remarkable structure-function relationships, iridium(III) complexes have become the most attractive class of phosphorescent heavy-metal complexes. In contrast to complexes based on other heavy metals (e.g., Ru(II), Rh(I), Os(II)), they show intense phosphorescence at room temperature,[103] which originates from a ^{3}MLCT excited state or in some cases from a ^{3}LC state. They have been used widely

as highly efficient emitters for organic light-emitting diodes (OLEDs),[79,104–108] as components of phosphorescent chemosensing systems,[109–115] and have been applied in electroluminescent devices.[116–119] More recent applications are found in the biomedical field as phosphorescence probes,[100,120,121] and in fields such as medicinal chemistry and molecular biology as replacements for radioactive biological labels.[122–126]

1.4.2 Huisgen cycloaddition reaction

In the past decade the heteroaromatic, five-membered 1,2,3-triazole ring has attracted interest of the wider scientific community. The great variety of properties of this type of compounds, such as high chemical stability, hydrogen-bond-accepting and -donating character, and strong dipole moment enable the application of the 1,2,3-triazole function in many different fields.[127] Some of the properties of the 1,2,3-triazole can be understood by looking at its structure. 1,2,3-Triazole has a flat structure, as revealed by molecular modelling studies and crystal structures.[7,128,129] Such a flat structure would be in line with a high degree of conjugation in the compound. However, several studies indicate that conjugation in the triazole-derived heteroaromatic structures is not extended through the N-1 of the triazole moiety (see Scheme 1.2 for numbering).[128,130–132] Interestingly, the electron density in the triazole ring is unevenly distributed among the three nitrogen atoms, with the highest density on the nitrogen at position N-3 and the lowest on the nitrogen at position N-2.[133] The presence of the three sp^2-hybridised nitrogen atoms in the triazole ring provides the additional feature that the triazole moiety can serve as a ligand to coordinate to metals or to bind guest molecules by hydrogen bonding, and thus, it can be considered as being a functional building block.[133–135]

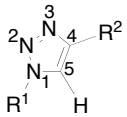

Scheme 1.2 *Structure and numbering of 1,4-disubstituted 1,2,3-triazole.*

The 1,2,3-triazole ring can be formed by the cycloaddition of an acetylene to an azido group. The thermal azide-alkyne cycloaddition reaction has been known for more than a century,[136] but no extensive investigation of this reaction had been carried out until the work of Huisgen and co-workers in the 1950s–1970s.[137] They studied this reaction as part of a large series of studies on the general family of 1,3-dipolar cycloaddition reactions.[138,139] When an asymmetrically substituted alkyne is employed, thermal activation of the azide-

alkyne cycloaddition usually leads to the formation of a mixture of two regioisomers, **1** and **2** (Scheme 1.3). In 2002, the introduction of a copper(I) catalyst to this reaction, independently discovered by the groups of Sharpless[140] and Tornøe,[141] led to major improvements in both rate and regioselectivity. The use of copper(I) catalyst results in the exclusive formation of 1,4-disubstituted product **1** (Scheme 1.3).

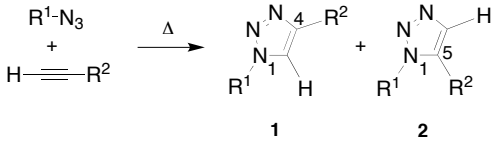

Scheme 1.3 *Huisgen 1,3-dipolar acetylene-azide cycloaddition reaction. In the absence of copper as a catalyst, the reaction leads to the formation of two regioisomers. In the presence of copper(I), regioisomer **1** is formed exclusively.*

This copper(I)-catalysed reaction is not only stereospecific, but also proceeds at room temperature and it is efficient in many protic and aprotic solvents, including water. Furthermore, it is fully bio-orthogonal (i.e., compatible with common moieties found in bio (macro)molecules).[142,143] As a result, the copper(I)-catalysed Huisgen cycloaddition reaction was rapidly adapted to play a prominent role in different fields, including those of materials science,[144,145] medicinal chemistry,[146] and bioconjugation chemistry.[146,147]

The strength of the copper(I)-catalysed reaction, also known as the "click" reaction,[140] in part, comes from the use of the azide moiety, which has several advantages over other functional groups. The azide group is by far the most convenient group of the 1,3-dipolar components that have to be introduced in a compound and can be kept in a molecule until it is needed. Indeed, it is stable toward a number of reactions, such as dimerisation and/or hydrolysis. The azide group is also convenient because it is easily accessible from primary amines by the diazo transfer reaction.[148] The remarkable stability (orthogonality) of aliphatic azides to a wide variety of other standard organic synthesis conditions make them "invisible" unless a good dipolarophile is present.

The cycloaddition of azides and acetylenes is ideally suited for the joining of macromolecular structures,[147] while its value for the preparation of lower molecular weight compounds, for example, triazole-linked glycopeptides, has also been established.[149]

In addition to the utilisation of the click reaction as a linking tool, 1,2,3-triazoles also play a role as coordination motifs. Regiospecific copper(I)-catalysed cycloaddition of azides and terminal alkynes is a methodology rapidly growing in the field of coordination chemistry, and

has recently been applied to the synthesis of palladium(II),[150] platinum(II),[150] iron(II),[151] ruthenium(II),[151] and europium(III) complexes.[151]

1.4.3 Click chemistry as a tool to prepare new chelating ligands

1,2,3-Triazoles are known monodentate ligands. In an example describing the ability of the 1,2,3-triazole to form coordination complexes,[150] van Koten and co-workers synthesised platinum and palladium metal complexes in which the 1,2,3-triazole was coordinated through its nitrogen N3.[150] They showed that the strength of the nitrogen–metal bond could conveniently be tuned both by steric and electronic factors, that is, by varying the substituents on the positions N1 and C4 of the triazole function (Scheme 1.4).[150]

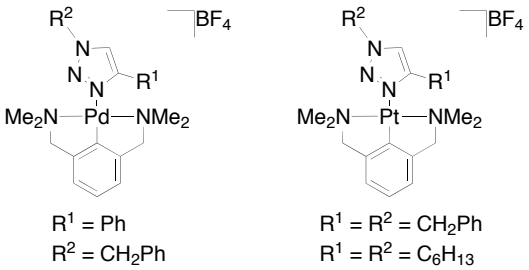

Scheme 1.4 *Schematic representation of the cationic Pd and Pt complexes synthesised by the van Koten group.[150]*

In principle, only two of the three nitrogen atoms of the 1,2,3-triazole are able to coordinate to transition metal ions. A complicating factor is that the presence of multiple coordination sites may enable these triazole ligands to possibly form isomeric structures or complicated multinuclear complexes. To eliminate this possibility and to increase the stability of the coordination complexes, ligands with an additional coordination site (e.g., a 2-pyridyl group) linked to the triazole unit have been developed.

The ability of 1,2,3-triazoles to act as a ligand in the formation of chelated coordination metal complexes has been known for a long time, and these metal complexes have been exploited extensively in different fields, such as organometallic catalysis.[133,152–154] However, few examples of luminescent metal complexes containing a 1,2,3-triazole-based ligand have been described. In this connection, ligands that contain an extended aromatic structure, such as the triazole-pyridine unit, are particularly interesting due to their extended conjugation and strong ligand field effect. An increasing number of papers in which 1,2,3-triazole is used as multidentate polyaromatic ligands have been published since 2006. At the time when these papers were published, the research described in this thesis had already begun.

To the best of our knowledge, the idea of using the bidentate 1,2,3-triazole-pyridine system as a chelating ligand was first suggested by Reek and co-workers in 2005.[131] In their study, the 2-(1-substituted-1*H*-1,2,3-triazol-4-yl)-pyridine unit (pytl; Chapter 2)[7] was inserted into a polymeric structure entirely synthesised by click chemistry. However, the authors did not report the preparation of the corresponding coordination metal complexes.

The first class of clicked multidentate ligands applied in the formation of luminescent coordination metal complexes was an analogue of the terdentate ligand tpy (Scheme 1.6). Two of the pyridine moieties of tpy were replaced by triazole rings to give the ligand 2,6-bis(1-R-1*H*-1,2,3-triazol-4-yl)pyridine (tripy; Scheme 1.5).[151] These tripy ligands were prepared by reacting bis-acetylene-appended pyridine with azides.[151] Besides being novel, a great advantage of the clicking approach lies in its high versatility; it allows, at least in principle, functionalisation of tripy with a large variety of functional groups. Flood and co-workers investigated the stability of homoleptic[155] ruthenium(II), europium(III), and iron(II) complexes (Scheme 1.5), and studied their electronic properties and emission behaviour.[151]

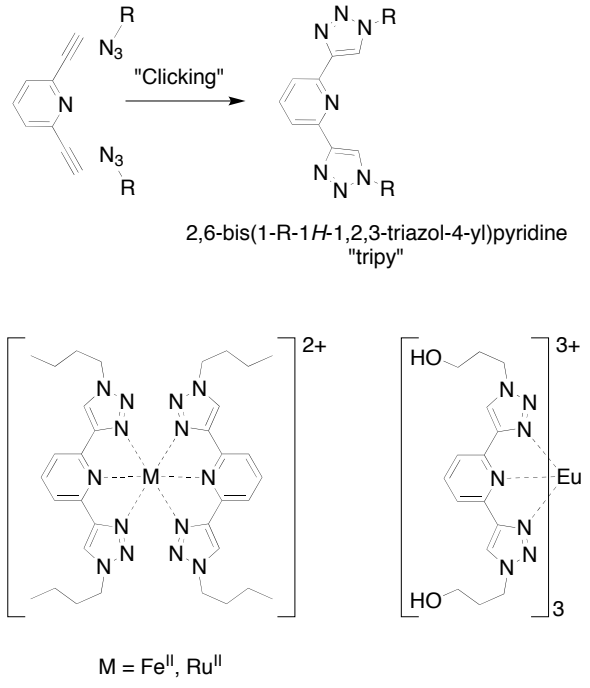

Scheme 1.5 *Structures of the terdentate ligand tripy and the corresponding homoleptic coordination complexes of this ligand.[151]*

It was observed that the electronic structures of the frontier orbitals of both the tpy and tripy complexes of iron(II) and ruthenium(II) were similar; the HOMOs were metal-based dπ orbitals and the π* LUMO was localised on the ligand. The MLCT absorption bands for the

iron(II) and ruthenium(II) tripy-based complexes (acetonitrile: $\lambda_{MLCT,Fe}$ = 443 nm, $\lambda_{MLCT,Ru}$ = 393 nm) were blueshifted with respect to the corresponding tpy-based complexes (acetonitrile: $\lambda_{MLCT,Fe}$ = 552 nm, $\lambda_{MLCT,Ru}$ = 475 nm), which indicated the presence of higher energy excited states. This results from a ligand-based π* LUMO that is higher in energy than that of the corresponding LUMO of the tpy ligand.

The triazole units are supposed to strongly reduce the emission quantum efficiency. Indeed, none of the triazole-containing complexes described in Scheme 1.6 exhibited photoluminescence at room temperature. For the homoleptic bis-tripy complex $[Ru(tripy)_2]^{2+}$ no emission was observed, not even at low temperature. This is caused by the stronger π-acceptor ability of tripy with respect to tpy, which lifts the ^{3}MLCT state and decreases the energy gap towards the ^{3}MC state.

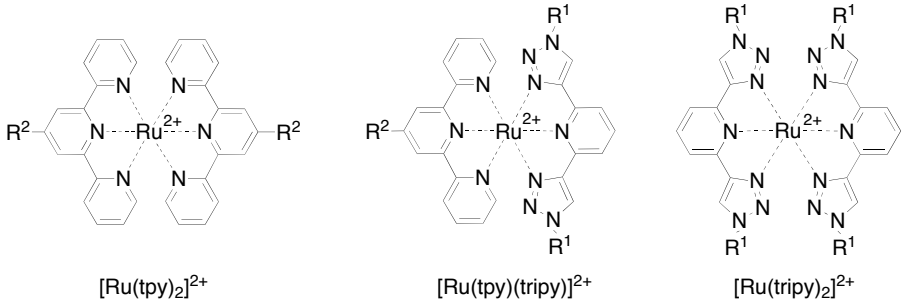

Scheme 1.6 *Schematic representation of the coordination complexes of general formula [Ru(tpy)$_{2-n}$(tripy)$_n$]$^{2+}$.*[157]

The application of bidentate ligands containing one triazole-pyridine unit as fluorescence sensors for metal ions was first described by Bunz and Xie.[158,159] Shortly after this, Schubert and co-workers reported the preparation of ruthenium(II) complexes containing pytl ligands as an alternative to bidentate bpy.[160] These authors prepared a small library of mono-functionalised ligands substituted with aromatic and aliphatic groups (Scheme 1.7). The photophysical and electrochemical behaviour of the corresponding ruthenium(II) homo- and heteroleptic complexes was found to be strongly influenced by the number of pytl ligands coordinated to the metal ion. In general, the complexes of formula $[Ru(dmbpy)_{3-n}(pytl\text{-}R)_n]^{2+}$ (dmbpy = 4,4'-dimethyl-2,2'-bipyridine) display properties that resemble those of their bpy-based counterparts, such as a strong orange emission at low temperature, when at least one dmbpy ligand is present (77 K in *n*-butyronitrile glassy matrix: for the complex with n = 1 $\lambda_{PL,max}$ = 575 nm; for the complex with n = 2 $\lambda_{PL,max}$ = 563 nm). The emission of the complexes at room temperature is fully quenched if at least one triazole-pyridine ligand is present; for the complex $[Ru(pytl\text{-}R)_n]^{2+}$ with n = 3 no emission was observed, even at low

temperature. Analysis of the photophysical and electrochemical properties revealed that the π^*_L LUMO of these complexes was mainly located on the dmbpy ligand. The increasing number of coordinated pytl ligands slightly stabilises the π_{metal} HOMO of the corresponding complex and significantly increases the π^*_{ligand} LUMO energy levels. This leads to a significant increase in the energy gap, and consequently, to lower emission quantum yields.

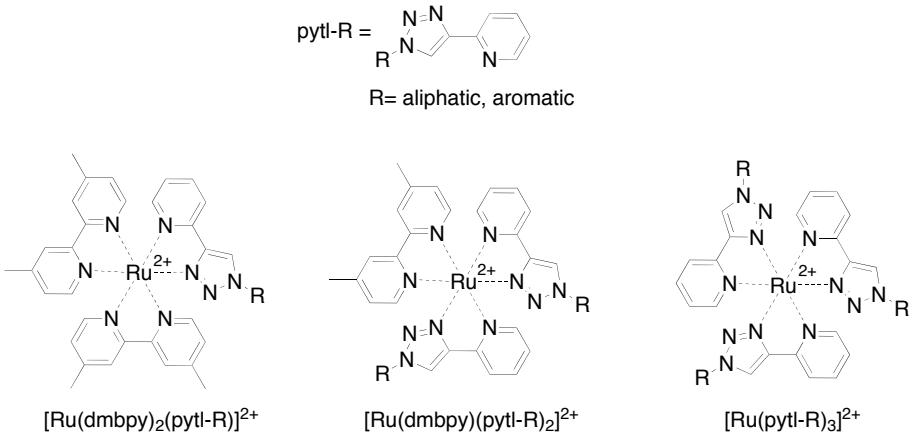

Scheme 1.7 *Schematic representation of the homo- and heteroleptic complexes of general formula* $[Ru(dmbpy)_{3-n}(pytl\text{-}R)_n]^{2+}$.[160]

In 2008 Yano and co-workers reported a bidentate ligand containing the 1,2,3-triazole ring coordinated to a rhenium(I) centre.[129] The crystal structure of the free ligand, and hence, of the 1,2,3-triazole ring was determined and compared with the crystal structure of 1,2,4-triazole (Scheme 1.8).[129] A significant difference was found in the length of the bonds. In particular, the N(3)–N(2) bond length of the 1,2,3-triazole ring is shorter than the adjacent N(3)–C(4) and N(1)–N(2) bonds, while the corresponding N(1)–N(2) bond length of 1,2,4-triazole was longer than those of the two adjacent bonds (Scheme 1.8). This structural feature suggests that, in the 1,2,3-triazole, the N(2)–N(3) bond has a strong double-bond character, while the N(3)–C(4) and N(1)–N(2) bonds have more single-bond character; thus, this triazole ring has an azo character (Scheme 1.8). In the 1,2,4-triazole, instead, the N(1)–N(2) bond has single-bond character, while N(1)–C(5) and N(2)–N(3) have double-bond character, suggesting that this triazole has an azine character (Scheme 1.8).[129] This conclusion is supported by the crystal structure that we obtained for pytl-R (R = adamantyl and methyl, see Chapter 2).[7]

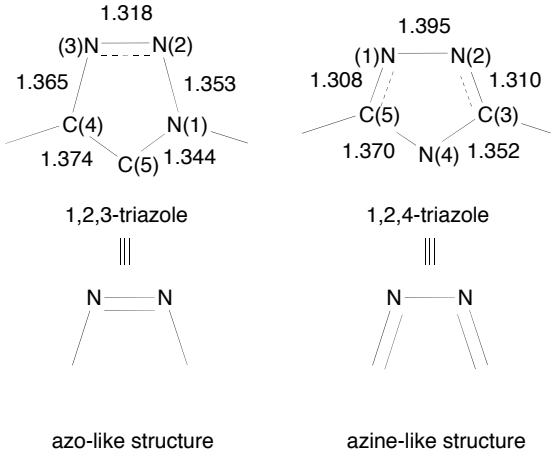

Scheme 1.8 *Bond length data obtained from crystal structures of 1,2,3-triazole and 1,2,4-triazole rings.*[129]

In 2009 the first report describing the synthesis and characterisation of heteroleptic iridium (III) complexes prepared by using triazole-derived compounds as coordinating ligands appeared. The ligands synthesised were not analogues of bpy, but belonged to the family of 1-substituted-4-phenyl-1*H*-1,2,3-triazole ligands (phtl; Chapter 6), which are analogues of the cyclometalating ligand 2-phenylpyridine (ppy; Scheme 1.9).[161]

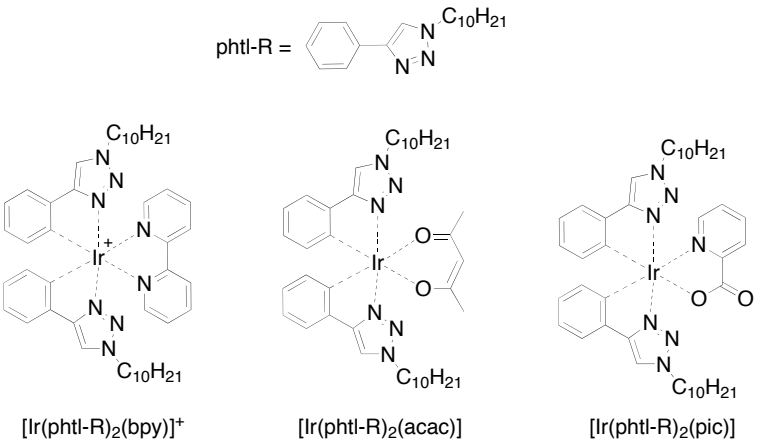

Scheme 1.9 *Schematic representation of heteroleptic complexes of iridium(III) with the cyclometalating ligands phtl-R.*[161]

These ligands were prepared by reacting 1-dodecyl azide with ethynylbenzene. A similar approach was used by us and is described in Chapter 6 of this thesis.[162] Spectroscopic measurements revealed that the emission of these heteroleptic iridium(III) complexes was strongly influenced by the nature of the ancillary ligand. In general, the presence of phtl

causes a blueshift of the maximum emission wavelength (in CH_2Cl_2: $[Ir(phtl\text{-}R)_2(bpy)]^{2+}$, $\lambda_{PL,max}$ = 560 nm; $[Ir(phtl\text{-}R)_2(acac)]^{2+}$ acac = acetylacetonate, $\lambda_{PL,max}$ = 435 nm; $[Ir(phtl\text{-}R)_2(pic)]^{2+}$ pic = picolinate, $\lambda_{PL,max}$ = 527 nm).[161] Comparison of these complexes with well-known phenyl-pyridine analogues shows that their optical and electronic properties can be tuned over a broad frequency range.[161] To the best of our knowledge no examples of iridium complexes containing triazole-pyridine bidentate ligands have been described before.

1.5 Aim and outline of this thesis

The work described in this thesis is aimed at the preparation and exploitation of new inorganic luminescent labels that contain the permethylated βCD unit and are water soluble as well as energetically efficient. The functionalisation of these coordination complexes with permethylated βCD provides luminescent labels that have the ability to self-assemble in a designed manner, enhancing their luminescence efficiency at the same time. The 1,2,3-triazole unit was the ligand of choice in these coordination complexes. Our major interest is focused on the preparation of a hydrogen evolution system in which a photosensitiser, an electron relay, and a metal nanoparticle self-organise into a linear structure, allowing an electron transfer process to be triggered by the absorption of light. **Chapter 2** describes the synthesis and characterisation of new pytl ligands prepared by click chemistry and used in the synthesis of heteroleptic complexes of ruthenium(II) and iridium(III). The already interesting photophysical properties of the iridium complex were remarkably enhanced by the functionalisation of the pytl with permethylated βCD. βCD plays an important role by acting as a second-sphere ligand and by shielding the coordination complex from quenching of its luminescence by dynamic collision or oxygen energy transfer, for example.

The iridium complex $[Ir(ppy)_2(pytl\text{-}\beta CD)]Cl$, which contains one permethylated βCD moiety, exists in two diastereoisomeric forms. **Chapter 3** reports a detailed structural investigation of the Δ diastereoisomer of $[Ir(ppy)_2(pytl\text{-}\beta CD)]Cl$ in D_2O by high-resolution liquid NMR spectroscopy. Supramolecular interactions between the iridium complex and the covalently attached CD enhance the photophysical properties of this complex. Two-dimensional NMR spectra were acquired to establish the molecular conformation of the iridium complex in solution.

Chapter 4 deals with the application of ionic iridium(III) complexes of the general formulas $[Ir(ppy)_2(pytl\text{-}R)]^+$ and $[Ir(F_2ppy)_2(pytl\text{-}R)]^+$ (F_2ppy = 2-(2,4-bisfluorophenyl)-pyridine) as luminophores in electrochemiluminescence (ECL). Emissive excited states of the metal complexes are generated by electron transfer reactions between electro-generated

species. Pytl ligands appended with various functional groups were used in the synthesis of the iridium(III) complexes. The intensity and stability of the ECL signal of the iridium(III) complexes in air-equilibrated aqueous media, and the effect of the substituent on the ECL emission, were investigated.

Chapter 5 describes our efforts to exploit the photophysical properties of pytl-appended iridium(III) complexes in a self-assembled system for the photocatalytic production of hydrogen. The activity of a linear, light-driven, catalytic, three-component system for the reduction of protons, comprised of a metal complex as a photosensitiser, a viologen-based electron relay, non-methylated βCD-modified platinum nanoparticles as the catalyst, and a sacrificial donor was investigated in a home-made setup. The photosensitisers were the polypyridine complexes described in Chapter 2. The modular approach introduced in this study allows the construction of several functional photo-active systems from a limited number of building blocks by self-assembly.

Chapter 6 describes the synthesis and characterisation of the bidentate cyclometalating ligands phtl, and their corresponding iridium(III) heteroleptic complexes.

Chapter 7 deals with the synthesis of a giant amphiphile consisting of polystyrene end-capped with permethylated βCD. This compound forms vesicular structures when injected as a solution in THF into water. The ability of the CDs on the surface of the polymersomes to form inclusion complexes was tested by carrying out a competition experiment with a fluorescent probe sensitive to the polarity of the surrounding medium. Furthermore, by using this system, we were able to mimic the recognition of molecules by cell membranes, which in nature is often based on interactions with specific membrane receptors. Furthermore, the enzyme horseradish peroxidase was modified with adamantane groups through a poly (ethylene glycol) spacer and its interaction with the polymersomes was investigated.

1.6 Acknowledgments

The work described in this thesis has been developed within the framework of the Marie Curie Research and Training Network (RTN) UNI-NANOCUPS. The EU (EU-FP MRTN-CT-2003-504233) is gratefully acknowledged for the financial support that made this work possible.

1.7 References

[1] P. Contreras-Carballada, *Thesis dissertation: Photoactivated Nano-Systems,* University of Amsterdam, Amsterdam, **2009**.

[2] B. Nelissen, *Thesis dissertation: Cyclodextrin Multimers. A Study of Their Design and Application in Optical and Mass-Sensitive Sensor Devices,* Radboud University, Nijmegen, **2002**.

[3] J. Szejtli, *Chem. Rev.* **1998**, *98,* 1743–1753.

[4] B. Casu, M. Reggiani, G. G. Gallo, A. Vigevani, *Tetrahedron* **1966**, *22,* 3061–3083.

[5] B. Gillet, D. J. Nicole, J. J. Delpuech, *Tetrahedron Lett.* **1982**, *23,* 65–68.

[6] Y. Yamamoto, Y. Inoue, *J. Carbohydr. Chem.* **1989**, *8,* 29–46.

[7] M. Felici, P. Contreras-Carballada, Y. Vida, J. M. M. Smits, R. J. M. Nolte, L. De Cola, R. M. Williams, M. C. Feiters, *Chem. Eur. J.* **2009**, *15,* 13124–13134.

[8] B. C. Gibb, *Isr. J. Chem.* **2011**, *51,* 798–806.

[9] R. J. Bergeron, M. P. Meeley, Y. Machida, *Bioorg. Chem.* **1976**, *5,* 121–126.

[10] M. V. Rekharsky, Y. Inoue, *Chem. Rev.* **1998**, *98,* 1875–1917.

[11] R. I. Gelb, L. M. Schwartz, B. Cardelino, H. S. Fuhrman, R. F. Johnson, D. A. Laufer, *J. Am. Chem. Soc.* **1981**, *103,* 1750–1757.

[12] M. Kitagawa, H. Hoshi, M. Sakurai, Y. Inoue, *Bull. Chem. Soc. Jpn* **1988**, *61,* 4255–4229.

[13] W. Saenger, *Angew. Chem. Int. Ed.* **1980**, *19,* 344–362.

[14] F. Cramer, W. Kampe, *J. Am. Chem. Soc.* **1965**, *87,* 1115–1120.

[15] H. Dodziuk, *Cyclodextrin and Their Complexes: Chemistry, Analytical Methods, Applications,* Wiley-VCH, Weinheim, **2006**.

[16] G. Patonay, K. Fowler, A. Shapira, G. Nelson, I. M. Warner, *J. Inclusion Phenom. Macrocyclic Chem.* **1987**, *5,* 717–723.

[17] S. Hamai, *J. Phys. Chem.* **1989**, *93,* 6527–6529.

[18] K. Kano, I. Takenoshita, T. Ogawa, *Chem. Lett.* **1982**, 321–324.

[19] G. Nelson, G. Patonay, I. M. Warner, *J. Inclusion Phenom. Macrocyclic Chem.* **1988**, *6,* 277–289.

[20] M. V. Rekharsky, M. P. Mayhew, R. N. Goldberg, P. D. Ross, Y. Yamashoji, Y. Inoue, *J. Phys. Chem. B* **1997**, *101,* 87–100.

[21] R. I. Gelb, L. M. Schwartz, *J. Inclusion Phenom. Mol. Recognit. Chem.* **1989**, *7,* 465–476.

[22] R. I. Gelb, L. M. Schwartz, D. A. Laufer, *Bioorg. Chem.* **1980**, *9,* 450–461.

[23] R. I. Gelb, L. M. Schwartz, D. A. Laufer, *J. Chem. Soc., Perkin Trans. 2* **1984**, 15–21.

[24] L. A. Blyshak, I. M. Warner, G. Patonay, *Anal. Chim. Acta* **1990**, *232,* 239–243.

[25] L. E. Briggner, X. R. Ni, F. Tempesti, I. Wadsö, *Thermochim. Acta* **1986**, *109,* 139–143.

[26] R. I. Gelb, L. M. Schwartz, *J. Inclusion Phenom. Mol. Recognit. Chem.* **1989**, *7,* 537–543.

[27] M. R. de Jong, J. F. J. Engbersen, J. Huskens, D. N. Reinhoudt, *Chem. Eur. J.* **2000**, *6,* 4034–4040.

[28] Y. Egawa, Y. Ishida, A. Yamauchi, J. Anzai, I. Suzuki, *Anal. Sci.* **2005**, *21,* 361–366.

[29] H. J. Schneider, F. Hacket, V. Rüdiger, H. Ikeda, *Chem. Rev.* **1998**, *98,* 1755–1785.

[30] J. B. Birks, *Phys. Lett.* **1965**, *19,* 25–26.

[31] J. B. Birks, J. M. De C. Conte, G. Walker, *Phys. Lett.* **1965**, *19,* 125–126.

[32] D. S. McClure, *J. Chem. Phys.* **1949**, *17,* 905–913.

[33] D. S. McClure, *J. Phys. Chem.* **1951**, *19,* 670–675.

[34] M. Kasha, *J. Chem. Phys.* **1952**, *20,* 71–74.

[35] V. Balzani, S. Campagna, *Top. Curr. Chem.* **2007**, *280,* 117–214.

[36] T. J. Meyer, *Pure Appl. Chem.* **1986**, *58,* 1193–1206.

[37] C. R. Hecker, A. K. I. Gushurst, D. R. McMillin, *Inorg. Chem.* **1991**, *30,* 538–541.

[38] J. M. Haider, R. M. Williams, L. De Cola, Z. Pikramenou, *Angew. Chem. Int. Ed.* **2003**, *42,* 1830–1833.

[39] J. M. Haider, R. M. Williams, L. De Cola, Z. Pikramenou, *Angew. Chem.* **2003**, *115,* 1874–1877.
[40] J. A. Faiz, R. M. Williams, M. J. J. Pereira Silva, L. De Cola, Z. Pikramenou, *J. Am. Chem. Soc.* **2006**, *128,* 4520–4521.
[41] H. F. M. Nelissen, M. Kercher, L. De Cola, M. C. Feiters, R. J. M. Nolte, *Chem. Eur. J.* **2002**, *8,* 5407–5414.
[42] D. Armspach, D. Matt, A. Harriman, *Eur. J. Inorg. Chem.* **2000**, 1147–1150.
[43] J. M. Haider, M. Chavarot, S. Weidner, I. Sadler, R. M. Williams, L. De Cola, Z. Pikramenou, *Inorg. Chem.* **2001**, *40,* 3912–3921.
[44] S. Weidner, Z. Pikramenou, *Chem. Commun.* **1998**, 1473–1474.
[45] F. Cacialli, J. S. Wilson, J. J. Michels, C. Daniel, C. Silva, R. H. Friend, N. Severin, P. Samori, J. P. Rabe, M. J. O'Connell, P. N. Taylor, H. L. Anderson, *Nat. Mater.* **2002**, *1,* 160–164.
[46] M. T. Stone, H. L. Anderson, *Chem. Commun.* **2007**, 2387–2389.
[47] J. Voskuhl, B. J. Ravoo, *Chem. Soc. Rev.* **2009**, *38,* 495–505.
[48] M. Felici, M. Marzá-Pérez, N. S. Hatzakis, R. J. M. Nolte, M. C. Feiters, *Chem. Eur. J.* **2008**, *14,* 9914–9920.
[49] B. J. Ravoo, R. Darcy, *Angew. Chem. Int. Ed. Engl.* **2000**, *39,* 4324–4326.
[50] P. Falvey, C. W. Lim, R. Darcy, T. Revermann, U. Karst, M. Giesbers, A. T. M. Marcelis, A. Lazar, A. W. Coleman, D. N. Reinhoudt, B. J. Ravoo, *Chem. Eur. J.* **2005**, *11,* 1171–1180.
[51] S. K. M. Nalluri, J. B. Bultema, E. J. Boekema, B. J. Ravoo, *Chem. Sci.* **2011**, *2,* 2383–2391.
[52] S. K. M. Nalluri, B. J. Ravoo, *Angew. Chem. Int. Ed.* **2010**, *49,* 5371–5374.
[53] Y. Liu, Y. L. Zhao, H. Y. Zhang, *Langmuir* **2006**, *22,* 3434–3438.
[54] C. T. Mallon, R. J. Forster, A. McNally, E. Campagnoli, Z. Pikramenou, T. E. Keyes, *Langmuir* **2007**, *23,* 6997–7002.
[55] O. Crespo-Biel, B. Dordi, D. N. Reinhoudt, J. Huskens, *J. Am. Chem. Soc.* **2005**, *127,* 7594–7600.
[56] F. Corbellini, A. Mulder, A. Sartori, M. J. W. Ludden, A. Casnati, R. Ungaro, J. Huskens, M. Crego-Calama, D. N. Reinhoudt, *J. Am. Chem. Soc.* **2004**, *126,* 17050–17058.
[57] C. A. Nijhuis, J. Huskens, D. N. Reinhoudt, *J. Am. Chem. Soc.* **2004**, *126,* 12266–12267.
[58] X. Y. Ling, D. N. Reinhoudt, J. Huskens, *Pure Appl. Chem.* **2009**, *81,* 2225–2233.
[59] C. Lagrost, G. Alcaraz, J. F. Bergamini, B. Fabre, I. Serbanescu, *Chem. Commun.* **2007**, 1050–1052.
[60] M. J. Hostetler, R. W. Murray, *Curr. Opin. Colloid Interface Sci.* **1997**, *2,* 42–50.
[61] C. R. Martin, D. T. Mitchell, *Anal. Chem.* **1998**, *70,* 322A–327A.
[62] M. Bruchez, M. Moronne, P. Gin, S. Weiss, A. P. Alivisatos, *Science* **1998**, *281,* 2013–2016.
[63] W. C. W. Chan, S. Nie, *Science* **1998**, *281,* 2016–2018.
[64] K. Mori, H. Yamashita, *J. Jpn. Petrol. Inst.* **2011**, *54,* 1–14.
[65] R. Klajn, K. J. M. Bishop, M. Fialkowski, M. Paszewski, C. J. Campbell, T. P. Gray, B. A. Grzybowski, *Science* **2007**, *316,* 261–264.
[66] G. A. DeVries, M. Brunnbauer, Y. Hu, A. M. Jackson, B. Long, B. T. Neltner, O. Uzun, B. H. Wunsch, F. Stellacci, *Science* **2007**, *315,* 358–361.
[67] V. Rotello, *Nanoparticles: Building Blocks for Nanotechnology,* Springer, New York, **2004**.
[68] L. Strimbu, J. Liu, A. E. Kaifer, *Langmuir* **2003**, *19,* 483–485.
[69] J. Alvarez, J. Liu, E. Roman, A. E. Kaifer, *Chem. Commun.* **2000**, 1151–1152.
[70] J. Liu, J. Alvarez, W. Ong, E. Román, A. E. Kaifer, *Langmuir* **2001**, *17,* 6762–6764.
[71] A. C. Templeton, W. P. Wuelfing, R. W. Murray, *Acc. Chem. Res.* **2000**, *33,* 27–36.
[72] Y. Liu, K. B. Male, P. Bouvrette, J. H. T. Luong, *Chem. Mater.* **2003**, *15,* 4172–4180.
[73] J. Liu, J. Alvarez, W. Ong, A. E. Kaifer, *Nano Lett.* **2001**, *1,* 57–60.
[74] Y. Liu, Y. W. Yang, Y. Chen, *Chem. Commun.* **2005**, 4208–4210.
[75] J. Liu, J. Alvarez, A. E. Kaifer, *Adv. Mater.* **2000**, *12,* 1381–1383.

[76] J. Liu, S. Mendoza, E. Román, M. J. Lynn, R. Xu, A. E. Kaifer, *J. Am. Chem. Soc.* **1999**, *121,* 4304–4305.
[77] I. M. Dixon, J. P. Collin, J. P. Sauvage, L. Flamigni, S. Encinas, F. Barigelletti, *Chem. Soc. Rev.* **2000**, *29,* 385–391.
[78] P. T. Chou, Y. Chi, *Chem. Eur. J.* **2007**, *13,* 380–395.
[79] S. J. Liu, Q. Zhao, R. F. Chen, Y. Deng, Q. L. Fan, F. Y. Li, L. H. Wang, C. H. Huang, W. Huang, *Chem. Eur. J.* **2006**, *12,* 4351–4361.
[80] S. Welter, N. Salluce, P. Belser, M. Groeneveld, L. De Cola, *Coord. Chem. Rev.* **2005**, *249,* 1360–1371.
[81] S. Welter, K. Brunner, J. W. Hofstraat, L. De Cola, *Nature* **2003**, *421,* 54–57.
[82] A. Juris, V. Balzani, F. Barigelletti, S. Campagna, P. Belser, A. von Zelewsky, *Coord. Chem. Rev.* **1988**, *84,* 85–277.
[83] M. W. Cooke, G. S. Hanan, F. Loiseau, S. Campagna, M. Watanabe, Y. Tanaka, *J. Am. Chem. Soc.* **2007**, *129,* 10479–10488.
[84] L. De Cola, P. Belser, A. von Zelewsky, F. Vogtle, *Inorg. Chim. Acta* **2007**, *360,* 775–784.
[85] O. Bossart, L. De Cola, S. Welter, G. Calzaferri, *Chem. Eur. J.* **2004**, *10,* 5771–5775.
[86] C. Dragonetti, S. Righetto, D. Roberto, R. Ugo, A. Valore, S. Fantacci, A. Sgamellotti, F. De Angelis, *Chem. Commun.* **2007**, 4116–4118.
[87] L. Flamigni, J. P. Collin, J. P. Sauvage, *Acc. Chem. Res.* **2008**, *41,* 857–871.
[88] A. B. Tamayo, S. Garon, T. Sajoto, P. I. Djurovich, I. M. Tsyba, R. Bau, M. E. Thompson, *Inorg. Chem.* **2005**, *44,* 8723–8732.
[89] W. J. Finkenzeller, M. E. Thompson, H. Yersin, *Chem. Phys. Lett.* **2007**, *444,* 273–279.
[90] J. Li, P. I. Djurovich, B. D. Alleyne, M. Yousufuddin, N. N. Ho, J. C. Thomas, J. C. Peters, R. Bau, M. E. Thompson, *Inorg. Chem.* **2005**, *44,* 1713–1727.
[91] F. Lafolet, S. Welter, Z. Popović, L. D. Cola, *J. Mater. Chem.* **2005**, *15,* 2820–2828.
[92] A. B. Tamayo, B. D. Alleyne, P. I. Djurovich, S. Lamansky, I. Tsyba, N. N. Ho, R. Bau, M. E. Thompson, *J. Am. Chem. Soc.* **2003**, *125,* 7377–7387.
[93] P. D. Fleischauer, P. Fleischauer, *Chem. Rev.* **1970**, *70,* 199–230.
[94] G. A. Crosby, *Acc. Chem. Res.* **1975**, *8,* 231–238.
[95] A. J. Lees, *Chem. Rev.* **1987**, *87,* 711–743.
[96] J. P. Sauvage, J. P. Collin, J. C. Chambron, S. Guillerez, C. Coudret, V. Balzani, F. Barigelletti, L. De Cola, L. Flamigni, *Chem. Rev.* **1994**, *94,* 993–1019.
[97] V. Balzani, A. Juris, M. Venturi, S. Campagna, S. Serroni, *Chem. Rev.* **1996**, *96,* 759–833.
[98] A. I. Baba, J. R. Shaw, J. A. Simon, R. P. Thummel, R. H. Schmehl, *Coord. Chem. Rev.* **1998**, *171,* 43–59.
[99] R. C. Evans, P. Douglas, C. J. Winscom, *Coord. Chem. Rev.* **2006**, *250,* 2093–2126.
[100] K. K. W. Lo, W. K. Hui, C. K. Chung, K. H. K. Tsang, T. K. M. Lee, C. K. Li, J. S. Y. Lau, D. C. M. Ng, *Coord. Chem. Rev.* **2006**, *250,* 1724–1736.
[101] A. Vlcek Jr, S. Zális, *Coord. Chem. Rev.* **2007**, *251,* 258–287.
[102] C. Kaes, A. Katz, M. W. Hosseini, *Chem. Rev.* **2000**, *100,* 3553–3590.
[103] H. Yersin, *Highly Efficient OLEDs with Phosphorescent Materials,* Wiley-VCH, Weinheim, **2008**.
[104] Y. You, S. Y. Park, *J. Am. Chem. Soc.* **2005**, *127,* 12438–12439.
[105] A. Tsuboyama, H. Iwawaki, M. Furugori, T. Mukaide, J. Kamatani, S. Igawa, T. Moriyama, S. Miura, T. Takiguchi, S. Okada, M. Hoshino, K. Ueno, *J. Am. Chem. Soc.* **2003**, *125,* 12971–12979.
[106] S. Y. Takizawa, J. I. Nishida, T. Tsuzuki, S. Tokito, Y. Yamashita, *Inorg. Chem.* **2007**, *46,* 4308–4319.
[107] Q. Zhao, C. Y. Jiang, M. Shi, F. Y. Li, T. Yi, Y. Cao, C. H. Huang, *Organometallics* **2006**, *25,* 3631–3638.
[108] X. Li, Z. Chen, Q. Zhao, L. Shen, F. Li, T. Yi, Y. Cao, C. Huang, *Inorg. Chem.* **2007**, *46,* 5518–5527.

[109] R. Gao, D. G. Ho, B. Hernandez, M. Selke, D. Murphy, P. I. Djurovich, M. E. Thompson, *J. Am. Chem. Soc.* **2002**, *124,* 14828–14829.
[110] M. L. Ho, F. M. Hwang, P. N. Chen, Y. H. Hu, Y. M. Cheng, K. S. Chen, G. H. Lee, Y. Chi, P. T. Chou, *Org. Biomol. Chem.* **2006**, *4,* 98–103.
[111] Q. Zhao, T. Cao, F. Li, X. Li, H. Jing, T. Yi, C. Huang, *Organometallics* **2007**, *26,* 2077–2081.
[112] Q. Zhao, S. Liu, M. Shi, F. Li, H. Jing, T. Yi, C. Huang, *Organometallics* **2007**, *26,* 5922–5930.
[113] H. Chen, Q. Zhao, Y. Wu, F. Li, H. Yang, T. Yi, C. Huang, *Inorg. Chem.* **2007**, *46,* 11075–11081.
[114] Q. Zhao, F. Li, S. Liu, M. Yu, Z. Liu, T. Yi, C. Huang, *Inorg. Chem.* **2008**, *47,* 9256–9264.
[115] Q. Zhao, S. Liu, F. Li, T. Yi, C. Huang, *Dalton Trans.* **2008**, 3836–3840.
[116] E. Holder, B. M. W. Langeveld, U. S. Schubert, *Adv. Mater.* **2005**, *17,* 1109–1121.
[117] H. J. Bolink, E. Coronado, S. Garcia Santamaria, M. Sessolo, N. Evans, C. Klein, E. Baranoff, K. Kalyanasundaram, M. Graetzel, M. K. Nazeeruddin, *Chem. Commun.* **2007**, 3276–3278.
[118] M. A. Baldo, D. F. O' Brien, Y. You, A. Shoustikov, S. Sibley, M. E. Thompson, S. R. Forrest, *Nature* **1998**, *395,* 151–154.
[119] H. J. Bolink, L. Cappelli, E. Coronado, M. Grätzel, E. Ortí, R. D. Costa, P. M. Viruela, M. K. Nazeeruddin, *J. Am. Chem. Soc.* **2006**, *128,* 14786–14787.
[120] K. K. W. Lo, S. P. Y. Li, K. Y. Zhang, *New J. Chem.* **2011**, *35,* 265–287.
[121] K. K. W. Lo, K. Y. Zhang, C. K. Chung, K. Y. Kwok, *Chem. Eur. J.* **2007**, *13,* 7110–7120.
[122] A. Waggoner, *Curr. Opin. Chem. Biol.* **2006**, *10,* 62–66.
[123] S. Jakobs, *Biochim. Biophys. Acta* **2006**, *1763,* 561–575.
[124] I. Chen, A. Y. Ting, *Curr. Opin. Biotechnol.* **2005**, *16,* 35–40.
[125] A. M. Pickering, K. J. A. Davies, *Free Radical Bio. Med.* **2012**, *52,* 239–246.
[126] H. Moshiri, R. Salavati, *Nucleic Acids Res.* **2010**, *38,* e138.
[127]. A. C. Tome, *Science of Synthesis: Houben-Weyl Methods of Molecular Transformations,* (Eds.: R. C. Storr, T. L. Gilchrist), Thieme, Stuttgart, **2004**, pp. 415–601.
[128] S. Bakbak, P. J. Leech, B. E. Carson, S. Saxena, W. P. King, U. H. F. Bunz, *Macromolecules* **2006**, *39,* 6793–6795.
[129] M. Obata, A. Kitamura, A. Mori, C. Kameyama, J. A. Czaplewska, R. Tanaka, I. Kinoshita, T. Kusumoto, H. Hashimoto, M. Harada, Y. Mikata, T. Funabiki, S. Yano, *Dalton Trans.* **2008**, 3292–3300.
[130] P. D. Zoon, I. H. M. van Stokkum, M. Parent, O. Mongin, M. Blanchard-Desce, A. M. Brouwer, *Phys. Chem. Chem. Phys.* **2010**, *12,* 2706–2715.
[131] D. J. V. C. van Steenis, O. R. P. David, G. P. F. van Strijdonck, J. H. van Maarseveen, J. N. H. Reek, *Chem. Commun.* **2005**, 4333–4335.
[132] M. Parent, O. Mongin, K. Kamada, C. Katan, M. Blanchard-Desce, *Chem. Commun.* **2005**, 2029–2031.
[133] T. L. Mindt, H. Struthers, L. Brans, T. Anguelov, C. Schweinsberg, V. Maes, D. Tourwé, R. Schibli, *J. Am. Chem. Soc.* **2006**, *128,* 15096–15097.
[134] Y. H. Lau, P. J. Rutledge, M. Watkinson, M. H. Todd, *Chem. Soc. Rev.* **2011**, *40,* 2848–2866.
[135] Y. Hua, A. H. Flood, *Chem. Soc. Rev.* **2010**, *39,* 1262–1271.
[136] A. Michael, *J. Prakt. Chem.* **1893**, *48,* 94–95.
[137] R. Huisgen, G. Szeimies, L. Möbius, *Eur. J. Inorg. Chem.* **1967**, *100,* 2494–2507.
[138] R. Huisgen, *Angew. Chem. Int. Ed.* **1963**, *2,* 565–598.
[139] R. Huisgen, *Angew. Chem. Int. Ed.* **1963**, *2,* 633–645.
[140] V. V. Rostovtsev, L. G. Green, V. V. Fokin, K. B. Sharpless, *Angew. Chem. Int. Ed.* **2002**, *41,* 2596–2599.
[141] C. W. Tornøe, C. Christensen, M. Meldal, *J. Org. Chem.* **2002**, *67,* 3057–3064.
[142] V. D. Bock, H. Hiemstra, J. H. van Maarseveen, *Eur. J. Org. Chem.* **2006**, 51–68.
[143] P. Wu, V. V. Fokin, *Aldrichim. Acta* **2007**, *40,* 7–17.

[144] W. H. Binder, R. Sachsenhofer, *Macromol. Rapid Commun.* **2007**, *28,* 15–54.
[145] J. F. Lutz, *Angew. Chem. Int. Ed.* **2007**, *46,* 1018–1025.
[146] H. C. Kolb, K. B. Sharpless, *Drug Discovery Today* **2003**, *8,* 1128–1137.
[147] R. Breinbauer, M. Köhn, *ChemBioChem* **2003**, *4,* 1147–1149.
[148] E. D. Goddard-Borger, R. V. Stick, *Org. Lett.* **2007**, *9,* 3797–3800.
[149] A. J. Dirks, J. J. L. M. Cornelissen, F. L. van Delft, J. C. M. van Hest, R. J. M. Nolte, A. E. Rowan, F. P. J. T. Rutjes, *QSAR Comb. Sci.* **2007**, *26,* 1200–1210.
[150] B. M. J. M. Suijkerbuijk, B. N. H. Aerts, H. P. Dijkstra, M. Lutz, A. L. Spek, G. van Koten, R. J. M. Klein Gebbink, *Dalton Trans.* **2007**, 1273–1276.
[151] Y. Li, J. C. Huffman, A. H. Flood, *Chem. Commun.* **2007**, 2692–2694.
[152] T. R. Chan, R. Hilgraf, K. B. Sharpless, V. V. Fokin, *Org. Lett.* **2004**, *6,* 2853–2855.
[153] Q. Dai, W. Gao, D. Liu, L. M. Kapes, X. Zhang, *J. Org. Chem.* **2006**, *71,* 3928–3934.
[154]. D. S. Moore, S. D. Robinson, A. G. Sykes, Catenated Nitrogen Ligands Part II. Transition Metal Derivatives of Triazoles, Tetrazoles, Pentazoles, and Hexazine, in *Advances in Inorganic Chemistry,* Elsevier, Amsterdam, **1988**, pp. 171–239.
[155] *Transition-metal complexes with only one type of ligand are said to be homoleptic.*
[156] *Transition-metal complexes with more than one type of ligand are said to be heteroleptic.*
[157] B. Schulze, C. Friebe, M. D. Hager, A. Winter, R. Hoogenboom, H. Görls, U. S. Schubert, *Dalton Trans.* **2009**, 787–794.
[158] D. Schweinfurth, K. I. Hardcastle, U. H. F. Bunz, *Chem. Commun.* **2008**, 2203–2205.
[159] O. David, S. Maisonneuve, J. Xie, *Tetrahedron Lett.* **2007**, *48,* 6527–6530.
[160] B. Happ, C. Friebe, A. Winter, M. D. Hager, R. Hoogenboom, U. S. Schubert, *Chem. Asian J.* **2009**, *4,* 154–163.
[161] B. Beyer, C. Ulbricht, D. Escudero, C. Friebe, A. Winter, L. Gonzalez, U. S. Schubert, *Organometallics* **2009**, *28,* 5478–5488.
[162] M. Felici, P. Contreras-Carballada, J. M. M. Smits, R. J. M. Nolte, R. M. Williams, L. De Cola, M. C. Feiters, *Molecules* **2010**, *15,* 2039–2059.

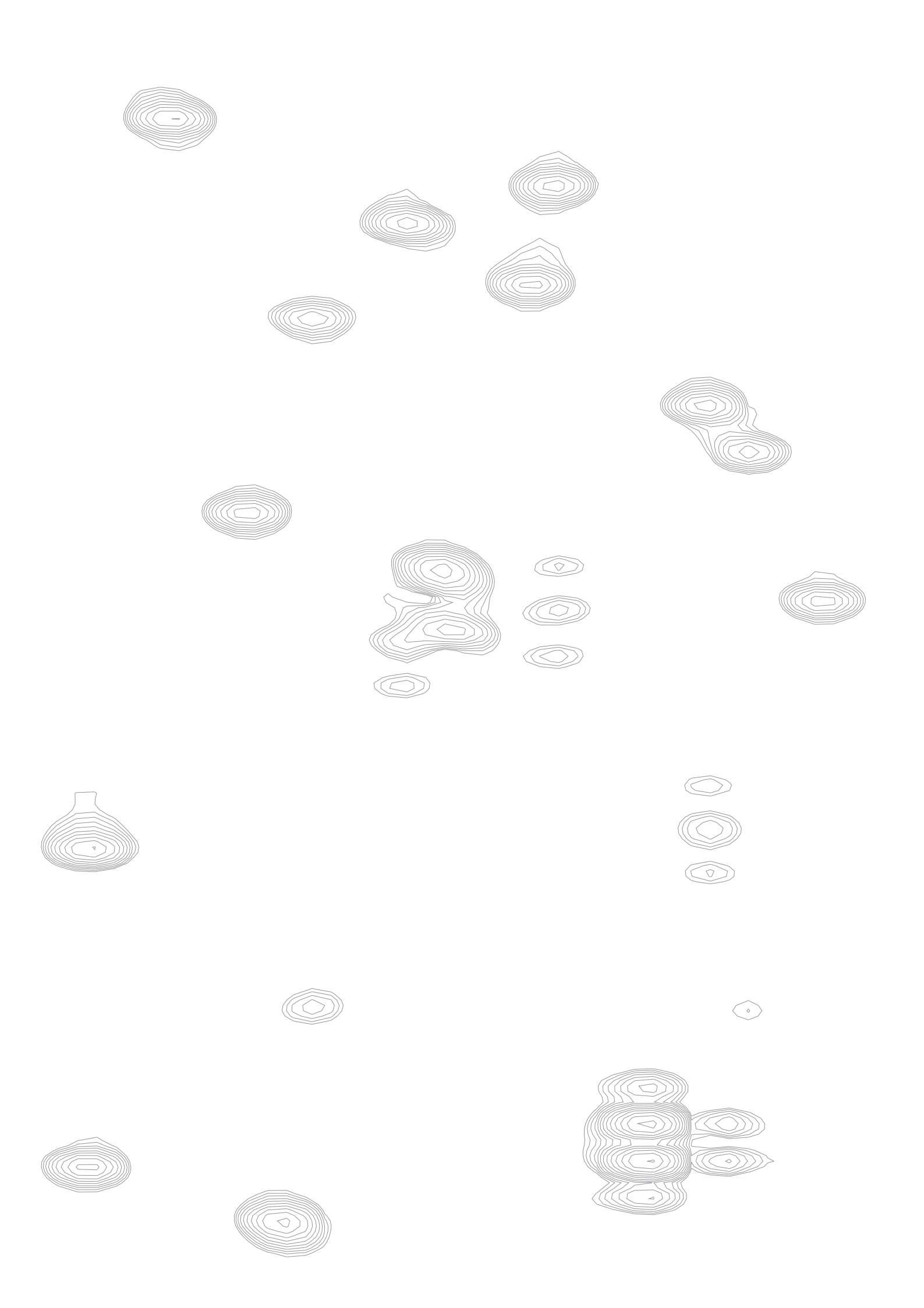

2

Ir^{III} and Ru^{II} Complexes Containing Triazole-Pyridine Ligands. Luminescence Enhancement upon Substitution with β-Cyclodextrin

Abstract

Novel 2-(1-substituted-1*H*-1,2,3-triazol-4-yl)pyridine (pytl) ligands have been prepared by "click" chemistry and used in the preparation of heteroleptic complexes of Ru and Ir with 2,2'-bipyridine (bpy) and 2-phenylpyridine (ppy) ligands, respectively, resulting in $[Ru(bpy)_2(pytl\text{-}R)]Cl_2$ and $[Ir(ppy)_2(pytl\text{-}R)]Cl$ (R = methyl, adamantyl, permethylated β-cyclodextrin (βCD)). The two diastereoisomers of the Ir complex with the appended βCD, $[Ir(ppy)_2(pytl\text{-}\beta CD)]Cl$, were separated. The $[Ru(bpy)_2(pytl\text{-}R)]Cl_2$ (R = methyl, adamantyl, or βCD) complexes have lower lifetimes and quantum yields than other polypyridine complexes. In contrast, the cyclometalated Ir complexes display rather long lifetimes and very high emission quantum yields. The emission quantum yield and lifetime (Φ = 0.23, τ = 1000 ns) of $[Ir(ppy)_2(pytl\text{-}ada)]Cl$ are surprisingly enhanced in $[Ir(ppy)_2(pytl\text{-}\beta CD)]Cl$ (Φ = 0.54, τ = 2800 ns). This behaviour is unprecedented for a metal complex and is most likely due to a number of factors, including (i) the increased rigidity of the complex, (ii) the protection from quenching by water molecules, and (iii) protection from dioxygen quenching, all being the result of the presence of the hydrophobic cavity of the βCD, which is covalently attached to pytl. The emissive excited state of the complex is localised on the cyclometalating ligands, as can be concluded from the blueshift (450 nm) of the emission, which takes place if two electron-withdrawing fluorine substituents are placed on the phenyl unit. The observed significant differences of the quantum yields of the two separate diastereoisomers of $[Ir(ppy)_2(pytl\text{-}\beta CD)]Cl$ (0.49 vs. 0.70) are attributed to different interactions of the chiral cyclodextrin substituent with the Δ and Λ isomers of the metal complex.

This work has been published as: M. Felici, P. Contreras-Carballada, Y. Vida, J. M. M. Smits, R. J. M. Nolte, L. De Cola, R. M. Williams, M. C. Feiters, Chem. Eur. J. ***2009****, 15, 13124–13134.*

2.1 Introduction

The copper(I)-catalysed dipolar [3+2] cycloaddition, better known as "click" reaction,[1] involves the formation of 1,2,3-triazole rings by coupling terminal alkynes and azides. It can be used to synthesise new bidentate ligands such as 2-(1-substituted-1*H*-1,2,3-triazol-4-yl) pyridine (pytl; Scheme 2.1).[2–4] Click chemistry is extremely flexible; it allows in principle for the transformation of any azide-appended compound into a triazole-pyridine ligand, as has been shown for 4-butoxyphenylazide[5] as well as for relatively small[6] and large carbohydrates, such as cyclodextrins.[7]

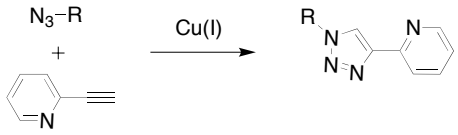

Scheme 2.1 *Preparation of pytl by the Cu-catalysed Huisgen dipolar [3+2] cycloaddition.*

Cyclodextrins are well-known cyclic oligosaccharides that can form inclusion complexes in aqueous solution with a variety of hydrophobic substrates, such as adamantane derivatives. They have been widely applied as supramolecular building blocks in various areas,[8–13] including photo-activated electron transfer processes.[14–19] By applying click chemistry to 2-ethynylpyridine and permethylated β-cyclodextrin (βCD) mono-azido derivative the cyclodextrin-appended triazole-pyridine (pytl-βCD; Scheme 2.2) could be readily prepared[20,21] and complexed with metal ions. Complexes of Ru[22–27] and especially of Ir[28–35] have received increasing attention in recent years because of their promising photophysical properties; they have been reported to be efficient photosensitisers, and were applied in the manufacture of optical devices (both in solution and in the solid state), and as components for organic light-emitting diodes (OLEDs). Because of our interest in such properties,[14–17] we prepared and characterised a series of heteroleptic[36] octahedral ruthenium and iridium complexes containing one substituted pytl ligand. In this chapter we report the synthesis and the photophysical properties of such complexes of pytl-βCD with Ru^{II} and Ir^{III} (Scheme 2.2), in which the coordination sphere is completed by 2,2'-bipyridine (bpy) for Ru^{II} and 2-phenylpyridine (ppy) for Ir^{III}, giving the complexes $[Ru(bpy)_2(pytl\text{-}\beta CD)]Cl_2$ and $[Ir(ppy)_2(pytl\text{-}\beta CD)]Cl$, respectively.

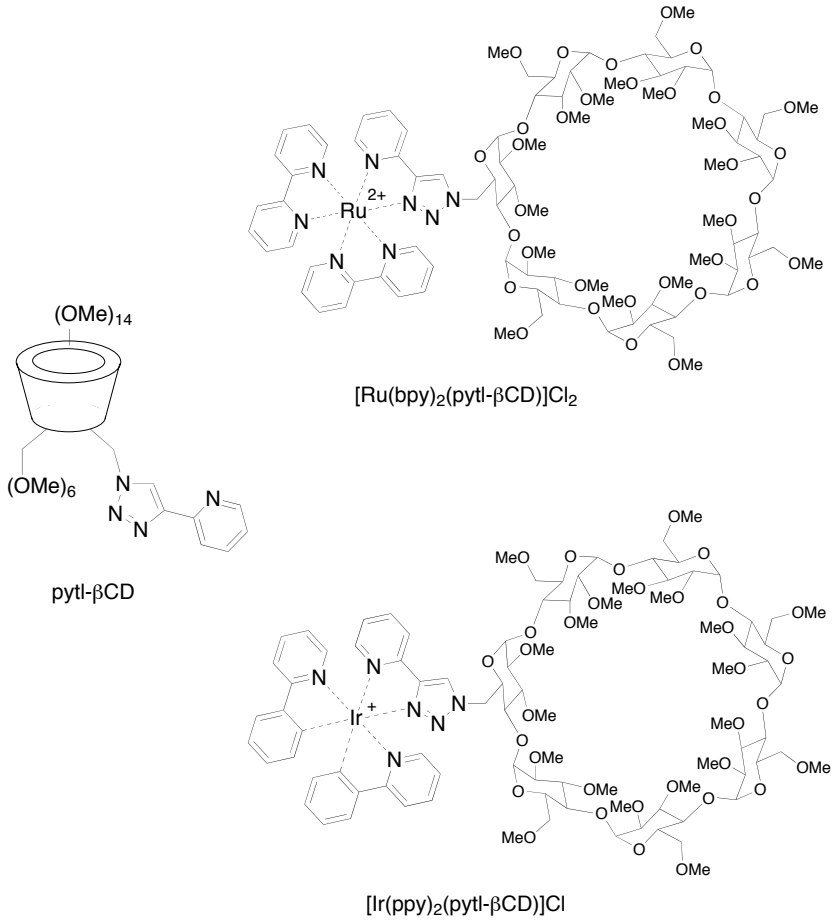

Scheme 2.2 *Structures of pytl-βCD and its heteroleptic complexes with Ir and Ru.*

By applying click chemistry to azide-appended adamantane and 2-ethynylpyridine, we also prepared 2-(1-adamantyl-1*H*-1,2,3-triazol-4-yl)pyridine (pytl-ada) and its Ru and Ir complexes $[Ru(bpy)_2(pytl\text{-}ada)]Cl_2$ and $[Ir(ppy)_2(pytl\text{-}ada)]Cl$ (Scheme 2.3). Furthermore, starting from methyl azide, 2-(1-methyl-1*H*-1,2,3-triazol-4-yl)pyridine (pytl-Me) was prepared, together with its Ru complex $[Ru(bpy)_2(pytl\text{-}Me)]Cl_2$ (Scheme 2.3).

Several approaches to tuning the emission energy of cyclometalated Ir complexes have focused on decreasing the highest occupied molecular orbital (HOMO) energy while keeping the lowest unoccupied molecular orbital (LUMO) energy relatively unchanged. The addition of electron-withdrawing groups to the phenyl ring, the most common one being fluorine,[35,37] has been used as one way to achieve this goal. For this reason, we prepared complexes of pytl-ada in which the coordination sphere of Ir was completed with either ppy or its fluorinated analogue 2-(2,4-bisfluorophenyl)-pyridine (F_2ppy). Some examples of ruthenium complexes containing 1,2,3-triazole ligands have been reported in the literature.[38–41]

Ru complexes in which the coordination sphere is occupied by one or three pytl ligands have been described but emission properties were not given.[38,39]

Analogues of ruthenium bisterpyridine in which each terpyridine ligand is substituted by a 2,6-bis(1-methyl-1*H*-1,2,3-triazol-4-yl)pyridine ligand (tripy; Scheme 1.5) have also been mentioned.[40,41] The preparation of Ir complexes containing pytl ligands has been published recently.[42] However, these ligands differ from ours because they do not have a substituent on the nitrogen atom in position 1, they are negatively charged, and the corresponding iridium complexes are neutral. The functionalisation of Ir complexes with βCD has never been described. An obvious advantage of the mono-functionalisation of βCD with pytl over the previously described functionalisation of all primary hydroxyls of this compound[7] is that it enables studies on a single metal ion bound to a cyclodextrin molecule. On the other hand, mono-functionalisation is responsible for the loss of symmetry in the cyclodextrin moiety, thus leading to rather complex NMR spectra. For this reason, high-resolution NMR spectroscopy techniques were applied for the characterisation of these derivatives (see Chapter 3).

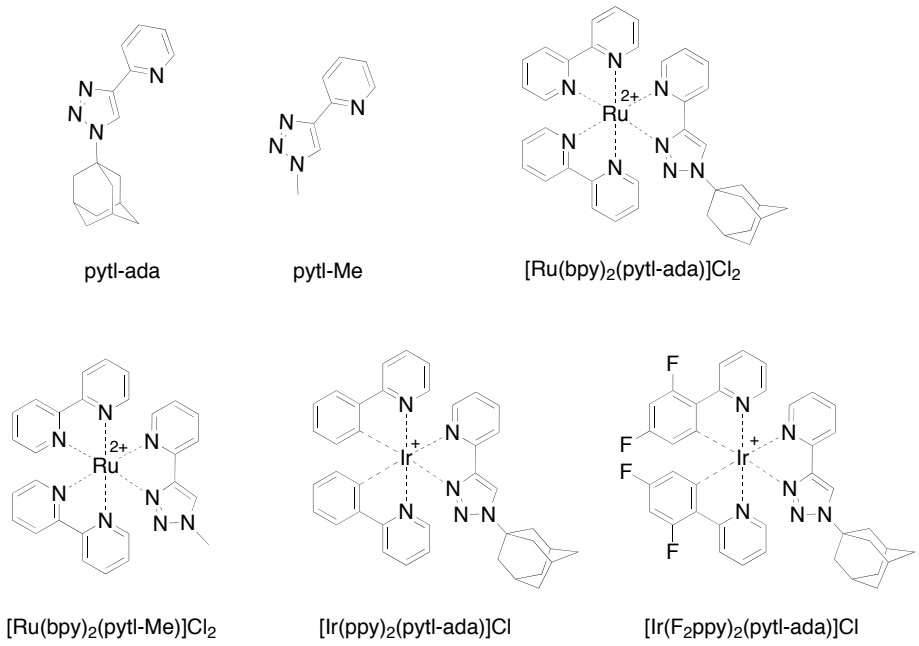

Scheme 2.3 *Structures of pytl-ada, pytl-Me, and their heteroleptic complexes with Ru and Ir.*

In this chapter we show that the cyclometalated Ir complexes [Ir(ppy)$_2$(pytl-R)]Cl (R = adamantyl, βCD) containing 1-substituted pytl ligands display blue-greenish emission accompanied by the characteristic long triplet lifetimes and surprisingly high emission quantum yields, especially for the βCD derivative, [Ir(ppy)$_2$(pytl-βCD)]Cl. By high-

performance liquid chromatography (HPLC) separation, NMR spectroscopy, circular dichroism, and X-ray crystallographic studies we established that the complex $[Ir(ppy)_2(pytl\text{-}\beta CD)]Cl$ exists in two diastereoisomeric forms. These diastereoisomers display an unexpectedly large difference in their emission quantum yields, which is remarkable considering the fact that the metal centres are in an enantiomeric relationship. To our knowledge such behaviour has not been reported before for metal complexes; it is due to a non-covalent interaction of the Ir complex with the covalently attached βCD, which acts as a chiral second-sphere ligand.

2.2 Results and discussion

2.2.1 Synthesis of pytl ligands and their Ru and Ir complexes

The established high efficiency and versatility of the click reaction[1] allowed us to prepare a small library of differently functionalised ligands (Schemes 2.2 and 2.3). Three different compounds all containing an azide were simply reacted with 2-ethynylpyridine under click conditions. In the case of the mono-functionalised β-cyclodextrin it was decided to methylate the 20 remaining hydroxyl groups, which made the compound soluble in a wider range of solvents[43] and easier to purify by chromatography.[43] Moreover, by methylation the hydrophobic cavity is extended: the βCD cavity has the same diameter as the cavity of a native cyclodextrin but its depth is increased by about 1.5 Å.[44]

The preparation of pytl-βCD from native β-cyclodextrin **1** (Scheme 2.4) proceeded through the mono-tosyl derivative **2**, the mono-azido derivative **3**, and the permethylated mono-azido β-cyclodextrin **4**, as described elsewhere.[21,45,46] Compound **4** was subsequently reacted with 2-ethynylpyridine (**5**) in deoxygenated THF, in the presence of CuBr and *N*,*N*,*N*′,*N*′,*N*-penta-methyldiethylenetriamine (PMDTA). This reaction was extremely selective and efficient, leading to the desired pytl-βCD in 93% yield without any side products. The novel ligands pytl-ada and pytl-Me were prepared analogously, by reaction of **5** with 1-azidoadamantane and methyl azide, respectively. The complex $[Ru(bpy)_2(pytl\text{-}\beta CD)]Cl_2$ was synthesised by reacting pytl-βCD with the commercially available *cis*-$[Ru(bpy)_2]Cl_2$ for 24 h (Scheme 2.4) to give, after purification by HPLC, an orange solid in 88% yield, which was found to be to the desired complex. The complexes $[Ru(bpy)_2(pytl\text{-}R)]Cl_2$ (R = adamantyl, methyl) were prepared by following an analogous synthetic path.

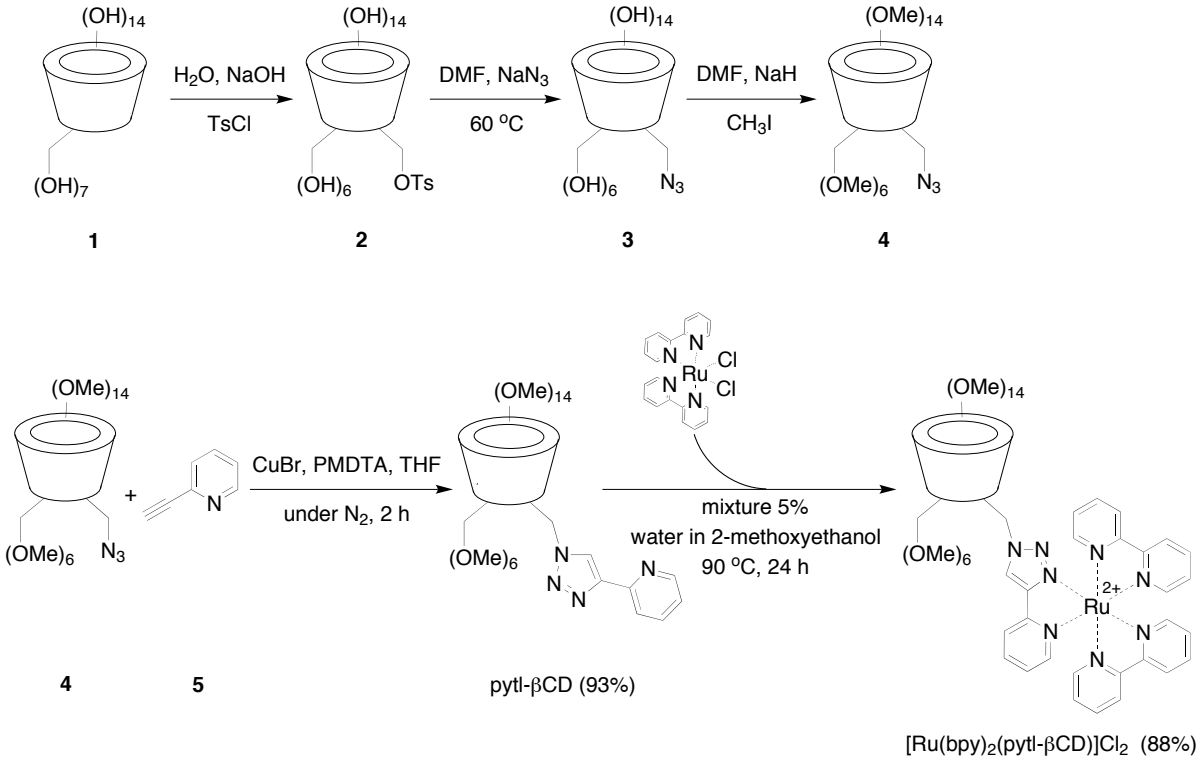

Scheme 2.4 *Synthesis of* ***4****, pytl-βCD, and [Ru(bpy)₂(pytl-βCD)]Cl₂.*

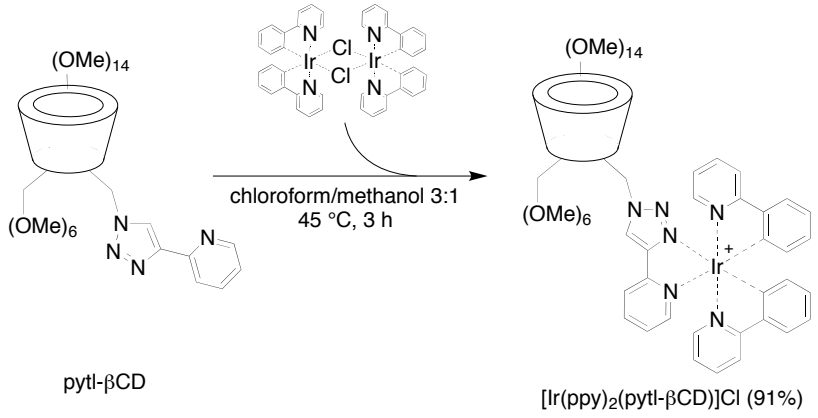

Scheme 2.5 *Synthesis of [Ir(ppy)₂(pytl-βCD)]Cl.*

The compounds [Ir(ppy)₂(pytl-R)]Cl (R = adamantyl, βCD) and [Ir(F₂ppy)₂(pytl-ada)]Cl were synthesised easily by replacing the bridging chlorides in the iridium(III) chloride-bridged complex [(ppy)₂Ir(μ-Cl)₂Ir(ppy)₂] with the appropriate bidentate pytl ligands. The pytl-βCD ligand reacted with the dinuclear species under quite mild conditions, in chloroform/methanol 3/1 (v/v) at 45 °C (Scheme 2.5). After 3 h the formation of only one new spot was observed by thin-layer chromatography (TLC), characterised (in contrast to the starting pytl-βCD) by an extremely bright green luminescence under a UV-vis lamp at

366 nm. $[Ir(ppy)_2(pytl\text{-}ada)]Cl$ and $[Ir(F_2ppy)_2(pytl\text{-}ada)]Cl$ were prepared analogously. In all cases, the purification was performed by silica gel chromatography or by HPLC using a preparative reversed-phase column (see Section 2.5) to give yellow solids in high yields (91–95%).

The structures of the ligands pytl-ada, pytl-Me, and of the Ir complex $[Ir(ppy)_2(pytl\text{-}ada)]Cl$ were determined by crystallography. Crystallographic details are given in Table 2.3, and the structures in the experimental part (Figures 2.6–2.8).[4] The packing of the molecules of the enantiomers of $[Ir(ppy)_2(pytl\text{-}ada)]Cl$ is discussed in the section describing the structural characterisation of $[Ir(ppy)_2(pytl\text{-}\beta CD)]Cl$ (Section 2.2.4).

2.2.2 Absorption and emission of the Ru and Ir complexes

The photophysical properties of the iridium and ruthenium pytl complexes were determined by steady-state and time-resolved spectroscopic methods. The absorption spectra of all Ru and Ir complexes in water at room temperature (Figure 2.1) showed intense bands in the UV region (290 nm) and moderately intense bands in the visible region (350–500 nm) which are typical for ruthenium and iridium polypyridyl complexes. All bands can be assigned by comparing the absorption spectra of the ruthenium complexes (Figure 2.1, left) with the spectrum of $[Ru(bpy)_3]^{2+}$.[27] The bands at wavelength shorter than 300 nm belong to the allowed π–π* transitions of the coordinated ligands and in particular to the bpy units, and the shoulder that appears at 280 nm is due to the substitution of one of the pyridine rings by the triazole ring.

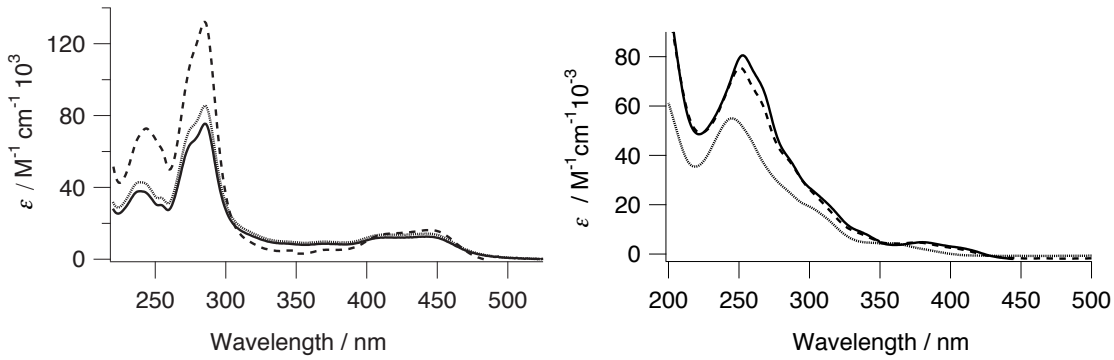

Figure 2.1 *UV-vis absorption spectra in water of the Ru complexes (left; solid line, $[Ru(bpy)_2(pytl\text{-}\beta CD)]Cl_2$; dotted line, $[Ru(bpy)_2(pytl\text{-}ada)]Cl_2$; dashed line, $[Ru(bpy)_2(pytl\text{-}Me)]Cl_2$) and of the Ir complexes (right; solid line, $[Ir(ppy)_2(pytl\text{-}ada)]Cl$; dashed line, $[Ir(ppy)_2(pytl\text{-}\beta CD)]Cl$; dotted line, $[Ir(F_2ppy)_2(pytl\text{-}ada)]Cl$) in water.*

All complexes displayed the typical singlet metal-to-ligand charge-transfer (^{1}MLCT) band between 400 and 500 nm; whereas $[Ru(bpy)_3]^{2+}$ shows a clear band with a maximum at 452 nm, in our complexes the presence of different ligands with similar properties leads to a set of MLCT bands due to the transitions from the metal to the bpys ligands or to the pytl ligand. In the case of the iridium complexes (Figure 2.1, right) the absorption spectra resembled those of triazole Ir complexes.[42,47] The bands in the 250–300 nm region again belong to the allowed intraligand π–π* transitions of the ppy units and pytl. The absorption spectra show ^{1}MLCT transitions at energies lower than the ligand π–π* transitions, in the 300–350 nm region, partially overlapping with the spin forbidden ^{3}MLCT transitions, which extend to 400 nm.[35,48]

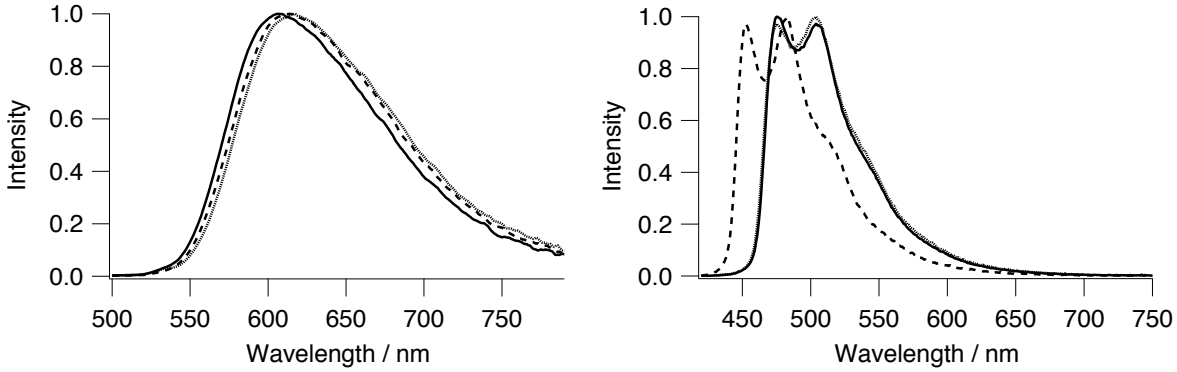

Figure 2.2 *Room-temperature emission spectra in water of the Ru complexes (left; λ_{exc} = 445 nm; solid line, [Ru(bpy)$_2$(pytl-βCD)]Cl$_2$; dotted line, [Ru(bpy)$_2$(pytl-ada)]Cl$_2$; dashed line, [Ru(bpy)$_2$(pytl-Me)]Cl$_2$) and of the Ir complexes (right; λ_{exc} = 380 nm; solid line, [Ir(ppy)$_2$ (pytl-βCD)]Cl; dotted line, [Ir(ppy)$_2$(pytl-ada)]Cl; dashed line, [Ir(F$_2$ppy)$_2$(pytl-ada)]Cl).*

The luminescence spectra of the ruthenium complexes (Figure 2.2, left) showed a broad band centred around 610 nm, which is typical for a radiative decay from a ^{3}MLCT state. In the case of the iridium complexes (Figure 2.2, right) which contain the ppy ligands and the substituted pytl we observed bands with a resolved vibronic fine structure, as expected for this type of complexes. For Ir the lowest excited state is also a ^{3}MLCT state, but for such high-energy emitting complexes a certain degree of mixing with the triplet ligand-centred (^{3}LC) state is present. Fluorination of the phenyl rings on the ppy ligands lowers the energy of the HOMO orbital in the molecules. The lowering of the LUMO energy is significantly less than for the HOMO, resulting in a widening of the HOMO–LUMO gap, leading to an increase in excited state energy. This is translated into a blueshift in the emission on going from the green emitters (non-fluorinated) to the blue emitters (fluorinated complexes) (Figure 2.2, right).

In the homoleptic[49] complex $[Ir(ppy)_3]$ and its fluorinated homologue $[Ir(F_2ppy)_3]$ a blueshift of 39 nm occurs in the emission spectrum.[50] The quantum yields of emission as well as the emission lifetimes for both the Ru and Ir complexes were determined in aqueous solutions under air-equilibrated and in argon-saturated conditions (Table 2.1). The pytl ligand appeared to influence the excited states of the ruthenium and iridium complexes in different ways.

Ruthenium complexes exhibit rather short lifetimes and low quantum yields[51] and their photophysical properties are therefore unaffected by the presence of dioxygen (Table 2.1).

Table 2.1 *Luminescence lifetimes and emission quantum yields of the Ru and Ir complexes.*

Complex	λ_{em} (nm)[a]	Φ(air)[a, c]	Φ(Ar)[a, d]	τ (ns, air)[b, c]	τ (ns, Ar)[b, d]	τ (ns, 77 K)[e]
$[Ru(bpy)_2(pytl\text{-}\beta CD)]Cl_2$	610	0.0054	0.0056	24.0	24.8	6300
$[Ru(bpy)_2(pytl\text{-}ada)]Cl_2$	615	0.0047	0.0048	19.1	19.6	6000
$[Ru(bpy)_2(pytl\text{-}Me)]Cl_2$	615	0.0060	0.0062	26.3	27.4	6000
$[Ir(ppy)_2(pytl\text{-}\beta CD)]Cl$	475	0.14	0.54	690	2800	5300
$[Ir(ppy)_2(pytl\text{-}ada)]Cl$	475	0.076	0.23	435	1000	5200
$[Ir(F_2ppy)_2(pytl\text{-}ada)]Cl$	450	0.071	0.16	480	1100	6000

a, ruthenium was excited at 448 nm and iridium at 402 nm; b, ruthenium was excited at 420 nm and iridium at 380 nm; c, the solutions were measured in air-equilibrated water (air); d, the solutions were measured in argon-saturated water which were prepared by bubbling argon through them for 20–30 min (Ar); e, the glassy EtOH/ MeOH (1/1, v/v) matrix samples were excited at 435 nm.

Their lowest excited states most likely involve the bpy ligands because the LUMO of the triazole is more electron-rich and therefore higher in energy than these of the pyridines. In the ruthenium complexes containing 1,2,4-triazole-pyridine ligands, the lowest energy excited electronic states are predominantly bpy-based.[51–55] We believe that in our case we are observing the same trend, but that this trend is affected by the nitrogen substitution of the triazole, which renders the substituted triazole a worse σ donor than the 1,2,4-unsubstituted triazole. As a consequence, we would expect a smaller ligand field for pytl, resulting in a lowering of the triplet metal-centred states (^{3}MC), which are known to be thermally populated and efficient non-radiative channels for the depopulation of the luminescent ^{3}MLCT state.[56]

A different situation is observed for the compounds that display excited state lifetimes in the microsecond range typical of cyclometalated iridium complexes;[30,33] they all decay with mono-exponential kinetics. They also show high emission quantum yields. Due to the long lifetime of their excited states, which is related to the triplet character of the emission, they are very sensitive to dioxygen, which can therefore quench their luminescent excited states. In general, the emission energies of luminescent cyclometalated iridium complexes are strongly

influenced by the triplet energy of the ligand.[57,58] Their HOMO's are principally composed of p orbitals of the phenyl ring and metal d orbitals of the Ir. The pyridine group on the other hand is more electronegative and therefore responsible for the LUMO. In many cases and in particular for blue emitters, the lowest excited state of the complex is best described as an admixture of ^{3}LC and ^{3}MLCT states.[50,59–61]

Very interestingly, the presence of a βCD group greatly alters the photophysical behaviour when compared to an adamantyl group. Even though the emission maximum is unchanged, indicating the same nature and involvement of coordinated ligands, the emission quantum yields, for both air-equilibrated and argon-saturated water solutions, increase dramatically (Φ(air) = 0.14, Φ(Ar) = 0.54). The excited state lifetimes also change and in particular become longer (Table 2.1). Such an elongation of the air-equilibrated lifetime points to a shielding of the emitting core from dioxygen. This is perhaps caused by the βCD, which could interact with the ppy ligands (see Chapter 3), partially keeping the water and the oxygen away from the iridium core. Such effects on phosphorescent molecules incorporated inside cyclodextrins complexes have been observed previously.[11,18,19,62] The βCD has a very flexible structure when compared to the native β-cyclodextrin, due to the breaking of its internal hydrogen bonds. The primary side of the βCD cavity is very close to the metal centre and, because of its flexibility, could approach the complex, partially shielding the ligands involved in the lowest excited states, and reducing the non-radiative decay processes.

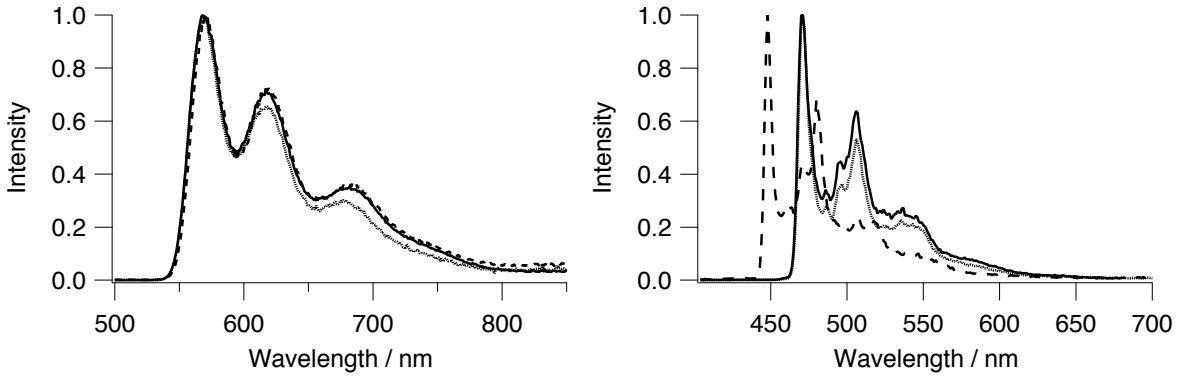

Figure 2.3 *77 K luminescence spectra of the ruthenium complexes (left; λ_{exc} = 445 nm; solid line, [Ru(bpy)$_2$(pytl-βCD)]Cl$_2$; dotted line, [Ru(bpy)$_2$(pytl-ada)]Cl$_2$; dashed line, [Ru(bpy)$_2$(pytl-Me)]Cl$_2$) and the iridium compounds (right; λ_{exc} = 380 nm; solid line, [Ir(ppy)$_2$(pytl-βCD)]Cl; dotted line, [Ir(ppy)$_2$(pytl-ada)]Cl; dashed line, [Ir(F$_2$ppy)$_2$(pytl-ada)]Cl) in a glassy EtOH/MeOH (1/1, v/v) matrix.*

2.2.3 Low temperature luminescence studies

Comparison of Figure 2.3, which shows the low temperature luminescence emission of the ruthenium and iridium complexes at 77 K in a EtOH/MeOH glassy matrix, with the spectra obtained at room temperature (Figure 2.2) reveals that the emission spectra become far more structured in the low temperature experiments. $[Ir(ppy)_2(pytl\text{-}\beta CD)]Cl$ and $[Ir(ppy)_2(pytl\text{-}ada)]Cl$ display spectra which almost overlap in peak position and relative peak intensities. As expected, the fluorinated complex $[Ir(F_2ppy)_2(pytl\text{-}ada)]Cl$ is different, showing a blueshift in the emission. All three emission spectra of the ruthenium compounds are clearly very similar with only a minor difference in the emission of $[Ru(bpy)_2(pytl\text{-}Me)]Cl_2$ in the higher wavelength region.

The vibronic structure of the iridium complexes corresponds to 1200 cm^{-1}, the ring-vibrations frequency of ppy, confirming the participation of the ligand in the emission process.[63]

For the ruthenium complexes the vibronic structure corresponds to 1400 and 1500 cm^{-1}, which are the ring-breathing frequencies of the bpy ligand, confirming the participation of this ligand in the excited-state luminescence emission of the complex as well.[64] This corroborates the assumption made above that the lowest emitting state involves the bpy ligands and that the triazole has little or no influence on the energy of the emissive state. The emission maximum is blueshifted (relative to room temperature), as expected for charge-transfer states and already observed for bpy complexes.[27]

2.2.4 Structural characterisation of $[Ir(ppy)_2(pytl\text{-}\beta CD)]Cl$ diastereoisomers

The iridium complexes $[Ir(ppy)_2(L)Cl]$ (L = ligand) are always prepared by reacting an ancillary ligand with the Ir^{III} chloride-bridged complex $[(ppy)_2Ir(\mu\text{-}Cl)_2Ir(ppy)_2]$ (*mer* configuration) in which the nitrogen atoms of the ppy ligands are always in a *trans* position with respect to the metal atom.[65] This fact limits the number of possible stereoisomers of the resulting complexes coordinating three bidentate ligands (two ppy, one pytl) to one pair of enantiomers. Our crystals of $[Ir(ppy)_2(pytl\text{-}ada)]Cl$ proved to be a racemic mixture (Figure 2.4), containing two pairs of enantiomers (Δ and Λ) in each unit cell (Z = 4).

The covalent functionalisation of a metal complex that exists in two enantiomeric forms with the chiral enantiopure βCD, composed of α-D-glucose building blocks, leads to the formation of diastereoisomeric species (Figure 2.5a,b). Since the geometry of metal

complexes can play an important role in photophysics, we investigated the effects of the existence of two diastereoisomers of [Ir(ppy)$_2$(pytl-βCD)]Cl in more detail.

The native β-cyclodextrin has a C_7 symmetry that is broken by the mono-functionalisation, and this fact is responsible for the high complexity of the carbohydrate region of the ^{1}H NMR spectra.

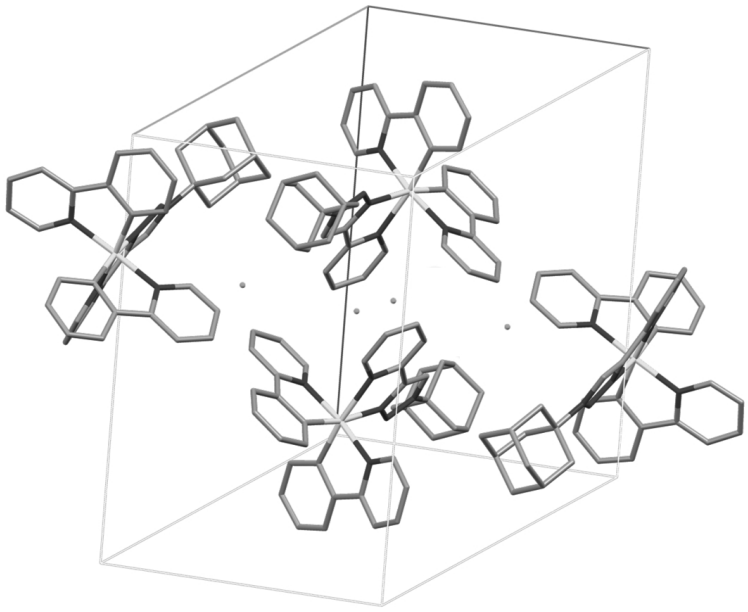

Figure 2.4 *Unit cell of [Ir(ppy)$_2$(pytl-ada)]Cl. The top and bottom structures toward the left are Δ; the top and bottom ones toward the right are Λ. Hydrogen atoms and solvent (water) molecules have been omitted for clarity.*

The situation becomes even more complex in the case of [Ir(ppy)$_2$(pytl-βCD)]Cl because two diastereoisomers are expected to display different NMR spectra. Indeed, the ^{1}H NMR spectrum of the mixture of [Ir(ppy)$_2$(pytl-βCD)]Cl (Figure 2.5d, top trace) suggests the presence of two different compounds in a 44:56 molar ratio. We found that these diastereoisomers can be separated on an achiral reversed-phase HPLC column with 0.1% (v/v) HCl or trifluoroacetic acid (TFA) in the mobile phase (Figure 2.5c); the ratio calculated from the peak areas corresponds to that derived from NMR. Under the same conditions in a semi-preparative HPLC column, the two isomeric compounds were isolated in milligram scale, fully characterised, and labelled [Ir(ppy)$_2$(pytl-βCD)]Cl (**A**) and (**B**) in order of elution.

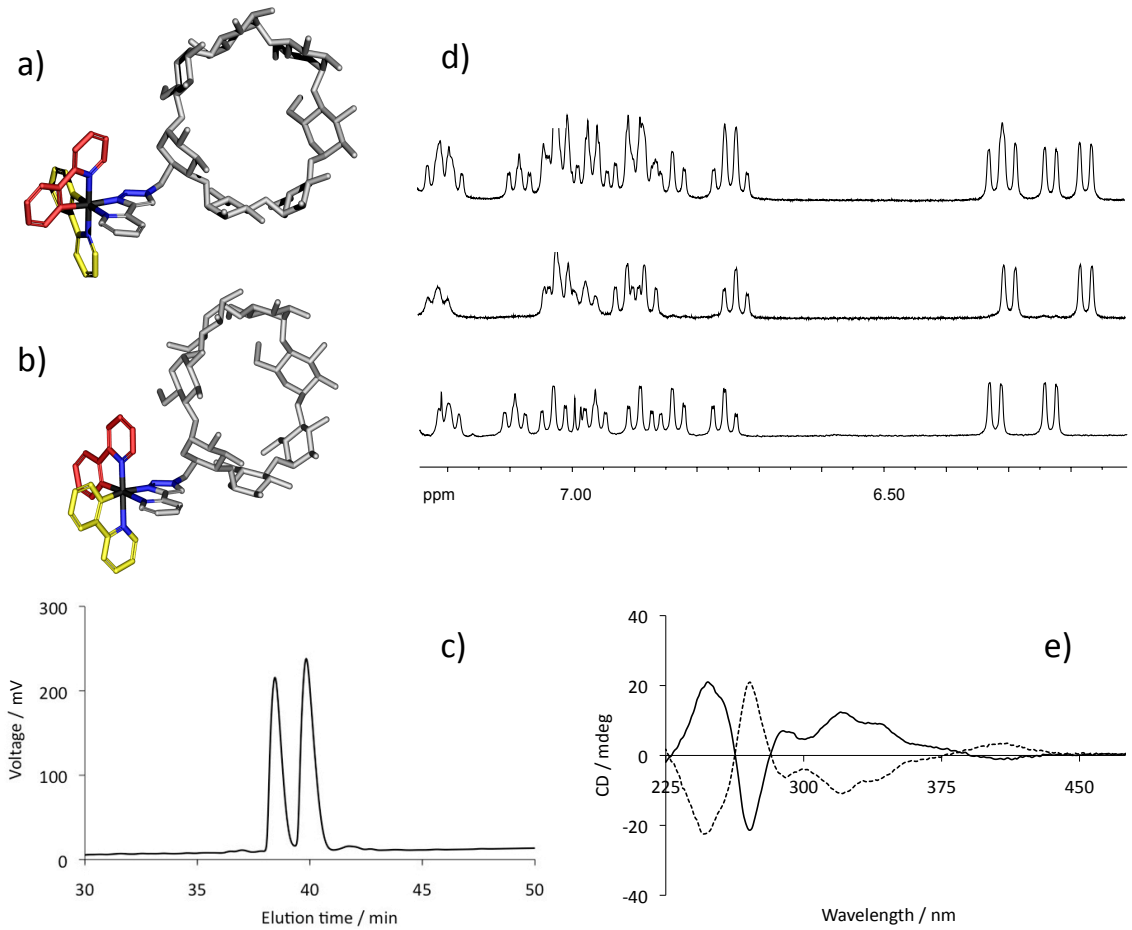

Figure 2.5 *a) Δ- and b) Λ- diastereoisomeric forms of [Ir(ppy)$_2$(pytl-βCD)]Cl; c) HPLC chromatogram: separation of the two Ir complexes was achieved by using a gradient of acetonitrile and water containing 0.1% v/v HCl; d) Part of the aromatic region of the ^{1}H NMR spectra of the mixture of diastereoisomers of [Ir(ppy)$_2$(pytl-βCD)]Cl (top trace), the 1st fraction corresponding to **A** (middle trace), and the 2nd fraction corresponding to **B** (bottom trace) (400 MHz, CDCl$_3$, 25 °C); e) Circular dichroism spectra in water of HPLC fractions: dashed line, 1st HPLC peak; solid line, 2nd HPLC peak.*

In the aromatic region of the ^{1}H NMR spectra in Figure 2.5d, the spectrum of the mixture of [Ir(ppy)$_2$(pytl-βCD)]Cl can be reproduced perfectly by overlapping the spectra of the two isolated isomers (**A**) and (**B**). The suggestion that these compounds are identical in the configuration of the βCD moiety, but have different arrangements of the bidentate ligands around the metal (Figure 2.5a, b), was further corroborated by their circular dichroism spectra (Figure 2.5e): the two isomers have identical spectra with ellipsicities of opposite sign. Comparison with circular dichroism spectra of enantiomerically pure cyclometalated Ir

complexes published in the literature[66] allowed assignment of the first peak (**A**) as the Δ- and the second (**B**) as the Λ-enantiomer.

2.2.5 Quantum yields and lifetimes of [Ir(ppy)$_2$(pytl-βCD)]Cl as mixture and of its separated isomers A and B

The mixture of isomers (**A**) and (**B**) and the individual components behaved similarly in air-equilibrated solutions, with luminescence quantum yields close to 14% (Tables 2.1 and 2.2). In argon-saturated conditions, however, we observed clear differences between the mixture and the isomers. The mixture had an intermediate quantum yield relative to the separated diastereoisomers; isomers (**A**) and (**B**) showed lower and higher emission quantum yields, respectively (Table 2.2).

As we discussed in the previous section, the replacement of an aliphatic group by the βCD in the complexes results in a long extension of the lifetimes and a large increase in emission quantum yields. We speculated that such an effect could be the result of a non-covalent interaction between the ppy ligands coordinated to the Ir and the hydrophobic cavity of the covalently attached βCD. Indeed, it is known that cyclodextrin can act simultaneously as both a first- and second-sphere ligand when covalently attached to a potential guest.[12] This may enhance the photophysical properties of the guest, mainly in three ways by: i) limiting the molecular degrees of freedom of the chemical bonds, thus reducing the non-radiative deactivation of the triplet excited state, ii) changing the microenvironmental polarity, and iii) preventing the excited state quenching due to dynamic collision or oxygen energy transfer.

Table 2.2 *Photophysical data for the separated diastereoisomeric (**A**, Δ; **B**, Λ) Ir complexes and their mixture.*[a]

Complex	λ_{exc} (nm)[b]	Φ(air)	Φ(Ar)	τ (ns, Air)	τ (ns, Ar)
[Ir(ppy)$_2$(pytl-βCD)]Cl mixture	380	0.14	0.54	690	2800
[Ir(ppy)$_2$(pytl-βCD)]Cl isomer (**A**)	380	0.13	0.49	670	2700
[Ir(ppy)$_2$(pytl-βCD)]Cl isomer (**B**)	380	0.14	0.70	680	2900

a, The solutions were measured in air-equilibrated solvent (air) and argon-saturated solvent prepared by bubbling argon through the solutions for 20–30 min (Ar); b, the optical density at the excitation wavelength was kept below 0.1.

The observed changes in phosphorescence in the presence of βCD hence provide evidence that an inclusion complex is formed but they give no structural information with regard to the geometry and mode of inclusion. Inspection of a molecular model (not shown) of our system

reveals that as a result of the methylation of the hydroxyl groups a hydrophobic pocket is formed on the primary side of the cavity. The metal complex with the appended βCD is forced to be close to this substituted rim because the covalent link is relatively short. High-resolution NMR spectroscopy investigations on the **A** (Δ) diastereoisomer show that there is an interaction between the iridium complex and the primary side of the attached βCD (Chapter 3). The rather large size of the Ir complex when compared with the diameter of the βCD cavity would not allow the formation of a real inclusion complex but a "semi-inclusion" complex with, for example, an aromatic ligand is possible.

The large and unexpected difference in the quantum yields of the two diastereoisomeric forms of the complex $[Ir(ppy)_2(pytl\text{-}\beta CD)]Cl$ is remarkable (Table 2.2). This result may be explained by a preferential interaction of the chiral βCD with one of the enantiomers of the attached metal complex. The inherent chirality of the octahedral trisbidentate complex (Figure 2.5) is most likely recognised by the βCD and probably leads to a stronger interaction in the case of one diastereoisomer than of the other. This idea is corroborated by the example of chiral recognition of helical metal complexes by cyclodextrins reported by Kano,[67] who has investigated the interaction of the $[Ru(phen)_3]$ in water with cyclodextrins that are fully carboxylated on their primary side.

2.3 Conclusion

We have described the design and preparation, by click chemistry, of novel βCD-, methyl-, and adamantane-appended triazole-pyridine ligands, namely, pytl-βCD, pytl-Me, and pytl-ada. The preparations of the heteroleptic complexes of Ru and Ir with bpy and ppy, respectively, resulting in $[Ru(bpy)_2(pytl\text{-}R)]Cl_2$ and $[Ir(ppy)_2(pytl\text{-}R)]Cl$ are reported. The two diastereoisomeric forms of the Ir complex of the βCD-appended ligand, $[Ir(ppy)_2(pytl\text{-}\beta CD)]Cl$, were separated by HPLC and characterised by NMR and circular dichroism spectroscopy. The luminescences of the Ru complexes (at 610–615 nm upon excitation at 448 or 420 nm) display low quantum yields (0.005–0.006) and short lifetimes (20–30 ns) and are not affected by oxygen. In contrast, the presence of the pytl ligand in the cyclometalated Ir complexes gives a series of highly luminescent compounds with emission quantum yields ranging between 0.23 and 0.70. Interestingly, it was found that the nature of the substituent strongly affects the Φ and τ values of such complexes; the emission intensity is enhanced on going from the adamantane-appendend ($[Ir(ppy)_2(pytl\text{-}ada)]Cl$ to the βCD-appended derivative $[Ir(ppy)_2(pytl\text{-}\beta CD)]Cl$. The luminescence enhancement is observed both in argon-saturated and in air-equilibrated water solutions. Large differences between the quantum yields of the

two diastereoisomers (**A**, Δ) and (**B**, Λ) of [Ir(ppy)$_2$(pytl-βCD)]Cl were also observed. These effects are ascribed to a partial self-inclusion of aromatic ligands of the Ir complex into the primary side of the chiral βCD cavity, which acts as an enantioselective second-sphere ligand. This limits the vibration modes of the ligands, changes the micropolarity around the emissive excited state, and shields it from a quencher such as oxygen. The excited state of the Ir complexes is an admixture of ^{3}LC and ^{3}MLCT states and it is mainly ligand (ppy) based. The phenyl and the pyridine moieties of the ppy ligand are expected to contribute the most to the HOMO and LUMO of the complex, respectively. This was also confirmed by studies on [Ir(F$_2$ppy)$_2$(pytl-ada)]Cl, in which the introduction of fluorine on the phenyl rings produces a bright blue emitting compound (450 nm), because it lowers the energy of the HOMO orbital.

We conclude that these new ligands for highly luminescent iridium complexes can be easily prepared by click chemistry, and that the luminescence wavelength and intensity can be tuned by introducing substituents on the ppy ligand or by appending a βCD. In particular, the presence of the βCD leads to highly luminescent species, also in air-equilibrated water solutions, by reducing the sensitivity of Ir complexes to dioxygen. This opens new horizons for the preparation and application of new luminescent iridium complexes, for example in electrochemiluminescent devices with highly improved efficiencies, and in hydrogen evolution systems. These applications will be discussed in Chapters 4, and 5, respectively.[68,69]

2.4 Acknowledgements

I thank Dr. Pablo Contreras-Carballada for the photophysical measurements and for fruitful discussions.

2.5 Experimental

2.5.1 Methods and materials

General. THF was purified by distillation under nitrogen from sodium/benzophenone; dry DMF was purchased from Fluka. The "magic mixture" eluent was a mixture of water (300 mL), NaCl (30 g), acetonitrile (1200 mL), and methanol (300 mL). Compounds **2**, **3**, and **4** were prepared according to literature procedures.[45,46] The Ir^{III} chloride-bridged complexes [(ppy)$_2$Ir(μ-Cl)$_2$Ir(ppy)$_2$] and [(F$_2$ppy)$_2$Ir(μ-Cl)$_2$Ir(F$_2$ppy)$_2$] were prepared according to literature procedures.[21,70] All other chemicals were purchased from Aldrich, Fluka, or Acros and used as received. Analytical TLC was performed on Merck precoated silica gel 60 F-254 plates (layer thickness 0.25 mm) and the compounds were visualised by UV irradiation at λ = 254 and/or 366 nm and by staining with phosphomolybdic acid reagent or KMnO$_4$. Purifications by silica gel chromatography were

performed using Acros (0.035–0.070 mm, pore diameter ca. 6 nm) silica gel. All click reactions were performed in an oxygen-free atmosphere of nitrogen under Schlenk conditions and distilled solvents.

NMR spectroscopy. ^{1}H NMR spectra were recorded at 25 °C on Varian Inova 400 or Bruker DMX-300 spectrometers operating at 400 and 300 MHz, respectively. ^{13}C NMR spectra were recorded on a Bruker DMX-300 spectrometer operating at 75 MHz. ^{1}H NMR chemical shifts (δ) are reported in parts per million (ppm) relative to the residual proton signal of the solvent, δ = 3.31 ppm for CD_3OD, and δ = 7.26 ppm for $CDCl_3$. Multiplicities are reported as follow: s (singlet), d (doublet), t (triplet), dd (doublet of doublets), ddd (doublet of doublet of doublets), or m (multiplet). Broad peaks are indicated by b. Coupling constants are reported as a *J* value in Hertz (Hz). The number of protons (*n*) for a given resonance is indicated as *n*H, and is based on spectral integration values. ^{13}C NMR chemical shifts (δ) are reported in ppm relative to the residual carbon signal of the solvent, δ = 49.0 ppm for CD_3OD, and δ = 77 ppm for $CDCl_3$.

Mass spectrometry (MS). All mass analyses were performed by using electrospray (ESI) techniques . High-resolution mass spectrometry (HRMS) measurements were performed on a JEOL AccuTOF instrument by using water, acetonitrile, or methanol as solvents.

HPLC. HPLC was carried out on a Shimadzu LC-20AT HPLC system equipped with a SPD-10AV UV-vis detector and a fraction collector. Columns were purchased from Dr. Maisch GmbH. The purity of the compounds was tested by analytical HPLC. An aliquot of solution (20 µL) was injected in a ReproSil 100 C18, 3 µm (150 × 3 mm) column operating at 30 °C. The detection wavelengths were fixed at 254 and 215 nm. A gradient of water and acetonitrile both containing 0.1% v/v TFA was used as the mobile phase, with a flow rate of 0.4 mL min^{-1}. The compounds were purified on the mg scale by using a semi-preparative reversed-phase column. An aliquot of solution (2 mL) was injected in a column ReproSil 100 C8, 5 µm (250 × 10 mm) operating at 30 °C. The detection wavelengths were fixed at 254 and 215 nm. A gradient of water and acetonitrile both containing 0.1% v/v HCl or TFA was used as the mobile phase, with a flow rate of 4 mL min^{-1}. HCl was used to ensure that chloride was the only counterion of the isolated compounds. In all cases, samples were prepared by dissolving the compound in mixtures of water/acetonitrile 95/5 or 1/1 v/v and filtering the solution on a Nylon syringe filter (0.2 µm).

X-ray crystallography. Single crystal of $[Ir(ppy)_2(pytl\text{-}ada)]Cl$ was grown by slow diffusion of diethyl ether into a solution of the pure compound in chloroform. Single crystals of pytl-ada and pytl-Me were grown by slow evaporation of a solution of the respective compounds in diethyl ether/heptane. Crystal data and summaries of the data collection and structure refinement are given in Table 2.3. The selected distances and bond angles are available in the literature.[4] The atomic coordinates, and equivalent isotropic displacement parameters for the non-hydrogen atoms, are available in the literature.[4] All measurements were performed at –65 °C. The structures of pytl-ada and pytl-Me were solved by the CRUNCH program.[71] All non-hydrogen atoms were refined with anisotropic temperature factors. The hydrogen atoms were placed at calculated positions and refined isotropically in riding mode. Crystallographic data (excluding structure factors) for the structure reported in this chapter has been deposited with the Cambridge Crystallographic Data Centre. CCDC-699148 (pytl-ada, MFLADA), 699149 (pytl-Me, MFLIGA), and 699147 ($[Ir(ppy)_2(pytl\text{-}ada)]Cl$, FELIC1) contain the supplementary crystallographic data for this chapter. These data can be obtained free of charge from the Cambridge Crystallographic Data Centre via www.ccdc.cam.ac.uk.

Circular dichroism. Circular dichroism spectra were recorded on a Jasco 810 spectropolarimeter equipped with a Jasco PTC-423S/L Peltier type temperature control unit, and were measured in MilliQ water at 20 °C.

Emission. Steady-state emission spectra were recorded on a Horiba Jobin-Yvon IBH FL-322 Fluorolog 3 spectrometer equipped with a 450 W xenon arc lamp, double-grating excitation and emission monochromators (2.1 nm mm^{-1} dispersion; 1200 grooves mm^{-1}), and a TBX-4-X single-photon-counting detector. Emission spectra were corrected for source intensity (lamp and grating) and emission spectral response (detector and grating) by standard correction curves. Luminescence quantum yields (Φ_{em}) were measured in optically dilute solutions (O.D. < 0.1 at excitation wavelength), using $[Ru(bpy)_3]Cl_2$ in aerated water (Φ_{em} = 0.028) or diphenylanthracene in cyclohexane (Φ_{em} = 0.9) as references.

Time-resolved measurements up to ≈5 μs were performed by using the time-correlated single-photon-counting (TCSPC) option on the Fluorolog 3. NanoLEDs (295 or 431 nm; full-width at half maximum (fwhm) < 750 ps) with repetition rates between 10 kHz and 1 MHz were used to excite the sample. The excitation sources were mounted directly on the sample chamber at 90 °C to a double-grating emission monochromator (2.1 nm mm^{-1} dispersion; 1200 grooves mm^{-1}) and collected by a TBX-4-X single-photon-counting detector. The photons collected at the detector are correlated by a time-to-amplitude converter (TAC) to the excitation pulse. Signals were collected using an IBH DataStation Hub photon-counting module and data was analysed by the commercially available DAS6 software (Horiba Jobin Yvon IBH). The goodness of fit was assessed by minimising the reduced chi-squared function (χ^2) and visual inspection of the weighted residuals.

2.5.2 Synthesis and characterisation

Pytl-βCD. Distilled THF was bubbled with nitrogen for 1 h prior to use to remove oxygen. Compounds **4** (300 mg, 0.21 mmol) and **5** (21.5 μL, 0.21 mmol) were added to a Schlenk tube under nitrogen atmosphere and dissolved in nitrogen-saturated THF (4 mL). A solution of CuBr (30 mg, 0.21 mmol) and PMDTA (46 μL, 0.22 mmol) was prepared by dissolving both reagents in nitrogen-saturated THF (2 mL) and bubbling nitrogen through the solution for 20 min to prevent oxidation of copper(I). When the CuPMDTA complex dissolved, the solution became slightly green and an aliquot of it (1 mL) was added to the Schlenk tube. The resulting mixture was stirred in the dark at room temperature under a nitrogen atmosphere for 2 h. The reaction was followed by TLC (eluent: methanol/chloroform 10/90 v/v). No workup was performed and, after removal of the solvent *in vacuo*, the obtained blue-green solid was directly purified by column chromatography (pure chloroform followed by methanol/chloroform 2/98 v/v). Pytl-βCD was obtained as a white solid (301 mg, 93%). The purity of the compound was verified by HPLC. ^{1}H NMR (400 MHz, $CDCl_3$): δ ppm 8.56 (bd, J = 4.17 Hz, 1H), 8.22 (s, 1H), 8.14 (bd, J = 7.90 Hz, 1H), 7.75 (ddd, J = 7.78, 7.75, 1.74 Hz, 1H), 7.20 (ddd, J = 7.48, 4.96, 1.01 Hz, 1H), 5.29 (d, J = 3.69 Hz, 1H), 5.17–5.06 (m, 7H), 4.69 (dd, J = 14.41, 7.34 Hz, 1H), 4.16 (ddd, J = 9.78, 7.42, 2.55 Hz, 1H), 4.00 (ddd, J = 9.73, 4.06, 2.10 Hz, 1H), 3.92–3.03 (m, 98H); ^{13}C NMR (75 MHz, $CDCl_3$): δ ppm 150.40, 149.42, 147.88, 136.75, 124.36, 122.72, 119.92, 99.35, 99.20, 98.99, 98.87, 98.82, 98.79, 98.32, 83.23, 82.16, 82.01–81.93 (m), 81.89, 81.81, 81.78–81.69 (m), 81.10, 80.22, 80.20, 80.13, 79.85, 79.72, 79.55, 71.46, 71.30, 71.29–71.21 (m), 71.10, 70.94, 70.90, 70.89, 70.72, 70.67, 70.48–70.41 (m), 61.74, 61.47, 61.45, 61.43, 61.38, 61.34, 61.19, 59.07, 59.02, 58.98, 58.94, 58.93, 58.72, 58.70, 58.56, 58.42, 58.38, 58.32, 51.64; HRMS (ES+): *m/z* calcd for $C_{69}H_{114}N_4NaO_{34}$: 1565.72121; found: 1565.71679 $[M+Na]^+$.

2-(1-Adamantyl-1*H*-1,2,3-triazol-4-yl)pyridine (pytl-ada). Distilled THF was bubbled with nitrogen for 1 h prior to use to remove oxygen. Compound **5** (156.5 μL, 1.41 mmol) and 1-azidoadamantane (250 mg, 1.41 mmol) were added to a Schlenk tube under a nitrogen atmosphere and dissolved in nitrogen-saturated THF (5 mL). A solution of CuBr (101.2 mg, 0.71 mmol) and PMDTA (151.5 μL, 0.73 mmol) was prepared by dissolving both reagents in nitrogen-saturated THF (2 mL) and bubbling nitrogen through the solution for 20 min to prevent oxidation of copper(I). When the CuPMDTA complex dissolved, the solution became slightly green and an aliquot of it (1.5 ml) was added to the Schlenk tube. The resulting mixture was stirred in the dark at room temperature under a nitrogen atmosphere for 2.5 h. The reaction was followed by TLC (eluent: diethyl ether/

heptane 80/20 v/v). No workup was performed and after removal of the solvent *in vacuo*, the obtained blue-green solid was directly purified by column chromatography (diethyl ether/heptane 30/70 v/v). Pytl-ada was obtained as a white solid (358 mg, 91%). Crystals were grown by slow evaporation of a solution of pytl-ada in diethyl ether/heptane. The structure was further confirmed by single-crystal X-ray diffraction. M.p. = 199.2 °C; ^{1}H NMR (300 MHz, $CDCl_3$): δ ppm 8.57 (ddd, J = 4.88, 1.78, 0.94 Hz, 1H), 8.22 (s, 1H), 8.19 (ddd, J = 7.97, 1.06, 1.06 Hz, 1H), 7.80–7.72 (m, 1H), 7.20 (ddd, J = 7.53, 4.90, 1.21 Hz, 1H), 2.29 (bs, 9H), 1.80 (bs, 6H); ^{13}C NMR (75 MHz, $CDCl_3$): δ ppm 150.76, 149.26, 147.32, 136.86, 122.57, 120.14, 118.54, 59.79, 42.95, 35.90, 29.45; HRMS (ES+): *m/z* calcd for $C_{17}H_{20}N_4Na$: 303.158571; found: 303.16037 [*M*+Na]$^+$.

2-(1-Methyl-1*H*-1,2,3-triazol-4-yl)pyridine (pytl-Me). Dry DMF was deoxygenated prior to use by performing three freeze-pump-thaw cycles. A two-necked round-bottomed flask was carefully dried with a flame under a flow of nitrogen. In the cooled flask, NaN_3 (0.198 g, 3 mmol) was added together with deoxygenated dry DMF (40 mL). CH_3I (0.3 mL, 4.8 mmol) was added dropwise and the solution was stirred in the dark at room temperature overnight. The methyl azide formed is a highly explosive intermediate and was therefore not isolated.[72] The clicking reagents were subsequently added to the reaction mixture and a large excess of **5** and catalyst were used to ensure the complete consumption of methyl azide. A solution of CuBr (430 mg, 3 mmol) and PMDTA (0.69 mL, 3.3 mmol) was prepared by dissolving both reagents in oxygen-free dry DMF (10 mL), bubbling nitrogen through the solution for 20 min to prevent oxidation of copper(I). When the CuPMDTA complex dissolved, an aliquot of the solution (8 ml), together with compound **5** (0.45 mL, 4.5 mmol) were added to the flask containing the methyl azide. The resulting mixture was stirred in the dark at room temperature under a nitrogen atmosphere for 24 h. The reaction was followed by TLC (eluent: diethyl ether/heptane 80/20 v/v). After removal of the solvent *in vacuo* (**CAUTION!** this solution may still contain methyl azide in case the conversion with **5** was not 100%), the obtained solid was purified by column chromatography (diethyl ether/ heptane 1/1 v/v followed by diethyl ether/ethyl acetate 90/10 v/v). Pytl-Me was obtained as a white solid (200 mg, overall yield 41%). Crystals were grown by slow evaporation of a solution of pytl-Me in diethyl ether/ heptane. The structure was further confirmed by single-crystal X-ray diffraction. ^{1}H NMR (400 MHz, $CDCl_3$): δ ppm 8.61–8.53 (m, 1H), 8.17 (ddd, *J* = 8.0, 1.1, 1.1 Hz, 1H), 8.12 (s, 1H), 7.82–7.72 (m, 1H), 7.23 (ddd, *J* = 7.5, 4.9, 1.2 Hz, 1H), 4.17 (s, 3H); ^{13}C NMR (75 MHz, $CDCl_3$): δ ppm 150.2, 149.4, 148.6, 136.8, 122.9, 122.8, 120.2, 36.8.

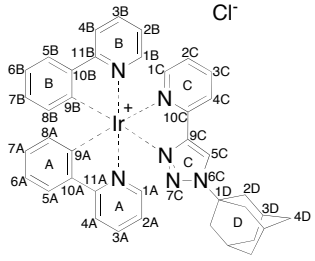

[Ir(ppy)$_2$(pytl-ada)]Cl. Ligand pytl-ada (32.2 mg, 0.12 mmol) was added as a solid to a suspension of [(ppy)$_2$Ir(μ-Cl)$_2$Ir(ppy)$_2$] (58.9 mg, 0.055 mmol) in methanol/chloroform 1/3 v/v (4 mL). The suspension was heated to 45 °C and stirred for 2 h, after which time a clear and yellow solution was obtained. The reaction was followed by TLC (eluent: methanol/chloroform 10/90 v/v) by which, under UV light at 366 nm, the compound appeared as a bright green luminescent spot. No workup was performed and after removal of the solvent *in vacuo*, the solid obtained was purified by column chromatography (methanol/chloroform 5/95 v/v followed by methanol/ chloroform 10/90 v/v). To obtain clear water solutions, suitable for photophysical measurements, the compound was dissolved in demineralised water, filtered on a Nylon syringe filter (0.2 μm) and freeze-dried. The product was obtained as a yellow solid (81.6 mg, 95%). The high purity of the compound, as required for photophysical

characterisation, was verified by analytical HPLC. Its structure was further confirmed by NOESY, gHSQC, HMBC, gDQCOSY NMR spectroscopy experiments in $CDCl_3$ and single-crystal X-ray diffraction. Crystals were grown by slow diffusion of diethyl ether in a solution of $[Ir(ppy)_2(pytl\text{-}ada)]Cl$ in chloroform. M.p. = 227.2 °C; ^{1}H NMR (400 MHz, $CDCl_3$): δ ppm 10.68 (s, 1H, 5C), 9.27 (bd, J = 7.98 Hz, 1H, 4C), 8.00 (ddd, J = 7.88, 7.84, 1.56 Hz, 1H, 3C), 7.88 (bd, J = 8.35 Hz, 2H, 4A, 4B), 7.77–7.70 (m, 2H, 3A, 3B), 7.68 (bdd, J = 5.48, 0.75 Hz, 1H, 1C), 7.63 (ddd, J = 9.30, 7.98, 1.06 Hz, 2H, 5A, 5B), 7.57 (bdd, J = 5.81, 0.77 Hz, 1H, 2A), 7.46 (bdd, J = 5.82, 0.75 Hz, 1H, 2B), 7.16 (ddd, J = 7.51, 5.54, 1.21 Hz, 1H, 2C), 7.03–6.91 (m, 4H, 6A, 1A, 1B, 6B), 6.88 (ddd, J = 7.43, 7.39, 1.29 Hz, 1H, 7A), 6.83 (ddd, J = 7.45, 7.38, 1.31 Hz, 1H, 7B), 6.29 (bdd, J = 7.60, 0.86 Hz, 2H, 8A, 8B), 2.28–2.16 (m, 9H, 2D, 3D), 1.73 (bs, 6H, 4D); ^{13}C NMR (75 MHz, $CDCl_3$): δ ppm 168.39 (11B), 167.65 (11A), 150.57 (10C), 150.33 (9A), 149.19 (2A), 149.17 (1C), 148.39 (2B), 147.98 (9C), 146.93 (9B), 143.70 (10A), 143.59 (10B), 139.78 (3C), 137.72 (3A), 137.58 (3B), 131.87 (8B), 131.65 (8A), 130.57 (7A), 129.75 (7B), 126.50 (5C), 125.50 (2C), 124.98 (4C), 124.56 (5A), 124.08 (5B), 123.08 (1A), 122.57 (1B), 122.44 (6A), 121.83 (6B), 119.29 (4A), 119.17 (4B), 63.18 (1D), 42.30 (3D), 35.45 (2D), 29.37 (4D); HRMS (ES+, H_2O): *m/z* calcd for $C_{39}H_{36}N_6Ir$: 781.26307; found: 781.26082 $[M]^+$.

$[Ir(ppy)_2(pytl\text{-}\beta CD)]Cl$. Ligand pytl-βCD (100 mg, 0.065 mmol) was added as a solid to a suspension of $[(ppy)_2Ir(\mu\text{-}Cl)_2Ir(ppy)_2]$ (33 mg, 0.031 mmol) in methanol/chloroform 1/3 v/v (3 mL). The suspension was heated to 45 °C and stirred for 3 h, after which time a yellow and clear solution was obtained. The reaction was followed by TLC (eluent: methanol/chloroform 10/90 v/v) by which, under UV light at 366 nm, the compound appeared as a bright green luminescent spot. No workup was performed and, after removal of the solvent *in vacuo*, the solid obtained was purified by column chromatography (methanol/chloroform 5/95 v/v followed by methanol/chloroform 10/90 v/v). To have clear water solutions, suitable for photophysical measurements, the compound was dissolved in demineralised water, filtered on a Nylon syringe filter (0.2 μm) and freeze-dried. The product was obtained as a yellow solid (117.4 mg, 91%). The high purity of the compound, as required for photophysical characterisation, was verified by analytical HPLC; HRMS (ES+, H_2O): *m/z* calcd for $C_{91}H_{130}N_6O_{34}Ir$: 2043.82571; found: 2043.82682 $[M]^+$.

Separation of the diastereoisomers A and B of $[Ir(ppy)_2(pytl\text{-}\beta CD)]Cl$. The two diastereosiomers **A** and **B** of $[Ir(ppy)_2(pytl\text{-}\beta CD)]Cl$ were separated on the milligram scale by using a semi-preparative HPLC equipped with a reversed-phase column. The mobile phase was a gradient of water and acetonitrile (from 34/66 to 28/72 v/v of water in 20 min) both containing 0.1% v/v HCl, with a flow rate of 4 mL min^{-1}. The separation of the diastereoisomers becomes less efficient on a semi-preparative scale and the HPLC peaks appeared partially overlapped. To limit this effect, aliquots (0.5 mL) of a low concentration (≈3 mg mL^{-1}) solution were injected and only the external parts of the two peaks were collected. The solvent was removed *in vacuo* at 40 °C. The products were dissolved in demineralised water, filtered on a Nylon syringe filter (0.2 μm) and freeze-dried.
Isomer **A**: ^{1}H NMR (400 MHz, $CDCl_3$): δ ppm 10.26 (s, 1H) 9.13 (bd, J = 7.16 Hz, 1H), 8.04 (t, J = 7.93 Hz, 1H), 7.90 (bd, J = 4.28 Hz, 1H), 7.88 (bd, J = 4.43 Hz, 1H), 7.86 (bd, J = 5.39 Hz, 1H), 7.81–7.71 (m, 2H), 7.70 (bd, J = 4.76 Hz, 1H), 7.67 (bd, J = 8.26 Hz, 1H), 7.55–7.51 (m, 1H), 7.50 (bd, J = 5.59 Hz, 1H), 7.20 (bt, 1H), 7.10 (ddd, J = 7.27, 5.87, 1.21 Hz, 1H), 7.03 (ddd, J = 7.76, 7.60, 1.09 Hz, 1H), 6.96 (ddd, J = 7.23, 5.88, 1.23 Hz, 1H), 6.89 (ddd, J = 7.58, 7.54, 1.25 Hz, 1H), 6.84 (ddd, J = 7.52, 7.50, 1.07 Hz, 1H), 6.76 (ddd, J = 7.50, 7.40, 1.27 Hz, 1H), 6.32 (dd, J = 7.61, 0.87 Hz, 1H), 6.23 (dd, J = 7.6, 0.95 Hz, 1H), 5.45 (d, J = 13.84 Hz, 1H), 5.16–5.09 (m, 5H), 4.99–4.94 (m, 2H), 4.85 (dd, J = 14.83, 4.53 Hz, 1H), 3.95–3.29 (m, 89H), 3.22–3.16 (m, 6H), 3.14 (s, 3H), 3.02 (dd, J = 9.68, 3.69 Hz, 1H), 2.25 (dd, J = 10.04, 3.28 Hz, 1H).
Isomer **B**: ^{1}H NMR (400 MHz, $CDCl_3$): δ ppm 10.31 (s, 1H), 9.18 (bs, 1H), 8.07 (bt, J = 9.02 Hz, 1H), 7.94 (bd, J = 8.45 Hz, 1H), 7.90 (bd, J = 7.88 Hz, 1H), 7.81–7.71 (m, 3H), 7.65 (bd, J = 7.46 Hz, 1H), 7.60 (bd, J = 9.94 Hz, 1H), 7.48 (bd, J = 5.56 Hz, 1H), 7.43 (d, J = 5.72 Hz, 1H), 7.22 (bt, J = 5.77 Hz, 1H), 7.06–6.95 (m, 3H), 6.92 (ddd, J = 7.70, 7.66, 0.89 Hz, 1H), 6.89 (ddd, J = 7.55, 7.39, 0.78 Hz, 1H), 6.74 (ddd, J =7.64, 7.48, 0.75

Hz, 1H), 6.30 (bd, *J* = 7.33 Hz, 1H), 6.17 (bd, *J* = 7.35 Hz, 1H), 5.42 (bd, *J* = 14.67 Hz, 1H), 5.24–5.07 (m, 6H), 4.84 (dd, *J* = 14.75, 4.01 Hz, 1H), 4.05 (bs, 1H), 3.91–3.35 (m, 89H), 3.28–3.15 (m, 9H), 3.02 (dd, *J* = 9.73 Hz, 1H), 2.84 (dd, *J* = 8.89 Hz, 1H).

[Ir(F_2ppy)$_2$(pytl-ada)]Cl. Ligand pytl-ada (23 mg, 0.082 mmol) was added as a solid to a suspension of [(F_2ppy)$_2$Ir(μ-Cl)$_2$Ir(F_2ppy)$_2$] (48.3 mg, 0.04 mmol) in methanol/chloroform 1/3 v/v (3mL). The suspension was heated to 40 °C and stirred for 3 h, after which time a yellow and clear solution was obtained. The reaction was followed by TLC (eluent: methanol/chloroform 10/90 v/v) by which, under UV light at 366 nm, the compound appeared as a bright blue luminescent spot. After removal of the solvent *in vacuo*, the solid obtained was purified by column chromatography (methanol/chloroform 5/95 v/v followed by methanol/chloroform 10/90 v/v). To have clear water solutions, suitable for photophysical measurements, the compound was dissolved in demineralised water, filtered on a syringe Nylon filter (0.2 μm) and freeze-dried. The product was obtained as a yellow solid (66.9 mg, 93.7%). The high purity of the compound, as required for photophysical characterisation, was verified by analytical HPLC. ^{1}H NMR (400 MHz, $CDCl_3$): *δ* ppm 11.06 (s, 1H), 9.51 (bd, *J* = 7.92 Hz, 1H), 8.32–8.26 (m, 2H), 8.06 (ddd, *J* = 7.88, 7.83, 1.58 Hz, 1H), 7.83–7.77 (m, 2H), 7.70 (ddd, *J* = 5.53, 1.46, 0.67 Hz, 1H), 7.49 (ddd, *J* = 5.83, 1.55, 0.67 Hz, 1H), 7.43 (ddd, *J* = 5.84, 1.54, 0.68 Hz, 1H), 7.28–7.24 (m, 1H), 7.05 (ddd, *J* = 7.35, 5.85, 1.36 Hz, 1H), 7.00 (ddd, *J* = 7.33, 5.86, 1.37 Hz, 1H), 6.58–6.46 (m, 2H), 5.71 (dd, *J* = 8.34, 2.35 Hz, 1H), 5.66 (dd, *J* = 8.56, 2.34 Hz, 1H), 2.24 (bs, 9H), 1.73 (bs, 6H); ^{13}C NMR (75 MHz, $CDCl_3$): *δ* ppm 165.26 (d, *J* = 12.36 Hz), 164.88 (d, *J* = 6.53 Hz), 164.65 (d, *J* = 12.46 Hz), 164.14 (d, *J* = 6.94 Hz), 162.99 (d, *J* = 12.83 Hz), 162.63 (d, *J* = 12.86 Hz), 161.84 (d, *J* = 12.44 Hz), 161.25 (d, *J* = 12.52 Hz), 159.53 (d, *J* = 12.77 Hz), 159.19 (d, *J* = 12.97 Hz), 154.03 (d, *J* = 6.66 Hz), 150.32 (s), 150.21 (d, *J* = 7.06 Hz), 148.95 (d, *J* = 10.01 Hz), 148.30 (s), 147.75 (s), 140.40 (s), 138.71 (d, *J* = 8.67 Hz), 127.69–127.47 (m), 127.38 (s), 125.76 (d, *J* = 21.91 Hz), 123.64–123.07 (m), 123.38 (s), 122.89 (s), 114.06 (dd, *J* = 11.03, 2.86 Hz), 113.83 (dd, *J* = 10.77, 2.86 Hz), 99.02 (t, *J* = 26.75 Hz), 98.50 (t, *J* = 26.83 Hz), 63.52 (s), 42.30 (s), 35.37 (s), 29.31 (s).

[Ru(bpy)$_2$(pytl-βCD)]Cl$_2$. Ligand pytl-βCD (39.0 mg, 0.025 mmol) and *cis*-[Ru^{II}(bpy)$_2$]Cl$_2$ (13.0 mg, 0.027 mmol) were added to a round-bottomed flask and dissolved by using a mixture of 2-methoxyethanol/water 95/5 v/v (6 mL). The resulting dark-violet solution was heated to 90 °C and stirred under nitrogen atmosphere for 24 h, after which time its colour became orange. The complexation reaction was tested at different temperatures and HRMS analysis clearly demonstrated the thermal instability of this Ru-appended βCD under these circumstances; in particular, at 100 °C it undergoes solvolysis with consequent ring opening of the βCD moiety and progressive loss of sugar units. For this reason the temperature was carefully kept below 95 °C. The reaction was followed by TLC (eluent: magic mixture) by which, under UV light at 366 nm, the compound appeared as an orange luminescent spot. No workup was performed and, after removal of the solvent *in vacuo*, a red-orange solid was obtained, which was subsequently purified by HPLC. The HPLC samples were prepared by dissolving the crude material in acetonitrile/water 1/1 v/v and filtering the solution on a Nylon syringe filter (0.2 μm). A semi-preparative reversed-phase column was used. A gradient of water and acetonitrile (from 70/30 to 40/60 v/v of water in 25 min) both containing 0.1% v/v HCl was used as the mobile phase. The HPLC fractions were collected and the solvent removed *in vacuo* at 40 °C. The product was dissolved in demineralised water, filtered on a Nylon syringe filter (0.2 μm) and freeze-dried. The product was obtained as an orange solid (44.62 mg, 88%). The high purity of the compound, as required for photophysical characterisation, was verified by analytical HPLC. ^{1}H NMR (300 MHz, $CDCl_3$): *δ* ppm 10.02 (s, 1H), 9.94 (s, 1H), 9.24–9.10 (m, 4H), 9.05–8.82 (m, 8H), 8.73–8.51 (m, 8H), 8.22–7.72 (m, 30H), 7.66–7.27 (m, 48H), 5.68–4.65 (m, 16H), 4.02–2.78 (m, 143H), 2.19–2.36 (m, 1H); ^{13}C NMR (75 MHz, $CDCl_3$): *δ* ppm 158.96–156.21 (m), 152.28–149.76 (m), 138.95–136.43 (m), 130.63–123.61 (m), 113.87 (s), 83.52–77.91 (m), 83.60–83.54 (m), 74.30–67.79 (m), 61.95–

57.23 (m), 100.68–94.96 (m), 54.56–51.19 (m), 37.91–18.88 (m), 14.05 (s); HRMS (ES+): *m/z* calcd for $C_{89}H_{130}N_8O_{34}Ru$: 1956.77329; found: 1956.76699 $[M]^{2+}$.

[Ru(bpy)$_2$(pytl-ada)]Cl$_2$. Compounds pytl-ada (70.65 mg, 0.25 mmol) and *cis*-$[Ru^{II}(bpy)_2]Cl_2$ (118 mg, 0.24 mmol) were added to a round-bottomed flask and dissolved by using a mixture of 2-methoxyethanol/water 95/5 v/v (7 mL). The resulting dark-violet solution was heated to 90 °C and stirred under nitrogen atmosphere for 24 h, after which time an orange solution was obtained. The reaction was followed by TLC (eluent: magic mixture) by which, under UV light at 366 nm, the compound appeared as an orange luminescent spot. No workup was performed and, after removal of the solvent *in vacuo*, a red-orange solid was obtained, which was subsequently purified by HPLC. The HPLC samples were prepared by dissolving the crude material in acetonitrile/water 1/1 v/v and filtering the solution on a Nylon syringe filter (0.2 μm). A semi-preparative reversed-phase column was used. A gradient of water and acetonitrile (from 95/5 to 30/70 v/v of water in 40 min) both containing 0.1% v/v HCl was used as the mobile phase. The HPLC fractions were collected and the solvent removed *in vacuo* at 40 °C. The product was dissolved in demineralised water, filtered on a Nylon syringe filter (0.2 μm) and freeze-dried. The compound was obtained as an orange solid (156 mg, 85%). The high purity, as required for photophysical characterisation, was verified by analytical HPLC. The hexafluorophosphate salt was obtained by adding a saturated aqueous solution of NH_4PF_6 to the solution of $[Ru(bpy)_2(pytl\text{-}ada)]Cl_2$ in water. The orange precipitate was filtered, washed with water and dried *in vacuo*. ^{1}H NMR (400 MHz, CD_3OD): δ ppm 9.17 (s, 1H), 8.71–8.60 (m, 4H), 8.26–8.23 (m, 1H), 8.15–8.04 (m, 4H), 8.05 (ddd, J = 7.86, 7.80, 1.42 Hz, 1H), 7.94 (bd, J = 5.68 Hz, 2H), 7.85–7.81 (m, 2H), 7.69 (bd, J = 5.61, 1H), 7.56–7.48 (m, 3H), 7.42 (ddd, J = 7.62, 5.68, 1.29 Hz, 1H), 7.36 (ddd, J = 7.66, 5.70, 1.37 Hz, 1H), 2.20 (bs, 3H), 2.16 (m, 6H), 1.78 (m, 6H); ^{13}C NMR (75 MHz, CD_3OD): δ ppm 159.25, 158.99, 158.98, 158.55, 153.19, 153.06, 153.02, 152.87, 152.79, 152.57, 148.51, 139.54, 139.16, 139.09, 139.07, 138.85, 129.06, 128.82, 128.79, 128.05, 127.19, 125.58, 125.48, 125.08, 124.79, 124.23, 123.81, 64.46, 43.39, 36.59, 31.00; HRMS (ES+): *m/z* calcd for $C_{37}H_{36}N_8Ru$: 694.21064; found: 694.20927 $[M]^{2+}$.

[Ru(bpy)$_2$(pytl-Me)]Cl$_2$. Ligand pytl-Me (34.7 mg, 0.22 mmol) and *cis*-$[Ru^{II}(bpy)_2]Cl_2$ (100 mg, 0.21 mmol) were added to a round-bottomed flask and dissolved by using a mixture of 2-methoxyethanol/water 95/5 v/v (5 mL). The resulting dark-violet solution was heated to 90 °C and stirred under nitrogen atmosphere for 24 h, after which time its colour became orange. The reaction was followed by TLC (eluent: magic mixture) by which, under UV light at 366 nm, the compound appeared as an orange luminescent spot. No workup was performed and, after removal of the solvent *in vacuo*, a red-orange solid was obtained, which was subsequently purified by HPLC. The HPLC samples were prepared by dissolving the crude material in water/acetonitrile 95/5 v/v and filtering the solution on a Nylon syringe filter (0.2 μm). A semi-preparative reversed-phase column was used. A gradient of water and acetonitrile (from 95/5 to 30/70 v/v of water in 40 min) both containing 0.1% v/v HCl was used as the mobile phase. The HPLC fractions were collected and the solvent removed *in vacuo* at 40 °C. The product was dissolved in demineralised water, filtered on a Nylon syringe filter (0.2 μm) and freeze-dried. The compound was obtained as an orange solid (117.8 mg, 87%). The high purity of the compound, as required for photophysical characterisation, was verified by analytical HPLC. ^{1}H NMR (300 MHz, CD_3OD): δ ppm 9.04 (s, 1H), 8.75–8.60 (m, 4H), 8.28 (bd, J = 7.97 Hz, 1H), 8.18–8.10 (m, 3H), 8.10–8.04 (m, 1H), 8.06 (ddd, J = 7.87, 7.72, 1.42 Hz, 1H), 7.99–7.89 (m, 3H), 7.82 (ddd, J = 5.63, 0.70, 0.62 Hz, 1H), 7.71–7.68 (m, 1H), 7.56–7.48 (m, 3H), 7.44–7.35 (m, 2H), 4.15 (s, 3H); ^{13}C NMR (75 MHz, CD_3OD): δ ppm 159.20, 159.00, 158.59, 153.20, 153.15, 152.97, 152.87, 152.65, 152.54, 149.04, 139.63, 139.24, 139.18, 139.15, 138.90, 128.98, 128.87, 128.85, 128.17, 128.12, 127.32, 125.65, 125.53, 125.28, 124.96, 123.96, 39.22; HRMS (ES+): *m/z* calcd for $C_{28}H_{24}N_8Ru$: 574.11674; found: 574.11314 $[M]^{2+}$.

X-ray crystallographic analysis and results. The structure of pytl-ada, pytl-Me, and $[Ir(ppy)_2(pytl\text{-}ada)]Cl$, and the atomic numbering are shown in Figures 2.6, 2.7, and 2.8, respectively. Geometrical calculations (PLATON[73]) revealed neither unusual geometric features, nor unusual short intermolecular contacts. The calculations revealed no higher symmetry and no (further) solvent accessible areas. The *trans*-oid structure of the uncomplexed pytl (Figures. 2.6 and 2.7) changed to a *cis*-oid structure for the Ir complex (Figure 2.8). Inspection of the geometry of the triazole part of the pytl ligand revealed that the bond between the nitrogen atoms that have bonds only to other atoms in the ring are the shortest (pytl-ada: 1.318 Å; pytl-Me: 1.314 Å; $[Ir(ppy)_2(pytl\text{-}ada)]$ Cl 1.317 Å); this is in line with the results for other structures reported recently[6] where it was concluded that the electronic structure of the ring is "azo-like" (Chapter 1, Section 1.4.3). The structure reported for pytl-Bn[6] showed a large angle between the least-square planes of the triazole and pyridine rings, viz. 15.46 deg.; this appears not to be a general feature of the pytl ligands as the corresponding values for our structures (pytl-ada: 2.90 deg.; pytl-Me: (A) 9.27, (B) 7.56 deg.; $[Ir(ppy)_2(pytl\text{-}ada)]Cl$, 11.19 deg.) are much lower (Table 2.3). The coordination geometry of the Ir atom in $[Ir(ppy)_2(pytl\text{-}ada)]Cl$ is slightly distorted from octahedral, with donor atom–Ir–donor atom angles ranging from 76.14 to 97.2 deg. for donor atoms with *cis*-orientation (with the shortest bite angle for the pytl chelator, N1–Ir1–N11), and between 168.8 an 172.0 deg. for *trans*-orientation (Table 2.3).

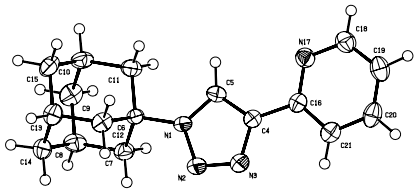

Figure 2.6 *Structure and atomic numbering of pytl-ada produced with PLATON.[73]*

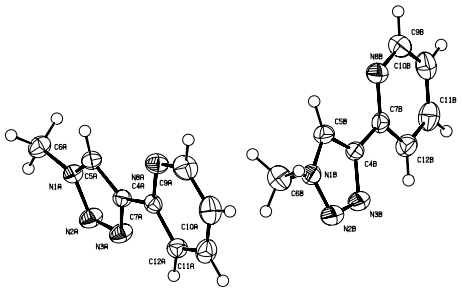

Figure 2.7 *Structure and atomic numbering of pytl-Me produced with PLATON.[73]*

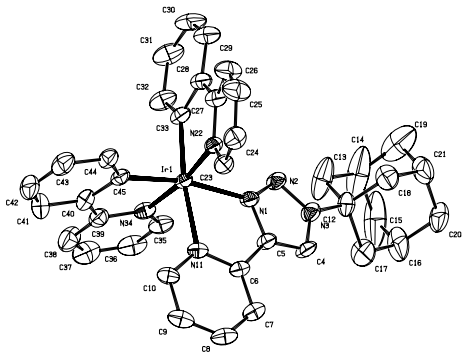

Figure 2.8 *Structure and atomic numbering of [Ir(ppy)$_2$(pytl-ada)]Cl produced with PLATON.[73]*

Table 2.3 *Crystal data and structure refinement of pytl-ada, pytl-Me, and [Ir(ppy)$_2$(pytl-ada)]Cl.*

Identification code	pytl-ada	pytl-Me	[Ir(ppy)$_2$(pytl-ada)]Cl
CCCD deposition number	699148	699149	699147
Crystal colour	translucent colourless	translucent colourless	translucent yellow
Crystal shape	rough thin platelet	rather regular needle	rough fragment
Crystal size (mm)	0.23 × 0.18 × 0.03	0.30 × 0.10 × 0.05	0.18 × 0.12 × 0.10
Empirical formula	$C_{17}H_{20}N_4$	$C_8H_8N_4$	$C_{39}H_{38}ClIrN_6O$
Formula weight	280.37	160.18	834.40
Temperature	208(2) K	208(2) K	208(2) K
Radiation/Wavelength	MoKα (graphite mon.)/ 0.71073 Å	MoKα (graphite mon.)/0.71073 Å	MoKα (graphite mon.)/ 0.71073 Å
Crystal system, space group	Orthorhombic, P b c a	Triclinic, P -1	Monoclinic, P 21/a
Unit cell dimensions.	*a*, *α* = 10.1387(3) Å, 90 deg. 173 reflections *b*, *β* = 11.0114(6) Å, 90 deg. 2.560 < *θ* < 25.000) *c*, *γ* = 25.7620(16) Å, 90 deg.	*a*, *α* = 5.49450(15) Å, 81.809(3) deg 82 reflections *b*, *β* = 9.4891(5) Å, 87.281(3) deg. 2.170 < θ < 27.490) *c*, *γ* = 15.1077(5) Å, 89.341(4) deg.	*a*, *α* = 12.5121(7) Å, 90 deg. 497 reflections *b*, *β* = 15.8248(12) Å, 99.180 (5) deg. 2.090 < θ < 25.000) *c*, *γ* = 17.3664(10) Å, 90 deg.
Volume	2876.1(3) Å^3	778.76(5) Å^3	3394.5(4) Å^3
Z, Calculated density	8, 1.295 mg m^{-3}	4, 1.366 mg m^{-3}	4, 1.633 mg m^{-3}
Absorption coefficient	0.080 mm^{-1}	0.090 mm^{-1}	4.054 mm^{-1}
Diffractometer / scan	Nonius KappaCCD with area detector *φ* and *ω* scan	Nonius KappaCCD with area detector *φ* and *ω* scan	Nonius KappaCCD with area detector *φ* and *ω* scan
F(000)	1200	336	1664
θ range for data collection	2.56 to 25.00 deg.	2.17 to 27.49 deg.	2.09 to 25.00 deg.
Index ranges	-9<=*h*<=12, -13<=*k*<=11, -30<=*l*<=30	-7<=*h*<=7, -12<=*k*<=12, -19<=*l*<=19	-14<=*h*<=14, -18<=*k*<=18, -20<=*l*<=20
Reflections collected /unique	22319 / 2520 [$R_{(int)}$ = 0.0462]	19115 / 3554 [$R_{(int)}$ = 0.0317]	53324 / 5952 [$R_{(int)}$ = 0.0368]
Reflections observed	1915 ([I_o>2σ(I_o)])	2640 ([I_o>2σ(I_o)])	4843 ([I_o>2σ(I_o)])
Completeness to 2*θ* = 25.00	97.1%	99.6%	95.8%
Absorption correction	SADABS multiscan correction[a]	SADABS multiscan correction[a]	SADABS multiscan correction[a]
Refinement method	Full-matrix least squares on F^2	Full-matrix least squares on F^2	Full-matrix least-squares on F^2
Computing	SHELXL-97[b]	SHELXL-97[b]	SHELXL-97[b]
Data/restraints/ parameters	2520/0/190	3554/0/219	5952/0/433
Goodness-of-fit on F^2	1.194	1.074	1.275
SHELXL-97 weight par's	0.0354, 1.6787	0.0519, 0.2841	0.0483, 4.8426
Final *R* indices [*I*>2*σ*(*I*)]	R_1 = 0.0633, wR_2 = 0.1098	R_1 = 0.0536, wR_2 = 0.1139	R_1 = 0.0307, wR_2 = 0.0826
R indices (all data)	R_1 = 0.0903, wR_2 = 0.1188	R_1 = 0.0817, wR_2 = 0.1251	R_1 = 0.0481, wR_2 = 0.0975
Largest diff. peak and hole	0.151 and -0.220 e. Å^{-3}	0.288 and -0.250 e.Å^{-3}	1.044 and -0.988 e.Å^{-3}

a, See reference[74]; b, see reference[75].

2.6 References

[1] H. C. Kolb, M. G. Finn, K. B. Sharpless, *Angew. Chem. Int. Ed.* **2001**, *40,* 2004–2021.

[2] *We prefer the designation pytl for the 2-(1-substituted-1H-1,2,3-triazol-4-yl)pyridine ligand rather than pyta coined by Obata et al. (see ref. [6]), because the latter is already in use for 4-pyridylthioacetate:* M. Kondo, M. Miyazawa, Y. Irie, R. Shinagawa, T. Horiba, A. Nakamura, T. Naito, K. Maeda, S. Utsuno, F. Uchida, *Chem. Commun.* **2002**, 2156–2157.

[3] D. J. V. C. van Steenis, O. R. P. David, G. P. F. van Strijdonck, J. H. van Maarseveen, J. N. H. Reek, *Chem. Commun.* **2005**, 4333–4335.

[4] M. Felici, P. Contreras-Carballada, Y. Vida, J. M. M. Smits, R. J. M. Nolte, L. De Cola, R. M. Williams, M. C. Feiters, *Chem. Eur. J.* **2009**, *15,* 13124–13134.

[5] D. Schweinfurth, K. I. Hardcastle, U. H. F. Bunz, *Chem. Commun.* **2008**, 2203–2205.

[6] M. Obata, A. Kitamura, A. Mori, C. Kameyama, J. A. Czaplewska, R. Tanaka, I. Kinoshita, T. Kusumoto, H. Hashimoto, M. Harada, Y. Mikata, T. Funabiki, S. Yano, *Dalton Trans.* **2008**, 3292–3300.

[7] O. David, S. Maisonneuve, J. Xie, *Tetrahedron Lett.* **2007**, *48,* 6527–6530.

[8] J. Szejtli, *Chem. Rev.* **1998**, *98,* 1743–1754.

[9] G. Wenz, *Angew. Chem. Int. Ed.* **1994**, *33,* 803–822.

[10] G. Wenz, B. H. Han, A. Müller, *Chem. Rev.* **2006**, *106,* 782–817.

[11] A. Douhal, *Cyclodextrin Materials Photochemistry, Photophysics and Photobiology,* Elsevier, Amsterdam, **2006**.

[12] F. Hapiot, S. Tilloy, E. Monflier, *Chem. Rev.* **2006**, *106,* 767–781.

[13] R. Breslow, S. D. Dong, *Chem. Rev.* **1998**, *98,* 1997–2011.

[14] J. M. Haider, R. M. Williams, L. De Cola, Z. Pikramenou, *Angew. Chem. Int. Ed.* **2003**, *42,* 1830–1833.

[15] J. M. Haider, Z. Pikramenou, *Chem. Soc. Rev.* **2005**, *34,* 120–132.

[16] H. F. M. Nelissen, M. Kercher, L. De Cola, M. C. Feiters, R. J. M. Nolte, *Chem. Eur. J.* **2002**, *8,* 5407–5414.

[17] J. A. Faiz, R. M. Williams, M. J. J. P. Silva, L. De Cola, Z. Pikramenou, *J. Am. Chem. Soc.* **2006**, *128,* 4520–4521.

[18] W. Xu, A. Jain, B. A. Betts, J. N. Demas, B. A. DeGraff, *J. Phys. Chem. A* **2002**, *106,* 251–257.

[19] D. Beck, J. Brewer, J. Lee, D. McGraw, B. A. DeGraff, J. N. Demas, *Coord. Chem. Rev.* **2007**, *251,* 546–553.

[20] M. Felici, P. Contreras-Carballada, R. M. Williams, Y. Vida, E. Orselli, L. De Cola, M. C. Feiters, R. J. M. Nolte, *Proc. 7th Netherlands Catalysis and Chemistry Conference* **2007**, 194.

[21] M. Felici, M. Marzá-Pérez, N. S. Hatzakis, R. J. M. Nolte, M. C. Feiters, *Chem. Eur. J.* **2008**, *14,* 9914–9920.

[22] S. Welter, N. Salluce, P. Belser, M. Groeneveld, L. De Cola, *Coord. Chem. Rev.* **2005**, *249,* 1360–1371.

[23] O. Bossart, L. De Cola, S. Welter, G. Calzaferri, *Chem. Eur. J.* **2004**, *10,* 5771–5775.

[24] S. Welter, K. Brunner, J. W. Hofstraat, L. De Cola, *Nature* **2003**, *421,* 54–57.

[25] L. De Cola, P. Belser, A. von Zelewsky, F. Vogtle, *Inorg. Chim. Acta* **2007**, *360,* 775–784.

[26] M. W. Cooke, G. S. Hanan, F. Loiseau, S. Campagna, M. Watanabe, Y. Tanaka, *J. Am. Chem. Soc.* **2007**, *129,* 10479–10488.

[27] A. Juris, V. J. Balzani, F. Barigelletti, S. Campagna, P. Belser, A. Vonzelewsky, *Coord. Chem. Rev.* **1988**, *84,* 85–277.

[28] C. Dragonetti, S. Righetto, D. Roberto, R. Ugo, A. Valore, S. Fantacci, A. Sgamellotti, F. De Angelis, *Chem. Commun.* **2007**, 4116–4118.

[29] L. Flamigni, J. P. Collin, J. P. Sauvage, *Acc. Chem. Res.* **2008**, *41,* 857–871.

[30] L. Flamigni, A. Barbieri, C. Sabatini, B. Ventura, F. Barigelletti, *Top. Curr. Chem.* **2007**, *281,* 143–203.

[31] A. B. Tamayo, S. Garon, T. Sajoto, P. I. Djurovich, I. M. Tsyba, R. Bau, M. E. Thompson, *Inorg. Chem.* **2005**, *44,* 8723–8732.

[32] W. J. Finkenzeller, M. E. Thompson, H. Yersin, *Chem. Phys. Lett.* **2007**, *444,* 273–279.

[33] J. Li, P. I. Djurovich, B. D. Alleyne, M. Yousufuddin, N. N. Ho, J. C. Thomas, J. C. Peters, R. Bau, M. E. Thompson, *Inorg. Chem.* **2005**, *44,* 1713–1727.

[34] F. Lafolet, S. Welter, Z. Popović, L. D. Cola, *J. Mater. Chem.* **2005**, *15,* 2820–2828.

[35] A. B. Tamayo, B. D. Alleyne, P. I. Djurovich, S. Lamansky, I. Tsyba, N. N. Ho, R. Bau, M. E. Thompson, *J. Am. Chem. Soc.* **2003**, *125,* 7377–7387.

[36] *Transition-metal complexes with more than one type of ligand are said to be heteroleptic.*

[37] P. Coppo, E. A. Plummer, L. De Cola, *Chem. Commun.* **2004**, 1774–1775.

[38] J. T. Fletcher, B. J. Bumgarner, N. D. Engels, D. A. Skoglund, *Organometallics* **2008**, *27,* 5430–5433.

[39] C. Richardson, C. M. Fitchett, F. R. Keene, P. J. Steel, *Dalton Trans.* **2008**, 2534–2537.

[40] Y. Li, J. C. Huffman, A. H. Flood, *Chem. Commun.* **2007**, 2692–2694.

[41] B. Schulze, C. Friebe, M. D. Hager, A. Winter, R. Hoogenboom, H. Görls, U. S. Schubert, *Dalton Trans.* **2009**, 787–794.

[42] E. Orselli, R. Q. Albuquerque, P. M. Fransen, R. Fröhlich, H. M. Janssen, L. De Cola, *J. Mater. Chem.* **2008**, *18,* 4579–4590.

[43] A. P. Croft, R. A. Bartsch, *Tetrahedron* **1983**, *39,* 1417–1474.

[44] H. Dodziuk, *Cyclodextrin and Their Complexes: Chemistry, Analytical Methods, Applications,* Wiley-VCH, Weinheim, **2006**.

[45] R. C. Petter, J. S. Salek, C. T. Sikorski, G. Kumaravel, F. T. Lin, *J. Am. Chem. Soc.* **1990**, *112,* 3860–3868.

[46] Z. Chen, J. S. Bradshaw, M. L. Lee, *Tetrahedron Lett.* **1996**, *37,* 6831–6834.

[47] E. Orselli, G. S. Kottas, A. E. Konradsson, P. Coppo, R. Fröhlich, L. De Cola, A. van Dijken, M. Büchel, H. Börner, *Inorg. Chem.* **2007**, *46,* 11082–11093.

[48] P. J. Hay, *J. Phys. Chem. A* **2002**, *106,* 1634–1641.

[49] *Transition-metal complexes with only one type of ligand are said to be homoleptic.*

[50] K. Dedeian, J. Shi, N. Shepherd, E. Forsythe, D. C. Morton, *Inorg. Chem.* **2005**, *44,* 4445–4447.

[51] R. Hage, J. G. Haasnoot, D. J. Stufkens, T. L. Snoeck, J. G. Vos, J. Reedijk, *Inorg. Chem.* **1989**, *28,* 1413–1414.

[52] M. Duati, S. Tasca, F. C. Lynch, H. Bohlen, J. G. Vos, S. Stagni, M. D. Ward, *Inorg. Chem.* **2003**, *42,* 8377–8384.

[53] T. E. Keyes, B. Evrard, J. G. Vos, C. Brady, J. J. McGarvey, P. Jayaweera, *Dalton Trans.* **2004**, 2341–2346.

[54] W. R. Browne, C. M. O'Connor, H. P. Hughes, R. Hage, O. Walter, M. Doering, J. F. Gallagher, J. G. Vos, *Dalton Trans.* **2002**, 4048–4054.

[55] R. Hage, J. G. Haasnoot, J. Reedijk, R. Wang, E. M. Ryan, J. G. Vos, A. L. Spek, A. J. M. Duisenberg, *Inorg. Chim. Acta* **1990**, *174,* 77–85.

[56] W. R. Browne, W. Henry, P. Passaniti, M. T. Gandolfi, R. Ballardini, C. M. O'Connor, C. Brady, C. G. Coates, J. G. Vos, J. J. McGarvey, *Photochem. Photobiol. Sci.* **2007**, *6,* 386–396.

[57] T. Sajoto, P. I. Djurovich, A. Tamayo, M. Yousufuddin, R. Bau, M. E. Thompson, R. J. Holmes, S. R. Forrest, *Inorg. Chem.* **2005**, *44,* 7992–8003.

[58] I. Avilov, P. Minoofar, J. Cornil, L. De Cola, *J. Am. Chem. Soc.* **2007**, *129,* 8247–8258.

[59] M. G. Colombo, H. U. Guedel, *Inorg. Chem.* **1993**, *32,* 3081–3087.

[60] G. F. Strouse, H. U. Guedel, V. Bertolasi, V. Ferretti, *Inorg. Chem.* **1995**, *34,* 5578–5587.

[61] F. W. M. Vanhelmont, H. U. Gudel, M. Fortsch, H. B. Burgi, *Inorg. Chem.* **1997**, *36,* 5512–5517.

[62] L. A. Sacksteder, M. Lee, J. N. Demas, B. A. Degraff, *J. Am. Chem. Soc.* **1993**, *115,* 8230–8238.

[63] C. S. K. Mak, A. Hayer, S. I. Pascu, S. E. Watkins, A. B. Holmes, A. Köhler, R. H. Friend, *Chem. Commun.* **2005**, 4708–4710.

[64] L. J. Bellamy, *The Infrared Spectra of Complex Molecules,* 1, 3rd, L. J. Bellamy Hastel Press, New York, **1975**.

[65] K. A. McGee, K. R. Mann*, Inorg. Chem.* **2007***, 46,* 7800–7809.

[66] F. J. Coughlin, M. S. Westrol, K. D. Oyler, N. Byrne, C. Kraml, E. Zysman-Colman, M. S. Lowry, S. Bernhard*, Inorg. Chem.* **2008***, 47,* 2039–2048.

[67] K. Kano, H. Hasegawa*, J. Am. Chem. Soc.* **2001***, 123,* 10616–10627.

[68] S. Zanarini, M. Felici, G. Valenti, M. Marcaccio, L. Prodi, S. Bonacchi, P. Contreras-Carballada, R. M. Williams, M. C. Feiters, R. J. M. Nolte, L. De Cola, F. Paolucci*, Chem. Eur. J.* **2011***, 17,* 4640–4647.

[69] N. Mourtzis, P. Contreras- Carballada, M. Felici, R. J. M. Nolte, R. M. Williams, L. De Cola, M. C. Feiters*, Phys. Chem. Chem. Phys.* **2011***, 13,* 7903–7909.

[70] I. R. Laskar, S. F. Hsu, T. M. Chen*, Polyhedron* **2005***, 24,* 189–200.

[71] R. de Gelder, R. A. G. de Graaff, H. Schenk*, Acta Cryst.* **1993***, A49,* 287–293.

[72] ***CAUTION!*** *In the first step of this synthesis methyl azide was formed, but never isolated. In fact, it is known that organic azides, especially low-molecular-weight ones, can be highly explosive. For organic azides, the "rule of six" is very useful: six carbon atoms (or other atoms of about the same size) per energetic functional group (azide, diazo, nitro, etc.) provides sufficient dilution to render the compound relatively safe. Sodium azide is relatively safe, unless acidified to form* HN_3*, which is volatile and highly toxic. For these reasons, azides should not be distilled or treated in a careless fashion. We have never experienced a safety problem with these materials. For more information, see H. C. Kolb, M. G. Finn, K. B. Sharpless, Angew. Chem. Int. Ed.* ***2001****, 40, 2004–2021.*

[73] A. L. Spek, *Platon. A Multipurpose Crystallographic Tool,* **2003**.

[74] G. M. Sheldrick, *SADABS. Program for Emperical Absorption Correction,* University of Göttingen, Germany, **1996**.

[75] G. M. Sheldrick, *SHELXL-97. Program for the Refinement of Crystal Structures,* University of Göttingen, Germany, **1997**.

3

Structural Characterisation of the Iridium Cyclodextrin Complex [Ir(ppy)$_2$(pytl-βCD)]Cl by NMR Spectroscopy

Abstract

The enhanced emission quantum yield and lifetime of the cyclometalated iridium complex [Ir(ppy)$_2$(pytl-βCD)]Cl (ppy = 2-phenylpyridine, pytl = 2-(1-substituted-1*H*-1,2,3-triazol-4-yl)-pyridine, βCD = permethylated β-cyclodextrin), relative to [Ir(ppy)$_2$(pytl-ada)]Cl (ada = adamantyl), suggest that an interaction is present between the iridium metal complex and the hydrophobic cavity of pytl attached to βCD. The compound [Ir(ppy)$_2$(pytl-βCD)]Cl exists in two diastereoisomeric forms, which are identical with respect to the configuration of the chiral centres in the cyclodextrin moiety, but have opposite chirality with respect to the configuration of the iridium complex. In this chapter we report a detailed structural investigation of isomer Δ (Figure 2.5a) of [Ir(ppy)$_2$(pytl-βCD)]Cl in D_2O by high-resolution liquid NMR spectroscopy. The assignments of the carbon and proton chemical shifts of [Ir(ppy)$_2$(pytl-βCD)]Cl, and analysis of the molecular structure were performed by two-dimensional NMR spectroscopy experiments. An interaction between the iridium complex and the covalently attached βCD cavity of isomer Δ (Figure 2.5a) was observed. Detailed analysis of the structure of the self-included compound indicated that only one ppy ligand was located inside the βCD cavity. The other ligands, ppy and pytl, are located above and outside the cavity, respectively. The excited state is mostly located on the ppy ligands; (partial) self-inclusion in the βCD cavity increases the rigidity of the iridium complex and protects the emissive excited state from quenching by water molecules as well as from dioxygen quenching.

3.1 Introduction

We have previously reported on the emission quantum yield and lifetime of cyclometalated iridium complexes, which were surprisingly enhanced in [Ir(ppy)$_2$(pytl-βCD)]Cl (ppy = 2-phenylpyridine, pytl = 2-(1-substituted-1*H*-1,2,3-triazol-4-yl)-pyridine, βCD = permethylated β-cyclodextrin) relative to [Ir(ppy)$_2$(pytl-ada)]Cl (ada = adamantyl; Chapter 2).[1] These results suggested that an interaction was present between the iridium metal complex and the hydrophobic cavity of βCD attached to the pytl ligand.[2,3] The formation of a (partial) self-included species was proposed; this would confer increased rigidity on the iridium complex and protect it from attaining an emissive excited state, which is localised on the cyclometalating ligands. Protection occurs from water molecules and dioxygen, which act as quenchers.[1] The compound [Ir(ppy)$_2$(pytl-βCD)]Cl exists in two diastereoisomeric forms, which are identical with respect to the configuration of the chiral centres in the βCD moiety, but have opposite chirality with regard to the iridium complex. In this chapter we report a detailed structural investigation of isomer Δ (Figure 2.5a) of [Ir(ppy)$_2$(pytl-βCD)]Cl in D_2O by high-resolution liquid NMR spectroscopy. This diastereoisomer was the only one that could be investigated by NMR spectroscopy, to date, although it displays a lower quantum yield than isomer Λ (Figure 2.5b and Table 2.2). This is because the Δ form is easier to isolate in a significant amount, since it elutes first from the HPLC column (Figure 2.5c). All of the carbon and proton chemical shifts of [Ir(ppy)$_2$(pytl-βCD)]Cl were assigned by two-dimensional NMR spectroscopy experiments: HSQC (Heteronuclear Single-Quantum Coherence),[4] HMBC (Heteronuclear Multiple-Bond Correlation),[4] and COSY (COrrelation SpectroscopY).[4] The structure of the compound was deduced by analysing the proximity of several hydrogen atoms within the molecule by means of ROESY (Rotating frame Overhauser Enhancement SpectroscopY) experiments.[4]

3.2 General

Native β-cyclodextrin has C_7 symmetry, which is broken by mono-functionalisation of the compound, and is responsible for the high complexity of the carbohydrate region of the ^{1}H NMR spectrum (Chapter 2).[1,5,6] The complexity of the spectrum is due to the high similarity of the resonances of the glucopyranose units, which are no longer chemically equivalent. Cyclodextrin protons resonate in a limited frequency range: δ = 0.2 ppm for H-1 and δ = 0.5 ppm for the set of protons H-2, H-3, H-4, H-5, and H-6,6'; due to overlap of the

peaks, assignment of the proton chemical shifts requires the use of a combination of two-dimensional NMR spectroscopy experiments.[6,7]

We found that the appearance of the ^{1}H NMR spectrum of [Ir(ppy)$_2$(pytl-βCD)]Cl in D_2O depended significantly on the concentration of the sample. At concentrations above approximately 3 mM the proton signals appear to be very broad, suggesting aggregation. This is probably due to intermolecular interactions among [Ir(ppy)$_2$(pytl-βCD)]Cl molecules, such as inclusion of part of the iridium moiety of one [Ir(ppy)$_2$(pytl-βCD)]Cl in the βCD cavity of another molecule. Considering that such interactions are more likely to take place at high concentrations, a spectrum with sharp peaks was obtained by diluting the sample to 1.8×10^{-3} M, below which concentration no further changes in the chemical shifts occurred. At this concentration [Ir(ppy)$_2$(pytl-βCD)]Cl exists as a monomeric species; this condition was used to prepare the NMR sample and a number of 2D NMR experiments were performed. It is worth noting that the concentration of the samples used in the photophysical measurements ($\approx10^{-6}$ M; Chapter 2)[1] was three orders of magnitude lower than the concentration used in the NMR studies presented herein. We believe that structural information on [Ir(ppy)$_2$(pytl-βCD)]Cl obtained by NMR spectroscopy is also valid at lower concentrations and can be used to rationalise the photophysical properties of the complex.

Inspection of a CPK model of [Ir(ppy)$_2$(pytl-βCD)]Cl indicates that βCD can act as a second-sphere ligand, allowing (partial) self-inclusion of the iridium complex. However, due to the small size of the βCD cavity with respect to the coordination complex, it is clear from the model that only one of the aromatic ligands of the iridium complex can be accommodated in the βCD cavity. In addition, the short methylene unit, which links the iridium complex to glucose moiety A, significantly limits the number of possible orientations of the aromatic ligands with respect to βCD (Scheme 3.1). This effect determines which ligand has the most favourable interaction with the βCD cavity.

3.3 Spectral assignment

To obtain structural information by NMR spectroscopy, it is necessary to first assign the chemical shifts of the hydrogen atoms of the molecule. A general approach for the assignment of the proton and carbon chemical shifts of a complicated spin system, such as a substituted βCD, involves two steps: i) identification of the chemical shifts of all the nuclei that belong to the same glucose moiety, and ii) determination of the position of the glucose moieties in the cyclodextrin ring.[6]

The HSQC spectrum, which correlates carbons and protons connected through a single covalent bond, was chosen as the reference spectrum in our strategy for ^{1}H and ^{13}C chemical shift assignment. In this 2D spectrum, the resonances of the protons are dispersed along the carbon dimension, according to the chemical shift of the carbon atoms to which they are bound. This feature significantly reduces overlap of the signals and allows identification of most of the peaks; this is otherwise not feasible in the 1D ^{1}H NMR spectrum. The HSQC spectrum it is not shown in this chapter because it does not provide useful information about the long-range H,C connectivity of the atoms in the molecule. More interesting in that sense is the HMBC spectrum, in which a cross-peak indicates a correlation between heteronuclei (^{13}C and ^{1}H) separated by a number of bonds larger than one.

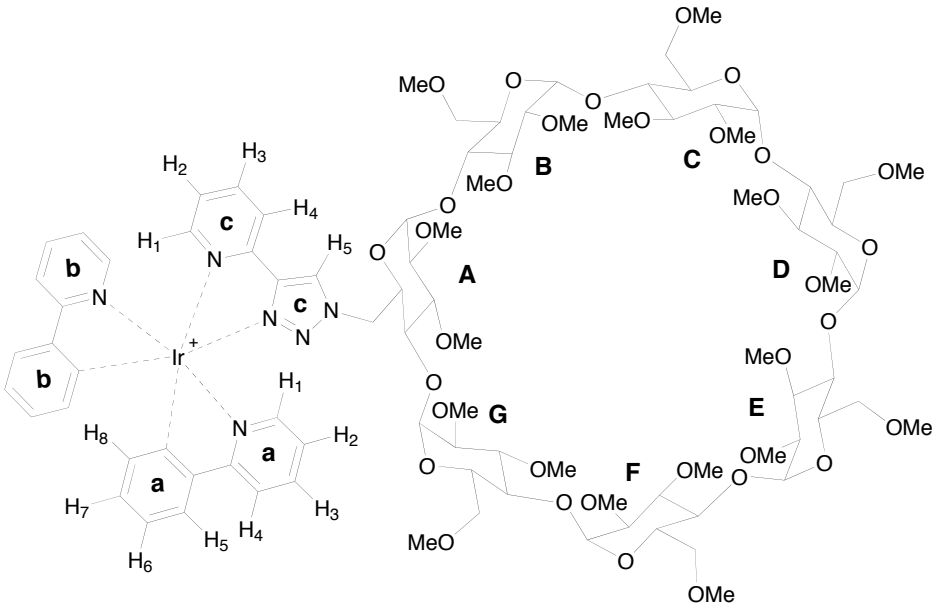

Scheme 3.1 *Structure and numbering of [Ir(ppy)$_2$(pytl-βCD)]Cl. The numbering of ligands **a** and **b** is identical.*

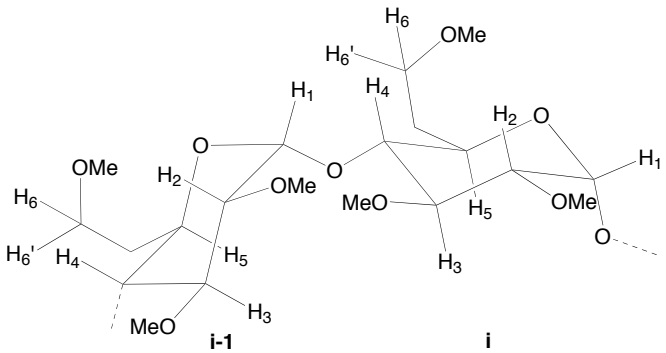

Scheme 3.2 *Structure of two adjacent glucose moieties in βCD (i = A, B, C, etc.).*

The proton and carbon chemical shifts within one glucose unit are usually identified by COSY experiments, which provide information about the connectivity of the ^{1}H atoms.[6] Unfortunately, our COSY spectrum was not sufficient in this case because the signals of H-3$_i$, H-4$_i$, H-5$_i$, H-6$_i$, and H-6'$_i$ (Scheme 3.2) of glucose residue i (i = A, B, C, etc.) were poorly resolved due to asymmetry of the mono-substituted βCD. To overcome this problem, we used HMBC experiments, which provide information about the connectivity of the ^{1}H and ^{13}C atoms. In these experiments the dephasing period was set to 71.5 ms to select mainly the long-range interactions ($J_{C\text{-}H} \approx 7$ Hz). The advantage of the HMBC spectrum over the COSY spectrum is the dispersion of the proton resonances along the carbon dimension. This significantly reduces the overlap of the peaks and allows the identification of most of the proton chemical shifts. We used the seven anomeric protons as starting points for the assignments, since they are easily identified because they appear in a specific and isolated region of the spectrum (H-1: δ = 5.3–5.1 ppm; C-1: δ = 97–101 ppm). By starting from one anomeric proton we assigned all proton and carbon chemical shifts of the nuclei of its glucose.

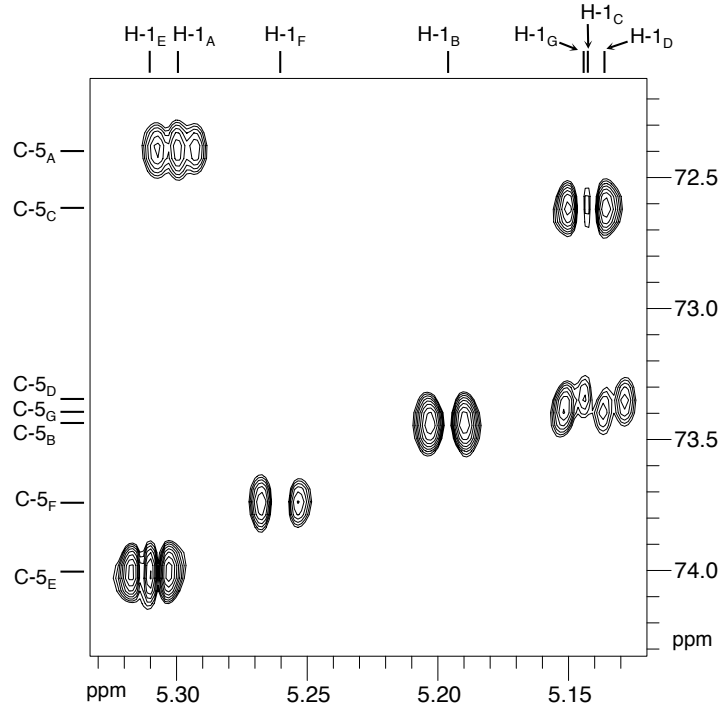

Figure 3.1 *(See text on the next page) Part of the 800 MHz HMBC spectrum of Δ-[Ir(ppy)$_2$(pytl-βCD)]Cl in D$_2$O at 25 °C. The chemical shifts of the seven C-5$_i$ are within the range δ = 72–75 ppm. The multiplicity along the proton dimension is due to vicinal homonuclear coupling.*

Most of the resonances of the glucose units, including the methyl groups, were identified by using the HMBC spectrum. An interesting example is the cross-peaks in the HMBC between C-5_i and H-1_i (Figure 3.1, see previous page), which contain information necessary to assign the chemical shifts of C-5_i (Tables 3.1 and 3.2), starting from the chemical shifts of the anomeric nuclei H-1_i.

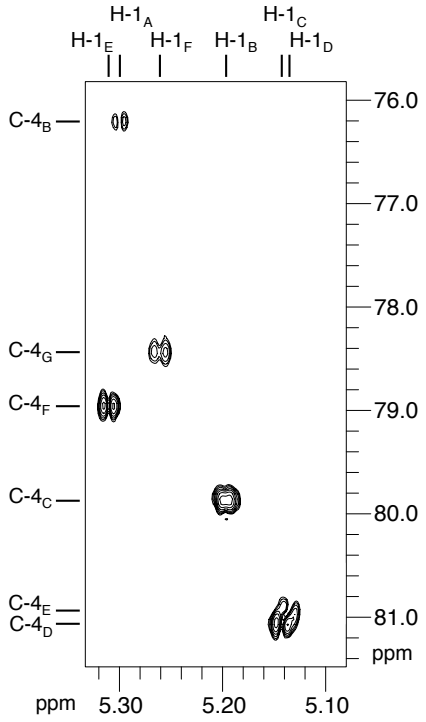

Figure 3.2 *Part of the 800 MHz HMBC spectrum of Δ-[Ir(ppy)$_2$(pytl-βCD)]Cl in D_2O at 25 °C. The chemical shifts of six C-4_i are within the range δ = 76–82 ppm. C-4_A appears outside the spectral region shown here (δ = 84.71 ppm). The multiplicity along the proton dimension is due to vicinal homonuclear coupling.*

The sequential assignment of the glucose moieties in the βCD ring was done by using HMBC and ROESY experiments. In the HMBC spectrum, the peaks corresponding to long-range coupling across the glycosidic bond, between anomeric proton H-1_{i-1} of residue i-1 and carbon C-4_i of the following residue i, were visible (Figure 3.2). We needed a starting point; the resonances of the protons of the modified glucose unit A, such as H-6,6'$_A$ and H-5_A (Scheme 3.1) are easily identified since they are shifted downfield due to the functionalisation with the iridium complex. Starting from the moiety A, the adjacent glucose unit was identified by means of the HMBC (Figure 3.2). This procedure was repeated for all glucose units. The resulting assignments were corroborated by analysis of the ROESY cross-peaks between H-1_{i-1} and H-4_i. The seven glucose units were named A, B, C, and so forth, and their

disposition along the cyclodextrin is presented in Scheme 3.1. The chemical shifts of the aromatic protons and carbons of the iridium complex were identified by a similar strategy (Tables 3.3 and 3.4).

Table 3.1 *^{1}H NMR chemical shifts, δ (ppm), of the βCD moiety of Δ-[Ir(ppy)$_2$(pytl-βCD)]Cl in D_2O.*

	H-1	H-2	H-3	H-4	H-5	H-6	H-6'	CH_3-2	CH_3-3	CH_3-6
A	5.30	3.27	3.84	3.53	4.34	5.10	4.71	3.50	3.58	–
B	5.20	3.23	3.57	3.74	3.69	3.60	3.43	3.50	3.61	3.25
C	5.14	3.27	3.68	3.77	3.83	3.29	3.53	3.47	3.58	3.27
D	5.13	3.23	3.59	3.63	3.38	2.88	3.26	3.46	3.55	3.11
E	5.31	3.33	3.76	3.68	3.92	n.f.[a]	n.f.[a]	3.53	3.62	3.25
F	5.26	3.32	3.67	3.91	3.81	3.60	3.93	3.52	3.70	3.42
G	5.15	3.30	3.59	3.64	3.63	3.39	2.97	3.42	3.55	2.76

a, Not found.

Table 3.2 *^{13}C NMR chemical shifts, δ (ppm), of the βCD moiety of Δ-[Ir(ppy)$_2$(pytl-βCD)]Cl in D_2O.*

	C-1	C-2	C-3	C-4	C-5	C-6	2-CH_3	3-CH_3	6-CH_3
A	97.07	83.39	82.65	84.71	72.39	55.73	60.98	63.03	–
B	100.19	83.87	84.60	76.21	73.44	73.77	61.54	63.16	61.18
C	100.69	82.81	83.35	79.86	72.62	73.08	60.52	61.81	61.71
D	100.40	82.60	83.10	81.06	73.36	72.55	60.45	62.31	61.08
E	98.97	83.89	83.66	80.96	74.01	n.f.[a]	60.92	63.16	61.20
F	100.19	83.20	83.68	78.96	73.74	73.14	61.30	63.20	61.17
G	100.51	82.14	83.71	78.43	74.42	73.16	59.92	61.91	58.19

a, Not found.

Table 3.3 *^{1}H NMR chemical shifts, δ (ppm), of the iridium complex of Δ-[Ir(ppy)$_2$(pytl-βCD)] Cl in D_2O.*

	H-1	H-2	H-3	H-4	H-5	H-6	H-7	H-8
a	7.82	7.09	7.95	8.07	7.82	7.08	6.95	6.37
b	7.64	7.13	7.90	8.13	7.87	7.09	6.95	6.33
c	7.88	7.32	8.05	8.18	8.88	–	–	–

Table 3.4 *^{13}C NMR chemical shifts, δ (ppm), of the iridium complex of Δ-[Ir(ppy)$_2$(pytl-βCD)] Cl in D_2O.*

	C-1	C-2	C-3	C-4	C-5	C-6	C-7	C-8
a	102.77	76.61	91.70	72.58	77.37	74.94	82.68	84.68
b	101.94	76.44	91.76	72.87	78.09	75.91	83.51	84.49
c	103.49	79.60	92.72	75.75	80.60	–	–	–

The carbon and proton resonances H-6$_E$, H-6'$_E$, and C-6$_E$ could not be assigned due to the absence of cross-peaks in the HMBC and COSY spectra. This is probably due to unfavourable values of the dihedral angles for the homo- and heteronuclear $^3J_{C\text{-}H}$ and $^3J_{H\text{-}H}$ couplings.

3.4 Conformational analysis

A ROESY experiment provides a map of the protons that are in close proximity and have through-space interactions. It is, therefore, possible to obtain information on the conformational behaviour of the [Ir(ppy)$_2$(pytl-βCD)]Cl complex in D_2O. Since we are interested in the intramolecular interactions between ligands of the iridium complex and the βCD moiety, protons H-3$_i$ and H-5$_i$ are particularly interesting; they are located inside the βCD cavity and can act as probe protons, providing information on the position of the guest (on the primary or secondary side).[5,7,8] In addition, analysis of the aromatic protons is important to establish which ligand interacts with the cavity of the βCD.

In the ROESY spectrum of [Ir(ppy)$_2$(pytl-βCD)]Cl in D_2O several cross-peaks indicate the presence of through-space interactions between aromatic and aliphatic protons (Figures 3.3 and 3.4). Careful examination of the spectrum revealed remarkable differences in the spatial orientation of the three ligands with respect to the βCD cavity. The pytl ligand **c** is located completely outside the βCD cavity, since it does not display any cross-peaks with the carbohydrate protons. The ppy ligand **a** instead shows several interactions (cross-peaks) with protons inside the βCD cavity and on the primary rim (Figure 3.3). Ligand **a** is directed towards the interior of the cavity; this is evident from the high number of ROESY cross-peaks between protons H-3$_a$, H-4$_a$, and H-5$_a$ and protons of the glucose moieties F and G (Figures 3.3 and 3.5). In particular, both nuclei H-4$_a$ and H-5$_a$ display intense cross-peaks with H-5$_F$. The comparable intensities of these peaks indicate that H-4$_a$ and H-5$_a$ are a similar distance from H-5$_F$ (Figure 3.3). However, proton H-4$_a$ is located closer to the primary rim because it also displays strong cross-peaks with H-6$_F$ (Figure 3.3). Proton H-5$_a$ shows an intense cross-peak with H-3$_F$, which reveals deep inclusion of the phenyl ring in the βCD cavity. An

interaction with H-5$_E$ from the preceding sugar moiety is also observed (Figure 3.3). Consistent with this model, proton H-3$_a$ is located approximately on the upper rim of the βCD, and indeed it displays only few weak cross-peaks, which are exclusively with H-6$_F$ and CH$_3$-6$_F$. As expected, protons H-2$_a$ and H-1$_a$ do not display any through-space interaction with the βCD nuclei because they are located above the cavity, in the proximity of the C_1 axis of βCD. In the ROESY spectrum, weaker interactions of aromatic protons H-4$_a$ and H-5$_a$ with the methyl group of moiety G, CH$_3$-2$_G$ (Figure 3.3) confirm deep inclusion of ligand **a** in the βCD cavity.

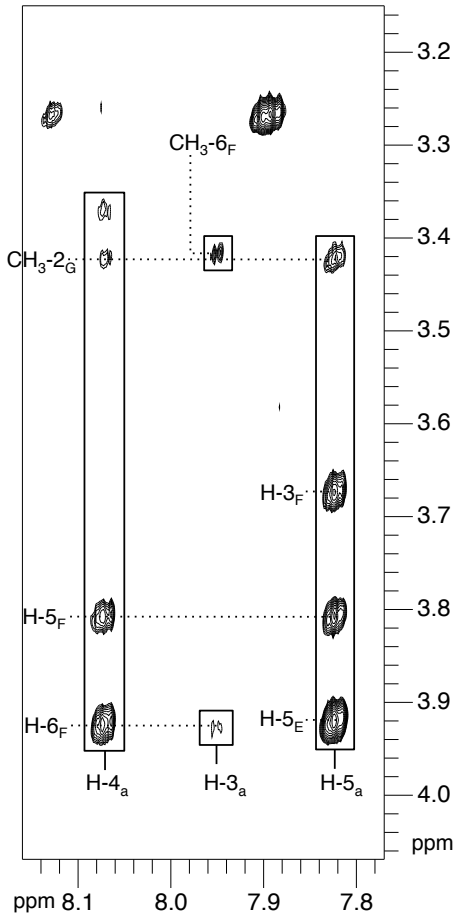

Figure 3.3 *ROESY spectrum of Δ-[Ir(ppy)$_2$(pytl-βCD)]Cl in D$_2$O at 25 °C, 800 MHz. Cross-peaks between protons of ligand **a** and some protons of the βCD are shown. The resonances of H-5$_E$ and H-6$_F$ are in close proximity, but are distinguishable.*

The iridium centre in [Ir(ppy)$_2$(pytl-βCD)]Cl displays octahedral geometry (Chapter 2),[1] which implies that the ppy ligand **b** is oriented orthogonally to ligand **a** (Figure 3.5). Our CPK model, in which ligand **a** is partially buried inside the βCD cavity, suggests that ligand **b**

is positioned close to the primary rim of βCD. This prediction is supported by NMR spectroscopy data. Analysis of the ROESY cross-peaks of the aromatic protons of ligand **b** reveals a number of through-space interactions, exclusively with protons located on the primary side of βCD. In particular, nuclei H-2$_b$ and H-1$_b$ of the pyridine ring are in proximity to methyl and methylene protons CH$_3$-6, H-6, and H-6' of glucose moiety B (Figures 3.4 and 3.5). Instead, the phenyl ring is located approximately above sugar moieties D and E, as indicated by the cross-peaks of H-8$_b$ and H-7$_b$ with CH$_3$-6$_E$ (Figures 3.4 and 3.5).

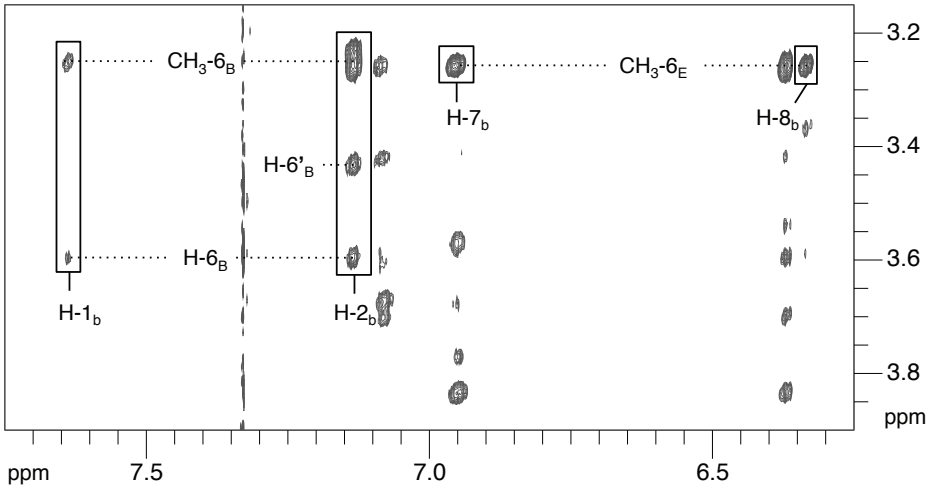

Figure 3.4 *ROESY spectrum of Δ-[Ir(ppy)$_2$(pytl-βCD)]Cl in D$_2$O at 25 °C, 800 MHz. Cross-peaks between protons of ligand **b** and some protons of the βCD are shown.*

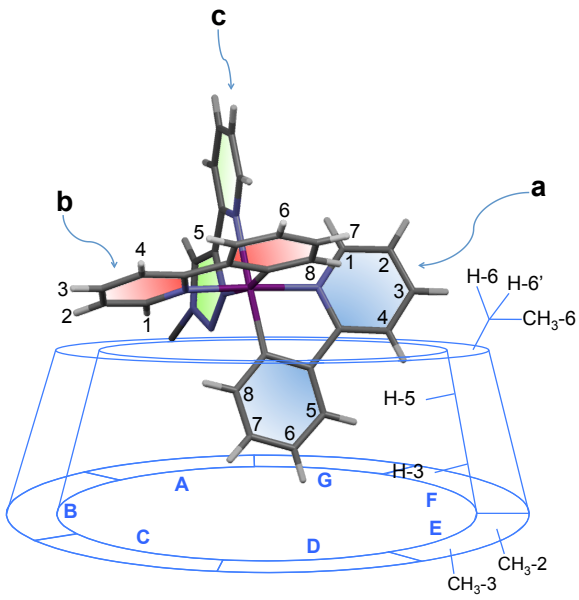

Figure 3.5 *Schematic representation of (partial) self-inclusion of the iridium complex in the cavity of βCD.*

3.5 Conclusion

Our NMR spectroscopy studies have revealed that a ligand of the iridium complex interacts with the covalently attached βCD cavity of isomer Δ (Figure 2.5a). Detailed analysis of the conformation of the self-included compound indicated that the ppy ligand **a** was the only ligand located inside the βCD cavity. It enters the βCD cavity from the primary side. Orthogonal ligands **b** and **c** are located above and outside the cavity, respectively. It is worth noting that this structure is consistent with the observed photophysical properties of [Ir(ppy)$_2$(pytl-βCD)]Cl in relation to the presence of βCD. The excited state is mostly located on the ppy ligands and (partial) self-inclusion in the βCD cavity increases the rigidity of the iridium complex. Furthermore, βCD protects the emissive excited state from quenching by water molecules as well as from dioxygen quenching. Even more effective ligand inclusion is probably present in isomer Λ (Figure 2.5b), which displays a higher luminescence quantum yield.

3.6 Acknowledgements

I thank Dr. Marco Tessari for the HR NMR spectroscopy measurements and for fruitful discussions.

3.7 Experimental

3.7.1 Methods and materials

NMR spectroscopy. NMR spectra were measured at 25 °C on a Varian Unity Inova 800 spectrometer equipped with a cryogenically cooled probe, operating at 799.646 MHz. The sample was prepared by dissolving the [Ir(ppy)$_2$(pytl-βCD)]Cl complex in D_2O (1.8×10^{-3} M). The ^1H–^{13}C correlation experiments were performed by using HSQC and HMBC standard echo/anti-echo pulse sequences. The HMBC spectra were acquired with a long-range $J_{H\text{-}C}$ dephasing period of 71.5 ms; for other experimental parameters see Table 3.5. The ^1H–^1H correlation experiments were performed by using COSY and ROESY standard pulse sequences (Table 3.5). The ROESY spectra were acquired with a mixing time of 400 ms; for other experimental parameters see Table 3.5. The spectra were processed using NMRPipe,[9] and analysed using CcpNmr Analysis software.[10] ^1H NMR chemical shifts (δ) are reported in parts per million (ppm) relative to the residual proton signal of D_2O (δ = 4.773 ppm).

Table 3.5 *Direct and indirect acquisition parameters for [Ir(ppy)$_2$(pytl-βCD)]Cl.*

Technique	**HSQC**		**HMBC**		**COSY**		**ROESY**	
	Direct dim.	Indirect dim.	Direct dim.	Indirect dim.	Direct dim.	Indirect dim.	Direct dim.	Indirect dim.
Spectral widths (kHz)	9	10	9	10	9	7.5	9	7.5
Number of complex data points	1350	210	2700	260	4500	400	5400	400
Carrier position (ppm)	4.773	80.100	4.773	80.100	4.773	4.773	4.773	4.773

3.8 References

[1] M. Felici, P. Contreras-Carballada, Y. Vida, J. M. M. Smits, R. J. M. Nolte, L. De Cola, R. M. Williams, M. C. Feiters*, Chem. Eur. J.* **2009***, 15,* 13124–13134.

[2] D. Beck, J. Brewer, J. Lee, D. McGraw, B. A. DeGraff, J. N. Demas*, Coord. Chem. Rev.* **2007***, 251,* 546–553.

[3] J. A. Fernandes, S. S. Braga, R. A. Sa Ferreira, M. Pillinger, L. D. Carlos, P. Ribeiro-Claro, I. S. Goncalves*, J. Inclusion Phenom. Macrocyclic Chem.* **2006***, 55,* 329–333.

[4] S. Berger, S. Braun, *200 and More NMR Experiments,* Wiley-VCH, Weineim, **1998**.

[5] N. Birlirakis, B. Henry, P. Berthault, F. Venema, R. J. M. Nolte*, Tetrahedron* **1998***, 54,* 3513–3522.

[6] H. J. Schneider, F. Hacket, V. Rudiger, H. Ikeda*, Chem. Rev.* **1998***, 98,* 1755–1786.

[7] Y. Liu, Z. X. Yang, Y. Chen*, J. Org. Chem.* **2008***, 73,* 5298–5304.

[8] H. F. M. Nelissen, M. Kercher, L. De Cola, M. C. Feiters, R. J. M. Nolte*, Chem. Eur. J.* **2002***, 8,* 5407–5414.

[9] F. Delaglio, S. Grzesiek, G. W. Vuister, G. Zhu, J. Pfeifer, A. Bax*, J. Biomol. NMR* **1995***, 6,* 277–293.

[10] W. F. Vranken, W. Boucher, T. J. Stevens, R. H. Fogh, A. Pajon, M. Llinas, E. L. Ulrich, J. L. Markley, J. Ionides, E. D. Laue*, Proteins* **2005***, 59,* 687–696.

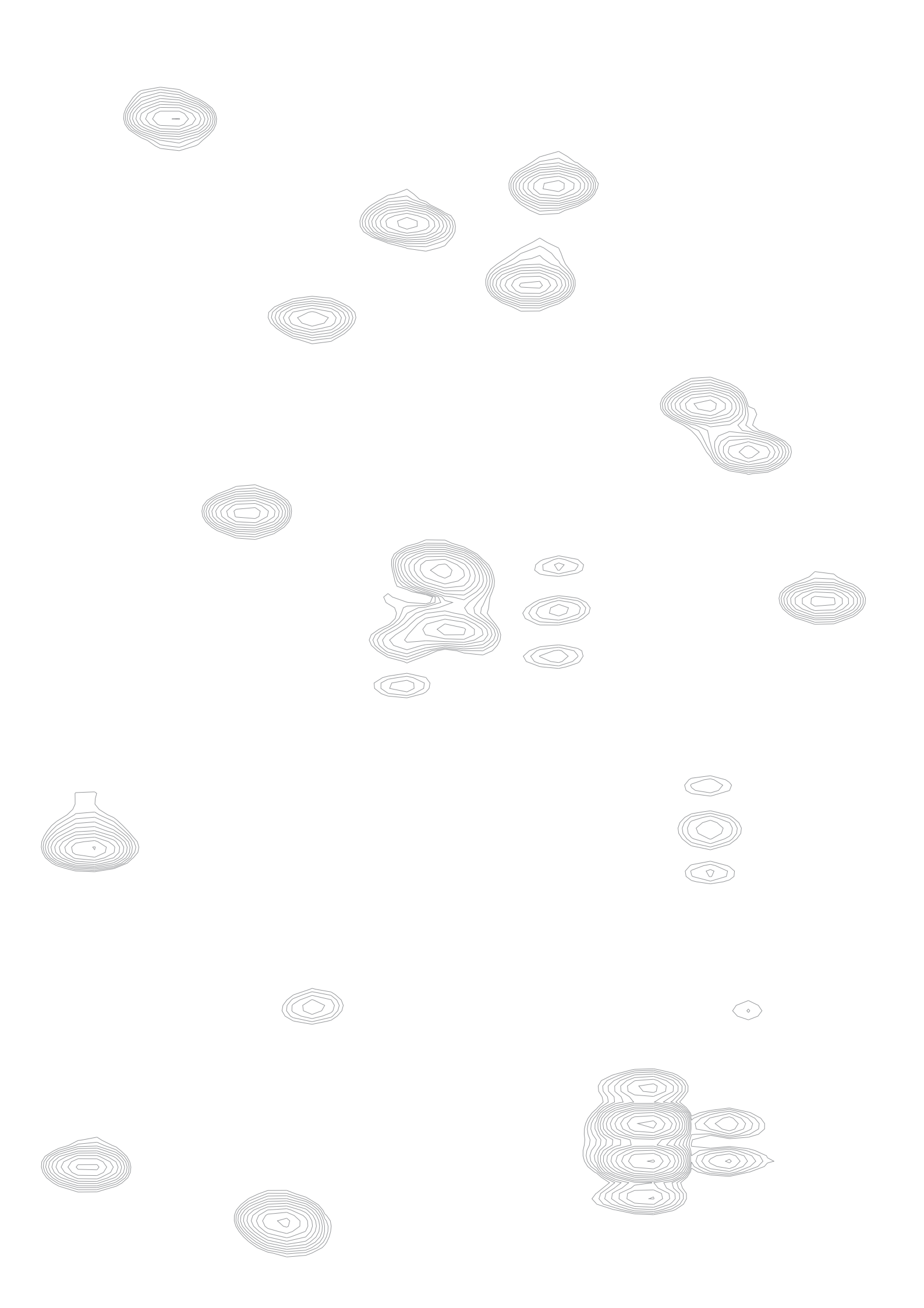

4

Iridium(III) Complexes as Potential Labels for Electrochemiluminescence

Abstract

Electrochemiluminescence (ECL) is the emission of light caused by electron transfer reactions between electro-generated species. This technique is a very promising and powerful analytical tool exploited in many different fields. The most important applications are in diagnostics, where various biologically relevant molecules (e.g., proteins and nucleic acids) can be recognised and quantified with a sensitivity and specificity previously not attainable. Five ionic Ir^{III} complexes of the general formulas $[Ir(ppy)_2(pytl\text{-}R)]^+$ (R = methyl, permethylated β-cyclodextrin (βCD), propylamine) and $[Ir(F_2ppy)_2(pytl\text{-}R)]^+$ (R = adamantyl, propylamine) (ppy = 2-phenylpyridine, pytl = 2-(1-substituted-1*H*-1,2,3-triazol-4-yl)-pyridine, F_2ppy = 2-(2,4-bisfluorophenyl)-pyridine) are shown to give bright green or blue ECL signals in air-equilibrated aqueous media. The straightforward functionalisation of the pytl ligand, prepared by click chemistry, allowed insertion of a solubilising group (βCD), which resulted in enhanced ECL emission in water. With the prospect of applying such luminophores in ECL-based biological assays, pytl was appended with a propylamino group. The presence of the amino group did not significantly affect the ECL properties, but provided a potential link for the covalent labelling of biomolecules and linking to solid substrates. Under the operating conditions, the free amino terminus underwent irreversible oxidation, resulting in electrode fouling. When functionalised, the amino group is, however, expected to be stable under oxidative conditions; hence its reactivity should not interfere with ECL when the iridium label is covalently linked to substrates. All luminophores displayed good solubility in aqueous buffers and gave an intense and stable ECL signal under physiological conditions.

This work is part of the publication: S. Zanarini, M. Felici, G. Valenti, M. Marcaccio, L. Prodi, S. Bonacchi, P. Contreras-Carballada, R. M. Williams, M. C. Feiters, R. J. M. Nolte, L. De Cola, F. Paolucci, Chem. Eur. J. ***2011****, 17, 4640–4647.*

4.1 Introduction

Electrochemiluminescence (ECL) is the process whereby species generated at electrode surfaces undergo high-energy electron transfer reactions to form excited states that emit light. The first detailed ECL studies were described by Hercules and Bard in the mid-1960s.[1,2] In about 50 years, ECL has become a powerful analytical method exploited in many different areas with the possibility of detecting very low analyte concentrations ($\leq 10^{-11}$ M).[3–5]

Because ECL involves the generation of light at an electrode, it is in fact a combination of electrochemical and spectroscopic methods. ECL has many distinct advantages over other spectroscopy-based detection systems.[4,6] For example, compared with fluorescence methods, ECL does not involve a light source; hence, the problems of scattered light and luminescent impurities are absent. Moreover, it has the possibility of accurate spatial control of the emission through the position of the working electrode. Last, but not least, the instrumentation is not expensive, especially in comparison with other techniques that can reach similar performances. Examples of applications of ECL are as ultra-sensitive detection methods for high-performance liquid chromatography (HPLC), flow injection analysis (FIA), and capillary electrophoresis.[7] The most interesting applications, however, are in the area of immunoassays for diagnostics, where a number of different biologically relevant molecules (e.g., proteins and nucleic acids) can be monitored and quantified with a sensitivity and specificity previously not attainable. The use of this technique in biological assays was made possible by the discovery of the intense ECL signal of water-soluble compounds such as $[Ru(bpy)_3]^{2+}$ (bpy = 2,2'-bipyridine).[8] Together with its derivatives, $[Ru(bpy)_3]^{2+}$ comprises one of the most extensively studied classes of coordination complexes due to their high stability in aqueous solution and excellent photo- and electrochemical properties, even in the presence of dissolved molecular oxygen.

A fundamental topic in ECL research is the development of new electroactive luminophores that give high ECL efficiency and stability under working conditions. Furthermore, luminophores that could display a red- or blueshifted emission with respect to $[Ru(bpy)_3]^{2+}$ are of great interest. These would allow the simultaneous detection of multiple analytes without the use of optical filters.

To be applied in ECL-based biological assays, a luminophore needs to meet a number of important criteria, such as i) possessing an intense and stable ECL signal under physiological conditions, ii) having good solubility in aqueous buffers, and iii) possessing suitable binding sites for the covalent functionalisation of biomolecules. The common drawbacks for most of the known dyes include limited solubility in water,[9,10] lack of stability during

electrochemical switching,[11,12] a low ECL efficiency, and the difficulty of introducing a binding site without interfering with the photophysical and electrochemical properties.

In the research described in this chapter, the ECL properties of ionic iridium(III) complexes synthesised according to the procedure described in Chapter 2[13] and which are potential luminophores for in-solution immunoassay methods and DNA analysis were investigated. These complexes contain two 2-phenylpyridine (ppy) cyclometalating ligands, and one variably substituted triazole-pyridine ligand (pytl) prepared by click chemistry (Chapter 2).[13–15] The complexes $[Ir(ppy)_2(pytl\text{-}Me)]^+$, $[Ir(ppy)_2(pytl\text{-}\beta CD)]^+$ (βCD = permethylated β-cyclodextrin) and $[Ir(F_2ppy)_2(pytl\text{-}ada)]^+$ (F_2ppy = 2-(2,4-bisfluorophenyl)-pyridine, ada = adamantyl; Scheme 4.1) combined remarkable solubility in water with excellent emission quantum yields and long lifetimes of their excited states. We reported previously in Chapter 2[13] on the very bright green and blue ECL emission of their solutions in air-equilibrated water. Taking advantage of the versatility of the adopted synthetic approach, pytl was also functionalised with a propylamino group; a suitable linker for covalent conjugation with biomolecules.[16] This feature, in combination with the high solubility and the intense photo- and electro-generated luminescence of the corresponding iridium(III) complexes $[Ir(F_2ppy)_2(pytl\text{-}NH_2)]^+$ and $[Ir(ppy)_2(pytl\text{-}NH_2)]^+$ (Scheme 4.1), met all of the requirements for an efficient ECL label for bio-analytical applications.

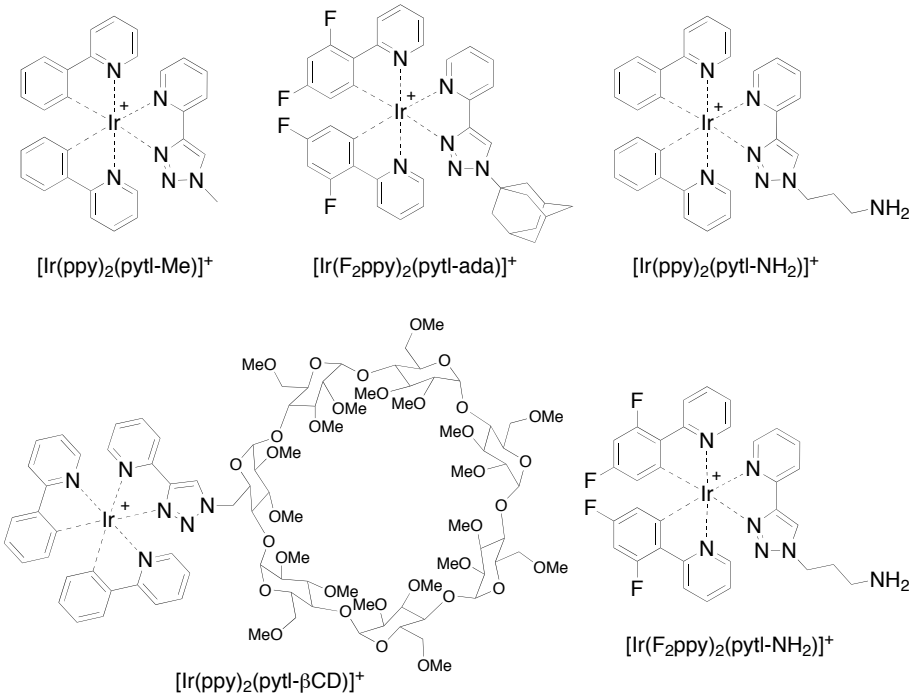

Scheme 4.1 *Chemical structures of the complexes investigated.*

4.2 Principle of ECL

4.2.1 Annihilation ECL

Electrochemiluminescence is a technique based on the conversion of electrical energy into radiative energy. This involves the formation of reactive intermediates from stable precursors, followed by their reaction to form a molecule in its excited state, which is deactivated by an emissive mechanism.

The first detailed studies on ECL involved electron transfer reactions between oxidised and reduced species, which were both generated at the same electrode by alternate pulsing of the electrode potential.[2,3,17,18] This approach is typically called "annihilation" and the general mechanism is outlined in Scheme 4.2.

(1) $R \longrightarrow R^{\bullet+} + e^-$ (oxidation at electrode)

(2) $R + e^- \longrightarrow R^{\bullet-}$ (reduction at electrode)

(3) $R^{\bullet+} + R^{\bullet-} \longrightarrow R + R^*$ (excited state formation)

(4) $R^* \longrightarrow R + h\nu$ (light emission)

Scheme 4.2 *Annihilation ECL mechanism.*

One example is the ECL from $[Ru(bpy)_3]^{2+}$, which was first reported in 1972 using acetonitrile as the solvent and in the presence of tetrabutylammonium tetrafluoroborate ($TBABF_4$) as an electrolyte.[19] ECL was generated by rapidly alternating the electrode potential to form oxidised $[Ru(bpy)_3]^{3+}$ and reduced $[Ru(bpy)_3]^{+}$ species (Figure 4.1).

In a typical annihilation experiment, a platinum electrode is immersed in a quiescent solution and the electrode potential is held at a value where no electrochemical activity occurs (such as 0.0 V). The potential is then quickly changed to anodic or cathodic values at which the first reagent is produced ($R^{\bullet+}$, Scheme 4.2, Eq. (1)) and then to the potential at which the second reagent is generated ($R^{\bullet-}$, Scheme 4.2, Eq. (2)). During the second step, both reagents exist in the diffusion layer near the electrode and can react, resulting in the emission of light (Scheme 4.2, Eq. (4)).

The exchange of one electron between the $R^{\bullet}$ (Scheme 4.2, Eq. (3)) species generates the excited molecule $[Ru(bpy)_3]^{2+*}$, which emits one photon of light, $h\nu$. The excited state formed in this process is similar to that formed during photoexcitation (i.e., photoluminescence (PL)). In PL, an electron is excited from metal-based $d\pi$ orbitals to ligand-based π^* orbitals (metal-

to-ligand charge transfer (MLCT)).[20–22] The excited electron then undergoes intersystem crossing to the lowest triplet states of $[Ru(bpy)_3]^{2+*}$.[20,21,23] The ^{3}MLCT excited state may be formed in ECL if an electron is transferred to the π^* orbital of one of the bipyridine ligands. $[Ru(bpy)_3]^{2+*}$ can then decay to the ground state, producing the same luminescence as that obtained from PL spectroscopy.[5]

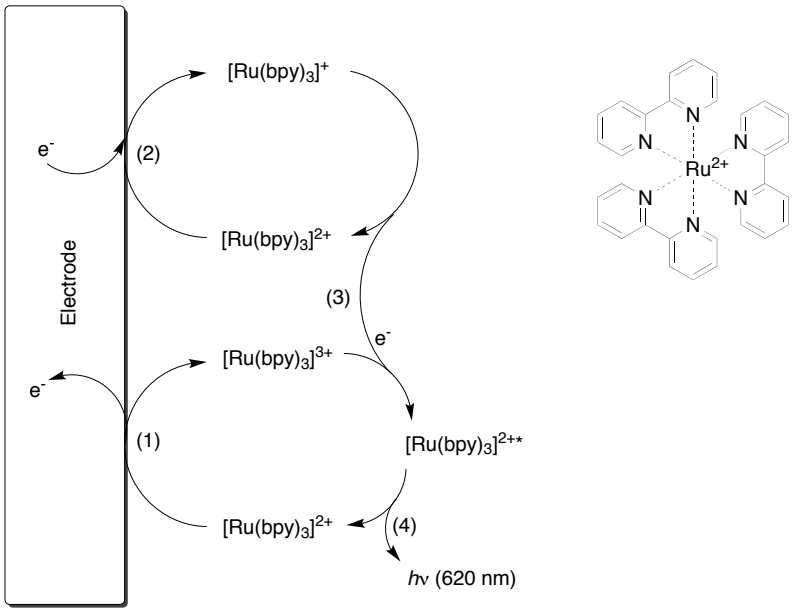

Figure 4.1 *Structure of $[Ru(bpy)_3]^{2+}$ and the proposed mechanism for the $[Ru(bpy)_3]^{3+}$/$[Ru(bpy)_3]^{+}$ ECL system.*

4.2.2 Coreactant ECL

Another mechanism to generate light through ECL is known as coreactant ECL. Unlike ion annihilation ECL, in which a double-potential step (e.g., oxidation followed by reduction) is required to generate the highly energetic precursors, in coreactant ECL the electrode oxidises *or* reduces all of the reagents in a *single*-potential step. The process is performed in a solution containing the luminophore and a specific reagent (coreactant) added deliberately. Depending on the polarity of the applied potential, both the luminophore and coreactant species can be oxidised *or* reduced to form radicals. Subsequently, the coreactant decomposes to produce a powerful reducing or oxidising species that reacts with the oxidised or reduced luminophore to generate emissive excited states. At present, all commercially available ECL analytical instruments are based on coreactant ECL technology. An example of such a system is the commercially important system $[Ru(bpy)_3]^{2+}$/TPrA (TPrA = tri-*n*-propylamine; Figure 4.2).[5,24]

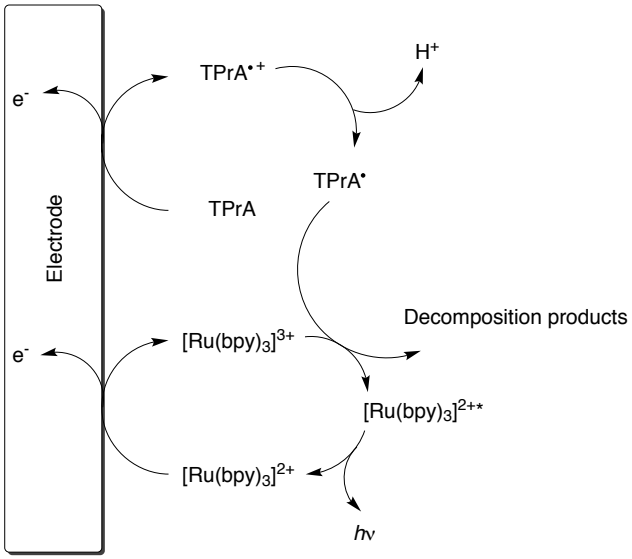

Figure 4.2 *The coreactant ECL mechanism.*

In this system, the ECL signal is produced upon concomitant oxidation of $[Ru(bpy)_3]^{2+}$ and TPrA (Figure 4.2). The short-lived TPrA radical cation ($[TPrA]^{\bullet+}$) is believed to lose a proton from one of the carbon atoms adjacent to the nitrogen, forming the strongly reducing intermediate $[TPrA]^{\bullet}$ (Scheme 4.3). This radical can then reduce $[Ru(bpy)_3]^{3+}$ to $[Ru(bpy)_3]^{2+*}$.

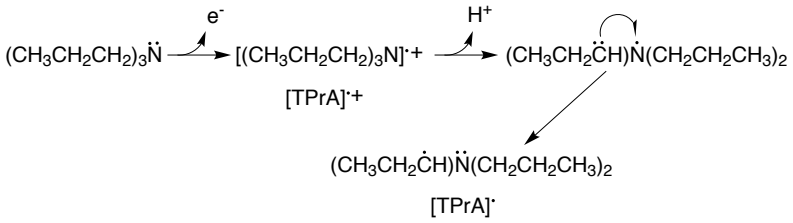

Scheme 4.3 *Proposed mechanism for the formation of the radical [TPrA]•.*

Details of the coreactant ECL mechanism are not completely understood and are still under investigation.[25–27] However, the great similarity of the PL and ECL spectra suggests that the emission process in ECL involves the MLCT state of $[Ru(bpy)_3]^{2+}$.

A good ECL coreactant needs to meet a number of criteria, which include solubility, stability, electrochemical properties, kinetics, ECL background, etc.[28] Amines are suitable candidates, but, as shown in Scheme 4.3, the presence of hydrogen on carbon bound to the nitrogen atom is required.

Analogous to TPrA, a wide range of amine compounds can be used as coreactants in redox reactions with a luminophore. Recently, 2-(dibutylamino)ethanol (DBAE) was reported as a

new oxidative coreactant for the $[Ru(bpy)_3]^{2+}$ ECL system.[29] This compound was preferred to the commonly used TPrA because it is less toxic, more water soluble, and gives a more intense ECL signal. The ECL intensity of the $[Ru(bpy)_3]^{2+}$/DBAE system at Pt electrodes in the presence of 0.10 M phosphate buffer (pH = 7.5) was approximately 100 times greater than that of the commonly used $[Ru(bpy)_3]^{2+}$/TPrA system.[29] The ECL enhancement of DBAE was attributed to the catalytic effect of hydroxyethyl group towards the direct oxidation of DBAE at the electrode. This promising coreactant was also highly efficient in combination with iridium complexes[30] and was, therefore, chosen in the investigation of our iridium complexes. The proposed ECL mechanism for the system Ir/DBAE is analogous to that of $[Ru(bpy)_3]^{2+}$/DBAE (Figure 4.2) and is schematically represented in Figure 4.3.

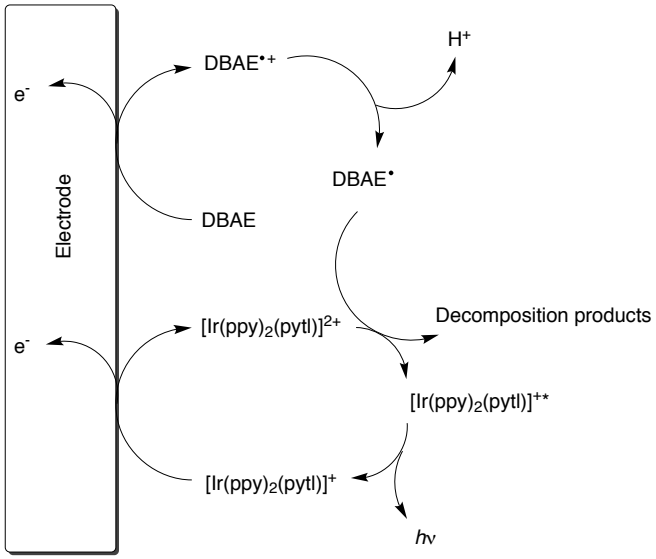

Figure 4.3 *Basic scheme for excited-state generation by electrochemical oxidation of DBAE and iridium complexes.*

The different mechanisms of annihilation and coreactant ECL imply different limitations to their applicability. Analytical applications are possible with annihilation ECL systems; however, they usually require purified, non-aqueous solvents. In fact, the potential window for the electrochemical oxidation and reduction of water is too narrow to generate both the radical anion and cation needed for annihilation. Coreactants, on the other hand, are generated by using potential steps in only one direction, allowing the generation of ECL in aqueous solution. Furthermore, this technology may eliminate the oxygen-quenching effect often encountered in ion annihilation ECL by working at oxidative potential. Thus, ECL analysis can also be performed in the presence of air. The use of a coreactants also makes it possible to

measure the ECL signal of fluorescent compounds for which either reduction or oxidation is a reversible process.

4.2.3 ECL in immunometric assays and clinical applications

ECL has been successfully applied in clinical analytical laboratories and in industry. Nowadays, several commercially available ECL immunoassays and methods for DNA analysis allow the detection of the concentration, or simply the presence, of specific proteins and DNA sequences. The assay format more commonly used for tests for biomolecules is the introduction of a traceable label in the analyte and the successive use of the specific signal of the marker for detection. The intensity of the detected signal is proportional to the analyte concentration. Classical labelling methodologies used in immunoassay are chemi-luminescence (e.g., fluorescein) and fluorescence. This approach has been successfully extended to electrochemiluminescent dyes. The majority of commercially available ECL-based detection systems are based on the concomitant oxidation of $[Ru(bpy)_3]^{2+}$ and TPrA in phosphate buffer solutions. An example of immunometric methods is the sandwich interaction antibody/antigen/antibody in which an antibody is immobilised on the working electrode surface (Figures 4.4 and 4.5 B).[31] The antigenic analytes in solution are captured by the immobilised antibody and then targeted by the labeled antibody specific for the analyte. When the sandwich interaction takes place, the ECL signal is detected, with an intensity proportional to the number of coupling sites. The use of different types of specific interactions lead to different assay formats (Figure 4.5).

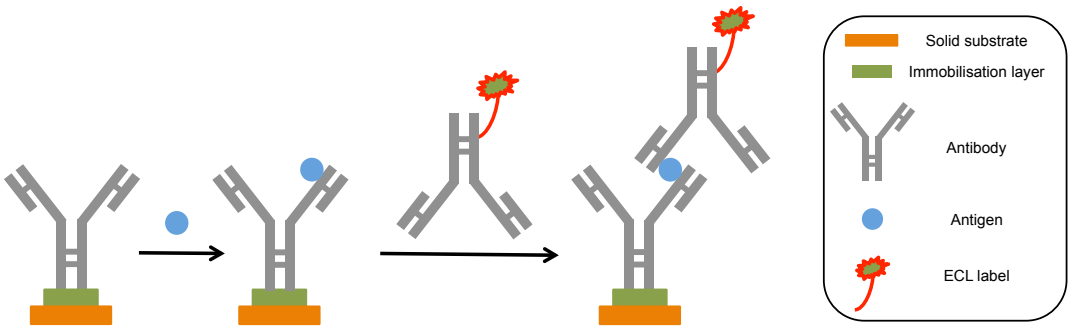

Figure 4.4 *Typical assay format of immunological methods based on ECL.*[31]

The most successful applications of ECL techniques are in the clinical area and are related to the monitoring of biomolecules, the presence of which is associated with genetic or viral diseases and dysfunctions of human metabolism. Examples of investigated compounds are hormones, enzymes, proteins, nucleic acids, and antibodies. The tests are normally performed

on biological fluids such as blood, serum, plasma, and urine. The high sensitivity and matrix independence of ECL allow its successful employment in clinical tests where well-established techniques (e.g., fluorescence) encounter difficulties. A number of ECL-based clinical tests have been summarised recently in a review;[32] the majority of methods employ TPrA as coreactant in aqueous buffer.

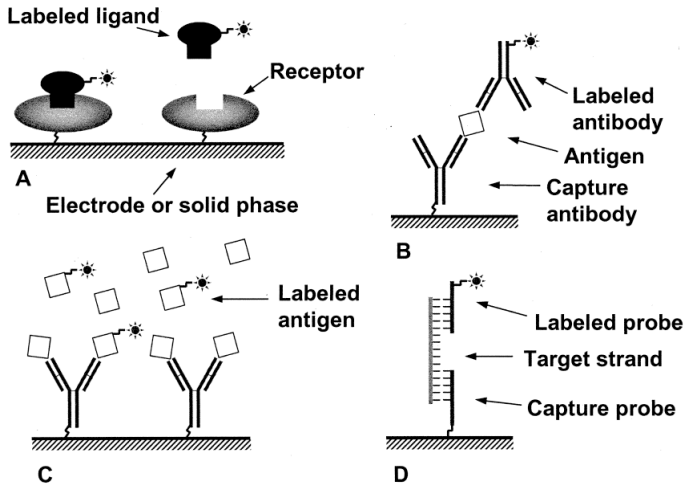

Figure 4.5 *Commonly used assay formats for ECL-based genomics and proteomics. a) Receptor-ligand assay, b) "sandwich" immunoassay, c) competition assay, and d) capture of a target oligonucleotide by using two partially complementary capture and labeled strands.*

Although ECL has found many interesting diagnostic applications, the most important one remains genomics. Inside a cell each protein is synthesised according to the sequence of the base pairs in a specific part of its DNA. Modification of a sequence can result in disease. Cancer is one of the possible consequences of DNA mutations; this consideration reveals the importance of a sensitive method to detect deviations in DNA structure. To recognise specific DNA sequences, synthetic oligonucleotides are used as probes and immobilised on a solid substrate. Only if the target nucleic acid strand is complementary to the probe will they combine to form a double strand (hybridisation). If at this point the target oligonucleotide interacts with a partially complementary strand labeled with an ECL-active molecule, such as $[Ru(bpy)_3]^{2+}$, detection of light is confirmation of the presence of the sequence in question in the sample.

4.3 ECL instrumentation

The basic components of an ECL instrument include an electrical energy supply necessary for redox processes, an electrochemical cell, and an optical detector for the measurement of either the emitted light intensity (as photocurrent or counts per second) or its spectroscopic response.[4,33] Although a number of ECL instruments are now commercially available, most of the ECL studies reported in the literature have been carried out on home-made instruments. The instrument used in these studies was a highly flexible and modular home-made instrument assembled by Dr. Simone Zanarini in the group of Prof. Paolucci in Bologna.[34] The ECL quantum efficiency is defined as the ratio of the number of photons emitted to the number of annihilations between the oxidised and reduced species. It is usually reported as a relative ECL value with respect to a reference compound with suitable, stable, and well-established ECL properties. In our studies the reference compound was the coordination complex $[Ru(bpy)_3]^{2+}$.[19]

The main spectroscopic components of this instrument are as follow: a dark box with a mobile cell holder (home-made), a dual-exit monochromator, a photo-diode silicon detector, a photomultiplier (PMT) detector, and a current-sensitive preamplifier (Figure 4.6).

The presence of two detectors allows the measurement of photoemission from both very weak (detector: PMT) and very intense (detector: silicon photodiode) sources. The detector change can easily be made by software controlling the position of a motorised mirror. The general setup of spectroscopic and electrochemical components is shown in Figure 4.6. The electrochemical cell is positioned inside a dark box, which is located in connection to the monochromator entrance slit. An opening in the dark box is directed towards the monochromator and allows the signal to reach the detector. The spectral hub interface allows control of the monochromator parameters and PMT high voltage through the operating software. This hub is also used to acquire data and direct them to the software. The monochromator is provided with one entrance slit and two exit slits. All slit widths can be adjusted by using micrometric screws positioned on the top of the slot.[34]

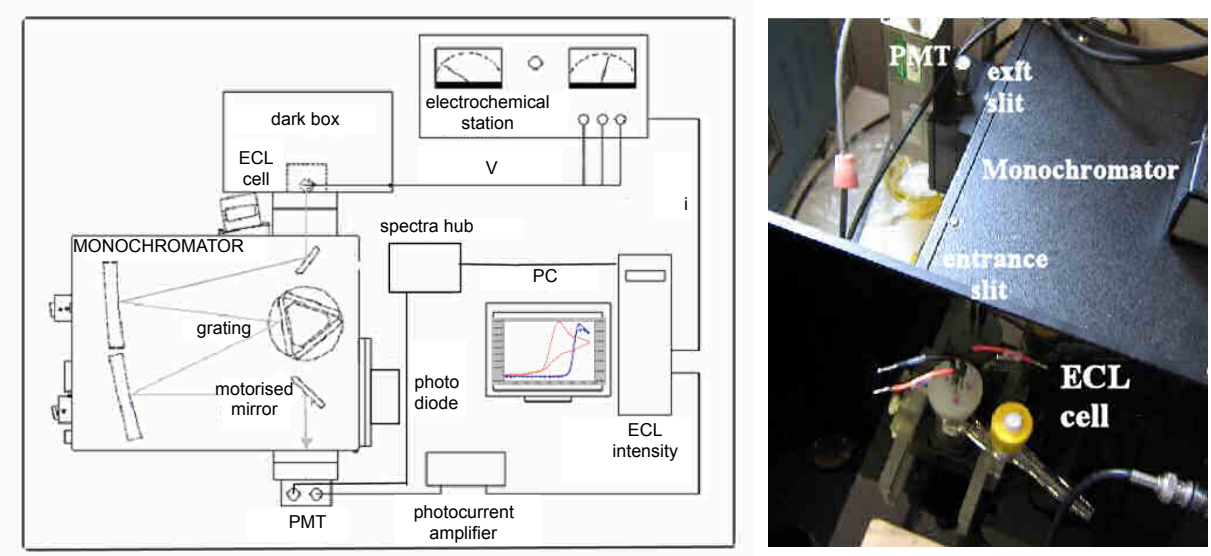

Figure 4.6 *Left: general scheme of the ECL instrument; right: top view of the ECL cell and monochromator from the entrance slit.*[34]

4.4 Results and discussion

In Chapter 2[13] we described the synthesis and characterisation of a series of new ionic heteroleptic iridium complexes containing two ppy cyclometalating ligands, and one variably substituted pytl prepared by click chemistry.[13] The complexes $[Ir(ppy)_2(pytl\text{-}Me)]^+$, $[Ir(ppy)_2(pytl\text{-}\beta CD)]^+$, and $[Ir(F_2ppy)_2(pytl\text{-}ada)]^+$ (Scheme 4.1) combined good solubility in water with excellent emission quantum yields and long lifetimes of their excited states.[13] Due to their interesting photophysical properties, these complexes were proposed as favourable emitters for ECL. Dr. Simone Zanarini investigated the ECL emission of their solutions in air-equilibrated phosphate buffer. Taking advantage of the versatility of our synthetic approach, the pytl ligand was then functionalised with an alkylamino group; a common linker for bio-conjugation reactions.[16] Such a property combines the solubility and intense photo- and electro-generated luminescence in the ensuing complexes, $[Ir(F_2ppy)_2(pytl\text{-}NH_2)]^+$ and $[Ir(ppy)_2(pytl\text{-}NH_2)]^+$ (Scheme 4.1), which thus meet all of the requirements for effective use as ECL labels in bio-analytical applications.

Preliminary electrochemical studies of the complexes were performed in aqueous media and argon-degassed acetonitrile. In the first case no electrochemical process was visible due to the rather narrow potential window of aqueous buffer solutions. Instead, quasi-reversible oxidation processes were, in general, detected for all compounds in acetonitrile. The only exceptions were the two amino derivatives, which showed a higher degree of irreversibility

(Figures 4.7 and 4.8 and Table 4.1). This is probably due to the irreversible oxidation of the free amino groups.

Based on the above results, ECL was generated in 0.1 mM[35] iridium complex, 0.1 M phosphate buffer solutions also containing 30 mM DBAE as coreactant, at potentials where the iridium complex and the coreactant were simultaneously oxidised.[29,30] The recorded light/potential profiles are shown in Figure 4.9. ECL and electrochemical measurements were carried out with a working electrode consisting of a side-oriented Pt disk electrode sealed in glass. The counter electrode consisted of a Pt spiral, while the reference electrode was a saturated KCl/Ag/AgCl electrode (aqueous media) or an Ag quasi-reference electrode (Ag/AgCl, with ferrocene standard; acetonitrile).

All complexes showed an ECL intensity comparable to that of $[Ru(bpy)_3]^{2+}$ under similar conditions (Table 4.1). The highest ECL intensity was obtained with $[Ir(ppy)_2(pytl\text{-}\beta CD)]^+$, which is an expected consequence of its relatively high PL quantum efficiency and solubility (Chapter 2).[13] In the case of $[Ir(ppy)_2(pytl\text{-}NH_2)]^+$and $[Ir(F_2ppy)_2(pytl\text{-}NH_2)]^+$, rapid electrode fouling was observed during the experiments; this brought about a large decrease in both the anodic current and ECL emission, as soon as during the second voltammetric cycle.

To stabilise and maximise the ECL emission, a very negative potential (–2.5 V vs. Ag) was applied at the working electrode prior to each measurement.

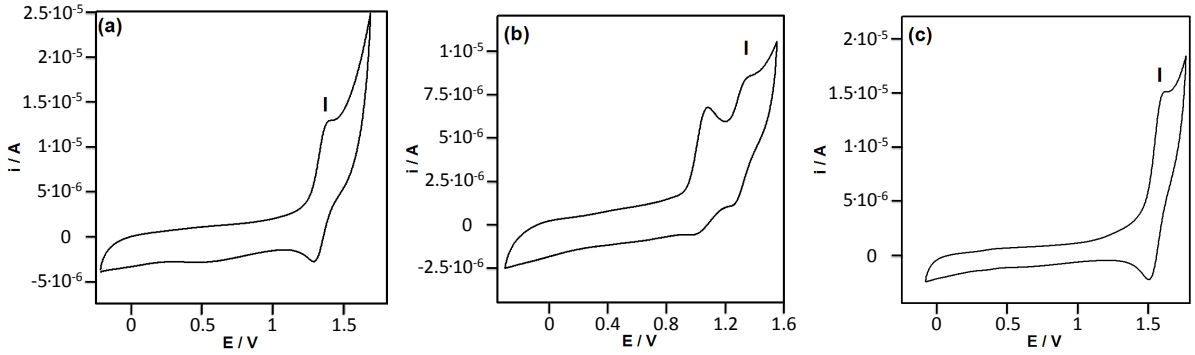

Figure 4.7 *Cyclic voltammetry curves in acetonitrile containing 0.1 M tetrabutylammonium hexafluorophosphate as the supporting electrolyte. Scan rate 0.2 V s^{-1}. The symbol "I" indicates the oxidation peak ascribed to our complexes. a) 1 mM $[Ir(ppy)_2(pytl\text{-}Me)]PF_6$; b) 0.5 mM $[Ir(ppy)_2(pytl\text{-}\beta CD)]Cl$; and c) 1 mM $[Ir(F_2ppy)_2(pytl\text{-}ada)]PF_6$. Potentials are versus Ag/AgCl. Please note that the first peak in (b) is related to partially reversible electrochemical oxidation of Cl^- to Cl_2.*

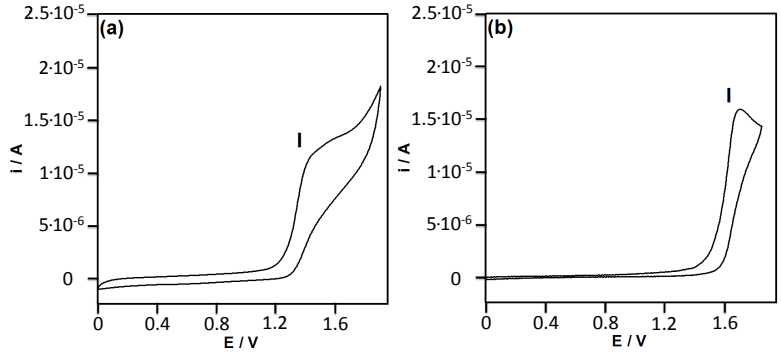

Figure 4.8 *Cyclic voltammetry curves in acetonitrile containing 1 mM tetrabutylammonium hexafluorophosphate as the supporting electrolyte. Scan rate 0.2 V/s. a) 1 mM [Ir(ppy)$_2$(pytl-NH$_2$)]PF$_6$ and b) 1 mM [Ir(F$_2$ppy)$_2$(pytl-NH$_2$)]PF$_6$. Potentials are versus Ag/AgCl. The oxidation peaks ascribed to our complexes are labeled with "I".*

The ensuing vigorous formation of hydrogen bubbles efficiently removed the passivating film and regenerated a clean electrode surface.[36] It is important to note that the irreversible oxidation of the free amino group and fouling of the electrode are problems that are not expect to interfere when the iridium complexes are conjugated to biological molecules. The amino group is probably stable when functionalised, such as with an amide, and the corresponding complexes will provide reliable electrochemical behaviour and a stable ECL signal.

Table 4.1 *Summary of relevant electrochemical, photophysical and ECL properties.*

Complex	E_{ox}[a]	Φ_{PL}[b]	$\lambda_{max,PL}$[b]	$E_{max,ECL}$[c]	$I_{max,rel}$[d]	$\lambda_{max,ECL}$
[Ru(bpy)$_3$]$^{2+}$	+1.23 V	0.04	615 nm	+1.21 V	1.00	615 nm
[Ir(ppy)$_2$(pytl-Me)]$^+$	+1.33 V	0.35	475 nm	+1.28 V	0.34	490 nm
[Ir(ppy)$_2$(pytl-βCD)]$^+$	+1.31 V	0.54	475 nm	+1.31 V	0.51	490 nm
[Ir(F$_2$ppy)$_2$(pytl-ada)]$^+$	+1.59 V	0.16	450 nm	+1.57 V	0.27	470 nm
[Ir(ppy)$_2$(pytl-NH$_2$)]$^+$	+1.30 V[e]	0.31	475 nm	+ 1.29 V	0.22	492 nm
[Ir(F$_2$ppy)$_2$(pytl-NH$_2$)]$^+$	+1.60 V[e]	0.10	452 nm	+ 1.59 V	0.15	473 nm

a, Ar-saturated 10^{-3} M complexes in MeCN at 0.2 V s^{-1} scan rate; potentials are versus Ag/AgCl; b, Ar-saturated water, excitation wavelength 402 nm for iridium and 448 nm for ruthenium from Chapter 2;[13] c, potentials are versus Ag/AgCl; d, ECL relative intensity with respect to [Ru(bpy)$_3$]$^{2+}$; e, irreversible process; anodic peak potential.

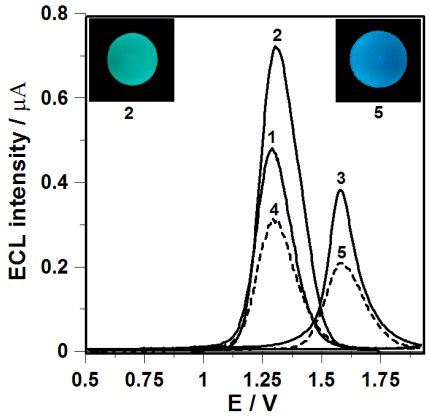

Figure 4.9 *ECL intensity versus potential profile in 0.1 M phosphate buffer/30 mM DBAE. The concentration of the Ir complex was 0.1 mM. 1) [Ir(ppy)$_2$(pytl-Me)]Cl; 2) [Ir(ppy)$_2$(pytl-βCD)]Cl; 3) [Ir(F$_2$ppy)$_2$(pytl-ada)]Cl; 4) [Ir(ppy)$_2$(pytl-NH$_2$)]Cl; and 5) [Ir(F$_2$ppy)$_2$(pytl-NH$_2$)]Cl. Switching method: CV; E_0 = 0 V, E_1 = +1.8 V, E_2 = –2.5 V, scan rate = 0.2 V s^{-1}. Working electrode: Pt disc. Potentials are versus Ag/AgCl. Insets: images of the electrode during emission with the specified compound.*

The ECL intensity versus potential curves given in Figure 4.9 show a single intense peak associated, in all cases, with electrochemical oxidation of the iridium centres. This is supported by the good agreement between the $E_{max,ECL}$ values in phosphate buffer and the E_{ox} values measured in acetonitrile/TBAPF$_6$ (see Table 4.1 and Figure 4.3 for a basic scheme of the mechanism). At the same time, the ECL spectra of the five iridium complexes (Figure 4.10) are characterised by a single emission band at a wavelength compatible with the photoemission of these compounds (Table 4.1 and Figure 4.11).

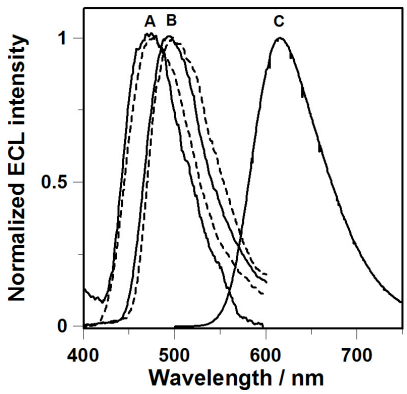

Figure 4.10 *ECL spectra in phosphate buffer/DBAE. A) [Ir(F$_2$ppy)$_2$(pytl-ada)]Cl (solid line) and [Ir(F$_2$ppy)$_2$(pytl-NH$_2$)]Cl (dashed line); B) [Ir(ppy)$_2$(pytl-Me)]Cl (solid line) and [Ir(ppy)$_2$(pytl-NH$_2$)]Cl (dashed line); and C) [Ru(bpy)$_3$]Cl$_2$. Switching program: E_1 = –2.5 V, t_1 =0.5 s; E_2 = +1.5 V, t_2 =0.3 s. Working electrode: Pt disc.*

This is in agreement with the hypothesis that the same excited states are involved in the generation of both luminescent phenomena. As a consequence, chemical variations in the coordination sphere should have similar effects on photo- and electrochemically generated luminescence. Fluorination of the phenyl rings in the ppy ligands gives rise to a blue shift of the PL (Chapter 2);[13] the same phenomenon was observed for the ECL (Table 4.1 and Figures 4.10 and 4.11). Importantly, the profiles reported in Figure 4.10 also show that none of the emissions of the complexes investigated have any significant overlap with that of $[Ru(bpy)_3]^{2+}$; their use in combination with $[Ru(bpy)_3]^{2+}$ would then allow at least two ECL colours in water to be registered without the need for an optical filter.

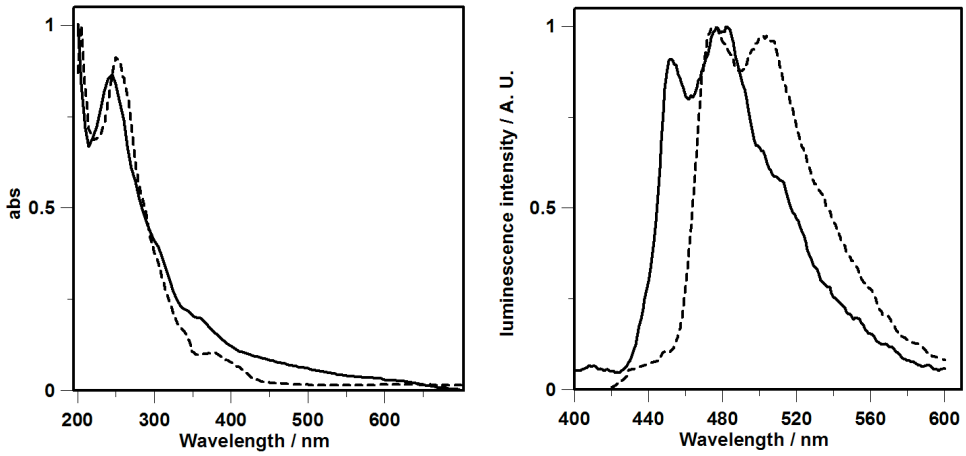

Figure 4.11 *Normalised absorption (left) and emission spectra (right) in Ar-saturated water. $[Ir(ppy)_2(pytl\text{-}NH_2)]PF_6$ (dashed line); $[Ir(F_2ppy)_2(pytl\text{-}NH_2)]PF_6$ (solid line).*

4.5 Conclusion

In summary, the present ionic triazole-pyridine-based Ir^{III} complexes showed enhanced ECL performance relative to previously reported Ir^{III} species.[9,37] Their very bright green and blue ECL emissions, observed earlier (Chapter 2)[13] as PL, were obtained in air-equilibrated aqueous media. Amine-appended side chains were easily introduced into the structures of the luminophores. The presence of the amino group did not significantly affect their ECL properties, but could provide a potential link for the functionalisation of biomolecules and solid substrates to be used in diagnostics. Under the operating conditions, the free amino terminus underwent irreversible oxidation, resulting in electrode fouling. This problem, however, should not occur when the iridium complex is conjugated to other molecules, since the functionalised amino group is expected to be stable under oxidative conditions. The emission energy was suitably modulated by fluorination of the ppy ligand. The new labels

developed herein summarise all of the fundamental characteristics required for efficient multicolour ECL-based nucleic acid and protein assays.

4.6 Acknowledgments

A special thanks to Dr. Simone Zanarini who performed the measurements described in this chapter. Many thanks also to Prof. Francesco Paolucci and Prof. Luca Prodi for the fruitful collaboration.

4.7 Experimental

4.7.1 Methods and materials

General. THF was purified by distillation under nitrogen from sodium/benzophenone. Compounds 3-azidopropan-1-amine,[38] $[(ppy)_2Ir(\mu\text{-}Cl)_2Ir(ppy)_2]$,[39] and $[(F_2ppy)_2Ir(\mu\text{-}Cl)_2Ir(F_2ppy)_2]$[39] were prepared according to literature procedures. Compounds pytl-Me, $[Ir(ppy)_2(pytl\text{-}\beta CD)]Cl$ and $[Ir(F_2ppy)_2(pytl\text{-}ada)]Cl$ were prepared as described in Chapter 2.[13] The complex $[Ir(F_2ppy)_2(pytl\text{-}ada)]Cl$ was obtained as the PF_6^- salt by precipitation from an aqueous solution by adding an excess of NH_4PF_6. All other chemicals were purchased from Aldrich, Fluka, or Acros and used as received. Analytical thin-layer chromatography (TLC) was performed on Merck precoated silica gel 60 F-254 plates (layer thickness 0.25 mm) and the compounds were visualised by UV irradiation at λ = 254 and/or 366 nm and by staining with phosphomolybdic acid reagent or $KMnO_4$. Purifications by silica gel chromatography were performed using Acros (0.035–0.070 mm, pore diameter ca. 6 nm) silica gel. The "magic mixture" eluent was a mixture of water (300 mL), sodium chloride (30 g), acetonitrile (1200 mL), and methanol (300 mL). All click reactions were performed under Schlenk conditions by using an oxygen-free atmosphere of nitrogen and solvents were dried and distilled according to standard laboratory procedures.

NMR spectroscopy. ^{1}H NMR spectra were recorded at 25 °C on Varian Inova 400 or Bruker DMX-300 spectrometers operating at 400 and 300 MHz, respectively. ^{13}C NMR spectra were recorded on a Bruker DMX-300 spectrometer operating at 75 MHz. ^{1}H NMR chemical shifts (δ) are reported in parts per million (ppm) relative to the residual proton signal of the solvent, δ = 3.31 ppm for CD_3OD, δ = 7.26 ppm for $CDCl_3$, and δ = 2.50 ppm for DMSO-d_6. Multiplicities are reported as follow: s (singlet), d (doublet), t (triplet), q (quartet), dd (doublet of doublets), ddd (doublet of doublet of doublets), or m (multiplet). Broad peaks are indicated by b. Coupling constants are reported as a J value in Hertz (Hz). The number of protons (n) for a given resonance is indicated as nH, and is based on spectral integration values. The signals of the protons on amino groups could not be observed due to fast exchange processes. ^{13}C NMR chemical shifts (δ) are reported in ppm relative to the carbon signal of the solvent, δ = 49.0 ppm for CD_3OD, δ = 77 ppm for $CDCl_3$, and δ = 40 ppm for DMSO-d_6. The resolution of ^{13}C spectra was increased when necessary by performing an exponential apodisation of the FID.

Mass spectrometry (MS). All mass analyses were performed with electrospray (ESI) techniques. High-resolution mass spectrometry (HRMS) measurements were performed on a JEOL AccuTOF instrument by using water, acetonitrile or methanol as solvents. Standard MS measurements were performed on a Finnigan LCQ Advantage Max instrument by using water, acetonitrile or methanol as solvents.

High-performance liquid chromatography (HPLC). HPLC was carried out on a Shimadzu LC-20AT HPLC system equipped with UV-vis detector SPD-10AV and a fraction collector. Columns were purchased from Dr. Maisch GmbH. The compounds were purified on a mg scale by using a semi-preparative reversed-phase column. An aliquot of solution (2 mL) was injected in a ReproSil 100 C8, 5 μm (250 × 10 mm) column operating at 30 °C. The detection wavelengths were fixed at 254 and 215 nm. A gradient of water and acetonitrile containing 0.1% v/v trifluoroacetic acid (TFA) was used as the mobile phase, with a flow rate of 4 mL min^{-1}. In all cases, the samples were prepared by dissolving the compound in a mixture of water/acetonitrile and filtering the solution on a Nylon syringe filter (0.2 μm).

Electrochemical and ECL experimental setup. ECL and electrochemical measurements were carried out with an Autolab electrochemical station (Ecochemie, Mod. PGSTAT 30). The working electrode consisted of a side-oriented Pt disk electrode sealed in glass (φ = 2 mm). The counter electrode consisted of a Pt spiral, while the reference electrode was a saturated KCl/Ag/AgCl electrode (aqueous media) or a Ag quasi-reference electrode (Ag/AgCl, ferrocene standard; acetonitrile). For ECL generation 30 mM DBAE was added as an oxidative co-reactant in 0.1 M phosphate buffer solution. The ECL signal was obtained in single oxidative steps by generating, at the same time, the amine and iridium complex in their oxidised forms, according to known mechanisms.[28,29] The ECL signal during cyclic voltammetry was measured with a photomultiplier tube (PMT, Hamamatsu model R928P) placed a few millimeters in front of the working electrode, inside a dark box. A voltage of 750 V was supplied to the PMT. The light/current/voltages curves were recorded by collecting the preamplified PMT output signal (by using a Keithley Mod. 6485 picoamperometer) with the second input channel of the ADC module of the Autolab instrument. ECL spectra were recorded by inserting the same PMT in a dual exit monochromator (Acton Research Spectra Pro2300i) and collecting the signal as described above.

Photophysical measurements. Absorbance spectra were collected with a Cary 5 UV-vis-NIR spectrophotometer and the PL was investigated with a Varian (model Cary Eclipse) fluorimeter by using a 10 mm quartz cuvette with fittings for Ar degassing and for connection to a vacuum line.

4.7.2 Synthesis and characterisation

3-[4-(Pyridin-2-yl)-1*H*-1,2,3-triazol-1-yl]propan-1-amine (pytl-NH_2). Distilled THF was bubbled with nitrogen for 1 h prior to use to remove oxygen. 3-Azidopropan-1-amine (563 mg, 5.62 mmol) and 2-ethynylpyridine (567.6 μL, 5.62 mmol) were added to a Schlenk tube under a nitrogen atmosphere and dissolved in deoxygenated THF (15 mL). A solution of CuBr (201.55 mg, 1.41 mmol) and *N*,*N*,*N*′,*N*′,*N*-pentamethyldiethylenetriamine (PMDTA; 352.0 μL, 1.69 mmol) was prepared by dissolving both reagents in deoxygenated THF (5 mL) and bubbling nitrogen through the solution for 20 min to prevent oxidation of copper(I). When the CuPMDTA complex dissolved, the solution became slightly green, and an aliquot of it (2 mL) was added to the Schlenk tube. The resulting mixture was stirred in the dark, at room temperature under a nitrogen atmosphere, for 2 h. The reaction was followed by TLC (eluent: methanol/chloroform/triethylamine 30/68.5/1.5 v/v/v). No workup was done and, after removal of the solvent *in vacuo*, the crude material was recrystallised twice from methanol/diethyl ether. The product was obtained as a white solid (982.3 mg, 86%). ^{1}H NMR (400 MHz, CD_3OD): δ ppm 8.55 (ddd, J = 4.9, 1.7, 0.9 Hz, 1H), 8.44 (s, 1H), 8.03 (ddd, J = 8.0, 1.1, 1.0 Hz, 1H), 7.88 (ddd, J = 7.9, 7.8, 1.8 Hz, 1H), 7.34 (ddd, J = 7.6, 4.9, 1.2 Hz, 1H), 4.57 (t, J = 7.0 Hz, 2H), 2.77 (t, J = 7.0 Hz, 2H), 2.16 (q, J = 7.0 Hz, 2H); ^{13}C NMR (75 MHz, CD_3OD): δ ppm 151.0, 150.5, 148.7, 138.8, 124.5, 124.3, 121.5, 49.1, 39.2, 33.2; HRMS (ES+, $CHCl_3/CH_3OH$): *m/z* calcd for $C_{10}H_{13}N_5Na$: 226.10686; found: 226.10544 $[M+Na]^+$.

[Ir(ppy)$_2$(pytl-NH$_2$)]PF$_6$. Solid pytl-NH$_2$ (85.36 mg, 0.42 mmol) was added to a suspension of [(ppy)$_2$Ir(μ-Cl)$_2$Ir(ppy)$_2$] (224 mg, 0.21 mmol) in methanol/chloroform (1/3 v/v; 9 mL). The suspension was heated to 50 °C and stirred for 2 h. The reaction was followed by TLC (eluent: magic mixture) by which, under UV light at 366 nm, the product appeared as a bright-green luminescent spot. No workup was done and, after removal of the solvent *in vacuo*, the crude material was purified by HPLC. The mobile phase was a gradient of water and acetonitrile (from 90/10 to 1/1 v/v of water in 30 min, to 10/90 v/v in 10 min). The HPLC fractions containing the desired iridium complex were identified by ESI-MS, collected, and a solution of NaOH (1 N) was added until the pH was between 7 and 8. The solvent was removed *in vacuo*. The yellow solid was dissolved in demineralised water, filtered on paper, and precipitated as the PF_6^- salt by the addition of a saturated aqueous solution of NH_4PF_6. The precipitate was filtered, washed with water, and dried. The pure product was obtained as a yellow solid (260.1 mg, 88%). To exchange the counterion to chloride, the yellow solid was first dissolved in dry acetone and the solution filtered on paper. The complex was then precipitated by the addition of a saturated solution of tetrabutylammonium chloride (TBACl) in acetone. The solid was filtered, washed with dry acetone, and dried *in vacuo*. ^{1}H NMR (400 MHz, CD_3OD): δ ppm 9.20 (s, 1H), 8.34 (ddd, J = 7.9, 1.3, 0.9 Hz, 1H), 8.10 (ddd, J = 7.7, 7.7, 1.6 Hz, 1H), 8.12–8.07 (m, 2H), 7.89–7.84 (m, 3H), 7.82–7.79 (m, 1H), 7.79 (ddd, J = 5.8, 1.5, 0.7 Hz, 1H), 7.72 (bdd, J = 7.7, 1.3 Hz, 1H), 7.65 (ddd, J = 5.8, 1.5, 0.8 Hz, 1H), 7.40 (ddd, J = 7.7, 5.5, 1.3 Hz, 1H),7.15 (ddd, J = 7.3, 5.8, 1.4 Hz, 1H), 7.06 (ddd, J = 7.3, 5.8, 1.4 Hz, 1H), 7.02 (ddd, J = 7.8, 7.3, 1.2 Hz, 1H), 6.92 (ddd, J = 7.8, 7.3, 1.2 Hz, 1H), 6.88 (ddd, J = 7.5, 7.4, 1.3 Hz, 1H), 6.77 (ddd, J = 7.5, 7.3, 1.3 Hz, 1H), 6.28 (ddd, J = 7.6, 1.2, 0.5 Hz, 1H), 6.25 (ddd, J = 7.6, 1.2, 0.5 Hz, 1H), 4.70–4.58 (m, 2H), 3.03–2.91 (m, 2H), 2.37–2.24 (m, 2H); ^{13}C NMR (75 MHz, CD_3OD): δ ppm 169.8, 169.0, 151.4, 150.91, 150.87, 150.7, 150.03, 150.02, 147.6, 145.5, 145.4, 141.0, 139.6, 139.5, 133.0, 132.6, 131.4, 130.6, 127.85, 127.84, 125.9, 125.4, 124.6, 124.18, 124.15, 123.7, 123.1, 120.9, 120.7, 50.3, 37.9, 28.6; HRMS (ES+, CH_3OH): *m/z* calcd for $C_{32}H_{29}IrN_7$: 704.21137; found: 704.20862 $[M]^+$.

[Ir(F$_2$ppy)$_2$(pytl-NH$_2$)]PF$_6$. Solid pytl-NH$_2$ (8.54 mg, 0.042 mmol) was added to a suspension of [(F$_2$ppy)$_2$Ir(μ-Cl)$_2$Ir(F$_2$ppy)$_2$] (25 mg, 0.021 mmol) in methanol/chloroform (1/3 v/v; 6 mL). The suspension was heated to 50 °C and stirred for 2 h. The reaction was followed by TLC (eluent: magic mixture) by which, under UV light at 366 nm, the product appeared as a bright-green luminescent spot. No workup was done and after removal of the solvent *in vacuo*, the crude material was purified by HPLC. The mobile phase was a gradient of water and acetonitrile (from 80/20 to 30/70 v/v of water in 30 min, to 10/90 v/v in 10 min). The HPLC fractions containing the desired iridium complex were identified by ESI-MS, collected, and a solution of NaOH (1 N) was added until pH = 7–8. The solvent was removed *in vacuo*. The yellow solid was dissolved in demineralised water, filtered on paper, and precipitated as the PF_6^- salt by the addition of a saturated aqueous solution of NH_4PF_6. The precipitate was filtered, washed with water, and dried *in vacuo*. The pure product was obtained as a yellow solid (25.42 mg, 78%). To exchange the counterion to chloride, the yellow solid was first dissolved in dry acetone and the solution filtered on paper. The complex was then precipitated by the addition of a saturated solution of TBACl in acetone. The solid was filtered, washed with dry acetone, and dried *in vacuo*. ^{1}H NMR (400 MHz, CD_3OD): δ ppm 9.04 (s, 1H), 8.36–8.28 (m, 3H), 8.15 (ddd, J = 7.9, 7.8 ,1.5 Hz, 1H), 7.97–7.90 (m, 3H), 7.81 (ddd, J = 5.8, 1.5, 0.6 Hz, 1H), 7.72 (ddd, J = 5.8, 1.5, 0.6 Hz, 1H), 7.48 (ddd, J = 7.6, 5.6, 1.3 Hz, 1H), 7.22 (ddd, J = 7.4, 5.8, 1.3 Hz, 1H), 7.15 (ddd, J = 7.4, 5.9, 1.3 Hz, 1H), 6.68 (ddd, J = 12.6, 9.2, 2.3 Hz, 1H), 6.58 (ddd, J = 12.7, 9.2, 2.4 Hz, 1H), 5.72 (dd, J = 8.5, 2.3 Hz, 1H), 5.66 (dd, J = 8.7, 2.4 Hz, 1H), 4.70–4.57 (m, 2H), 3.04–2.92 (m, 2H), 2.36–2.24 (m, 2H); HRMS (ES+, CH_3OH): *m/z* calcd for $C_{32}H_{25}F_4IrN_7$: 776.17368; found: 776.17458 $[M]^+$.

[Ir(ppy)$_2$(pytl-Me)]PF$_6$. Solid pytl-Me (29.88 mg, 0.187 mmol) was added to a suspension of [(ppy)$_2$Ir(μ-Cl)$_2$Ir(ppy)$_2$] (100 mg, 0.093 mmol) in methanol/chloroform (1/3 v/v; 6 mL). The suspension was heated to 50 °C and stirred for 1 h. The reaction was followed by TLC (eluent: methanol/chloroform 15/85 v/v)

by which, under UV light at 366 nm, the product appeared as a bright-green luminescent spot. No workup was done and after removal of the solvent *in vacuo*, the crude material was purified by column chromatography (methanol/chloroform 5/95 v/v followed by methanol/chloroform 15/85 v/v). The solvent was removed *in vacuo*, yielding the product as the Cl^- salt. The yellow solid was dissolved in demineralised water, filtered on paper, and precipitated as the PF_6^- salt by adding a saturated aqueous solution of NH_4PF_6. The pure product was obtained as a yellow solid (141.6 mg, 94%). ^{1}H NMR (400 MHz, $CDCl_3$): δ ppm 10.86 (s, 1H), 9.10 (d, J = 8.2 Hz, 1H), 7.99 (ddd, J = 7.8, 7.8, 1.6 Hz, 1H), 7.93–7.87 (m, 2H), 7.77 (ddd, J = 7.4, 2.2, 1.5 Hz, 1H), 7.75 (ddd, J = 7.4, 2.2, 1.5 Hz, 1H), 7.74 (ddd, J = 5.4, 1.6, 0.7 Hz, 1H), 7.68–7.66 (m, 2H), 7.65 (ddd, J = 4.9, 1.4, 0.5 Hz, 1H), 7.45 (ddd, J = 5.8, 1.5, 0.8 Hz, 1H), 7.21 (ddd, J = 7.6, 5.5, 1.2 Hz, 1H), 7.05–7.00 (m, 2H), 6.98 (ddd, J = 7.8, 7.4, 1.3 Hz, 1H), 6.96 (ddd, J = 7.3, 5.8, 1.4 Hz, 1H), 6.90 (ddd, J = 7.4, 7.4, 1.4 Hz, 1H), 6.87 (ddd, J = 7.4, 7.4, 1.4 Hz, 1H), 6.31 (ddd, J = 7.6, 1.2, 0.5 Hz, 1H), 6.30 (ddd, J = 7.6, 1.2, 0.5 Hz, 1H), 4.22 (s, 3H). ^{13}C NMR (75 MHz, $CDCl_3$): δ ppm 168.2, 167.5, 150.0, 149.8, 149.5, 149.2, 148.4, 148.2, 146.3, 143.6, 143.5, 139.6, 137.9, 137.8, 131.7, 131.6, 130.5, 130.0, 129.8, 125.9, 124.6, 124.5, 124.2, 123.1, 122.7, 122.5, 122.1, 119.4, 119.3, 38.7; HRMS (ES+, CH_3OH): *m/z* calcd for $C_{30}H_{24}IrN_6$: 661.16917; found: 661.16861 $[M]^+$.

4.8 References

[1] D. M. Hercules, *Science* **1964**, *145,* 808–809.

[2] K. S. V. Santhanam, A. J. Bard, *J. Am. Chem. Soc.* **1965**, *87,* 139–140.

[3] R. E. Visco, E. A. Chandross, *J. Am. Chem. Soc.* **1964**, *86,* 5350–5351.

[4] A. J. Bard, Chapter 2, in *Electrogenerated Chemiluminescence,* Dekker, New York, **2004**.

[5] J. K. Leland, M. J. Powell, *J. Electroanal. Chem.* **1991**, *318,* 91.

[6] R. A. Meyers, *Encyclopedia of Analytical Chemistry: Applications, Theory and Instrumentation, Vol.* 11, Wiley, New York, **2000**.

[7] X. B. Yin, S. Dong, E. Wang, *Trends Anal. Chem.* **2004**, *23,* 432–441.

[8] I. Rubinstein, A. J. Bard, *J. Am. Chem. Soc.* **1981**, *103,* 512–516.

[9] D. Bruce, M. M. Richter, *Anal. Chem.* **2002**, *74,* 1340–1342.

[10] B. D. Muegge, M. M. Richter, *Anal. Chem.* **2004**, *76,* 73–77.

[11] L. R. Faulkner, A. J. Bard, *J. Am. Chem. Soc.* **1968**, *90,* 6284–6290.

[12] T. C. Richards, A. J. Bard, *Anal. Chem.* **1995**, *67,* 3140–3147.

[13] M. Felici, P. Contreras-Carballada, Y. Vida, J. M. M. Smits, R. J. M. Nolte, L. De Cola, R. M. Williams, M. C. Feiters, *Chem. Eur. J.* **2009**, *15,* 13124–13134.

[14] O. David, S. Maisonneuve, J. Xie, *Tetrahedron Lett.* **2007**, *48,* 6527–6530.

[15] D. Schweinfurth, K. I. Hardcastle, U. H. F. Bunz, *Chem. Commun.* **2008**, 2203–2205.

[16] G. T. Hermanson, *Bioconjugate Techniques,* Academic Press, Burlington, **2008**.

[17] D. M. Hercules, *Science* **1964**, *146,* 387–388.

[18] J. M. Bader, T. J. Kuwana, *J. Electroanal. Chem.* **1965**, *10,* 104–109.

[19] N. E. Tokel, A. J. Bard, *J. Am. Chem. Soc.* **1972**, *94,* 2862–2863.

[20] J. N. Demas, G. A. Crosby, *J. Mol. Spectrosc.* **1968**, *26,* 72–77.

[21] J. N. Demas, G. A. Crosby, *J. Am. Chem. Soc.* **1971**, *93,* 2841–2847.

[22] D. M. Roundhill, *Photochemistry and Photophysics of Coordination Complexes,* Plenum, New York, **1994**.

[23] J. Van Houten, R. J. Watts, *J. Am. Chem. Soc.* **1976**, *98,* 4853–4858.

[24] E. M. Gross, J. D. Anderson, A. F. Slaterbeck, S. Thayumanavan, S. Barlow, Y. Zhang, S. R. Marder, H. K. Hall, M. Flore Nabor, J. F. Wang, E. A. Mash, N. R. Armstrong, R. M. Wightman, *J. Am. Chem. Soc.* **2000**, *122,* 4972–4979.

[25] W. Miao, J. P. Choi, A. J. Bard, *J. Am. Chem. Soc.* **2002**, *124,* 14478–14485.

[26] F. Kanoufi, Y. Zu, A. J. Bard, *J. Phys. Chem. B* **2001**, *105,* 210–216.

[27] Y. Zu, A. J. Bard, *Anal. Chem.* **2000**, *72,* 3223–3232.
[28] A. J. Bard, Chapter 5, in *Electrogenerated Chemiluminescence,* Dekker, New York, **2004**.
[29] X. Liu, L. Shi, W. Niu, H. Li, G. Xu, *Angew. Chem. Int. Ed.* **2007**, *46,* 421–424.
[30] S. Zanarini, E. Rampazzo, S. Bonacchi, R. Juris, M. Marcaccio, M. Montalti, F. Paolucci, L. Prodi, *J. Am. Chem. Soc.* **2009**, *131,* 14208–14209.
[31] W. Miao, A. J. Bard, *Anal. Chem.* **2003**, *75,* 5825–5834.
[32] M. M. Richter, *Chem. Rev.* **2004**, *104,* 3003–3036.
[33] C. G. Zoski, *Handbook of Electrochemistry,* Elsevier, Amsterdam, **2007**.
[34] S. Zanarini, *Thesis dissertation: New Materials for Electrochemiluminescence,* University of Bologna, Bologna, **2007**.
[35] *At this concentration all the complexes were easily dissolved, except* $[Ir(F_2ppy)_2(pytl\text{-}ada)]^+$ *which needed some sonication and heating because of adamantane hydrophobicity.*
[36] S. Hughes, P. L. Meschi, D. C. Johnson, *Anal. Chim. Acta* **1981**, *132,* 1–10.
[37] B. D. Muegge, M. M. Richter, *Luminescence* **2005**, *20,* 76–80.
[38] B. Carboni, A. Benalil, M. Vaultier, *J. Org. Chem.* **1993**, *58,* 3736–3741.
[39] I. R. Laskar, S. F. Hsu, T. M. Chen, *Polyhedron* **2005**, *24,* 189–200.

5

Self-Assembled Systems for Hydrogen Evolution

Abstract

Light-driven, catalytic, three-component systems for the reduction of protons, composed of an iridium complex as the photosensitiser, a viologen-based electron relay, cyclodextrin-modified platinum nanoparticles as the catalyst, and a sacrificial donor, are capable of producing molecular hydrogen. The photosensitiser, electron relay, and catalyst were appended with host and guest molecules, such as β-cyclodextrin, adamantane, and ursodeoxycholic acid, which were used to assemble the components of the photocatalytic system in a supramolecular manner. The modular approach introduced in this study allows the generation of several functional photo-active systems by self-assembly from a limited number of building blocks. We established that the polypyridine iridium complexes of general formula $[Ir(ppy)_2(pytl\text{-}R)]Cl$ (ppy = 2-phenylpyridine, pytl = 2-(1-substituted-1*H*-1,2,3-triazol-4-yl)-pyridine) are active in the production of H_2, with yields that in our conditions are 2.5–450 times higher than the classical three-component system Ru-bpy/Me-V-Me/Pt-βCD/EDTA. (bpy = 2,2'-bipyridine, Ru-bpy = $[Ru(bpy)_3]^{2+}$, Me-V-Me = methyl viologen, Pt-βCD = non-methylated β-cyclodextrin-functionalised platinum nanoparticles, EDTA = ethylenediamine-tetraacetic acid). By investigating different photocatalytic systems, it was found that the electron relay plays an essential role and it is necessary to guarantee an efficient electron transfer process, and the amount of hydrogen produced is directly proportional to the quantum yield of the photosensitiser. The attempt to increase the efficiency of our systems by using guest-appended viologens led us to unexpected observations. The presence of adamantane or bile acid groups induced the aggregation and increased the stabilisation of the radical cations which is disadvantageous for hydrogen formation.

Part of this work has been published as:

N. Mourtzis, P. Contreras-Carballada, M. Felici, R. J. M. Nolte, R. M. Williams, L. De Cola, M. C. Feiters, Phys. Chem. Chem. Phys. ***2011****, 13, 7903–7909.*

P. Contreras-Carballada, N. Mourtzis, M. Felici, S. Bonnet, R. J. M. Nolte, R. M. Williams, L. De Cola, M. C. Feiters, Eur. J. Org. Chem. ***2012****, 6729–6736.*

5.1 Introduction

The large-scale production of clean energy is one of the major challenges society is currently facing. The exhaustion of fossil fuels and the tangible influence of the greenhouse effect on the environment have created the need to switch from carbon-based fuels (coal, gas, oil) to renewable energy sources with less or no impact on the environment (solar, wind, wave power, biomass, wood).[1] Molecular hydrogen is commonly recognised as a key sustainable fuel for the future because of its high energy content and combustion produces only water.[2] However, hydrogen is not an energy source (not available as such) but an energy carrier, and it becomes a sustainable alternative to classical fuels only if it is produced in a clean fashion. Molecular hydrogen does not occur in large amounts on earth, but has to be produced from substances containing hydrogen atoms such as water or fossil fuels. Globally, industry already produces and uses hydrogen on a massive scale. However, its current production is largely based on fossil fuels; this is relatively energy inefficient and leads to the emission of a significant amount of greenhouse gases.[3] The production of hydrogen by using solar energy represents an ideal example of the production of sustainable energy.[4]

The development of hydrogen as an energy carrier requires several technical aspects to be considered. Governments and industries, particularly in the United States, Japan, and Europe, have been investing heavily in research and development to overcome the technical barriers for the use of hydrogen, which include[4] i) sustainable production, ii) purification,[5] iii) storage/distribution,[6] and iv) utilisation.[7]

More than thirty years ago, the groups of Lehn and Grätzel showed independently[8–10] that the now classical three-component heterogeneous photocatalytic system can be used for the generation of molecular hydrogen from water. Such a system consists of a sacrificial donor, a photosensitiser, an electron carrier, and a hydrogen evolution catalyst. Several studies have been reported on systems containing different photosensitisers, sacrificial electron donors, variously substituted viologens and a variety of catalysts, such as semiconductor metal oxides and noble-metal particles.[2] The catalysts initially used by Grätzel and Lehn were semiconductors, which were effective only under UV light because of their wide band gap. The development of new photocatalysts that are able to produce H_2 from water to make systems active over the whole visible spectrum has, therefore, attracted much attention.[11–17] Metal complexes have long been explored as photosensitisers for the evolution of hydrogen in combination with different catalysts.[18–25] There is a wide range of molecules that can act as photosensitiser such as organic dyes, inorganic systems as well as organometallic complexes.[26–28] In a typical catalytic cycle, the photosensitiser, which has been oxidised by

the catalyst, needs to be regenerated by an electron source (sacrificial donor), which is consumed during hydrogen production. In combination with a colloidal Pt catalyst, methyl viologen ([Me-V-Me]Cl_2) is frequently employed as an electron carrier between the sensitiser and the catalyst. The important steps in these systems are photo-induced electron transfer from a photo-excited sensitiser to Me-V-Me and subsequent electron transport to the colloidal Pt catalyst by reduced methyl viologen ([Me-V-Me]$^{\bullet+}$).

The typical structure of photocatalytic systems with an organometallic complex as a sensitising dye is shown in Scheme 5.1. These complexes are photo- and electro-active molecules and typical examples are Ru and Ir polypyridine complexes.[29–33] These compounds are capable of absorbing light from the UV into the visible part of the electromagnetic spectrum, creating a long-lived excited state that is able to transfer one electron to the electron relay (viologen) in a reversible redox process. The reduced viologen is then a strong reductant capable of transferring electrons to the platinum particle surface where it combines with H^+ to reduce it to molecular hydrogen. In these systems, light acts as a pump, forcing electrons in the direction of the catalytic centre. It is likely that the largest disadvantages of these kind of catalytic cycles are that they depend on the limited efficiency of collisions between participants in the electron transfer, and the deactivation processes, such as dimerisation of reduced viologen into electro-inactive species or its irreversible hydrogenation.[34]

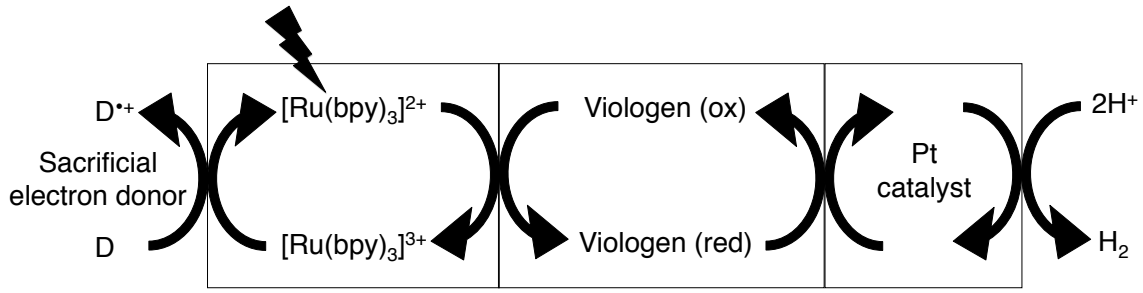

Scheme 5.1 *Representation of a system for hydrogen evolution based on colloidal platinum as the catalyst, viologen as the electron relay and* $[Ru(bpy)_3]^{2+}$ *(bpy = 2,2'-bipyridine) as the sensitising dye.*

In our approach we decided to investigate an analogously constructed three-component system containing the complexes $[Ru(bpy)_2(pytl\text{-}\beta CD)]^{2+}$ (pytl = 2-(1-substituted-1*H*-1,2,3-triazol-4-yl)-pyridine, βCD = permethylated β-cyclodextrin) or $[Ir(ppy)_2(pytl\text{-}\beta CD)]^+$ (ppy = 2-phenylpyridine; introduced in Chapter 2 of this thesis) as sensitisers,[35] and a substituted viologen as an electron relay that can promote the transfer of electrons to the platinum

catalyst (Scheme 5.2). The photo-induced electron transfer step may be improved by linking electron donor and acceptor molecules in a more strict fashion, but without covalent bonds, by mimicking photo-induced electron transfer processes in the natural photosynthetic reaction centre.[36,37] Similar to natural systems, in which a series of redox- and photo-active molecules are closely packed and well organised through non-covalent interactions with membranes, in our supramolecular architecture the components are held together by hydrophobic interactions. For our purposes, cyclodextrins seemed perfect candidates to assemble molecules of interest in a versatile way. Moreover, in the literature there are examples of the use of cyclodextrins as protection agents against dimerisation of the intermediates of the catalytic cycle (i.e., the highly reactive viologen radical cation $[Me\text{-}V\text{-}Me]^{\bullet+}$)[38–40] and against the chemical reduction of $[Me\text{-}V\text{-}Me]^{\bullet+}$ by evolving hydrogen.[40,41] Cyclodextrins have also been used as "molding matrices"[42] or "supports"[43,44] for platinum colloids, showing a significant influence on the overall hydrogen production, probably due to stabilisation of the platinum colloid in solution.

Typical total efficiencies of similar systems reported in the literature are around or below 0.1%, hydrogen evolution rates range from about 1 to 9 mL h^{-1} (≈40 to 375 μmol h^{-1}); typical light sources are 150 W Xe lamps. Because no standard experimental conditions have yet been established in the photo-catalytic community, it is difficult to compare the efficiencies of systems described in the literature.

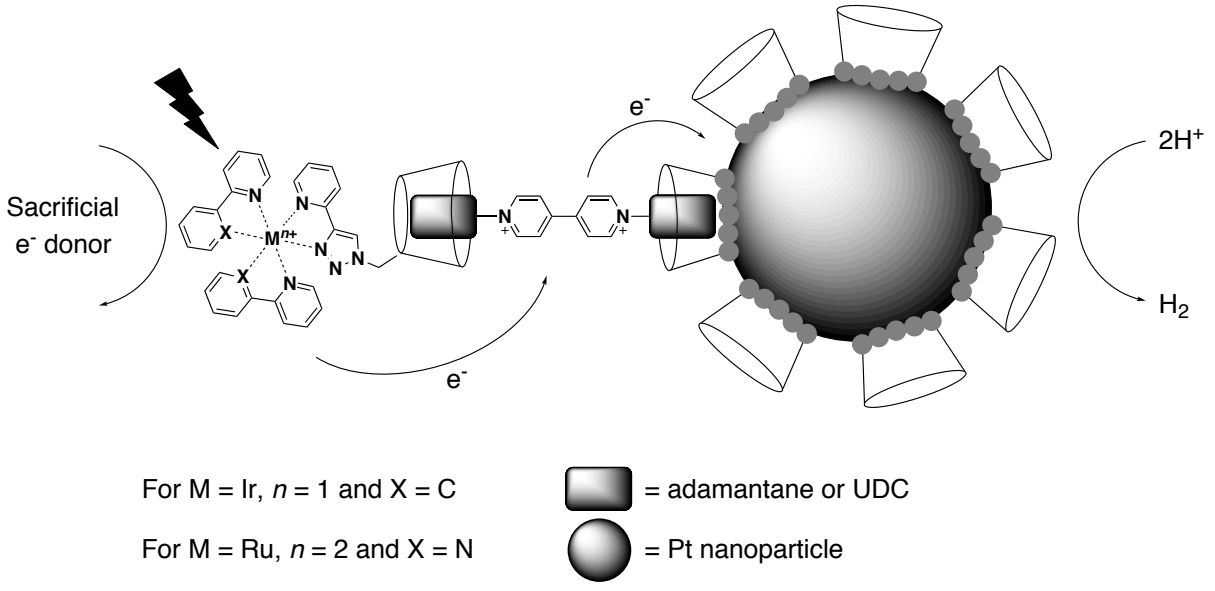

Scheme 5.2 *Schematic representation of the self-assembled three component catalytic system for a more efficient photo-induced electron transfer towards the platinum particle.*

The modular supramolecular approach we are introducing in this study has the great advantage, relative to a covalently linked multicomponent system, that it allows the generation of several functional photo-active systems by self-assembly from a limited number of building blocks. By combining different elements, it is possible to investigate different self-assembled systems, and thus, optimise experimental conditions. Our aim is to establish whether these three-component systems are able to generate hydrogen and whether supramolecular interactions can provide an efficiency higher than that of collision-controlled analogues. Firstly an assessment of the individual components is presented.

5.2 Photosensitiser, catalyst, and electron relay

5.2.1 Selection of photosensitiser and catalyst

To establish whether our design could lead to the desired goal, we need to select the most suitable components and study their processes separately. It is clear that the chromophoric units must have a number of characteristics for them to be used as sensitisers for our purposes. Among others, high photostability and a long excited state lifetime are a prerequisite. Also, the excited state of the photosensitiser has to transfer an electron to the relay before it returns to the ground state, resulting in a charge-separated state that we can utilise further. Polypyridine complexes are good candidates, since they can be excited over a wide range of wavelengths along the visible spectrum and they can be easily functionalised with cyclodextrins (Chapters 2 and 6).[35,45] Moreover, electron transfer from a ruthenium polypyridine complex to viologen, for example, has been widely documented.[30,46,47]

The complex $[Ir(ppy)_2(pytl\text{-}\beta CD)]^+$ (Ir-CD), investigated in Chapter 2,[35] possesses unique photophysical properties, in particular, high quantum yield (0.54) and long lifetime (28 μs). It also shows great water solubility provided by the permethylated cyclodextrin derivative, the cavity of which can also serve as a binding site for modified viologens. In the inclusion complex, the close proximity of the two components will facilitate the electron transfer from the photosensitiser to the mediator and finally to the catalyst. These facts make this complex a perfect candidate as a photosensitiser for the production of molecular hydrogen from aqueous acidic solutions. For comparison, the complexes $[Ir(ppy)_2(pytl\text{-}Me)]^+$ (Ir-Me), $[Ir(ppy)_2(pytl\text{-}ada)]^+$ (ada = adamantyl; Ir-ada), $[Ru(bpy)_2(pytl\text{-}\beta CD)]^{2+}$ (Ru-CD), and $[Ru(bpy)_3]^{2+}$ (Ru-bpy) were also examined because experiments with them should give useful information about the behaviour of our supramolecular photocatalytic system (Scheme 5.3). The ability of the excited state of our iridium and ruthenium complexes to transfer an electron to a viologen

molecule and to form a long-lived charge-separated state was investigated by Dr. Pablo Contreras-Carballada in Amsterdam by means of steady-state and time-resolved spectroscopy techniques.[48] The electron relay used was the asymmetric viologen Me-V-ada with one methyl group and an adamantane moiety, which makes it a suitable guest for inclusion in cyclodextrins.

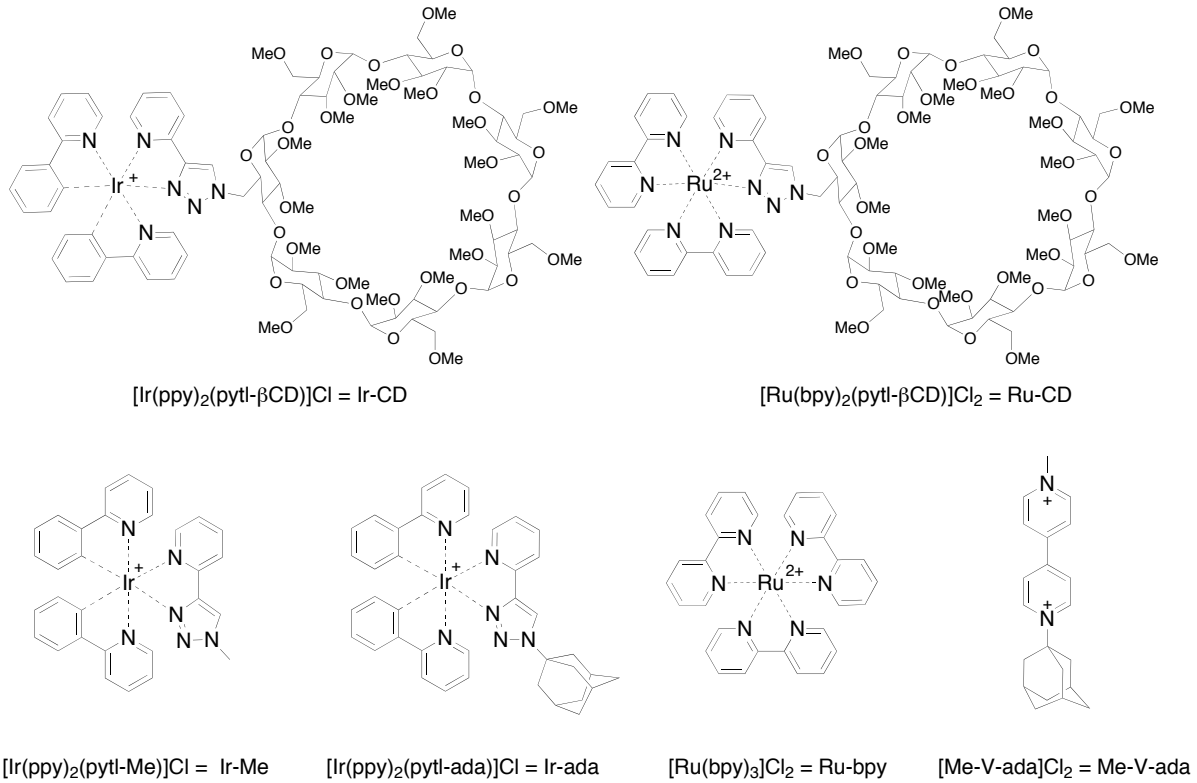

Scheme 5.3 *Structures of iridium and ruthenium complexes with methyladamantyl viologen.*

The catalysts we decided to use for our studies were Pt nanoparticles functionalised with perthiolated non-methylated β-cyclodextrin receptors (Scheme 5.4), which were prepared by our co-workers in Amsterdam.[44,48] The presence of cyclodextrins on the surface of the nanoparticles surface stabilises them by preventing aggregation phenomena.[49,50] At the same time, their surface remains accessible to the substrate and they retain their catalytic activity.[51,52] The presence of cyclodextrin also prevents the adsorption of larger viologen molecules on the surface of the particle, avoiding their irreversible catalytic hydrogenation in the presence of molecular hydrogen.[53] Cyclodextrins also make the nanoparticles soluble in water; this is an essential feature for our applications.

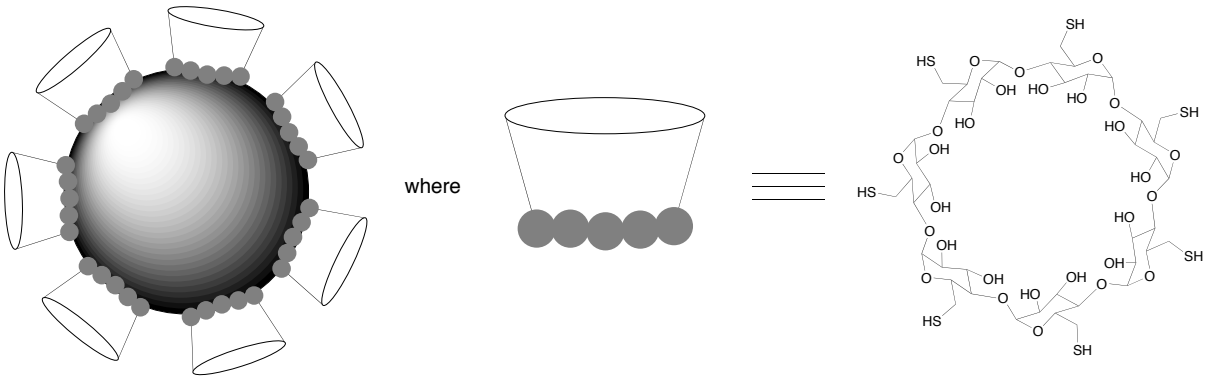

Scheme 5.4 *Schematic representation of the platinum nanoparticles and the stabilising molecule. The stabiliser is a perthiolated non-methylated β-cyclodextrin; sulfur atoms are represented by grey circles.*

The electro-catalytic activity of Pt nanoparticles towards hydrogen reduction is a well-documented process.[54] The catalyst functions as a negatively charged condenser/capacitor to provide the necessary electrochemical potential and number of electrons for the reduction of aqueous protons and serves as a gas evolution site.[55] This process can be described by the following mechanism when the electron carrier is a reduced viologen:[56,57]

$$n[\text{Me-V-Me}]^{\bullet+} + \text{Pt} \leftrightarrows \text{Pt}^{n-} + n[\text{Me-V-Me}]^{2+}$$
$$\text{Pt}^{n-} + \text{H}^{+} \leftrightarrows \text{Pt}^{(n-1)-} + \text{H}_{ads}$$
$$2\text{H}_{ads} \leftrightarrows \text{H}_2 \uparrow$$

The platinum particles have been investigated by means of cyclic voltammetry which has established that they were active towards the reduction of protons to hydrogen as expected, even at relatively high pH (≈6) values.[48] The particle size observed for our preparations by TEM (1.5–2.5 nm)[48] is in the range appropriate for application in catalytic reactions;[52] it allows the diffusion of sufficient H^+ ions to the surface of the catalyst for reduction to H_2 to take place.[48]

5.2.2 Selection and synthesis of the electron relay

Viologen is a very promising electron relay for use in our systems, with electrochemical properties that make it suitable to accept one electron from the excited state of iridium and ruthenium metal complexes. We decided to use 1,1′-disubstituted-4,4′-bipyridine-1,1'-diium species, as chloride salts, where the nitrogen atoms are located in the *para* position; thus having the correct geometry to yield linear self-assembled structures. During the research

described in this chapter we used three different viologens Me-V-Me, ada-V-ada and ada-V-DC (DC = ursodeoxycholic acid (UDC) derivative), with different moieties, symmetrically and asymmetrically substituted (Scheme 5.5).[58] The simplest of the series is the methyl viologen Me-V-Me, also known as paraquat, is a commercially available product; others were synthesised in our laboratory.

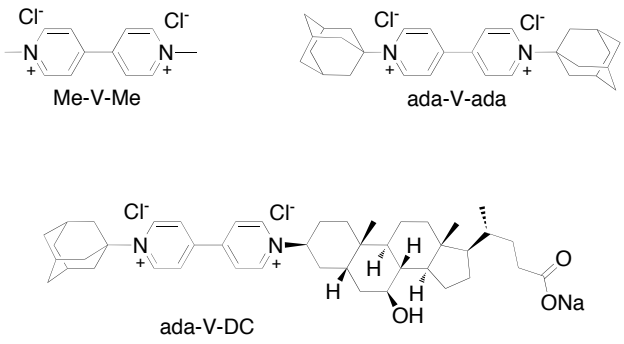

Scheme 5.5 *Structures of viologens Me-V-Me, ada-V-ada and ada-V-DC.*

The synthesis of a viologen requires different approaches depending on the chemical reactivity of the substituents to be attached to the nitrogen atoms. Primary electrophiles react directly with the nitrogen atoms of 4,4′-bipyridine (**1**); for example, reaction with methyl iodide gives Me-V-Me. In the case of weak electrophiles, or in any other case, it is necessary to react the desired substituent as an amino derivative (e.g., 1-adamantylamine) with the 1,1'-bis(2,4-dinitrophenyl)-4,4'-bipyridine-1,1'-diium compound (**3**), in which the two pyridinium rings are activated towards nucleophilic attack by the electron-withdrawing 2,4-dinitrophenyl group (Scheme 5.6). The interesting mechanism of this reaction, known as the Zincke reaction, involves the opening and closing of the pyridine rings, which lead to exchange of the pyridinium nitrogen atoms with the nitrogen atoms of the entering groups.[59] The efficiency of the reaction was tested on different substrates and allowed the preparation of viologens ada-V-ada and ada-V-DC.

Methyladamantyl viologen (Me-V-ada) mentioned in the previous paragraph was kindly provided by Dr. Pablo Contreras-Carballada.[48] In the first step, the preparation of the viologen ada-V-ada involved the synthesis of the symmetrically substituted intermediate **3**, which was further reacted with 1-adamantylamine (Scheme 5.6). The final compound ada-V-ada was obtained as a pure chloride salt by ion exchange.

The synthesis of the asymmetric viologen ada-V-DC was achieved by separate activation of the two nitrogen atoms of **1** (Scheme 5.7).

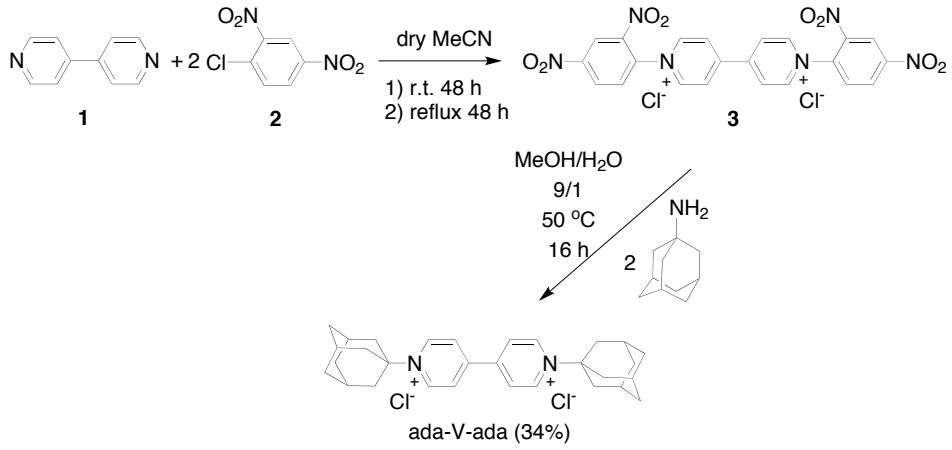

Scheme 5.6 *Synthesis of the symmetric bisadamantyl viologen ada-V-ada.*

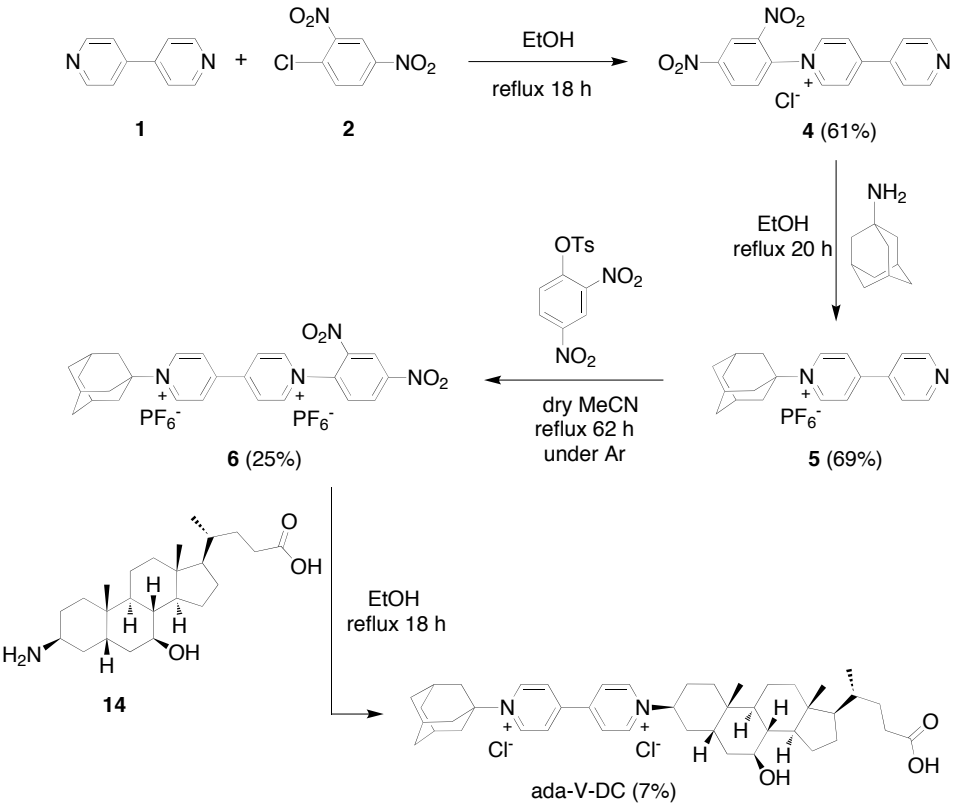

Scheme 5.7 *Synthesis of the asymmetric adamantyl-DC viologen ada-V-DC.*

Compound **1** was first reacted with one equivalent of 1-chloro-2,4-dinitrobenzene (**2**) and then with 1-adamantylamine to yield **5** selectively (Scheme 5.7).

Due to the positive charge present, the unreacted nitrogen of **5** became a weaker nucleophile and we had to use 2,4-dinitrophenyl 4-methylbenzene-1-sulfonate to prepare **6**, since *p*-toluene sulfonate is a better leaving group than chloride. Compound **6** was then reacted with 3β-amino-7β-hydroxy-5β-cholan-24-oic acid (**14**), yielding the asymmetric

viologen ada-V-DC. While 1-adamantylamine is a commercially available product, the preparation of **14** has never been described in the literature and we therefore designed the following synthesis: The carboxylic functionality of 3α,7β-dihydroxy-5β-cholan-24-oic acid (UDC, **7**) was protected as a methyl ester to avoid undesired reactions during the chemical modification of the molecule. By adapting a synthetic scheme for the tosylation of lithocholic acid available in the literature,[60] we prepared **9** in which the hydroxyl group at C3 was converted into a better leaving group. This step produced a mixture of tosylated derivatives that was further reacted without purification. Substitution of the tosylate by sodium azide afforded a mixture of **11** and **12**, which were isolated by chromatography. Compound **12** was then converted into an amine by reduction with triphenylphosphine and the carboxylic functionality was deprotected to yield **14** (Scheme 5.8).

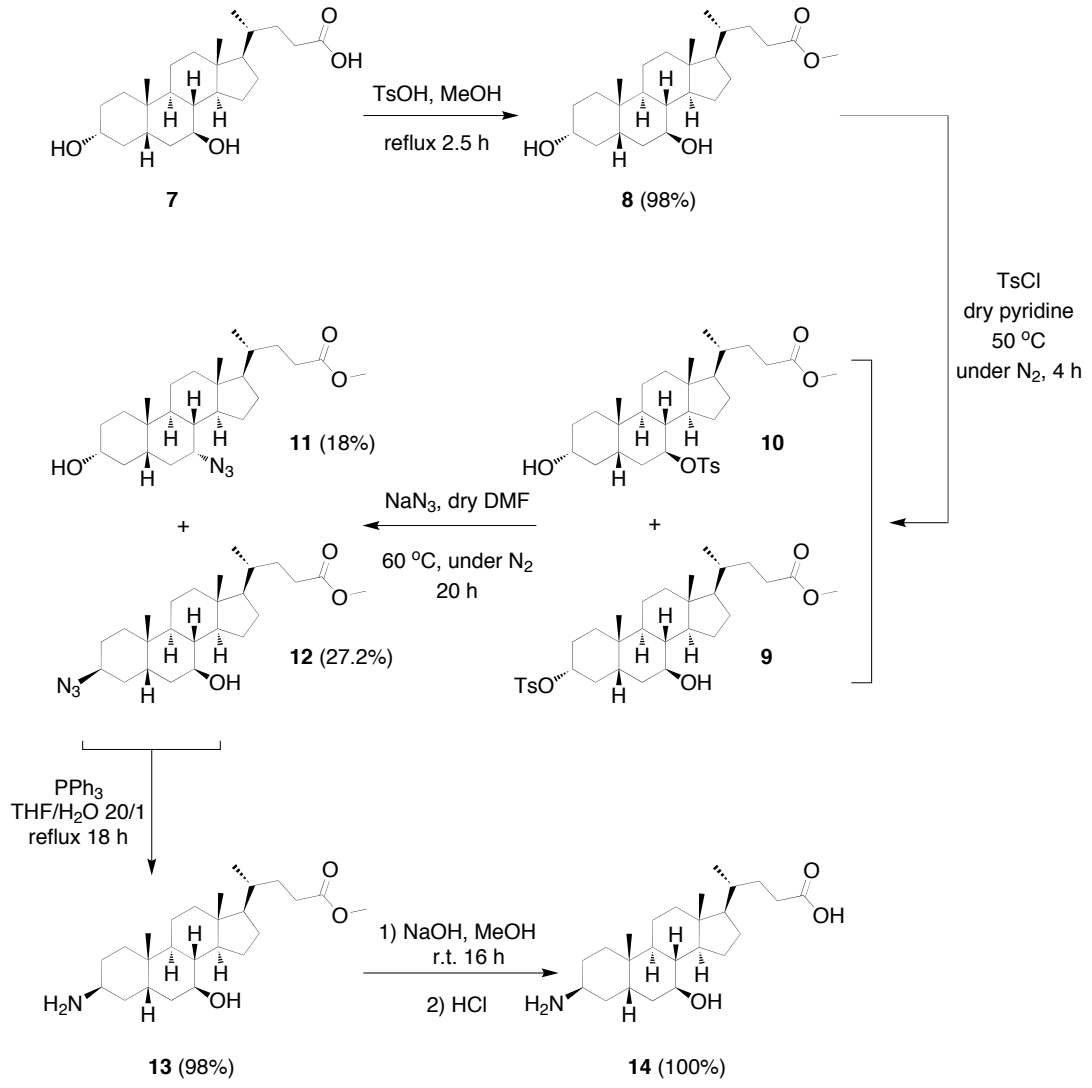

Scheme 5.8 *Synthesis of **14**.*

Hydrolysis of the methyl esters **11** and **12** yielded the free acids **11a** and **12a** (Scheme 5.9). In addition to the full characterisation by NMR spectroscopy, the crystal structures of the carboxylic acid derivatives **11a** and **12a** (Scheme 5.9) were determined by single-crystal X-ray diffraction.[45] Nucleophilic substitution of the tosyl group on **9** occurred with a bimolecular mechanism, resulting in inverted stereochemistry at the carbon atom. This was proved by the crystal structures of **11a** and **12a**, which clearly showed the azide in an axial position (Scheme 5.9). This aspect is particularly important in the case of **12a** because it results in a viologen derivative with a molecular rod-like shape when the 4,4′-bipyridine moiety is attached. This would ensure the highest binding constant for the inclusion complex of the viologen with the βCD-appended sensitiser ($K \approx 10^5$ M^{-1}),[61] due to a better fit of the bile acid into the cyclodextrin cavity, and probably the most efficient geometry for the electron transfer process. Due to inversion at C3 and C7 in UDC, compounds **11a** and **12a** have the configurations of chenodeoxycholic and isoursodeoxycholic acid, respectively, according to accepted bile acid nomenclature.[62]

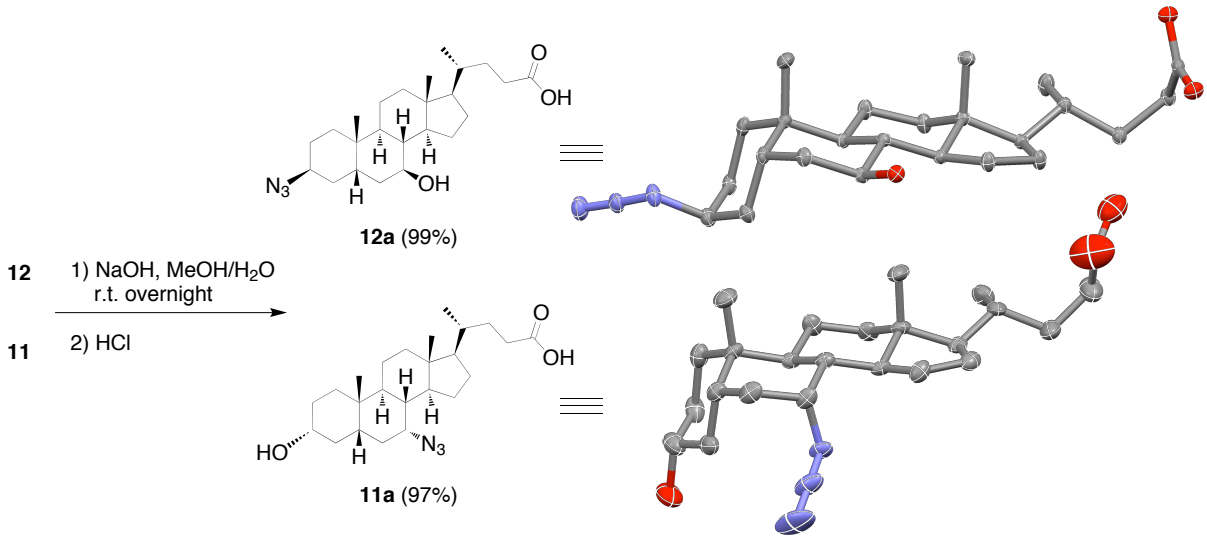

Scheme 5.9 *Preparation and crystal structures of **12a** and **11a**. Grey, carbon; blue, nitrogen; red, oxygen. The thermal ellipsoids for the image represent the 25% probability limit. Hydrogen atoms are omitted for clarity.*

5.3 Hydrogen evolution experiments

We showed above that Pt nanoparticles were catalytically active and that triazole-pyridine complexes together with viologen were suitable components.[48] Scheme 5.10 shows the structures of the selected complexes used as photosensitisers, the modified viologen compound that acts as an electron relay, and the platinum catalyst where the catalytic reaction

takes place assembled in one of the possible supramolecular architectures which have been investigated for H_2 production.

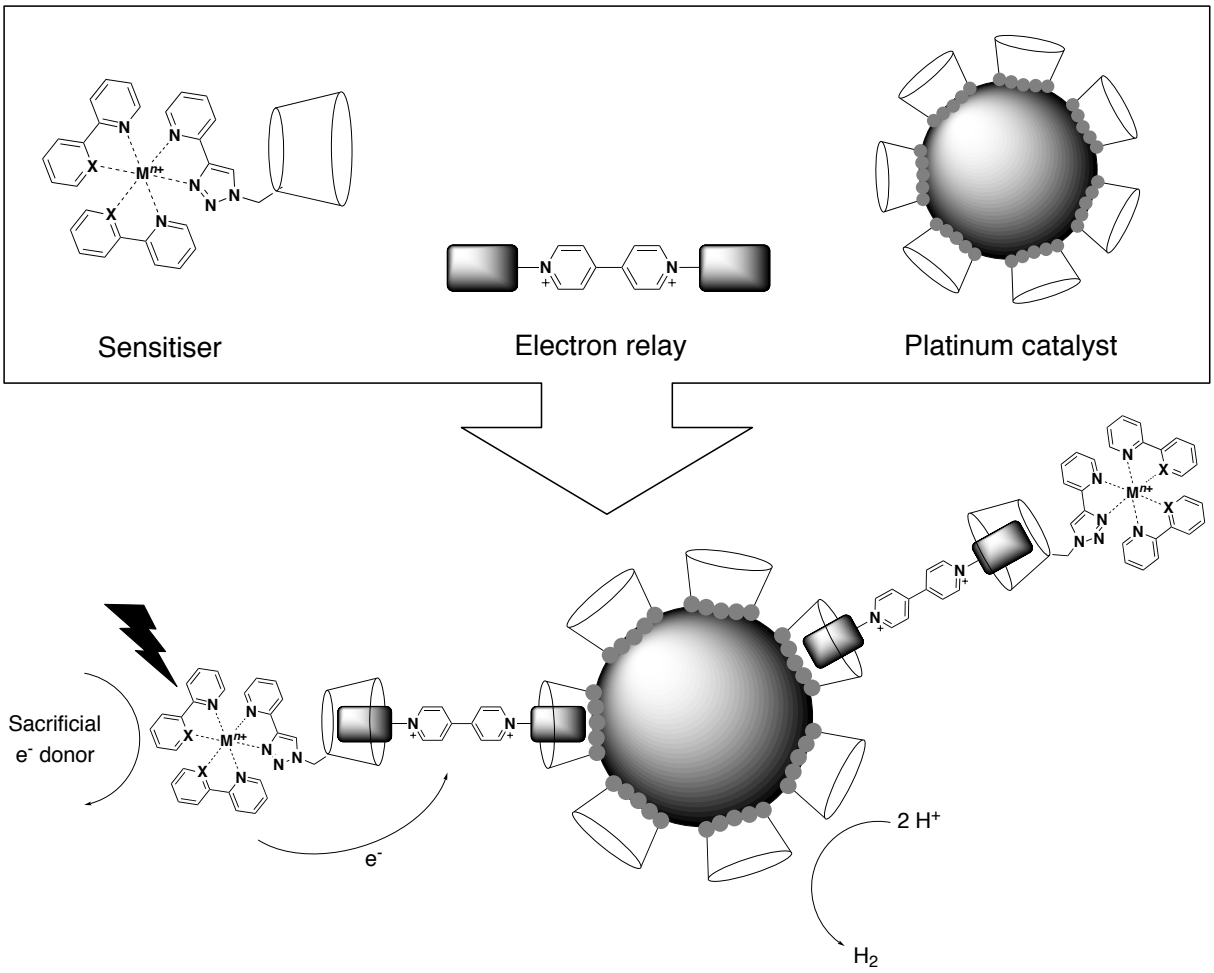

Scheme 5.10 *Chemical structures of the compounds studied in the hydrogen evolution process. Iridium and ruthenium complexes used as the sensitising dye, viologen modified with various guests (grey block) used as an electron relay, and a schematic representation of the platinum nanoparticle where the actual reduction process occurs. For M = Ir, n = 1 and X = C; for M = Ru, n = 2 and X = N. The sacrificial donors tested were methanol, ethylenediaminetetraacetic acid (EDTA), or triethanolamine (TEOA).*

The components were mixed in aqueous solution to obtain self-assembled system A, represented in Scheme 5.11, as well as several other combinations that are also possible when starting from these building blocks. It should be noted that only assembly A, and perhaps B ("dimer" of sensitising dye), of those reported in Scheme 5.11 are expected to be able to produce H_2. The second system, in fact, can yield a viologen radical cation, which

subsequently dissociates and reaches the catalyst surface. In spite of the purely statistical nature of the assembly, which leads to non-productive assemblies in addition to functional ones, we are convinced that this approach represents an improvement to the collision-controlled redox process.

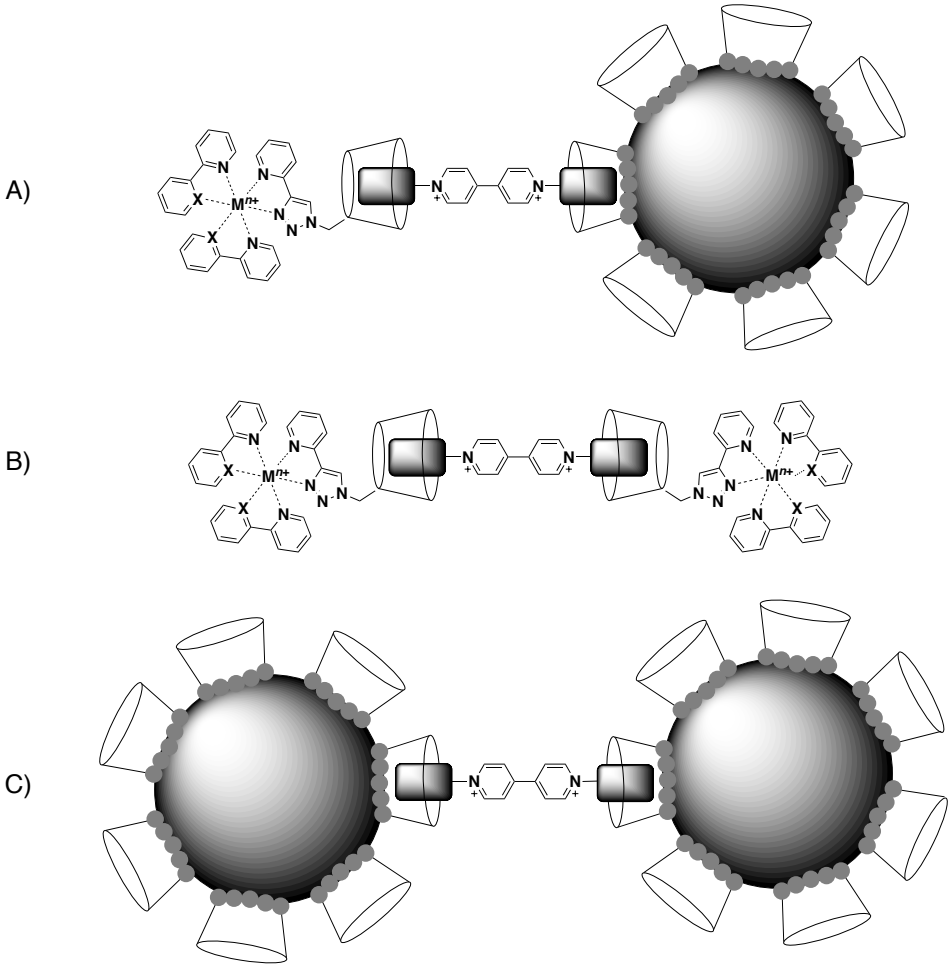

Scheme 5.11 *Possible assemblies formed in solution by the building blocks present during the experiments. For M = Ir, n = 1 and X = C; for M = Ru, n = 2 and X = N.*

To facilitate efficient electron transfer to the Pt centre, an electron donor was utilised to re-reduce the photochemically formed photosensitiser.[10,63] Three candidates were tested as electron donors: TEOA because of its good reducing properties, methanol because of its availability from biomass, and the sodium salt of EDTA because it is a classical example of an electron donor. TEOA was soon discarded because of the formation of insoluble decomposition products that turned the reaction mixtures heavily turbid. Methanol proved to be unsuitable under the experimental conditions used, since it resulted in low hydrogen production yields, probably due to partial evaporation during the degassing procedure.

Furthermore, the use of large amounts of methanol decreases the binding abilities of cyclodextrins. Therefore, every experiment described hereafter involved the use of EDTA as a sacrificial donor.

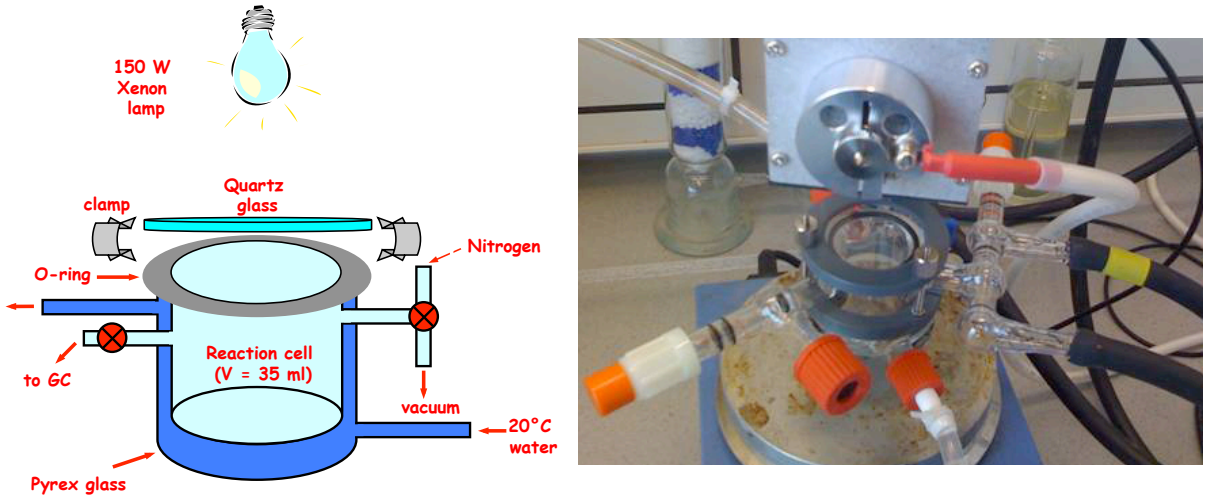

Figure 5.1 *Schematic representation (left) and picture (right) of the reaction vessel employed in the hydrogen evolution experiments. The cell is covered with a quartz glass lid that is kept air-tight with three metal screws. The xenon lamp (150 W) continuously irradiates the cell from above. The cell has one inlet for vacuum/nitrogen connected to a Schlenk line and another inlet for taking samples of gas with a microsyringe. The system is kept at a constant temperature.*

Experiments were carried out under constant irradiation. The system was studied in a home-made cell designed by Dr. Nikos Mourtzis and constructed in our University (Figure 5.1). In a typical experiment, an aqueous solution (10 mL) was prepared with the sensitising dye at a concentration in the millimolar range (0.1 mM), combined with a 10-fold excess of a viologen relay (Scheme 5.5) and 1 mg of freshly prepared platinum nanoparticles stabilised with perthiolated non-methylated β-cyclodextrin. A sacrificial electron donor was added to this solution in 100-fold excess with respect to the sensitising dye. Finally, to assure the presence of enough H^+ ions, the concentration of HCl was set to approximately 200 molar equivalents. The solution was then carefully degassed. The total volume of the aqueous solution was always kept to 10 mL in a cell with a capacity for 35 mL. The size of the nanoparticles could greatly affect the efficiency of hydrogen production; therefore, freshly prepared samples, which were stored under inert atmosphere, were used. To break possible aggregates, solutions containing the nanoparticles were sonicated for 30 min prior to use.

Solutions were monitored for molecular hydrogen evolution by directly measuring the amount of molecular hydrogen contained *in the gas phase* inside the reaction cell through GC analysis. To calculate the moles of hydrogen gas from the chromatographic peak areas, a calibration curve was constructed by preparing different mixtures of N_2 and H_2 of known ratios and measuring their H_2 peak integrals. The gas mixing and injecting processes, as well as the illumination experiment itself, were performed at T = 20 °C meaning that 1 mol of gas occupies 24.05 L. It is important to notice that all the H_2 amounts described hereafter and produced in the photocatalytic cell were determined by analysing only the gas phase. H_2 that remained dissolved in the solution (at most 8 μmol), or even trapped inside bubbles on the solution surface, was not measured. The amount of hydrogen dissolved in solution is in equilibrium and therefore proportional to that in the head space.

In our approach we designed a modular three-component system for hydrogen evolution in which units were linked to each other by reversible supramolecular interactions. A great advantage of a self-assembled system, compared with other systems containing elements that are covalently linked, is the possibility to change any of the three components without requiring the synthesis of an entirely new system. This allows optimisation of the entire process by precisely tuning the physical properties of each molecular component. We investigated different combinations of photosensitisers and electron relays and compared the efficiency of the resulting systems in terms of amount of hydrogen produced.

5.3.1 Role and supramolecular interactions of the photosensitiser

To evaluate the effect of the metal centre on the efficiency of our systems independently from any other aspects, we investigated the systems Ru-CD/Me-V-Me/Pt-βCD/EDTA and Ir-CD/Me-V-Me/Pt-βCD/EDTA, which differed only in the nature of photosensitisers Ru-CD and Ir-CD, respectively. The electron mediator used in both cases was Me-V-Me. Illumination of the Ru-CD/Me-V-Me/Pt-βCD/EDTA system resulted in very low hydrogen production; only 0.15 μmol of H_2 was produced after the first 15 min and then the reaction continued at a very low rate, giving 0.36 μmol of gas after 28 h (Figure 5.2). In the case of Ir-CD/Me-V-Me/ Pt-βCD/EDTA, where the βCD-appended ruthenium complex was replaced by the iridium analogue, 4.6 μmol of H_2 was produced during the first 15 min (Figure 5.2) and gas evolution was apparent by bubble formation in the solution. The higher efficiency of this system was also shown by the fact that, 3 h after the illumination started, EDTA was largely consumed as the solution became completely transparent (the limited solubility of EDTA, even at low concentrations, was responsible for a turbid solution). As a consequence of the lack of a

sacrificial donor, the photosensitiser could no longer be regenerated and the production of H_2 stopped. The total amount of H_2 produced was 137 μmol. In all of the experiments we also observed the formation of CO_2 (not reported in Figure 5.2), which originated from the decomposition of EDTA. As expected, the amount of CO_2 produced followed the same trend as the production of H_2. Taking into consideration that the initial concentration of HCl was 20 mM, which means that 200 μmol of H^+ in the solution can be reduced to give 100 μmol of H_2, part of the H_2 produced was likely to have derived from the reduction of protons from water or EDTA. In the latter case protons are produced during the irreversible decomposition of oxidised EDTA which comprises the hydrolysis of unstable intermediates.[4] Substitution of ruthenium with iridium as the light-harvesting unit increased the efficiency of the system in the initial phase by approximately 30 times and more than 900 times after 3 h of illumination (in the case of iridium, 100 equivalents of the sacrificial donor had already been consumed). This remarkable difference underlines the crucial importance, in the photocatalytic production of H_2, of choosing a very efficient sensitiser to guarantee the largest amount of electrons reaching the metallic catalyst.

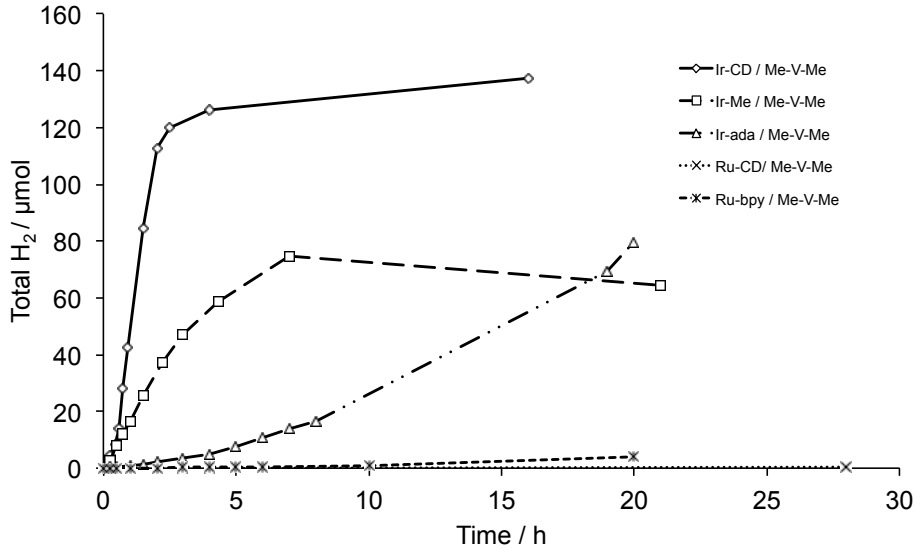

Figure 5.2 *Plots of molecular hydrogen produced inside the cell head space as a function of illumination time. The different photosensitisers used (0.1 mM) are shown with different lines. In all cases, the sacrificial donor was EDTA (10 mM), the electron mediator was Me-V-Me (1 mM) and the catalyst was β-cyclodextrin-modified Pt (0.1 mg mL^{-1}) in the form of nanoparticles.*

The presence of βCD in the photosensitisers Ir-CD and Ru-CD is meant to ensure efficient interaction with a properly modified viologen. As established in Chapter 2,[35] however, βCD

can also act as a second-sphere ligand with respect to the metal complex, enhancing, in the case of the iridium species, the excited-state quantum yield and lifetime. To investigate the effect of this interaction on the H_2 production efficiency, we replaced the βCD moiety on the iridium complex with a methyl group and used this complex in a similar experiment. The new photosensitiser Ir-Me lacks the host properties of Ir-CD and is characterised by a lower quantum yield (0.35) and shorter lifetime (2.1 μs). Interestingly, in the Ir-Me/Me-V-Me/Pt-βCD/EDTA system, after 15 min of irradiation, only 2.8 μmol of H_2 was produced and when the maximum amount of H_2 was reached after 7 h 75 μmol was present inside the cell (Figure 5.2). The efficiency of the system containing Ir-CD is approximately double that of the system with Ir-Me (Table 5.1). If we consider that Me-V-Me is not capable of supramolecular interactions with the cycloextrin cavity, since it does not contain any hydrophobic groups, it is clear that the different efficiency of the two systems is proportional to the different quantum yields of the sensitising dyes ($\Phi_{\text{Ir-CD}} = 0.54$, $\Phi_{\text{Ir-Me}} = 0.35$). Some other observations can also be made. For the Ir-Me experiment, i) the reaction was finished before EDTA was totally consumed and ii) a plateau was reached after 7 h, compared with 3 h in the Ir-CD experiment. These facts indicate that the limiting factor in the case of Ir-CD was the initial concentration of the sacrificial donor, whereas in the other experiment termination of the reaction should be attributed to other causes, possibly because the turnover number of Ir-Me may be lower, due to fewer regeneration cycles.

As another variation of the system, the photosensitiser Ir-ada was used. It has an adamantyl group on the pytl ligand and displays an even lower quantum yield and shorter lifetime ($\Phi = 0.23$, $\tau = 1$ μs) than Ir-Me, as reported in Chapter 2.[35] After 15 min of illumination, the Ir-ada/Me-V-Me/Pt-βCD/EDTA system produced only 0.2 μmol of hydrogen gas (Figure 5.2). The amount of gas continued to increase almost linearly with time and when the experiment was stopped after 20 h 80 μmol of H_2 was present inside the cell (Table 5.1). Due to the low reaction rate, we could not determine the maximum amount of hydrogen that could be produced by this system. However, we could estimate that, when Ir-ada was the photosensitiser, the resulting system was less efficient than that with Ir-CD by a factor of approximately two. The different kinetic behaviour displayed by this system (Figure 5.2) might be explained by considering the amphiphilic nature of the photosensitiser. Compound Ir-ada, as observed by NMR spectroscopy, forms aggregates in water even at low concentrations (0.57×10^{-3} M); this could interfere with the catalytic process by limiting the directional flow of electrons towards the catalytic centre. No further investigation was carried out in this direction.

On the basis of the data collected in these studies, we may conclude that the efficiency of

our system is directly related to the quantum yield of the photosensitiser. The sensitising dye should be chosen by taking into account all of the factors that affect its photophysical properties (e.g., formation of inclusion complexes, hydrophobic interactions) because such factors will also have a direct impact on the efficiency of the hydrogen evolution system. The most efficient system was Ir-CD/Me-V-Me/Pt-βCD/EDTA, in which the metal centre was protected from quenching of the luminescence by the βCD. At this time, the higher amount of hydrogen produced is only due to the improved photophysical properties of the sensitiser, since no interactions with βCD on either side of methylviologen are expected.

To compare our supramolecular systems with others already reported in the literature, we investigated Ru-bpy/Me-V-Me/Pt-βCD/EDTA, one of the first systems used for photocatalytic production of H_2 from water.[26,43] We carried out some experiments in which the efficiency of this system was evaluated under our working conditions. Surprisingly, during the first hour of illumination, no gas evolution was observed and after three h the amount of H_2 produced was only 0.2 μmol. The reaction rate did not increase until approximately 8 h after illumination was started (Figure 5.2). The reaction kept on going, even after 20 h, and the final amount of H_2 sampled at this time was 3.9 μmol. Under the conditions used in our experiments, the three iridium complexes Ir-CD, Ir-Me and Ir-ada are much better antenna molecules for H_2 production from acidic aqueous solutions than Ru-bpy. In terms of *final* gas amount ratios, this is translated as Ir-CD, Ir-Me and Ir-ada being approximately 35, 20 and 21 times more efficient than Ru-bpy (Table 5.1).

Table 5.1 *Total amount of hydrogen produced by using different photosensitisers.*

Photosensitiser	Electron relay	Time at maximum conc. H_2	H_2 produced (μmol)
Ir-CD	Me-V-Me	16 h	137
Ir-Me	Me-V-Me	7 h	75
Ir-ada	Me-V-Me	20 h (continuing)	80
Ru-CD	Me-V-Me	28 h	0.4
Ru-bpy	Me-V-Me	20 h (continuing)	3.9

5.3.2 Optimisation of the electron relay

In all experiments described in the previous paragraph we used the electron mediator Me-V-Me. To increase the efficiency of our system, however, we would need an electron relay able to interact strongly with both sensitiser and catalyst. A good candidate is the modified

viologen ada-V-ada in which both methyl groups of Me-V-Me are replaced by adamantyl moieties. These viologens were chosen because they are capable of forming inclusion complexes with the cyclodextrin cavity of the photosensitiser and of the Pt nanoparticles. Substituted adamantane usually has a good affinity for the βCD cavity ($K_{bind} \approx 10^3$–10^4 M^{-1}), [64] but we noticed that this affinity decreased by approximately an order of magnitude ($K_{bind} \approx 10^2$–10^3 M^{-1}, estimated by isothermal calorimetry (ITC)) upon appending a viologen residue, probably due to the proximity of a positively charged nitrogen atom. Despite this fact, we decided that it would be of interest to investigate how the host-guest interactions between photosensitiser, electron relay, and catalyst would influence the photocatalytic efficiency of the systems studied above.

The most promising photosensitiser to be used in combination with ada-V-ada was selected by taking into consideration two aspects. Firstly, only Ir-CD and Ru-CD can play the role of the host for the adamantyl-functionalised viologen, since Ir-Me, Ir-ada, and Ru-bpy do not have a βCD moiety. Secondly, compound Ru-CD has a poorer photophysical profile than Ir-CD (Chapter 2),[35] as was also reflected by its very low efficiency towards photocatalytic H_2 production in combination with Me-V-Me (see Section 5.3.1). Therefore, the only system involving the ada-V-ada mediator worth studying seemed to be Ir-CD/ada-V-ada/Pt-βCD/EDTA.

During the first 20 min of illumination, only 0.15 μmol of H_2 was produced (Figure 5.3) and the reaction stopped after 2 h, giving a total H_2 amount of less than 0.4 μmol. This value is definitely much lower than what we achieved with any iridium complex previously examined in combination with Me-V-Me (Table 5.1). During the experiment the solution became slightly blue a few minutes after illumination started. This coloration was most probably due to the formation of the viologen radical cation [ada-V-ada]$^{\bullet+}$. It is known that, under certain conditions, the reduced form of viologen gives a strong blue colour to solutions.[65] The reduced form of the viologen mediator [ada-V-ada]$^{\bullet+}$ apparently associates in solution because of the reduced repulsion forces between the less positively charged mono-cation radicals when compared with the dication analogues. This leads to the formation of dimers and/or multimers, which hamper the directional flow of electrons towards the catalytic centre or even block it completely.[40] The aggregation process stabilises the viologen mono-radical cation and accounts for the very low amount of hydrogen produced (Figure 5.3). This process is promoted by the presence of hydrophobic substituents, such as long alkyl chains or even adamantyl groups, which have the tendency to aggregate in an aqueous environment. Another factor that could contribute to the stability of [ada-V-ada]$^{\bullet+}$ is a different electronic effect of the adamantyl groups with respect to the methyl group. It is known that the

substituents on the nitrogen atoms are involved in stabilisation of the radical cation.[66] In particular, it has been observed that larger alkyl groups can increase, to a certain extent, the redox potential of the viologen, which, therefore, becomes a less efficient reducing agent.[65] This would also account for the lower efficiency of the corresponding hydrogen evolution system. To better understand and quantify this phenomenon, cyclic voltammetry studies of the different viologens are currently being carried out.[67] With this in mind, it is clear why the system containing the bisadamantyl viologen mediator (ada-V-ada) is less efficient than the bismethyl analogue Me-V-Me.

To enhance the selectivity of system A shown in Scheme 5.11, which has (as discussed before) optimal functionality, or at least to obtain better control in the binding of the three components, we would need an asymmetrically substituted viologen with one group that shows a stronger affinity towards one of the cyclodextrin binding sites. In this way, the binding constant between the photosensitiser and viologen could be differentiated from the one between the viologen and cyclodextrin-modified Pt catalyst. UDC is known to be one of the best guests for β-cyclodextrin with a binding constant that is two orders of magnitude higher than that of adamantane (K_{bind} = 7.8×10^5 M^{-1}).[61] Therefore, one possible solution to our problem would be to use the electron relay ada-V-DC, which has one adamantyl and one ursodeoxycholic acid moiety. The Ir-CD/ada-V-DC/Pt-βCD/EDTA system, when studied in our setup, produced a bright blue solution after only a few minutes of illumination, which was retained until the light source was turned off (more than 20 h). The amount of H_2 produced was around 0.2 μmol after 15 min, 1.9 μmol after 3 h, and became almost constant (4.3 μmol) after approximately 11 h (Figure 5.3). Bile acids are known to be surfactants, with a low critical micelle concentration in aqueous solutions.[62,68] The mono-radical cation of the viologen ada-V-DC is further stabilised compared to ada-V-ada due to enhanced aggregation. However, the increased stability of the reduced viologen is not reflected in a lower yield of the photocatalytic reaction, since the amount of hydrogen produced was in fact higher than in the case of Ir-CD/ada-V-ada (Table 5.2). Possible explanations are i) the higher binding constant expected between the βCD of Ir-CD and the DC moiety on ada-V-DC facilitates electron transfer between these two components and ii) there is a different electronic effect of DC with respect to adamantane in the radical cation.[67] The first factor would increase the concentration of the viologen radical (blue colour intensity) in solution, which would shift the electron transfer equilibria towards reduction of the catalyst; thus increasing the yield of the H^+ reduction process. The second factor would decrease the redox potential, making the radical cation a slightly better reducing agent.[67] As observed, a serious problem related to the use of modified viologens is their high tendency to aggregate. We expected the high affinity

of cyclodextrins to disrupt the aggregates to a certain extent, thus leading to the desired self-assembled system. Unfortunately, that was not the case and resulted in a difficult evaluation of the role of the substituents on the viologen in terms of efficiency of our hydrogen evolution systems.

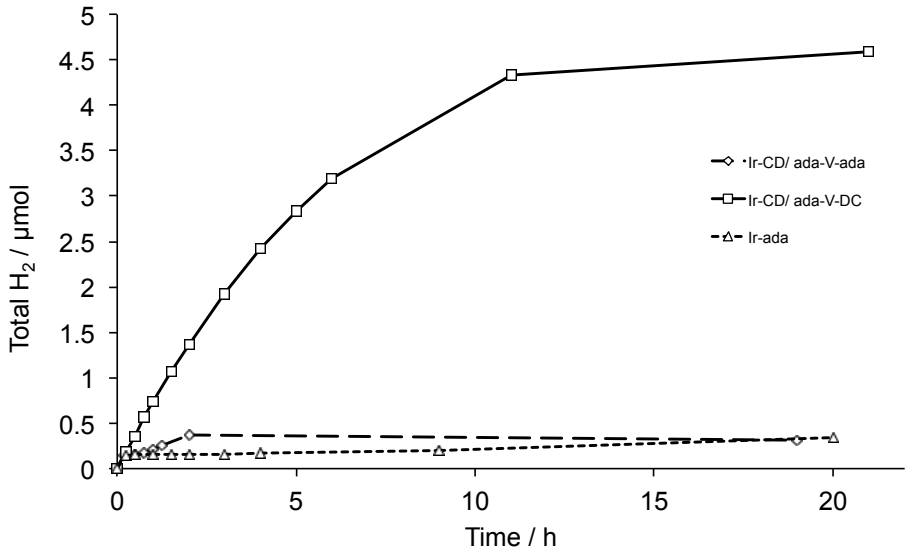

Figure 5.3 *Plots of molecular hydrogen produced inside the cell head space as a function of illumination time. The different combinations of photosensitiser (0.1 mM) and mediator (1 mM) are shown with different lines. In all cases, the sacrificial donor was EDTA (10 mM) and the catalyst was β-cyclodextrin-modified Pt nanoparticles (0.1 mg mL $^{-1}$).*

Table 5.2 *Total amount of hydrogen produced by using different electron relays. In the last experiment no electron relay was used.*

Electron relay	Photosensitiser	Time at maximum conc. H_2	H_2 produced (µmol)
Me-V-Me	Ir-CD	16 h	137
ada-V-ada	Ir-CD	2 h	0.36
ada-V-DC	Ir-CD	11 h	4.3
–	Ir-ada	20 h	0.34

One possible solution to this problem could be the covalent attachment of the βCD to the viologen and the adamantane to the iridium centre. In such a system interference due to aggregation phenomena would surely be limited. A similar procedure was recently described by Forster and co-workers.[69] No aggregation or micellation was reported by these authors.

It is interesting to note that the photosensitiser Ir-ada is the only one studied herein that can bind directly to the cyclodextrin-decorated catalyst through host-guest interactions because it has an adamantane group. To investigate the efficiency of a system where no viologen mediation was present, we examined the Ir-ada/Pt-βCD/EDTA combination. It was found that the efficiency was very low, giving only 0.34 μmol of H_2 after 20 h (Figure 5.3). The amount of hydrogen produced was more than 200 times lower than that of the Ir-ada/Me-V-Me/Pt-βCD/EDTA system, where methyl viologen was present (Figure 5.2). These results confirm the essential role of viologen for electronic communication between the photosensitiser and catalyst; close proximity of the two components through supramolecular interactions cannot compensate for the absence of the relay.

5.4 Conclusion

Various light-driven catalytic systems for the reduction of H^+, composed of an Ir complex photosensitiser, a viologen-based electron relay, cyclodextrin-modified platinum nanoparticles as the catalyst, and a sacrificial donor, are capable of producing molecular hydrogen. The yields measured were 2.5–450 times higher than the known Ru-bpy/Me-V-Me/Pt-βCD/EDTA system. The most efficient combination was Ir-CD/Me-V-Me/Pt-βCD/EDTA, which produced almost 32 μmol (≈0.75 mL) of H_2 per hour from a 10 mL solution (actual yields were higher, since part of the gas remained in solution). We investigated the effect of the photosensitiser on the efficiency of our systems and found that the total amount of hydrogen produced was directly proportional to the quantum yield of the photosensitiser.

An attempt to increase the efficiency of our self-assembled three-component system by using guest-appended viologens gave rise to unexpected phenomena. When ada-V-ada and ada-V-DC were used, the presence of adamantane or bile acid groups induced stabilisation and aggregation of the radical cations. This resulted in a decrease of the electron transfer rate towards the catalyst and an overall decrease of the reaction yield. The electron relay plays an essential role, as evidenced by our experiments, and it is necessary to establish an efficient electron transfer process. A different design of the components, taking into account their amphiphilic properties, could probably overcome the problems we encountered and will be the aim of future investigations.

5.5 Acknowledgements

Special thanks to Dr. Nikos Mourtzis and Dr. Pablo Contreras-Carballada for the fruitful collaboration.

5.6 Experimental

5.6.1 Methods and materials

General. THF was purified by distillation under nitrogen from sodium/benzophenone; dry acetonitrile was obtained by distillation under nitrogen from phosphorus pentoxide. Dry DMF was purchased from Fluka and anhydrous pyridine from Aldrich. Other chemicals were purchased from Aldrich, Fluka, or Acros and used as received. Analytical thin-layer chromatography (TLC) was performed on Merck precoated silica gel 60 F-254 plates (layer thickness 0.25 mm) and the compounds were visualised by UV irradiation at λ = 254 and/or 366 nm and by staining with phosphomolybdic acid reagent or $KMnO_4$. Purifications by silica gel chromatography were performed using Acros (0.035–0.070 mm, pore diameter ca. 6 nm) silica gel. The "magic mixture" eluent was a mixture of water (300 mL), sodium chloride (30 g), acetonitrile (1200 mL), and methanol (300 mL). Compounds **3**, **4** and **5** were prepared by following a procedure different from that described in the literature (vide infra). We performed a more extensive characterisation, which was also in agreement with the published data.

NMR spectroscopy. ^{1}H NMR spectra were recorded at 25 °C on Varian Inova 400 or Bruker DMX-300 spectrometers operating at 400 and 300 MHz, respectively. ^{13}C NMR spectra were recorded on a Bruker DMX-300 spectrometer operating at 75 MHz. ^{1}H NMR chemical shifts (δ) are reported in parts per million (ppm) relative to the residual proton signal of the solvent, δ = 4.79 ppm for D_2O, δ = 3.31 ppm for CD_3OD, δ = 7.26 ppm for $CDCl_3$, and δ = 2.50 ppm for DMSO-d_6. Multiplicities are reported as follow: s (singlet), d (doublet), t (triplet), q (quartet), dd (doublet of doublets), ddd (doublet of doublet of doublets), or m (multiplet). Broad peaks are indicated by b. Coupling constants are reported as a *J* value in Hertz (Hz). The number of protons (*n*) for a given resonance is indicated as *n*H, and is based on spectral integration values. ^{13}C NMR chemical shifts (δ) are reported in ppm relative to the carbon signal of the solvent, δ = 49.0 ppm for CD_3OD, δ = 77 ppm for $CDCl_3$, and δ = 40 ppm for DMSO-d_6; when the solvent was D_2O sodium-3-trimethylsilylpropionate-2,2,3,3-d_4 was added as an internal standard, δ = 0 ppm.[70] The signals of the protons on hydroxyl, amino, and carboxylic groups could not be observed due to fast exchange processes. The resolution of the ^{13}C NMR spectra was increased when necessary by performing an exponential apodisation of the FID.

Mass spectrometry (MS). All mass analyses were performed by using electrospray (ESI) techniques. High-resolution mass spectrometry (HRMS) measurements were performed on a JEOL AccuTOF instrument by using water, acetonitrile, or methanol as solvents. Standard MS measurements were performed on a Finnigan LCQ Advantage Max by using water, acetonitrile, or methanol as solvents.

High-performance liquid chromatography (HPLC). HPLC was carried out on a Shimadzu LC-20AT HPLC system equipped with an SPD-10AV UV-vis detector and a fraction collector. Columns were purchased from Dr. Maisch GmbH. The compounds were purified on a mg scale by using a semi-preparative reversed-phase column. An aliquot of solution (2 mL) was injected in a column ReproSil 100 C8, 5 μm (250 × 10 mm) operating at 30 °C. The detection wavelengths were fixed at 254 and 215 nm. A gradient of water and

acetonitrile both containing 0.1% v/v HCl or trifluoroacetic acid (TFA) was used as the mobile phase, with a flow rate of 4 mL min^{-1}. HCl was used to ensure that chloride was the only counterion of the isolated compounds. In all cases, samples were prepared by dissolving the compound in a suitable mixture of water/ acetonitrile and filtering the solution on a Nylon syringe filter (0.2 μm).

X-ray crystallography. Single crystals of **11a** and **12a** were grown by slow evaporation of slightly acidic solutions in water/acetonitrile. Crystal data and summaries of the data collection and structure refinement of **11a**, and **12a** are available in the Supplementary Information of our publication (open-access journal);[45] selected distances and bond angles as well as atomic coordinates and equivalent isotropic displacement parameters for the non-hydrogen atoms, are also given in the above-mentioned Supplementary Information. All measurements were performed at –65 °C. The structures of **11a** and **12a** were solved by the SHELXS program.[71] All non-hydrogen atoms were refined with anisotropic temperature factors. The hydrogen atoms were placed at calculated positions and refined isotropically in riding mode. Crystallographic data (excluding structure factors) for the structures reported in this chapter have been deposited with the Cambridge Crystallographic Data Centre. CCDC-757884 (**10a**, MFR99) and 757885 (**11a**, MFR99B) contain the supplementary crystallographic data for this chapter. These data can be obtained free of charge from the Cambridge Crystallographic Data Centre via www.ccdc.cam.ac.uk.

Hydrogen evolution experiments. The ratio of photosensitiser/EDTA of 1:100 was fixed as a consequence of solubility problems. The donor (Na_4EDTA) was already quite insoluble in the solution volume used and a higher excess would have resulted in a completely turbid solution. It was decided not to use less dye to decrease the dye/donor ratio because that could reduce the amount of hydrogen produced, in some cases below the detection limit. The 1:10 ratio of dye/electron relay was chosen to reduce the amount of viologen molecules with two dye-CDs (or two Pt-CDs) at their ends (undesirable, non-effective complexes; Scheme 5.11). In the case of methyl viologen, which does not form inclusion complexes (at least not strong ones), the same ratio was used for comparison. The amount of acid used was chosen to give a low pH in order to have a high concentration of H^+ that could be reduced to H_2, whilst avoiding low values that could cause decomposition of metal-CD or full protonation of Na_4EDTA. The amount of catalyst used was the maximum amount that could be dissolved by 30 min sonication; adding more would have given a very dark suspension resulted in very low yields. The light source was a 150 W xenon lamp (Hamamatsu L2274). Xenon lamps are popular for demanding absorbance and fluorescence applications as high-intensity broadband sources. Because of its sun-like spectrum, the xenon lamp is commonly used for solar simulation. The power supply was a Hamamatsu C2577 and the lamp housing a Hamamatsu E2420. The system was subjected to a number of cycles of degassing and purging with nitrogen and was then illuminated under nitrogen. The amount of hydrogen evolved in the gas phase was measured by gas chromatography.

5.6.2 Synthesis and characterisation

1,1'-Bis(2,4-dinitrophenyl)-4,4'-bipyridine-1,1'-diium dichloride (3). The synthetic procedure was adapted from a reported publication.[72] ^1H NMR (300 MHz, D_2O): δ ppm 9.64–9.42 (m, 6H), 9.08–8.92 (m, 6H), 8.37 (d, J = 8.7 Hz, 2H); ^{13}C NMR (75 MHz, D_2O): δ ppm 155.5, 152.7, 149.7, 145.7, 141.1, 134.0, 133.6, 130.4, 125.7; HRMS (ES+, H_2O): *m/z* calcd for $C_{22}H_{14}N_6O_8$: 490.08731; found: 490.08721 $[M]^{2+}$.

1,1'-Bis(adamantyl)-4,4'-bipyridine-1,1'-diium dichloride (ada-V-ada). Compound **3** (1.02 g, 1.8 mmol) was added to a 100 mL round-bottomed flask and dissolved in a 90/10 v/v mixture of methanol/water (50 mL) at 50 °C. 1-Adamantylamine (1.21 g, 8 mmol) was added in small portions and the dark-red mixture was subsequently stirred at 50 °C for 16 h. The reaction was followed by TLC (eluent: magic mixture). The solvent

was removed *in vacuo* and the brown-red residue was stirred in diethyl ether (100 mL) at room temperature for 1 h and filtered. The solid was stirred in water (70 mL) at 100 °C for 14 h and then the solution was cooled to room temperature and filtered. Soon after heating, a brown solid lighter than water separated from the solution; this became orange and clear. The solvent of the filtrate was removed under reduced pressure and the product was purified by column chromatography (eluent: magic mixture). The desired fractions were collected and the solvent removed *in vacuo*. To remove sodium chloride from the eluent, the product was dissolved in water (10 mL) and precipitated by addition of a 0.6 M aqueous solution of NH_4PF_6 (10 mL). The pure product, ada-V-ada, was obtained by filtration of the light-yellow precipitate and drying *in vacuo* (440 mg, 34%). The counterion, PF_6^-, was exchanged with Cl^- by means of semi-preparative HPLC (see Section 5.6.1). The mobile phase was a gradient of water and acetonitrile (80/20 to 0/100 v/v of water in 55 min) containing 0.1% v/v HCl. ^{1}H NMR (400 MHz, D_2O): δ ppm 9.39–9.35 (m, 4H, AA' of AA'XX'), 8.59–8.54 (m, 4H, XX' of AA'XX'), 2.46–2.38 (m, 18H), 1.92–1.79 (m, 12H); ^{13}C NMR (75 MHz, D_2O): δ ppm 152.2, 145.3, 129.3, 73.9, 44.7, 37.4, 32.9; HRMS (ES+, CH_3OH): *m/z* calcd for $C_{30}H_{38}N_2$: 426.30350; found: 426.30431 $[M]^{2+}$.

1-(2,4-Dinitrophenyl)-4-(pyridin-4-yl)pyridinium chloride (4).[73] 4,4'-Bipyridine (1.56 g, 10 mmol) and 2,4-dinitrochlorobenzene (2.03 g, 10 mmol) were added to a 50 mL round-bottomed flask and dissolved in ethanol (20 mL) at room temperature. The resulting mixture was stirred under reflux for 18 h, then cooled to room temperature and poured into diethyl ether (250 mL) while stirring vigorously. After filtration of the golden-brown precipitate formed, washing with diethyl ether (200 mL), and drying *in vacuo*, product **4** was obtained as a pale-yellow solid (2.18 g, 61%). ^{1}H NMR (300 MHz, D_2O): δ ppm 9.42 (d, J = 2.5 Hz, 1H), 9.32–9.27 (m, 2H, AA' of AA'XX'), 8.97 (dd, J = 8.7, 2.5 Hz, 1H), 8.89–8.85 (m, 2H, AA' of AA'XX'), 8.74–8.70 (m, 2H, XX' of AA'XX'), 8.31 (d, J = 8.7 Hz, 1H), 8.09–8.05 (m, 2H, XX' of AA'XX').

1-(Adamantyl)-4-(pyridin-4-yl)pyridinium hexafluorophosphate (5).[73] Compound **4** (1.43 g, 4 mmol) was added to a 100 mL round-bottomed flask and dissolved in ethanol (30 mL) by heating the solution at 60 °C. 1-Adamantylamine (1.61 g, 11 mmol) was added and the resulting mixture was stirred under reflux for 20 h. The reaction was followed by TLC (eluent: magic mixture). The solvent was removed *in vacuo* and diethyl ether (200 mL) was added to the resulting dark-red viscous oil. The mixture was stirred at room temperature for 10 min and filtered. This procedure was repeated two more times, until the filtrate was colourless. The filtered brown-yellow solid was stirred with water (200 mL) at room temperature for 30 min and filtered. An aqueous 1.5 M solution of NH_4PF_6 (8 mL, 12 mmol) was added dropwise to the yellow filtrate. The resulting precipitate was filtered, washed with water (20 mL), and dried *in vacuo*, affording product **5** as a slightly yellow solid (1.2 g, 69%). ^{1}H NMR (400 MHz, CD_3OD): δ ppm 9.34–9.28 (m, 2H, AA' of AA'XX'), 8.85–8.79 (m, 2H, AA' of AA'XX'), 8.49–8.44 (m, 2H, XX' of AA'XX'), 8.00–7.96 (m, 2H, XX' of AA'XX'), 2.45–2.39 (m, 9H), 1.92–1.88 (m, 6H); ^{13}C NMR (75 MHz, CD_3OD): δ ppm 154.7, 151.8, 143.6, 143.3, 126.9, 123.7, 71.3, 43.1, 36.1, 31.7.

2,4-Dinitrophenyl 4-methylbenzene-1-sulfonate. 2,4-Dinitrophenol (3.68 g, 20 mmol) was added to a 100 mL round-bottomed flask and dissolved in acetone (50 mL). Immediately after triethylamine (2.82 mL, 20.2 mmol) and tosyl chloride (4.19 g, 22 mmol) were added to the solution, a precipitate formed and the mixture was stirred at 30 °C for 15 h. The solvent was then removed *in vacuo* and the residue was dissolved in chloroform (50 mL). Most of the impurities were removed by washing the organic phase with 5 mM aqueous K_2CO_3 (50 mL). The organic phase was then dried over Na_2SO_4, filtered, and the solvent removed *in vacuo*. The resulting residue was added to a 1:2 v/v mixture of ethanol/water (150 mL) and the solution was cooled to 0 °C for 30 min. The precipitate formed was filtered, washed with water (100 mL), and dried *in vacuo*, affording the pure product as a white solid (4.9 g, 72%). ^{1}H NMR (300 MHz, $CDCl_3$): δ ppm 8.76 (d, J = 2.8 Hz, 1H), 8.48 (dd, J = 9.0, 2.8 Hz, 1H), 7.83–7.77 (m, 2H, AA' of AA'XX'), 7.72 (d, J = 9.1 Hz, 1H), 7.42–7.37 (m, 2H, XX' of AA'XX'), 2.49

(s, 3H); ^{13}C NMR (75 MHz, $CDCl_3$): δ ppm 147.2, 145.7, 145.2, 142.4, 130.7, 130.2, 128.6, 128.5, 126.2, 121.5, 21.7.

1-(2,4-Dinitrophenyl)-1'-adamantyl-4,4'-bipyridine-1,1'-diium bis(hexafluorophosphate) (6). Compound **5** (440 mg, 1 mmol) was added to a 100 mL round-bottomed flask and dissolved in dry acetonitrile (40 mL). The previously prepared 2,4-dinitrophenyl 4-methylbenzene-1-sulfonate (510 mg, 1.5 mmol) was added to this solution and the mixture was stirred under reflux in an argon atmosphere for 62 h. The reaction was followed by TLC (eluent: magic mixture). The solution was then cooled to room temperature, resulting in the formation of a precipitate. The solvent was removed *in vacuo* and the residue was stirred in diethyl ether (100 mL) at room temperature for 15 min before the solution was filtered. This procedure was repeated once more. To convert the product from a mixture of salts into a PF_6^- salt, the brown-yellow solid from the filtration was initially dissolved in acetone (40 mL) and the product re-precipitated as a chloride salt, by the addition of a 0.15 M solution of tetrabutylammonium chloride (TBACl) in acetone (20 mL). The resulting yellow solid was filtered and dissolved in water (100 mL). The product was precipitate as a PF_6^- salt by the addition of an aqueous 1.5 M solution of NH_4PF_6 (5 mL). The light-pink precipitate was filtered and dried *in vacuo* (190 mg, 25%). ^{1}H NMR (300 MHz, DMSO-d_6): δ ppm 9.71–9.67 (m, 2H, AA' of AA'XX'), 9.66–9.62 (m, 2H, AA' of AA'XX'), 9.18 (d, J = 2.5 Hz, 1H), 9.13–9.09 (m, 2H, XX' of AA'XX'), 9.03 (dd, J = 8.7, 2.5 Hz, 1H), 8.89–8.84 (m, 2H, XX' of AA'XX'), 8.44 (d, J = 8.7 Hz, 1H), 2.42–2.34 (m, 9H), 1.83–1.77 (m, 6H); ^{13}C NMR (75 MHz, DMSO-d_6): δ ppm 151.2, 149.3, 147.9, 147.1, 143.1, 143.00, 138.3, 131.9, 130.3, 126.8, 126.6, 121.5, 70.4, 41.1, 39.5, 23.0, 13.4.

3α,7β-Dihydroxy-5β-cholan-24-oic acid methyl ester (8). Compound **7** (277.1 mg, 0.71 mmol) was dissolved in methanol (10 mL). A catalytic amount of *p*-toluenesulfonic acid was added and the solution was stirred under reflux for 2.5 h. The reaction was followed by TLC (eluent: ethyl acetate/heptane 80/20 v/v). After removal of the solvent *in vacuo*, the crude product was dissolved in chloroform and washed with an aqueous solution of K_2CO_3 (1 M, 1 × 100 mL). The organic phase was dried over anhydrous Na_2SO_4 and the solvent removed under reduced pressure to yield **8** as a white solid (282.3 mg, 98%). ^{1}H NMR (300 MHz, $CDCl_3$): δ ppm 3.64 (s, 3H), 3.61–3.48 (m, 2H), 2.41–2.10 (m, 2H), 2.01–0.96 (m, 24H), 0.92 (s, 3H), 0.90 (d, J = 6.4 Hz, 3H), 0.65 (s, 3H); ^{13}C NMR (75 MHz, $CDCl_3$): δ ppm 174.7, 71.3, 71.2, 55.7, 54.9, 51.4, 43.69, 43.66, 42.4, 40.1, 39.2, 37.3, 36.9, 35.2, 34.9, 34.0, 31.01, 30.96, 30.3, 28.5, 26.8, 23.3, 21.1, 18.3, 12.1.

3α-(4-Methylphenyl)sulfonyloxy-7β-hydroxy-5β-cholan-24-oic acid methyl ester (9) and **3α-hydroxy-7β-(4-methylphenyl)sulfonyloxy-5β-cholan-24-oic acid methyl ester (10).** Compound **8** (254.5 mg, 0.62 mmol) was added to a Schlenk tube under a nitrogen atmosphere and dissolved in dry pyridine (5 mL). Tosyl chloride (178.4 mg, 0.94 mmol) was added and the solution was heated to 50 °C under nitrogen for 4 h. The reaction was followed by TLC (eluent: ethyl acetate/heptane 50/50 v/v). After removal of the solvent *in vacuo*, the crude product was dissolved in ethyl acetate, washed with HCl (1 N, 3 × 80 mL) and water (1 × 80 mL). The organic phase was dried over anhydrous Na_2SO_4 and the solvent removed under reduced pressure. The crude product (348.4 mg) was further reacted without purification.

3α-Hydroxy-7α-azido-5β-cholan-24-oic acid methyl ester (11) and **3β-azido-7β-hydroxy-5β-cholan-24-oic acid methyl ester (12).** The crude material containing compounds **9** and **10** (348.4 mg) was added to a Schlenk tube under a nitrogen atmosphere and dissolved in dry DMF (15 mL). Sodium azide (201.5 mg, 3.1 mmol) was added and the solution was heated to 60 °C under nitrogen for 20 h. The reaction was followed by TLC (eluent: ethyl acetate/heptane 50/50 v/v). After removal of most of the solvent *in vacuo*, the crude material was dissolved in ethyl acetate and washed with water (2 × 80 mL). The organic phase was dried over anhydrous Na_2SO_4 and the solvent removed under reduced pressure. The crude material was purified by column chromatography (eluent: ethyl acetate/heptane 15/85 v/v). Product **11** was obtained as a slightly yellow viscous

oil (48.2 mg, overall yield = 18%). Product **12** was obtained as a slightly yellow viscous oil (72.8 mg, overall yield = 27.2%).

11: ^{1}H NMR (300 MHz, $CDCl_3$): δ ppm 3.73–3.68 (m, 1H), 3.66 (s, 3H), 3.55–3.43 (m, 1H), 2.43–0.95 (m, 26H), 0.92 (d, J = 6.1 Hz, 3H), 0.91 (s, 3H), 0.63 (s, 3H); ^{13}C NMR (75 MHz, $CDCl_3$): δ ppm 174.7, 71.8, 60.5, 55.6, 51.5, 51.1, 42.6, 41.0, 39.3, 38.3, 38.2, 35.3, 35.2, 34.9, 33.7, 31.0, 30.9, 30.6, 30.4, 28.0, 23.3, 22.9, 20.4, 18.3, 11.7.

12: ^{1}H NMR (300 MHz, $CDCl_3$): δ ppm 3.93–3.88 (m, 1H), 3.66 (s, 3H), 3.59–3.46 (m, 1H), 2.41–2.15 (m, 2H), 2.04–0.99 (m, 24H), 0.97 (s, 3H), 0.92 (d, J = 6.4 Hz, 3H), 0.67 (s, 3H); ^{13}C NMR (75 MHz, $CDCl_3$): δ ppm 174.6, 71.3, 58.3, 55.8, 54.9, 51.5, 43.7, 43.6, 40.1, 38.9, 37.8, 36.3, 35.2, 34.4, 31.2, 31.01, 30.98, 30.3, 28.5, 26.8, 24.5, 23.7, 21.3, 18.3, 12.1.

3α-Hydroxy-7α-azido-5β-cholan-24-oic acid (11a) and **3β-azido-7β-hydroxy-5β-cholan-24-oic acid (12a).** A solution of NaOH was prepared by adding an aqueous solution of NaOH (2 N, 2 mL) to methanol (7 mL). Compounds **11** (20 mg, 0.046 mmol) or **12** (20 mg, 0.046 mmol) were dissolved in this solution and the resulting mixture was stirred at room temperature overnight. The reaction was followed by TLC (eluent: ethyl acetate). While cooling the reaction in ice bath, HCl (4 N) was added until pH = 7. After removal of the solvent *in vacuo*, the crude material obtained was purified by column chromatography (eluent: ethyl acetate). Product **11a** was obtained as a white solid (18.6 mg, 97%). Product **12a** was obtained as a white solid (19 mg, 99%). Single crystals of **11a** and **12a** were grown by slow evaporation of their slightly acidic solutions in water/acetonitrile. The structures were further confirmed by single-crystal X-ray diffraction. Alternatively, compounds **11a** and **12a** could be isolated from the crude mixture by semi-preparative HPLC (see Section 5.6.1). The mobile phase was a gradient of water and acetonitrile (30/70 to 0/100 v/v of water in 35 min) containing 0.1% v/v TFA.

11a: ^{1}H NMR (300 MHz, $CDCl_3$): δ ppm 3.73–3.68 (m, 1H), 3.56–3.44 (m, 1H), 2.46–0.95 (m, 26H), 0.95–0.90 (m, 6H), 0.64 (s, 3H); ^{13}C NMR (75 MHz, $CDCl_3$): δ ppm 179.0, 71.8, 60.4, 55.6, 51.1, 42.6, 41.0, 39.3, 38.3, 38.1, 35.3, 35.2, 34.9, 33.7, 30.8, 30.7, 30.6, 30.4, 28.0, 23.6, 22.9, 20.5, 18.2, 11.8.

12a: ^{1}H NMR (300 MHz, $CDCl_3$): δ ppm 3.93–3.89 (m, 1H), 3.57–3.45 (m, 1H), 2.45–2.22 (m, 2H), 2.04–1.0 (m, 24H), 0.98 (s, 3H), 0.94 (d, J = 6.4 Hz, 3H), 0.69 (s, 3H); ^{13}C NMR (75 MHz, $CDCl_3$): δ ppm 178.8, 71.4, 58.3, 55.8, 54.9, 43.8, 43.6, 40.1, 38.9, 37.9, 36.3, 35.2, 34.5, 31.3, 30.8, 30.3, 29.7, 28.6, 26.8, 24.6, 23.8, 21.4, 18.4, 12.1.

3β-Amino-7β-hydroxy-5β-cholan-24-oic acid methyl ester (13). Compound **12** (340 mg, 0.79 mmol) was added to a 25 mL round-bottomed flask and dissolved in a 20/1 v/v mixture of THF/water (10.5 mL). Triphenylphosphine (1.56 g, 6.2 mmol) was added to this solution and the mixture was stirred under reflux for 18 h. The reaction was followed by TLC (eluent: ethyl acetate/heptane 1/2 v/v). The solvent was removed *in vacuo* and the crude product was purified by column chromatography (eluent: ethyl acetate/heptane 1/2 v/v to remove impurities followed by methanol/triethylamine 50/1 v/v to elute the product). The appropriate fractions were collected and the solvent was removed *in vacuo*. Finally, the residue was dissolved in chloroform (50 mL) and the solvent was removed *in vacuo* to remove triethylamine remaining from the eluent. This procedure was repeated three times, affording pure product **13** as a light-yellow viscous oil (320 mg, 98%). ^{1}H NMR (300 MHz, $CDCl_3$): δ ppm 3.55 (s, 3H), 3.46–3.35 (m, 1H), 3.11–3.05 (m, 1H), 2.31–2.04 (m, 2H), 1.93–0.88 (m, 24H), 0.87 (s, 3H), 0.81 (d, J = 6.2 Hz, 3H), 0.57 (s, 3H); ^{13}C NMR (75 MHz, $CDCl_3$): δ ppm 174.4, 70.8, 55.7, 54.7, 51.2, 45.7, 43.4, 43.2, 40.0, 38.5, 36.8, 36.7, 35.0, 34.6, 34.5, 30.76, 30.75, 29.5, 28.3, 27.7, 26.6, 23.7, 21.2, 18.1, 11.9.

3β-Amino-7β-hydroxy-5β-cholan-24-oic acid (14). Compound **13** (150 mg, 0.37 mmol) was added to a 25 mL round-bottomed flask and dissolved in methanol (10 mL). A 2 M aqueous solution of NaOH (5 mL, 10 mmol) was added to this solution and the mixture was stirred at room temperature for 16 h. The reaction was followed

by TLC (eluent: methanol). The solution was then neutralised (pH = 8) by the addition of a 2 M aqueous solution of HCl (5 mL, 10 mmol) and the solvent was removed *in vacuo*. Sodium chloride formed was removed by selective dissolution of the product in the minimum amount of methanol (30 mL) and filtration. Removal of the solvent of the filtrate *in vacuo* afforded the pure product **14** as a white solid (145 mg, 100%). ^{1}H NMR (300 MHz, CD_3OD): δ ppm 3.52–3.43 (m, 1H), 3.43–3.37 (m, 1H), 3.35 (s, 3H), 2.29–2.15 (m, 1H), 2.11–1.06 (m, 22H), 1.04 (s, 3H), 0.96 (d, J = 6.2 Hz, 3H), 0.71 (s, 3H); ^{13}C NMR (75 MHz, CD_3OD): δ ppm 183.7, 71.7, 57.4, 56.8, 48.6, 44.7, 44.2, 41.5, 40.2, 38.1, 37.8, 37.2, 36.2, 35.6, 34.1, 32.2, 30.5, 29.7, 27.9, 25.5, 23.9, 22.6, 19.1, 12.6; HRMS (ES+, CH_3OH): *m/z* calcd for $C_{24}H_{42}NO_3$: 392.31647; found: 392.31491 $[M+H]^+$.

1-(7β-Hydroxy-5β-cholan-24-oic acid-3β-yl)-1'-(adamantyl)-[4,4'-bipyridine]-1,1'-diium dichloride (ada-V-DC). Compound **14** (120 mg, 0.3 mmol) was added to a 50 mL round-bottomed flask and dissolved in ethanol (20 mL). Compound **6** (130 mg, 0.3 mmol) was then added and an immediate colour change from pink to orange was observed. The mixture was stirred under reflux for 18 h. The reaction was followed by TLC (eluent: magic mixture). The solution was cooled to room temperature, resulting in the formation of a small amount of a crystalline precipitate. The solvent was removed *in vacuo* and the resulting brown-yellow residue was purified by semi-preparative HPLC (see Section 5.6.1). The mobile phase was a gradient of water and acetonitrile (30/70 to 0/100 v/v of water in 40 min) containing 0.1% v/v HCl. The desired fractions were collected and the solvent was removed *in vacuo*, affording pure product ada-V-DC as a white solid (16 mg, 7%). ^{1}H NMR (300 MHz, CD_3OD): δ ppm 9.58–9.49 (m, 2H, AA' of AA'XX'), 9.44–9.34 (m, 2H, AA' of AA'XX'), 8.76–8.61 (m, 4H, AA'XX'), 5.10–4.98 (m, 1H), 3.71–3.53 (m, 1H), 2.49–1.14 (m, 41H), 1.12 (s, 3H), 0.98 (d, J = 6.4 Hz, 3H), 0.74 (s, 3H); ^{13}C NMR (75 MHz, CD_3OD): δ ppm 179.2, 151.0, 150.8, 146.0, 144.1, 128.2, 128.0, 73.1, 72.2, 69.9, 57.8, 56.8, 44.5, 44.3, 43.1, 42.8, 41.1, 38.2, 37.1, 36.8, 36.07–36.03 (m), 35.3, 34.1, 33.8, 32.5, 31.7, 29.4, 28.3, 27.1, 23.0, 22.4, 18.9, 12.4; HRMS (ES+, H_2O): *m/z* calcd for $C_{44}H_{62}N_2O_3$: 666.47604; found: 666.47935 $[M]^{2+}$.

5.7 References

[1] T. Nussbaumer, *Energy Fuels* **2003**, *17,* 1510–1521.

[2] E. Amouyal, *Sol. Energy Mater. Sol. Cells* **1995**, *38,* 249–276.

[3] W. Lubitz, W. Tumas, *Chem. Rev.* **2007**, *107,* 3900–3903.

[4] A. J. Esswein, D. G. Nocera, *Chem. Rev.* **2007**, *107,* 4022–4047.

[5] N. W. Ockwig, T. M. Nenoff, *Chem. Rev.* **2007**, *107,* 4078–4110.

[6] V. V. Struzhkin, B. Militzer, W. L. Mao, H. K. Mao, R. J. Hemley, *Chem. Rev.* **2007**, *107,* 4133–4151.

[7] R. Borup, J. Meyers, B. Pivovar, Y. S. Kim, R. Mukundan, N. Garland, D. Myers, M. Wilson, F. Garzon, D. Wood, P. Zelenay, K. More, K. Stroh, T. Zawodzinski, J. Boncella, J. E. McGrath, M. Inaba, K. Miyatake, M. Hori, K. Ota, Z. Ogumi, S. Miyata, A. Nishikata, Z. Siroma, Y. Uchimoto, K. Yasuda, K. I. Kimijima, N. Iwashita, *Chem. Rev.* **2007**, *107,* 3904–3951.

[8] J. Kiwi, M. Grätzel, *Nature* **1979**, *281,* 657–658.

[9] M. Kirch, J. M. Lehn, J. P. Sauvage, *Helv. Chim. Acta* **1979**, *62,* 1345–1384.

[10] K. Kalyanasundaram, J. Kiwi, M. Grätzel, *Helv. Chim. Acta* **1978**, *61,* 2720–2730.

[11] P. Ritterskamp, A. Kuklya, M. A. Wüstkamp, K. Kerpen, C. Weidenthaler, M. Demuth, *Angew. Chem. Int. Ed.* **2007**, *46,* 7770–7774.

[12] D. W. Hwang, H. G. Kim, J. S. Lee, J. Kim, W. Li, S. Hyuk Oh, *J. Phys. Chem. B* **2005**, *109,* 2093–2102.

[13] W. Shangguan, A. Yoshida, *J. Phys. Chem. B* **2002**, *106,* 12227–12230.

[14] I. Tsuij, H. Kato, A. Kudo, *Chem. Mater.* **2006**, *18,* 1969–1975.

[15] M. Anpo, *Catal. Sur. Jpn.* **1997**, *1,* 169–179.

[16] A. Kudo, *Int. J. Hydrogen Energy* **2006**, *31,* 197–202.

[17] K. Maeda, K. Teramura, D. Lu, T. Takata, N. Saito, Y. Inoue, K. Domen, *Nature* **2006**, *440,* 295.
[18] J. R. Darwent, P. Douglas, A. Harriman, G. Porter, M. C. Richoux, *Coord. Chem. Rev.* **1982**, *44,* 83–126.
[19] I. Okura, *Coord. Chem. Rev.* **1985**, *68,* 53–99.
[20] Y. Amao, I. Okura, *J. Mol. Catal. B: Enzym.* **2002**, *17,* 9-21.
[21] J. Handman, A. Harriman, G. Porter, *Nature* **1984**, *307,* 534–535.
[22] I. Okura, H. Hosono, *J. Phys. Chem.* **1992**, *96,* 4466–4469.
[23] D. L. Jiang, C. K. Choi, K. Honda, W. S. Li, T. Yuzawa, T. Aida, *J. Am. Chem. Soc.* **2004**, *126,* 12084–12089.
[24] Y. Astuti, E. Palomares, S. A. Haque, J. R. Durrant, *J. Am. Chem. Soc.* **2005**, *127,* 15120–15126.
[25] N. Himeshima, Y. Amao, *Energy Fuels* **2003**, *17,* 1641–1644.
[26] M. Grätzel, *Acc. Chem. Res.* **1981**, *14,* 376–384.
[27] N. Serpone, E. Pelizzetti, M. Grätzel, *Coord. Chem. Rev.* **1985**, *64,* 225–245.
[28] C. G. Garcia, J. F. de Lima, N. Y. Murakami Iha, *Coord. Chem. Rev.* **2000**, *196,* 219–247.
[29] G. M. Brown, S. F. Chan, C. Creutz, H. A. Schwarz, N. Sutin, *J. Am. Chem. Soc.* **1979**, *101,* 7638–7640.
[30] E. H. Yonemoto, G. B. Saupe, R. H. Schmehl, S. M. Hubig, R. L. Riley, B. L. Iverson, T. E. Mallouk, *J. Am. Chem. Soc.* **1994**, *116,* 4786–4795.
[31] A. Auffrant, A. Barbieri, F. Barigelletti, J. Lacour, P. Mobian, J. P. Collin, J. P. Sauvage, B. Ventura, *Inorg. Chem.* **2007**, *46,* 6911–6919.
[32] L. L. Tinker, N. D. McDaniel, P. N. Curtin, C. K. Smith, M. J. Ireland, S. Bernhard, *Chem. Eur. J.* **2007**, *13,* 8726–8732.
[33] J. I. Goldsmith, W. R. Hudson, M. S. Lowry, T. H. Anderson, S. Bernhard, *J. Am. Chem. Soc.* **2005**, *127,* 7502–7510.
[34] D. R. Rosseinsky, P. M. S. Monk, *J. Chem. Soc., Faraday Trans.* **1990**, *86,* 3597–3601.
[35] M. Felici, P. Contreras-Carballada, Y. Vida, J. M. M. Smits, R. J. M. Nolte, L. De Cola, R. M. Williams, M. C. Feiters, *Chem. Eur. J.* **2009**, *15,* 13124–13134.
[36] N. Krauss, W. Hinrichs, I. Witt, P. Fromme, W. Pritzkow, Z. Dauter, C. Betzel, K. S. Wilson, H. T. Witt, W. Saenger, *Nature* **1993**, *361,* 326–331.
[37] W. Kuhlbrandt, D. N. Wang, Y. Fujiyoshi, *Nature* **1994**, *367,* 614–621.
[38] J. W. Park, N. H. Choi, J. H. Kim, *J. Phys. Chem.* **1996**, *100,* 769–774.
[39] A. Diaz, P. A. Quintela, J. M. Schuette, A. E. Kaifer, *J. Phys. Chem.* **1988**, *92,* 3537–3542.
[40] Y. Okuno, Y. Chiba, O. Yonemitsu, *Chem. Commun.* **1984**, 1638–1639.
[41] O. Johansen, A. Launikonis, J. W. Loder, A. W. H. Mau, W. H. F. Sasse, J. D. Swift, D. Wells, *Aust. J. Chem.* **1981**, *34,* 2347–2354.
[42] N. P. Luneva, V. Y. Shafirovich, A. E. Shilov, *Kinet. Katal.* **1988**, *30,* 250–251.
[43] Y. Okuno, Y. Chiba, O. Yonemitsu, *Chem. Lett.* **1983**, 893–896.
[44] J. Alvarez, J. Liu, E. Roman, A. E. Kaifer, *Chem. Commun.* **2000**, 1151–1152.
[45] M. Felici, P. Contreras-Carballada, J. M. M. Smits, R. J. M. Nolte, R. M. Williams, L. De Cola, M. C. Feiters, *Molecules* **2010**, *15,* 2039–2059.
[46] H. F. M. Nelissen, M. Kercher, L. De Cola, M. C. Feiters, R. J. M. Nolte, *Chem. Eur. J.* **2002**, *8,* 5407–5414.
[47] T. Hiraishi, T. Kamachi, I. Okura, *J. Mol. Catal. A: Chem.* **2000**, *151,* 7–15.
[48] P. Contreras-Carballada, *Thesis dissertation: Photoactivated Nano-Systems,* University of Amsterdam, Amsterdam, **2009**.
[49] A. C. Templeton, W. P. Wuelfing, R. W. Murray, *Acc. Chem. Res.* **2000**, *33,* 27–36.
[50] Y. Liu, K. B. Male, P. Bouvrette, J. H. T. Luong, *Chem. Mater.* **2003**, *15,* 4172–4180.
[51] J. Liu, J. Alvarez, W. Ong, E. Roman, A. E. Kaifer, *Langmuir* **2001**, *17,* 6762–6764.
[52] L. Strimbu, J. Liu, A. E. Kaifer, *Langmuir* **2003**, *19,* 483–485.
[53] V. E. Maier, V. Y. Shafirovich, *Kinet. Katal.* **1988**, *29,* 417–420.

[54] S. Trasatti, O. A. Petrii, *J. Electroanal. Chem.* **1992**, *327,* 353–376.
[55] A. J. Bard, M. A. Fox, *Acc. Chem. Res.* **1995**, *28,* 141–145.
[56] M. S. Matheson, P. C. Lee, D. Meisel, *J. Phyc. Chem.* **1983**, *87,* 394–399.
[57] W. J. Albery, P. N. Bartlett, A. J. J. McMahon, *J. Electronanal. Chem.* **1985**, *182,* 7–23.
[58] N. Mourtzis, P. Contreras-Carballada, M. Felici, R. J. M. Nolte, R. M. Williams, L. De Cola, M. C. Feiters, *Phys. Chem. Chem. Phys.* **2011**, *13,* 7903–7909.
[59] S. Kunugi, T. Okubo, N. Ise, *J. Am. Chem. Soc.* **1976**, *98,* 2282–2287.
[60] E. H. Ryu, A. Ellern, Y. Zhao, *Tetrahedron* **2006**, *62,* 6808–6813.
[61] M. R. de Jong, J. F. J. Engbersen, J. Huskens, D. N. Reinhoudt, *Chem. Eur. J.* **2000**, *6,* 4034–4040.
[62] A. F. Hofmann, K. J. Mysels, *J. Lipid Res.* **1992**, *33,* 617–626.
[63] S. Rau, B. Schäfer, D. Gleich, E. Anders, M. Rudolph, M. Friedrich, H. Görls, W. Henry, J. G. Vos, *Angew. Chem. Int. Ed.* **2006**, *45,* 6215–6218.
[64] M. V. Rekharsky, Y. Inoue, *Chem. Rev.* **1998**, *98,* 1875–1918.
[65] P. M. S. Monk, Chapter 9, in *The Viologens: Physicochemical Properties, Synthesis and Applications of the Salts of 4,4'-Bipyridine,* Wiley, Chichester, **1998**.
[66] A. G. Evans, J. C. Evans, M. W. Baker, *J. Am. Chem. Soc.* **1977**, *99,* 5882–5884.
[67] *Those experiments have been completed after the thesis manuscript was approved and are published in: P. Contreras-Carballada, N. Mourtzis, M. Felici, S. Bonnet, R. J. M. Nolte, R. M. Williams, L. De Cola, M. C. Feiters, Eur. J. Org. Chem.* ***2012****, 6729–6736.*
[68] T. Nakashima, T. Anno, H. Kanda, Y. Sato, T. Kuroi, H. Fujii, S. Nagadome, G. Sugihara, *Colloids Surf., B* **2002**, *24,* 103–110.
[69] Y. Pellegrin, R. J. Forster, T. E. Keyes, *Inorg. Chim. Acta* **2008**, *361,* 2683–2691.
[70] P. A. Sigala, M. A. Tsuchida, D. Herschlag, *Proc. Natl. Acad. Sci. USA* **2009**, *106,* 9232–9237.
[71] G. M. Sheldrick, *SHELXL-97. Program for the Refinement of Crystal Structures,* University of Göttingen, Germany, **1997**.
[72] H. Kamogawa, S. Sato, *Bull. Chem. Soc. Jpn.* **1991**, *64,* 321–323.
[73] J. W. Park, H. E. Song, S. Y. Lee, *J. Phys. Chem. B* **2002**, *106,* 7186–7192.

6

Cationic Heteroleptic Cyclometalated Ir^{III} Complexes Containing Phenyl-Triazole and Triazole-Pyridine Clicked Ligands

Abstract

The [3+2] Huisgen dipolar cycloaddition method ("click" chemistry) was utilised to prepare a class of bidentate 1-substituted-4-phenyl-1*H*-1,2,3-triazole cyclometalating ligands (phtl) with different substituents on the triazole moiety. By using various ligands (phtl-R^1 and pytl-R^2; pytl = 2-(1-substituted-1*H*-1,2,3-triazol-4-yl)pyridine; R^1 = adamantyl, methyl and R^2 = adamantyl, methyl, permethylated β-cyclodextrin, ursodeoxycholic acid), we prepared a small library of new luminescent heteroleptic ionic iridium complexes [Ir(phtl-R^1)$_2$(pytl-R^2)]Cl and investigated their photophysical properties. The flexibility of the clicking approach allows straightforward control of the physico-chemical properties of the complexes by varying the nature of the substituent on the ligand.

*This work has been published as: M. Felici, P. Contreras-Carballada, J. M. M. Smits, R. J. M. Nolte, R. M. Williams, L. De Cola, M. C. Feiters, Molecules **2010**, 15, 2039–2059.*

6.1 Introduction

The photoluminescence of organometallic complexes has attracted much interest, since it can be utilised for a variety of applications, such as oxygen sensors, biological probes, and phosphorescent dopants in optoelectronic devices.[1,2] In particular, cyclometalated complexes of iridium(III) have received a great deal of attention because of the high tunability of their emission in terms of colour and efficiency. This has been achieved by screening a large variety of cyclometalating and ancillary ligands, often bearing functional groups with electron-withdrawing or -releasing properties. While much has been done to investigate the photophysical properties of iridium(III) complexes, little attention has been focused on controlling other properties such as solubility and polarity. The increasing number of applications of such compounds has made this aspect more appealing; it is indeed important, for example, to create photo-active materials that are water soluble to incorporate them in electrochemiluminescence (ECL) devices, or that are apolar with high affinity for hydrophobic matrices or possess "sticky" tails capable of selectively recognising guests on modified surfaces.[3] The best approach to obtain complexes with designed physico-chemical properties is through the functionalisation of ligands with selected substituents. Unfortunately, most of the ligands are difficult to prepare or their synthesis requires a large number of steps.[4–7] Their functionalisation is not always trivial because it usually implies aromatic substitution reactions (on the phenyl or pyridyl moieties) and coupling reactions. This all leads to an increase in the cost of the material itself and to limited applicability. We now report an exploration of the application of the Huisgen copper(I)-catalysed [3+2] cycloaddition as an efficient and flexible means to prepare a class of bidentate cyclometalated ligands, namely, 1-substituted-4-phenyl-1*H*-1,2,3-triazole (phtl; **1** and **2**; Scheme 6.1);[8] we have also investigated whether these ligands can be used to form stable luminescent heteroleptic iridium complexes (Scheme 6.1) and the properties that emerge from the use of such ligands. The substituents we used to functionalise 2-(1-substituted-1*H*-1,2,3-triazol-4-yl) pyridine (pytl) and phtl, namely, permethylated β-cyclodextrin (βCD), adamantyl (ada), an ursodeoxycholic acid (UDC) derivative and the methyl group, are examples of moieties provided with different physico-chemical properties. Decoration of a metal complex with these residues does not influence the electronic properties of the molecule, and hence, does not directly affect its correlated luminescent properties. However, it can add other features to the metal complex, providing us with multi-functional materials. We prepared a small library of phosphorescent complexes containing host (βCD) or guest molecules (adamantane, UDC-derivative). Cyclodextrins are well-known cyclic oligosaccharides that can form inclusion

complexes in aqueous solution with a variety of hydrophobic substrates, such as adamantane derivatives, and they have been widely applied as supramolecular building blocks in various areas,[9–14] including photo-activated electron transfer processes.[6,15–18] With βCD attached to [Ir(**1**)$_2$(pytl-βCD)]Cl, the phosphorescent dye can be immobilised on guest-appended polymeric membranes, which are used as responsive materials for oxygen sensors. βCD can also act as second-sphere ligand, enhancing the photophysical properties of [Ir(**1**)$_2$(pytl-βCD)]Cl.[19] The presence of adamantanes in [Ir(**2**)$_2$(pytl-ada)]Cl and [Ir(**1**)(**2**)(pytl-ada)]Cl allows the surface of vesicles and nanoparticles covered with cyclodextrins to be decorated with iridium complexes.[20]

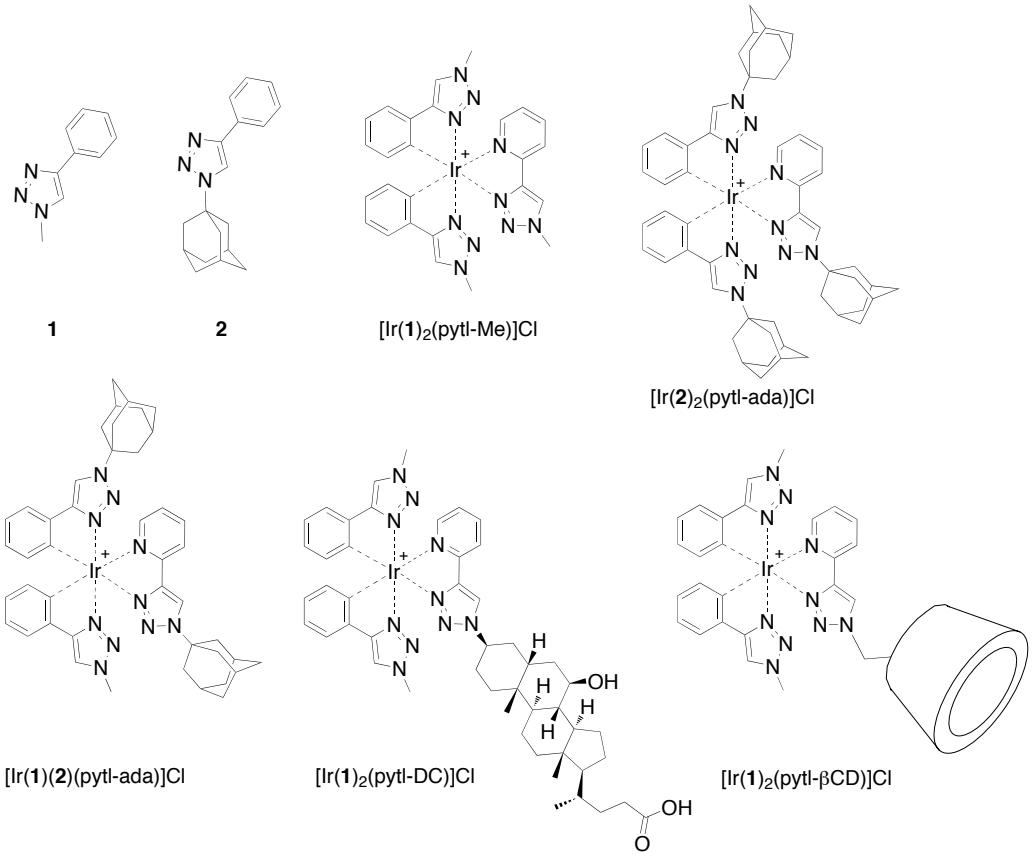

Scheme 6.1 *Structures of **1** and **2** and their heteroleptic iridium complexes.*

Complex [Ir(**1**)$_2$(pytl-DC)]Cl is particularly interesting, in which a UDC derivative instead of adamantane was used as host. Native UDC is an amphiphilic molecule that has high affinity for β-cyclodextrin[21] as well as for bilayer membranes.[22–25] As we show herein, UDC can be easily functionalised through the azido group (Scheme 6.3 below). Its affinity for membranes, combined with the sensitivity of polyamine iridium(III) complexes to the polarity of their environment, provides us with an interesting luminescent polarity probe for the study

of the dynamics of natural and artificial membranes.[4,5,26] Besides the supramolecular aspects, the nature of the substituents in complex [Ir(phtl-R^1)$_2$(pytl-R^2)]Cl strongly affects other properties such as solubility. This can be tuned by changing the hydrophilicity of the ligands: the simplest complex of the series, methylated [Ir(**1**)$_2$(pytl-Me)]Cl, displays poor solubility in water, which is dramatically increased in [Ir(**1**)$_2$(pytl-βCD)]Cl by the introduction of one βCD.

6.2 Results and discussion

6.2.1 Synthesis of phtl and pytl ligands and their iridium complexes

The Huisgen cycloaddition, also known as the "click" reaction,[27] involves the formation of 1,2,3-triazole rings by coupling terminal alkynes and azides. It can be used to prepare the phtl ligand in one step, by reacting ethynylbenzene with an azide-containing molecule. The known high efficiency of this reaction, combined with its tolerance to other functional groups,[27] allows linking of the phtl (and pytl) ligand to many different groups (i.e., methyl, adamantyl, bile acid),[19,28,29] requiring only the presence of at least one azido group in the molecule of interest. Therefore, this approach makes a large library of cyclometalating ligands readily accessible. Ligands **1** and **2** were prepared by reacting azidomethane and 1-azidoadamantane with ethynylbenzene for 2 h in deoxygenated THF, in the presence of CuBr and *N*,*N*,*N*′,*N*′,*N*-pentamethyldiethylenetriamine (PMDTA). The products were isolated in 43 and 76% yield, respectively. This click reaction was also used to prepare the ancillary ligands pytl-ada, pytl-βCD, and pytl-Me by reacting 2-ethynylpyridine with the corresponding azido-appended derivatives under identical conditions (Scheme 6.2), as reported previously in this thesis (Chapter 2). The click approach was also used to prepare the ligand 3β-[4-(pyridin-6-yl)-1*H*-1,2,3-triazol-1-yl]-7β-hydroxy-5β-cholan-24-oic acid (pytl-DC), starting from the intermediate compound 3β-azido-7β-hydroxy-5β-cholan-24-oic acid methyl ester (**3**). The latter was synthesised by selective functionalisation of commercially available UDC, as described in Chapter 5 (Scheme 5.8). In addition to full characterisation by NMR spectroscopy and mass spectrometry, the crystal structures of ligands **1**, **2**, and pytl-DC were obtained by single-crystal X-ray diffraction.[30] The crystal structure of pytl-DC confirmed that the inverted stereochemistry of the carbon bearing the azide in **3**, with respect to UDC, resulted in a derivative with a molecular rod-like shape (Figure 6.1).

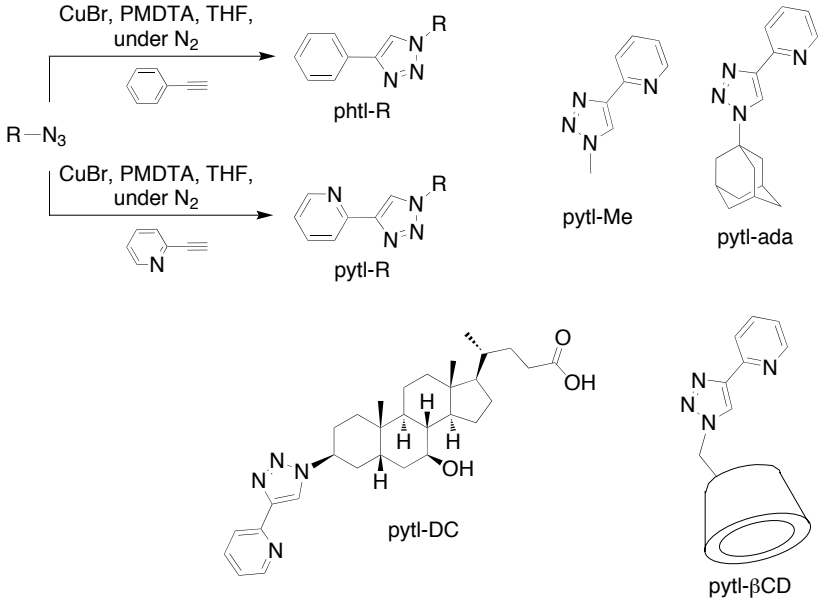

Scheme 6.2 *Synthesis and structures of the ligands phtl-R and pytl-R.*

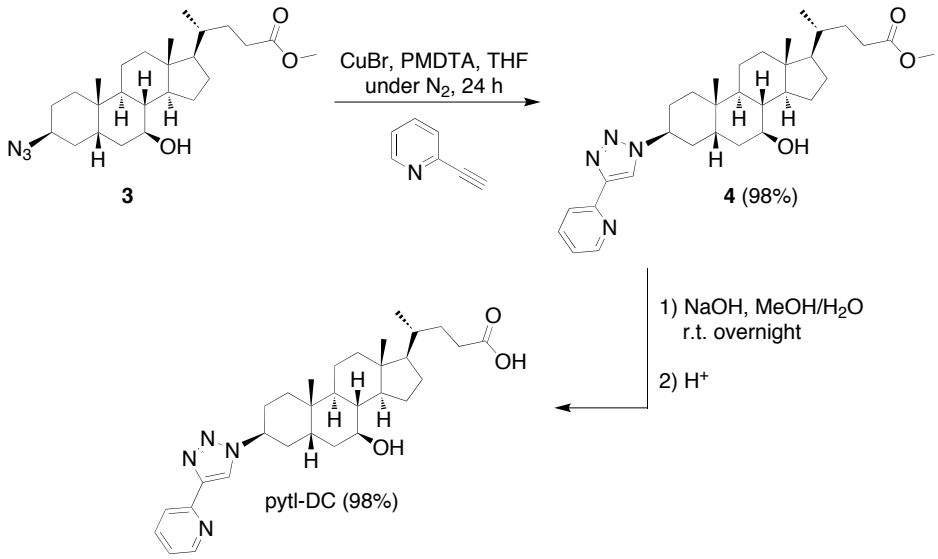

Scheme 6.3 *Synthesis of the bile acid derivatives pytl-DC.*

It is interesting to note that the click approach allows the functionalisation of phtl and pytl with substituents that display very different molecular complexity. We explored herein the range from a simple methyl group to a bile acid, which has a four-ring steroidal structure with two hydroxyl groups and one carboxylic acid functionality. The efficiency and high flexibility of such an approach provides a powerful tool for the preparation of large libraries of bidentate ligands.

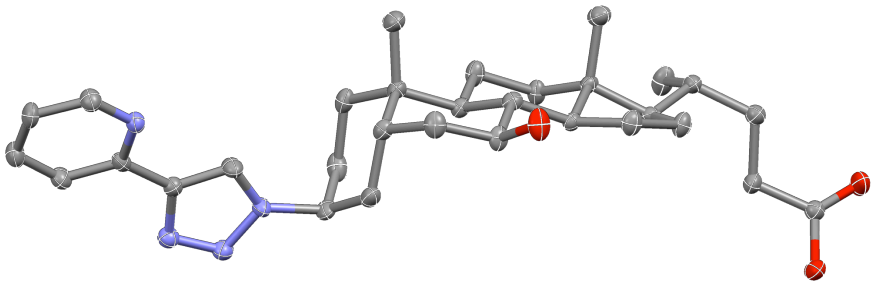

Figure 6.1 *Crystal structure of pytl-DC. Grey, carbon; blue, nitrogen; red, oxygen. The thermal ellipsoids in the image represent the 25% probability limit. Hydrogen atoms are omitted for clarity.*

The synthesis of an iridium(III) complex is usually accomplished through a two-step process, namely, the Nonoyama reaction, which yields a chloride-bridged dinuclear iridium species,[31] followed by substitution of the chlorides with an ancillary ligand (Scheme 6.4). The iridium(III) dimers [(**1**)$_2$Ir(μ-Cl)$_2$Ir(**1**)$_2$] and [(**2**)$_2$Ir(μ-Cl)$_2$Ir(**2**)$_2$] were prepared by reacting **1** or **2** with $IrCl_3$ in a mixture of water/2-methoxyethanol 1/3 (v/v) at 97 °C. Compound [(**1**)(**2**)Ir(μ-Cl)$_2$Ir(**1**)(**2**)] was prepared by using an equimolar mixture of **1** and **2**, which afforded a mixture of dinuclear species that was difficult to separate; it was used further without purification. All of the complexes were obtained by reacting the corresponding iridium dimers with a bidentate pytl ligand (Scheme 6.4) under mild conditions in a mixture of chloroform/methanol 3:1 (v/v) at 45 °C. After 3 h, the formation of only one new spot on TLC was observed, characterised (in contrast to the starting compound) by bright luminescence under a UV-vis lamp at 366 nm. All of the complexes, except for [Ir(**1**)(**2**)(pytl-ada)]Cl, were purified by silica column chromatography or preparative-layer chromatography (PLC). In the case of [Ir(**1**)(**2**)(pytl-ada)]Cl, the non-selective synthesis resulted in a mixture of different iridium species that could not be isolated by traditional silica chromatography. This problem was overcome by using an HPLC apparatus equipped with a semi-preparative reversed-phase column. Characterisation was achieved by means of NMR spectroscopy and high-resolution mass spectrometry (HRMS). Compound [Ir(**1**)(**2**)(pytl-ada)]Cl is an example of a cyclometalated complex in which three different ligands are present: **1**, **2** and pytl-ada. It was synthesised to investigate the possibility of preparing complexes with a higher degree of functionalisation. To the best of our knowledge, complexes with these structural characteristics have not yet been reported.

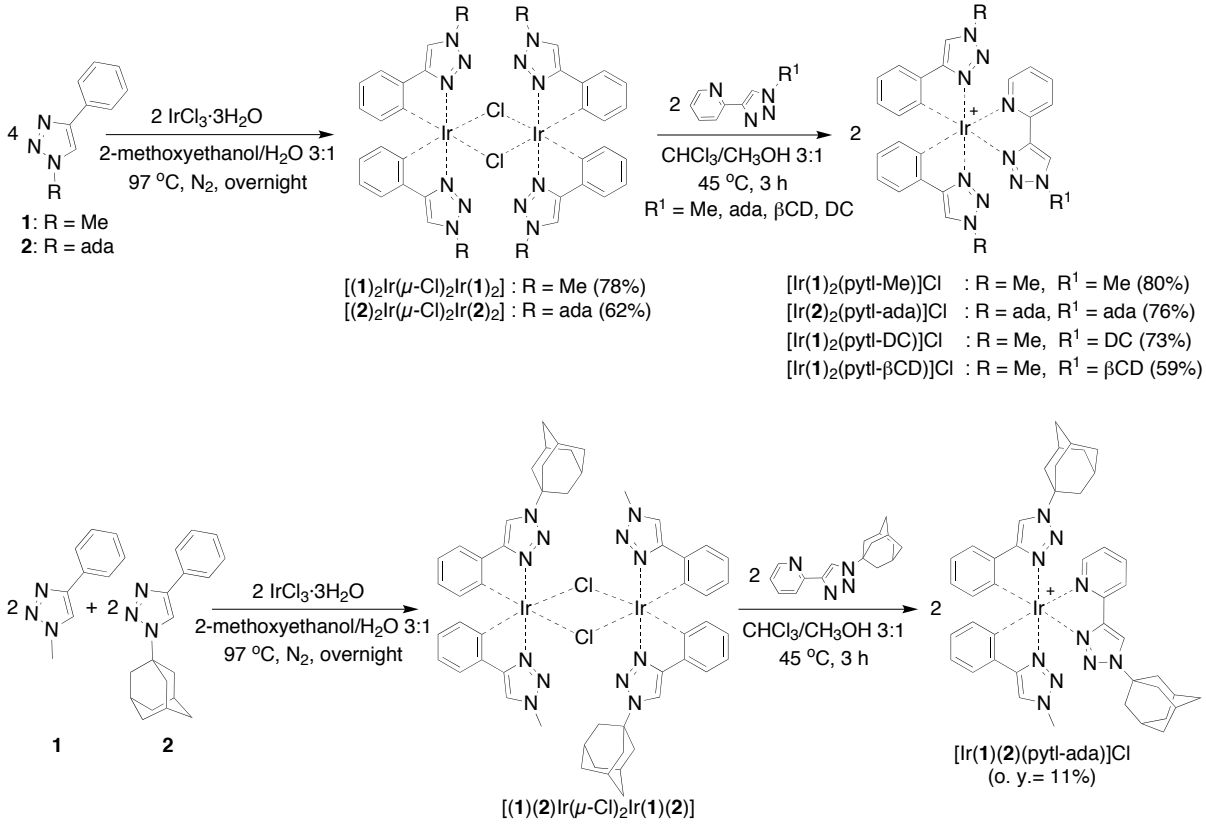

Scheme 6.4 *Synthesis of the iridium(III) complexes.*

Cyclometalated iridium complexes have an octahedral geometry. The relative spatial orientation of the substituents around the metal centre depends on whether they are attached to the cyclometalating or ancillary ligands. In fact, it is known that in the chloride-bridged dinuclear iridium complex prepared by the Nonoyama reaction the cyclometalating ligands are always oriented in a *trans* position with respect to each other. In particular, the two nitrogen atoms of the phtl ligands are aligned along a common axis through the central iridium atom.[32] The pytl ligand, which is inserted in the second synthetic step, is located on the plane perpendicular to that axis. By taking advantage of the well-established orientation of the ligands around the complex, considering that both phtl and pytl can be prepared from the same azide-appended molecule, we were able to control the location of the substituents in the iridium complex with our approach simply by clicking them to either 2-ethynylpyridine or ethynylbenzene.

6.2.2 Photophysical characterisation

All of the iridium complexes are soluble in acetonitrile and these solutions were used to measure the absorption and emission spectra. The UV-vis spectra of all of the complexes were very similar;[30] we show herein only the spectrum of the iridium complex [Ir(**1**)(**2**)(pytl-ada)] Cl (Figure 6.2). The intense absorption bands present in the UV region (190–240 nm) are assigned to the $^1(\pi–\pi^*)$ transitions of the phtl and pytl ligands (Figure 6.2). The shoulders appearing between 290 and 350 nm are likely to be due to weaker charge-transfer (CT) transitions, being of both spin-allowed ^{1}MLCT and forbidden ^{3}MLCT nature (MLCT = metal-to-ligand charge transfer). All complexes are luminescent in solution at room temperature and display very similar, broad, featureless emission spectra between 410 and 650 nm (for the emission of [Ir(**1**)(**2**)(pytl-ada)]Cl see Figure 6.2) with a maximum for the emission at 510 nm.

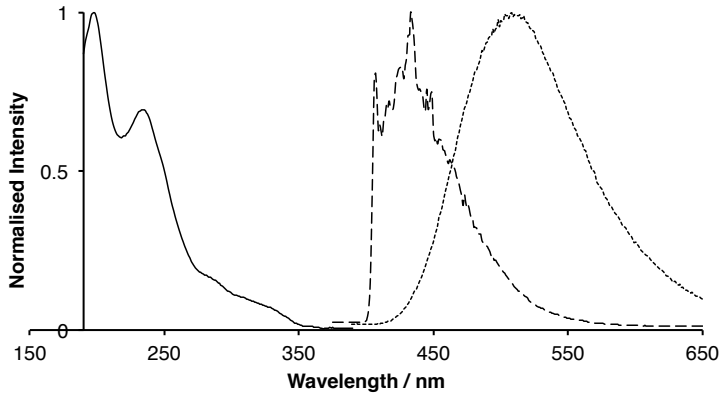

Figure 6.2 *UV-vis absorption spectrum (solid line) and room-temperature emission spectrum (dotted line) of [Ir(**1**)(**2**)(pytl-ada)]Cl (λ_{exc} = 335 nm) in acetonitrile. The emission spectrum of [Ir(**1**)(**2**)(pytl-ada)]Cl (λ_{exc} = 335 nm) at 77 K (dashed line) in a glassy butyronitrile matrix is also shown.*

According to previously published work concerning analogous cyclometalated iridium(III) complexes,[33] such a broad emission is characteristic for a MLCT excited state in which, formally speaking, an electron is transferred from the metal centre to the ligand with the lowest reduction potential. If this transfer is understood as a HOMO–LUMO transition, the HOMO would be localised on the metal core and the LUMO orbital on the ligand. This is also consistent with the emission quantum efficiencies of all of the complexes measured in air-equilibrated solutions, which range from 0.021 to 0.052 (Table 6.1). In deaerated conditions

compounds [Ir(**1**)$_2$(pytl-Me)]Cl, [Ir(**2**)$_2$(pytl-ada)]Cl, and [Ir(**1**)(**2**)(pytl-ada)]Cl exhibit a two- to three-fold increase in the emission quantum yields; for [Ir(**1**)$_2$(pytl-DC)]Cl and [Ir(**1**)$_2$(pytl-βCD)]Cl the increase is very large and reaches a five-fold higher value. For [Ir(**1**)$_2$(pytl-βCD)]Cl, the quantum yields are comparable to the value measured for [Ir(ppy)$_2$(pytl-ada)]Cl, in which the cyclometalating ligands are 2-phenylpyridine (ppy).[19] This behaviour could be explained by the tendency of molecules such as βCD, and especially UDC, to interact (aggregate or form inclusion complexes) even in very diluted solutions; this interaction could increase the emission efficiencies by reducing the non-radiative decay promoted by vibrational modes. Organisation of organometallic complexes in solution through micelle or vesicle formation, inclusion in a cyclodextrin cavity, or otherwise has been shown to influence greatly the properties of these complexes.[34] These changes in the emissive properties of the compounds studied are always assigned to changes in the surrounding environment. For example, vesicle formation with metallosurfactants leads to the observation of fast components in the excited-state decay of the individual metal complexes.[35]

Table 6.1 *Luminescence lifetimes and quantum yields of the emission of iridium complexes. For quantum yield measurements, λ_{exc} = 335 nm; for lifetime measurements, λ_{exc} = 324 nm. The solutions were measured in air-equilibrated acetonitrile (air) and argon-saturated acetonitrile (Ar), which was degassed by bubbling argon for 20–30 min through the solution.*

Complex	Φ(air)	Φ(Ar)	τ (ns, air)	τ (ns, Ar)
[Ir(**1**)$_2$(pytl-Me)]Cl	0.037	0.097	24.8	27.1
[Ir(**2**)$_2$(pytl-ada)]Cl	0.021	0.048	17.4	18.0
[Ir(**1**)(**2**)(pytl-ada)]Cl	0.024	0.071	11.8 (60%) 23.6 (40%)	19.7
[Ir(**1**)$_2$(pytl-DC)]Cl	0.039	0.203	24	28.3 (84%) 2.22 (16%)
[Ir(**1**)$_2$(pytl-βCD)]Cl	0.052	0.254	26.4	34.1

All complexes undergo large hypsochromic shifts upon cooling to 77 K (see spectrum of [Ir(**1**)(**2**)(pytl-ada)]Cl; Figure 6.2). In a butyronitrile solid matrix, the maximum of the emission wavelength is blueshifted and appears at 435 nm. Such behaviour is expected for compounds emitting from a charge-transfer excited state and is due to the impossibility for the solvent molecules to rearrange around the excited state. The consequent lack of stabilisation of the excited state leads to a more energetic (blueshifted) emission. The emission spectra

show a series of vibronic transitions (see emission of [Ir(**1**)(**2**)(pytl-ada)]Cl; Figure 6.2) that are not resolved at room temperature and which imply that a considerable ligand-centred character develops in these species at low temperature.[36]

6.3 Conclusion

In this chapter, we reported the preparation and photophysical properties of new highly luminescent heteroleptic iridium(III) complexes. Click chemistry was used as an efficient tool to introduce the phtl and pytl ligands functional groups with various level of complexity. The flexibility of such an approach provides access to a large library of clicked ligands and therefore to multi-functional iridium(III) complexes with tuneable physico-chemical properties. In particular, complex [Ir(**1**)$_2$(pytl-DC)]Cl is a promising luminescent polarity probe for the study of membrane dynamics; complexes [Ir(**1**)$_2$(pytl-βCD)]Cl and [Ir(**2**)$_2$(pytl-ada)]Cl are interesting building blocks for the preparation of supramolecular systems.

6.4 Acknowledgements

I thank Dr. Pablo Contreras-Carballada for the photophysical measurements and for fruitful discussions.

6.5 Experimental

6.5.1 Methods and materials

General. THF was purified by distillation under nitrogen from sodium/benzophenone; dry DMF was purchased from Fluka. The compounds pytl-Me, pytl-ada, and pytl-βCD were prepared as described in Chapter 2.[19] The synthesis of 3β-azido-7β-hydroxy-5β-cholan-24-oic acid methyl ester (**3**) is described in Chapter 5.[30] All other chemicals were purchased from Aldrich, Fluka, or Acros and used as received. Analytical thin-layer chromatography (TLC) was performed on Merck precoated silica gel 60 F-254 plates (layer thickness 0.25 mm) and the compounds were visualised by UV irradiation at λ = 254 and/or 366 nm and by staining with phosphomolybdic acid reagent or $KMnO_4$. PLC was performed on Merck precoated silica gel 60 F-254 plates (layer thickness 1 mm, concentrating zone 20 × 4 cm) and the compounds were visualised by UV irradiation at λ = 254 and/or 366 nm. Purifications by silica gel chromatography were performed by using Acros (0.035–0.070 mm, pore diameter ca. 6 nm) silica gel. All click reactions were performed in an oxygen-free atmosphere of nitrogen under Schlenk conditions and solvents were dried and distilled according to standard laboratory procedures.

NMR spectroscopy. ^{1}H NMR spectra were recorded at 25 °C on Varian Inova 400 or Bruker DMX-300 spectrometers operating at 400 and 300 MHz, respectively. ^{13}C NMR spectra were recorded on a Bruker

DMX-300 spectrometer operating at 75 MHz. ^{1}H NMR chemical shifts (δ) are reported in parts per million (ppm) relative to the residual proton signal of the solvent, δ = 3.31 ppm for CD_3OD, δ = 7.26 ppm for $CDCl_3$, and δ = 2.50 ppm for DMSO-d_6. Multiplicities are reported as follow: s (singlet), d (doublet), t (triplet), q (quartet), dd (doublet of doublets), ddd (doublet of doublet of doublets), or m (multiplet). Broad peaks are indicated by b. Coupling constants are reported as a *J* value in Hertz (Hz). The number of protons (*n*) for a given resonance is indicated as *n*H, and is based on spectral integration values. ^{13}C NMR chemical shifts (δ) are reported in ppm relative to the carbon signal of the solvent, δ = 49.0 ppm for CD_3OD, δ = 77 ppm for $CDCl_3$, and δ = 40 ppm for DMSO-d_6. The signals of the protons on hydroxyl and carboxylic groups could not be observed due to fast exchange processes. The resolution of the ^{13}C spectra was increased when necessary by performing an exponential apodisation of the FID.

Mass spectrometry (MS). All mass analyses were performed by using electrospray (ESI) techniques. HRMS measurements were performed on a JEOL AccuTOF instrument by using water, acetonitrile, or methanol as solvents. Standard MS measurements were performed on a Finnigan LCQ Advantage Max by using water, acetonitrile, or methanol as solvents.

High-performance liquid chromatography (HPLC). HPLC was carried out on a Shimadzu LC-20AT HPLC system equipped with a SPD-10AV UV-vis detector and a fraction collector. Columns were purchased from Dr. Maisch GmbH. The compounds were purified on the mg scale by using a semi-preparative reversed-phase HPLC column. An aliquot of solution (2 mL) was injected in a ReproSil 100 C8, 5 μm (250 × 10 mm) column operating at 30 °C. The detection wavelengths were fixed at 254 and 215 nm. A gradient of water and acetonitrile both containing 0.1% v/v HCl or trifluoroacetic acid (TFA) was used as the mobile phase, with a flow rate of 4 mL min^{-1}. HCl was used to ensure that chloride was the only counterion of the isolated compounds. In all cases, samples were prepared by dissolving the compound in a mixture of water/acetonitrile 95/5 or 1/1 v/v, and filtering the solution on a Nylon syringe filter (0.2 μm).

X-ray crystallography. Single crystals of **1** (phtl-Me) and **2** (phtl-ada) were grown by slow evaporation of a solution of compounds **1** and **2** in chloroform/heptane. Single crystals of pytl-DC were grown by slow evaporation of a solution of pytl-DC in methanol. Crystal data and summaries of the data collection and structure refinement are given in Table 6.2 for pytl-DC; for compounds **1** and **2** the data is reported in the literature.[30] All measurements were performed at –65 °C. The structure of **1** was solved by the SHELXS program,[37] and that of **2** and pytl-DC by the program CRUNCH.[38] All non-hydrogen atoms were refined with anisotropic temperature factors. The hydrogen atoms were placed at calculated positions and refined isotropically in riding mode. Crystallographic data (excluding structure factors) for all the structures have been deposited with the Cambridge Crystallographic Data Centre. CCDC-757888 (**1**, FELIC3), 757886 (**2**, MFR130), and 757887 (pytl-DC, PYTLUD) contain the supplementary crystallographic data for this chapter. These data can be obtained free of charge from the Cambridge Crystallographic Data Centre via www.ccdc.cam.ac.uk.

Emission and UV-vis spectroscopy. Electronic absorption spectra were recorded in a quartz cuvette (1 cm, Hellma) on a Hewlett-Packard 8543 diode array spectrometer (range 190 nm–1100 nm). Steady-state fluorescence spectra were recorded by using a Spex 1681 fluorimeter, equipped with a Xe arc light source, a Hamamatsu R928 photomultiplier tube detector and double excitation and emission monochromator. Emission spectra were corrected for source intensity and detector response by standard correction curves, unless otherwise noted. Luminescence quantum yields (Φ_{em}) were measured in optically dilute solutions (O.D. < 0.1 at excitation wavelength), using $[Ru(bpy)_3]Cl_2$ in aerated and deoxygenated water ($\Phi_{em,air}$ = 0.028; $\Phi_{em,deox}$ = 0.042) or diphenylanthracene in aerated and deoxygenated cyclohexane ($\Phi_{em,air}$ = 0.77; $\Phi_{em,deox}$ = 0.91) as references.

Lifetimes of excited states were determined by using a coherent Infinity Nd:YAG-XPO laser (2 ns pulses full-width at half maximum (fwhm)) and a Hamamatsu C5680-21 streak camera equipped with a Hamamatsu M5677 low-speed single sweep unit. Streak cameras are high-speed light detectors, which enable detection of the fluorescence as a function of the spectral and the time evolution simultaneously.

6.5.2 Synthesis and characterisation

1-Methyl-4-phenyl-1*H*-1,2,3-triazole (1). Dry DMF was deoxygenated prior to use by performing three freeze-pump-thaw cycles. A two-necked round-bottomed flask was carefully dried with a flame under a flow of nitrogen. In the cooled flask, NaN_3 (198 mg, 3 mmol) was added together with deoxygenated dry DMF (40 mL). CH_3I (0.3 mL, 4.8 mmol) was added dropwise and the solution was stirred in the dark overnight. The methyl azide formed is a highly explosive intermediate and was therefore not isolated.[39] The clicking reagents were subsequently added to the reaction mixture and a large excess of ethynylbenzene (658.9 µL, 6 mmol) and catalyst were used to ensure the complete consumption of methyl azide. A solution of CuBr (430 mg, 3 mmol) and PMDTA (0.67 mL, 3.2 mmol) was prepared by dissolving both reagents in oxygen-free dry DMF (10 mL); bubbling nitrogen through the solution for 20 min to prevent oxidation of Cu(I). When the CuPMDTA complex dissolved, an aliquot of the solution (5 mL), together with ethynylbenzene (0.45 mL, 4.5 mmol) were added to the flask. The resulting mixture was stirred in the dark at room temperature under a nitrogen atmosphere for 24 h. The reaction was followed by TLC (eluent: diethyl ether). After removal of the solvent in vacuo (CAUTION! this solution may still contain methyl azide in case the conversion with ethynylbenzene was not 100%), the solid obtained was purified by column chromatography (diethyl ether/heptane 50/50 v/v followed by diethyl ether/ethyl acetate 90/10 v/v). Product **1** was obtained as a white solid (208 mg, overall yield 43%). Crystals were grown by slow evaporation of a solution of **1** in chloroform/heptane. The structure was further confirmed by single-crystal X-ray diffraction. ^{1}H NMR (300 MHz, $CDCl_3$): δ ppm 7.86–7.78 (m, 2H), 7.73 (s, 1H), 7.47–7.38 (m, 2H), 7.37–7.29 (m, 1H), 4.14 (s, 3H); ^{13}C NMR (75 MHz, $CDCl_3$): δ ppm 148.0, 130.6, 128.8, 128.1, 125.7, 120.5, 36.7; HRMS (ES+, $CHCl_3/CH_3OH$): *m/z* calcd for $C_9H_{10}N_3$: 160.08747; found: 160.08768 $[M+H]^+$.

1-Adamantyl-4-phenyl-1*H*-1,2,3-triazole (2). Distilled THF was bubbled with nitrogen for 1 h prior to use to remove oxygen. Ethynylbenzene (185.6 µL, 1.69 mmol) and 1-azidoadamantane (300 mg, 1.69 mmol) were added to a Schlenk tube under a nitrogen atmosphere and dissolved in deoxygenated THF (15 mL). A solution of CuBr (242.4 mg, 1.69 mmol) and PMDTA (365.8 µL, 1.75 mmol) was prepared by dissolving both reagents in deoxygenated THF (15 mL) and bubbling nitrogen through the solution for 20 min to prevent oxidation of Cu(I). When the CuPMDTA complex dissolved, the solution became slightly green and an aliquot of it (3 mL) was added to the Schlenk tube. The resulting mixture was stirred in the dark at room temperature under a nitrogen atmosphere for 2.5 h. The reaction was followed by TLC (eluent: diethyl ether/heptane 80/20 v/v). No workup was performed and after removal of the solvent *in vacuo*, the blue-green solid obtained was directly purified by column chromatography (diethyl ether/heptane 30/70 v/v). Product **2** was obtained as a white solid (358.8 mg, 76%). Crystals were grown by slow evaporation of a solution of **2** in chloroform/heptane. The structure was further confirmed by single-crystal X-ray diffraction. ^{1}H NMR (300 MHz, $CDCl_3$): δ ppm 7.86–7.81 (m, 2H), 7.82 (s, 1H), 7.45–7.38 (m, 2H), 7.34–7.28 (m, 1H), 2.32–2.26 (m, 9H), 1.85–1.79 (m, 6H); ^{13}C NMR (75 MHz, $CDCl_3$): δ ppm 137.8, 131.1, 128.8, 127.8, 125.6, 118.2, 59.6, 43.0, 35.9, 29.5; HRMS (ES+, $CHCl_3/CH_3OH$): *m/z* calcd for $C_{18}H_{22}N_3$: 280.18137; found: 280.18165 $[M+H]^+$.

3β-[4-(Pyridin-6-yl)-1*H*-1,2,3-triazol-1-yl]-7β-hydroxy-5β-cholan-24-oic acid methyl ester (4). Distilled THF was bubbled with nitrogen for 1 h prior to use to remove oxygen. 2-Ethynylpyridine (58.6 μL, 0.58 mmol) and **3** (250 mg, 0.58 mmol) were added to a Schlenk tube under a nitrogen atmosphere and dissolved in deoxygenated THF (10 mL). A solution of CuBr (83.2 mg, 0.58 mmol) and PMDTA (125.4 μL, 0.6 mmol) was prepared by dissolving both reagents in deoxygenated THF (10 mL) and bubbling nitrogen through the solution for 20 min to prevent oxidation of Cu(I). When the CuPMDTA complex had dissolved, the solution became slightly green and an aliquot of it (4 mL) was added to the Schlenk tube. The resulting mixture was stirred in the dark at room temperature under a nitrogen atmosphere for 24 h. The reaction was followed by TLC (eluent: ethyl acetate). After removal of the solvent *in vacuo*, the blue-green solid obtained was directly purified by column chromatography (eluent: ethyl acetate/heptane 50/50 v/v followed by ethyl acetate/heptane 60/40 v/v). Product **4** was obtained as a white solid (303.9 mg, 98%). ^{1}H NMR (400 MHz, $CDCl_3$): δ ppm 8.57 (ddd, J = 4.9, 1.7, 0.9 Hz, 1H), 8.24 (s, 1H), 8.20 (ddd, J = 8.0, 1.0, 1.0, Hz, 1H), 7.77 (ddd, J = 7.8, 7.8, 1.8 Hz, 1H), 7.22 (ddd, J = 7.6, 4.9, 1.1 Hz, 1H), 4.72–4.68 (m, 1H), 3.66 (s, 3H), 3.67–3.57 (m, 1H), 2.40–1.02 (m, 26H), 0.94–0.91 (m, 6H), 0.68 (s, 3H); ^{13}C NMR (75 MHz, $CDCl_3$): δ ppm 174.5, 150.3, 149.1, 147.6, 136.8, 122.6, 121.0, 120.1, 70.9, 56.5, 55.8, 54.8, 51.3, 43.5, 43.2, 39.9, 39.4, 37.6, 36.2, 35.1, 34.2, 30.94–30.77 (m), 30.4, 28.4, 26.7, 24.8, 23.4, 21.3, 18.2, 12.0; HRMS (ES+, CH_3OH): *m/z* calcd for $C_{32}H_{46}N_4NaO_3$: 557.34676; found: 557.34578 [M+Na]$^+$.

3β-[4-(Pyridin-6-yl)-1*H*-1,2,3-triazol-1-yl]-7β-hydroxy-5β-cholan-24-oic acid (pytl-DC). A solution of NaOH was prepared by adding an aqueous solution of NaOH (2 N, 2 mL) to methanol (7 mL). Compound **4** (55.9 mg, 0.10 mmol) was dissolved in this solution and the resulting mixture was stirred at room temperature overnight. The reaction was followed by TLC (eluent: methanol/ethyl acetate 10/90 v/v). While cooling the reaction in an ice bath, HCl (4 N) was added until pH = 7–8. After removal of the solvent *in vacuo*, the crude material was purified by column chromatography (methanol/ethyl acetate 10/90 v/v). Pytl-DC was obtained as a white solid (55.6 mg, 98%). Crystals were grown by slow evaporation of a solution of pytl-DC in methanol. The structure was further confirmed by single-crystal X-ray diffraction. ^{1}H NMR (300 MHz, DMSO-d_6): δ ppm 8.67 (s, 1H), 8.59 (ddd, J = 4.9, 1.8, 1.0 Hz, 1H), 8.05 (ddd, J = 8.0, 1.1, 1.1 Hz, 1H), 7.89 (ddd, J = 8.0, 7.8, 1.8 Hz, 1H), 7.33 (ddd, J = 7.7, 4.9, 1.1 Hz, 1H), 4.74–4.68 (m, 1H), 3.44–3.32 (m, 1H), 2.29–0.93 (m, 26H), 0.89 (d, J = 6.4 Hz, 3H), 0.85 (s, 3H), 0.63 (s, 3H); ^{13}C NMR (75 MHz, DMSO-d_6): δ ppm 175.8, 150.7, 149.9, 147.4, 137.6, 123.3, 122.9, 119.9, 69.8, 56.6, 56.2, 55.3, 43.5, 43.2, 40.2, 39.3, 38.1, 37.2, 35.3, 34.4, 31.6, 31.4, 31.0, 30.7, 28.6, 27.1, 24.8, 24.0, 21.6, 18.8, 12.5; HRMS (ES+, CH_3OH): *m/z* calcd for $C_{31}H_{44}N_4NaO_3$: 543.33111; found: 543.33058 [M+Na]$^+$.

[(1)$_2$Ir(μ-Cl)$_2$Ir(1)$_2$]. A mixture 3/1 v/v of 2-methoxyethanol/water (9 mL) was deoxygenated by bubbling nitrogen through it for 10–15 min. Ligand **1** (91.5 mg, 0.57 mmol) and $IrCl_3 \cdot 3H_2O$ (70 mg, 0.23 mmol) were added and the solution was heated to 97 °C in the dark for 24 h under a nitrogen atmosphere (without bubbling). After cooling to room temperature, the yellow solid was filtered off, washed with water (3 × 100 mL), diethyl ether (3 × 100 mL), and dried. After purification by column chromatography (eluent: from methanol/chloroform 5/95 v/v to methanol/chloroform 10/90 v/v), chloride-bridged complex [(**1**)$_2$Ir(μ-Cl)$_2$Ir(**1**)$_2$] was obtained as a yellow solid (97.4 mg, 78%). ^{1}H NMR (400 MHz, DMSO-d_6): δ ppm 8.61 (s, 2H), 8.59 (s, 2H), 7.42 (ddd, J = 7.4, 1.4, 0.5 Hz, 2H), 7.41 (ddd, J = 7.5, 1.4, 0.5 Hz, 2H), 6.81 (ddd, J = 7.4, 7.4, 1.2 Hz, 2H), 6.80 (ddd,

J = 7.4, 7.4, 1.2 Hz, 2H), 6.64 (ddd, *J* = 7.4, 7.4, 1.4 Hz, 2H), 6.63 (ddd, *J* = 7.4, 7.4, 1.5 Hz, 2H), 6.05 (ddd, *J* = 7.6, 1.2, 0.5 Hz, 2H), 6.00 (ddd, *J* = 7.6, 1.2, 0.5 Hz, 2H), 4.30–4.26 (m, 12H); ESI-MS (ES+, $CHCl_3$/CH_3OH): *m/z* 1053.1 $[M\text{-Cl}]^+$.

[(2)$_2$Ir(μ-Cl)$_2$Ir(2)$_2$]. A mixture 3/1 v/v of 2-methoxyethanol/water (9 mL) was deoxygenated by bubbling nitrogen through it for 10–15 min. Ligand **2** (50 mg, 0.18 mmol) and $IrCl_3 \cdot 3H_2O$ (21.4 mg, 0.072 mmol) were added and the solution was heated to 97 °C in the dark for 24 h under a nitrogen atmosphere (without bubbling). After cooling to room temperature, the yellow solid was filtered off, washed with water (3 × 80 mL), and dried. After purification by column chromatography (eluent: ethyl acetate), chloride-bridged complex [(**2**)$_2$Ir(μ-Cl)$_2$Ir(**2**)$_2$] was obtained as a yellow solid (35 mg, 62%). ^{1}H NMR (400 MHz, $CDCl_3$): *δ* ppm 7.83 (s, 2H), 7.77 (s, 2H), 7.27–7.22 (m, 4H), 6.75 (ddd, *J* = 7.4, 7.4, 1.1 Hz, 2H), 6.70 (ddd, *J* = 7.3, 7.3, 1.2 Hz, 2H), 6.64 (ddd, *J* = 7.2, 7.2, 1.1 Hz, 2H), 6.62 (ddd, *J* = 7.3, 7.3, 1.2 Hz, 2H), 6.15 (dd, *J* = 7.4, 0.8 Hz, 2H), 6.04 (dd, *J* = 7.6, 0.5 Hz, 2H), 2.48–2.28 (m, 36H), 1.90–1.79 (m, 24H); ^{13}C NMR (75 MHz, $CDCl_3$): *δ* ppm 157.0, 156.8, 145.9, 143.9, 136.3, 135.8, 132.9, 132.3, 127.24, 127.22, 121.08, 121.06, 120.8, 120.6, 113.9, 113.7, 61.9, 61.4, 42.9, 42.8, 35.79, 35.75, 29.49, 29.46; ESI-MS (ES+, $CHCl_3$/CH_3OH): *m/z* 807.0 $[(M/2)+\text{Na}]^+$

[(1)(2)Ir(μ-Cl)$_2$Ir(1)(2)]. A mixture 3/1 v/v of 2-methoxyethanol/water (12 mL) was deoxygenated by bubbling nitrogen through it for 10–15 min. Ligands **1** (40 mg, 0.25 mmol) and **2** (70.2 mg, 0.25 mmol), and $IrCl_3 \cdot 3H_2O$ (62.5 mg, 0.21 mmol) were added and the solution was heated to 97 °C in the dark for 24 h under a nitrogen atmosphere (without bubbling). After cooling to room temperature, the yellow solid was filtered off, washed with water (3 × 80 mL), and dried. This reaction is expected to yield a mixture of chloride-bridged complexes [(**X**)(**Y**)Ir(μ-Cl)$_2$Ir(**X**)(**Y**)] (**X** = **1**,**2**; **Y** = **1**,**2**). The reaction was followed by TLC (eluent: methanol/chloroform 20/80 v/v) where several spots, corresponding to different dimeric species, could be observed. The crude material was used for further experiments without purification.

[Ir(1)$_2$(pytl-Me)]Cl. Ligand pytl-Me (14.6 mg, 0.086 mmol) was added as a solid to a suspension of precursor [(**1**)$_2$Ir(μ-Cl)$_2$Ir(**1**)$_2$] (47.2 mg, 0.043 mmol) in methanol/chloroform 1/3 v/v (4 mL). The suspension was heated to 45 °C and stirred in the dark for 3 h, after which time a clear and yellow solution was obtained. The reaction was followed by TLC (eluent: methanol/chloroform 30/70 v/v) by which, under UV light at 366 nm, the compound appeared as a bright green-blue luminescent spot. After removal of the solvent *in vacuo*, the solid obtained was purified by PLC (eluent: methanol/chloroform 25/75 v/v). The product was obtained as a slightly yellow solid (47.4 mg, 80%). ^{1}H NMR (400 MHz, $CDCl_3$): *δ* ppm 10.48 (s, 1H), 8.88 (d, *J* = 7.9 Hz, 1H), 7.93–7.87 (m, 2H), 7.77 (s, 1H), 7.73 (s, 1H), 7.43 (dd, *J* = 7.5, 1.1 Hz, 1H), 7.39 (dd, *J* = 7.4, 1.1 Hz, 1H), 7.12 (ddd, *J* = 7.5, 5.6, 1.3 Hz, 1H), 6.96 (ddd, *J* = 7.5, 7.5, 1.2 Hz, 1H), 6.92 (ddd, *J* = 7.4, 7.4, 1.2 Hz, 1H), 6.85 (ddd, *J* = 7.5, 7.5, 1.4 Hz, 1H), 6.81 (ddd, *J* = 7.5, 7.5, 1.4 Hz, 1H), 6.32–6.28 (m, 2H), 4.16 (s, 3H), 4.08 (s, 3H), 4.05 (s, 3H); ^{13}C NMR (75 MHz, $CDCl_3$): *δ* ppm 157.9, 157.5, 151.1, 150.3, 149.3, 146.1, 142.3, 139.0, 135.3, 135.0, 132.75, 132.73, 128.9, 128.6, 128.1, 124.8, 123.7, 122.6, 122.3, 122.2, 122.1, 118.9, 118.8, 38.60, 38.56, 38.5; HRMS (ES+, CH_3OH): *m/z* calcd for $C_{26}H_{24}IrN_{10}$: 669.18146; found: 669.18464 $[M]^+$.

[Ir(2)$_2$(pytl-ada)]Cl. Ligand pytl-ada (7.29 mg, 0.026 mmol) was added as a solid to a suspension of precursor [(**2**)$_2$Ir(μ-Cl)$_2$Ir(**2**)$_2$] (20.0 mg, 0.013 mmol) in methanol/chloroform 1/3 v/v (4 mL). The suspension was heated to 45 °C and stirred in the dark for 3 h, after which time a clear and yellow solution was obtained. The reaction was followed by TLC (eluent: methanol/chloroform 20/80 v/v) by which, under UV light at 366 nm, the compound appeared as a bright green-blue luminescent spot. After removal of the solvent *in vacuo*, the solid obtained was purified by column chromatography (eluent: from chloroform to methanol/chloroform 5/95 v/v). The product was obtained as a slightly yellow solid (20.3 mg, 76%). ^{1}H NMR (400 MHz, $CDCl_3$): *δ* ppm 10.56 (s, 1H), 9.16 (d, *J* = 7.8 Hz, 1H), 7.96 (bd, *J* = 5.4 Hz, 1H), 7.92 (ddd, *J* = 7.8, 7.8, 1.4 Hz, 1H), 7.76 (s, 1H),

7.71 (s, 1H), 7.34 (dd, *J* = 5.7, 1.3 Hz, 1H), 7.32 (dd, *J* = 5.6, 1.2 Hz, 1H), 7.07 (ddd, *J* = 7.2, 5.8, 1.2 Hz, 1H), 6.91 (ddd, *J* = 6.7, 6.7, 1.2 Hz, 1H), 6.88 (ddd, *J* = 6.6, 6.6, 1.2 Hz, 1H), 6.82 (ddd, *J* = 7.4, 7.4, 1.4 Hz, 1H), 6.77 (ddd, *J* = 7.5, 7.5, 1.4 Hz, 1H), 6.16 (dd, *J* = 7.6, 0.6 Hz, 1H), 6.13 (dd, *J* = 7.5, 0.6 Hz, 1H), 2.30–2.19 (m, 15H), 2.13–2.10 (m, 12H), 1.81–1.68 (m, 18H); ^{13}C NMR (75 MHz, $CDCl_3$): δ ppm 156.7, 156.1, 151.7, 150.0, 148.9, 146.8, 143.3, 138.9, 136.1, 135.7, 133.0, 132.3, 128.2, 127.4, 125.2, 124.01, 123.95, 122.1, 121.7, 121.5, 121.2, 114.1, 114.0, 62.2, 61.9, 61.8, 42.70, 42.67, 42.5, 35.67, 35.63, 29.7, 29.5, 29.37, 29.36; HRMS (ES+, CH_3OH): *m/z* calcd for $C_{53}H_{60}IrN_{10}$: 1029.46316; found: 1029.46242 $[M]^+$.

[Ir(1)(2)(pytl-ada)]Cl. Ligand pytl-ada (44.8 mg, 0.16 mmol) was added as a solid to a suspension of the crude mixture of precursors [(**X**)(**Y**)Ir(μ-Cl)$_2$Ir(**X**)(**Y**)] (**X** = **1**,**2**; **Y** = **1**,**2**) (76.2 mg) in methanol/ chloroform 1/3 v/v (8 mL). The suspension was heated to 45 °C and stirred in the dark for 3 h, after which time a yellow solution was obtained. The reaction was followed by TLC (eluent: methanol/ chloroform 20/80 v/v). The mixture of products obtained could not be separated by column chromatography. After removal of the solvent *in vacuo*, the crude material was purified by using a semi-preparative reversed-phase column. The mobile phase was a gradient of water and acetonitrile (1/1 v/v for 20 min + gradient 1/1 to 100/0 v/v of acetonitrile in 40 min) containing 0.1% v/v HCl. The complex [Ir(**1**)(**2**)(pytl-ada)]Cl was a mixture of four stereoisomeric forms: two diastereoisomers **A** and **B**, and their corresponding enantiomers (Λ,Δ). The diastereoisomeric species **A**(Λ+Δ) and **B**(Λ+Δ) could be separated by HPLC using the conditions described above. However, we did not isolate these compounds and instead collected them as a mixture. The HPLC fractions containing the desired iridium complex were identified by ESI-MS. The retention times of the two peaks of [Ir(**1**)(**2**)(pytl-ada)]Cl were t = 41.9 and 43.3 min. After collecting the fractions, the solvent was removed *in vacuo* at 40 °C. The product was obtained as a slightly yellow solid (21.1 mg, overall yield = 11%) containing the two diastereoisomers in a molar ratio of 1:0.8 as calculated from the NMR spectrum. ^{1}H NMR (400 MHz, $CDCl_3$): δ ppm 10.49 (s, 0.8H), 10.45 (s, 1H), 9.12–9.05 (m, 1H+0.8H), 7.93–7.83 (m, 2H+1.6H), 7.77 (bs, 1.6H), 7.76 (s, 1H), 7.73 (s, 1H), 7.33 (dd, *J* = 7.4, 1.1 Hz, 1.6H), 7.32 (dd, *J* = 7.2, 1.1 Hz, 1H), 7.29 (dd, *J* = 7.4, 1.2 Hz, 1H), 7.08–7.02 (m, 1H+0.8H), 6.92–6.76 (m, 3H+2.4H), 6.75 (ddd, *J* = 7.4, 7.4, 1.3 Hz, 0.8H) 6.74 (ddd, *J* = 7.4, 7.4, 1.3 Hz, 1H), 6.31 (d, *J* = 7.5 Hz, 0.8H), 6.24 (d, *J* = 7.5 Hz, 1H), 6.12 (d, *J* = 7.5 Hz, 1H), 6.08 (d, *J* = 7.5 Hz, 0.8H), 4.02 (s, 2.4H), 4.00 (s, 3H), 2.28–2.22 (m, 9H+7.2H), 2.22–2.17 (m, 3H+2.4H), 2.14–2.09 (m, 6H+4.8H), 1.82–1.66 (m, 12H+9.6H); ^{13}C NMR (75 MHz, $CDCl_3$): δ ppm 157.8, 157.2, 156.6, 156.0, 151.48, 151.47, 150.1, 149.9, 148.84, 148.79, 146.5, 146.2, 143.2, 142.9, 138.9–138.8 (m), 135.9, 135.63, 135.60, 135.4, 133.1, 132.9, 132.4, 132.2, 128.2, 128.1, 127.5, 127.3, 125.1, 124.9, 124.3, 124.2, 123.7, 123.6, 122.23, 122.19, 122.1, 121.8, 121.7, 121.56, 121.55, 121.3, 119.2, 119.0, 114.3, 114.1, 62.4, 62.3, 61.9, 61.8, 42.62, 42.57, 42.4, 42.3, 38.5, 38.4, 35.60, 35.58, 35.55, 29.41–29.37 (m), 29.32, 29.30; HRMS (ES+, CH_3OH): *m/z* calcd for $C_{44}H_{48}IrN_{10}$: 909.36926; found: 909.37012 $[M]^+$.

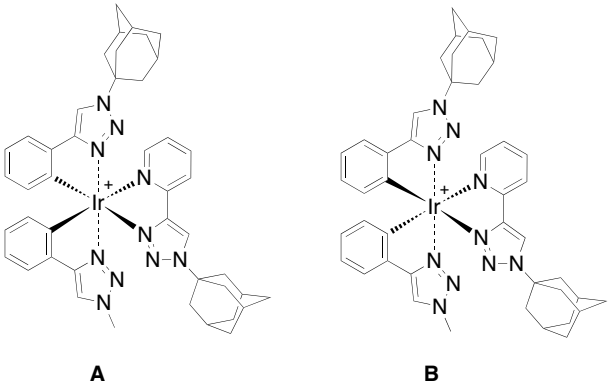

[Ir(1)$_2$(pytl-DC)]Cl. Ligand pytl-DC (26.8 mg, 0.052 mmol) was added as a solid to a suspension of precursor [(**1**)$_2$Ir(μ-Cl)$_2$Ir(**1**)$_2$] (28.3 mg, 0.026 mmol) in methanol/chloroform 1/3 v/v (4 mL). The suspension was heated to 45 °C and stirred in the dark for 17 h, after which time a clear and yellow solution was obtained. The reaction was followed by TLC (eluent: methanol/chloroform 20/80 v/v) by which, under UV light at 366 nm, the compound appeared as a bright green-blue luminescent spot. After removal of the solvent *in vacuo*, the solid

obtained was purified by PLC (eluent: methanol/chloroform 20/80 v/v). The product was obtained as a slightly yellow solid (39.1 mg, 73%) containing a 1:1 molar mixture of two diastereoisomers, as also confirmed by the NMR spectrum. ^{1}H NMR (400 MHz, CD_3OD): δ ppm 9.041 (s, 1H), 9.038 (s, 1H), 8.24–8.23 (m, 1H), 8.23–8.22 (m, 3H), 8.20–8.16 (m, 2H), 8.08–7.99 (m, 4H), 7.50–7.46 (m, 2H), 7.44–7.40 (m, 2H), 7.34–7.30 (m, 2H), 6.97–6.92 (m, 2H), 6.88–6.79 (m, 4H), 6.71 (ddd, J = 7.4, 1.4, 1.4 Hz, 2H), 6.29 (ddd, J = 7.5, 1.1, 0.5 Hz, 1H), 6.28 (ddd, J = 7.6, 1.1, 0.5 Hz, 1H), 6.25–6.22 (m, 2H), 4.81–4.76 (m, 2H), 4.07–4.06 (m, 6H), 4.05 (bs, 6H), 3.51–3.42 (m, 2H), 2.37–0.89 (m, 64H), 0.72 (s, 6H); HRMS (ES+, CH_3OH): *m/z* calcd for $C_{49}H_{60}IrN_{10}O_3$: 1029.44791; found: 1029.44633 $[M]^+$.

[Ir(1)$_2$(pytl-βCD)]Cl. Ligand pytl-βCD (20.1 mg, 0.013 mmol) was added as a solid to a suspension of precursor $[(\mathbf{1})_2Ir(\mu\text{-}Cl)_2Ir(\mathbf{1})_2]$ (7.04 mg, 0.006 mmol) in methanol/chloroform 1/3 v/v (4 mL). The suspension was heated to 45 °C and stirred in the dark for 3 h, after which time a clear and yellow solution was obtained. The reaction was followed by TLC (eluent: methanol/chloroform 15/85 v/v) by which, under UV light at 366 nm, the compound appeared as a bright green-blue luminescent spot. After removal of the solvent *in vacuo*, the solid obtained was purified by column chromatography (eluent: methanol/chloroform 5/95 v/v). The product was obtained as a slightly yellow solid (16.0 mg, 59%) containing a 1:1 molar mixture of two diastereoisomers, as also confirmed by the NMR spectrum. ^{1}H NMR (300 MHz, $CDCl_3$): δ ppm 9.73 (s, 1H), 9.63 (s, 1H), 8.87–8.68 (m, 2H), 7.95–7.87 (m, 2H), 7.81 (s, 1H), 7.78 (s, 1H), 7.744 (s, 1H), 7.736 (s, 1H), 7.40–7.21 (m, 6H), 7.17–7.11 (m, 2H), 6.97–6.65 (m, 8H), 6.30–6.21 (m, 2H), 6.17–6.06 (m, 2H), 5.57–5.46 (m, 1H), 5.39–5.03 (m, 13H), 4.95–4.83 (m, 1H), 4.78–4.69 (m, 1H), 4.17 (s, 3H), 4.12 (s, 3H), 4.11 (s, 3H), 4.05 (s, 3H), 4.15–2.98 (m, 200H), 2.96–2.89 (m, 1H), 2.81–2.74 (m, 1H); HRMS (ES+, CH_3OH): *m/z* calcd for $C_{87}H_{130}IrN_{10}O_{34}$: 2051.83801; found: 2051.83965 $[M]^+$.

Table 6.2 Data for the crystallographic structural determination of pytl-DC.

Identification code	PYTLUD (pytl-DC)
Crystal colour	translucent colourless
Crystal shape	rather regular fragment
Crystal size	0.29 × 0.25 × 0.16 mm
Empirical formula	$C_{31}H_{44}N_4O_3$
Formula weight	520.70
Temperature	208(2) K
Radiation/Wavelength	Mo$K\alpha$ (graphite mon.)/0.71073 Å
Crystal system, space group	Orthorhombic, $P2_12_12_1$
Unit cell dimensions	a = 11.1262(14) Å b = 11.5765(14) Å c = 64.786(7) Å
Volume	8344.6(17) Å^3
Z, Calculated density	12, 1.243 mg m^{-3}
Absorption coefficient	0.081 mm^{-1}
Diffractometer/scan	Nonius KappaCCD with area detector φ and ω scan
F(000)	3384
θ range for data collection	2.06–27.51 deg.
Index ranges	-14<=h<=14, -14<=k<=13, -82<=l<=83

Reflections collected/unique	40445/14003 [$R_{(int)}$ = 0.0385]
Reflections observed	8397 ([I_o>2σ(I_o)])
Completeness	to 2θ = 25.00 90.5%
Absorption correction	SADABS multiscan correction[a]
Refinement method	Full-matrix least-squares on F^2
Computing	SHELXL-97[b]
Data/restraints/parameters	14003/0/1042
Goodness-of-fit on F^2	1.038
SHELXL-97 weight parameters	0.0379, 1.1082
Final R indices [I>2σ(I)]	R_1 = 0.0504, wR_2 = 0.0860
R indices (all data)	R_1 = 0.1139, wR_2 = 0.1024
Largest diff. peak and hole	0.278 and –0.186 e. Å^{-3}

a, See reference[40]; b, see reference[37].

6.6 References

[1] E. Holder, B. M. W. Langeveld, U. S. Schubert, *Adv. Mater.* **2005**, *17,* 1109–1121.

[2] H. Yersin, *Top. Curr. Chem.* **2004**, *241,* 1–26.

[3] F. Neve, A. Crispini, *Eur. J. Inorg. Chem.* **2000**, 1039–1043.

[4] K. K. W. Lo, K. Y. Zhang, S. K. Leung, M. C. Tang, *Angew. Chem. Int. Ed. Engl.* **2008**, *120,* 2245–2248.

[5] K. K. W. Lo, K. Y. Zhang, C. K. Chung, K. Y. Kwok, *Chem. Eur. J.* **2007**, *13,* 7110–7120.

[6] H. F. M. Nelissen, M. Kercher, L. De Cola, M. C. Feiters, R. J. M. Nolte, *Chem. Eur. J.* **2002**, *8,* 5407–5414.

[7] O. Lohse, P. Thevenin, E. Waldvogel, *Synlett* **1999**, *1,* 45–48.

[8] B. Beyer, C. Ulbricht, D. Escudero, C. Friebe, A. Winter, L. Gonzalez, U. S. Schubert, *Organometallics* **2009**, *28,* 5478–5488.

[9] J. Szejtli, *Chem. Rev.* **1998**, *98,* 1743–1753.

[10] G. Wenz, B. H. Han, A. Müller, *Chem. Rev.* **2006**, *106,* 782–817.

[11] F. Hapiot, S. Tilloy, E. Monflier, *Chem. Rev.* **2006**, *106,* 767–781.

[12] H. Dodziuk, *Cyclodextrin and Their Complexes: Chemistry, Analytical Methods, Applications,* Wiley-VCH, Weinheim, **2006**.

[13] R. Breslow, S. D. Dong, *Chem. Rev.* **1998**, *98,* 1997–2011.

[14] A. Douhal, *Cyclodextrin Materials Photochemistry, Photophysics and Photobiology,* Elsevier, Amsterdam, **2006**.

[15] J. M. Haider, R. M. Williams, L. De Cola, Z. Pikramenou, *Angew. Chem. Int. Ed.* **2003**, *42,* 1830–1833.

[16] J. M. Haider, Z. Pikramenou, *Chem. Soc. Rev.* **2005**, *34,* 120–132.

[17] J. A. Faiz, N. Spencer, Z. Pikramenou, *Org. Biomol. Chem.* **2005**, *3,* 4239–4245.

[18] D. Beck, J. Brewer, J. Lee, D. McGraw, B. A. DeGraff, J. N. Demas, *Coord. Chem. Rev.* **2007**, *251,* 546–553.

[19] M. Felici, P. Contreras-Carballada, Y. Vida, J. M. M. Smits, R. J. M. Nolte, L. De Cola, R. M. Williams, M. C. Feiters, *Chem. Eur. J.* **2009**, *15,* 13124–13134.

[20] C. W. Lim, O. Crespo-Biel, M. C. A. Stuart, D. N. Reinhoudt, J. Huskens, B. J. Ravoo, *Proc. Natl. Acad. Sci. USA* **2007**, *104,* 6986–6991.

[21] H. F. M. Nelissen, A. F. J. Schut, M. C. Feiters, R. J. M. Nolte, F. Venema, *Chem. Commun.* **2000**, 577–578.

[22] J. Voskuhl, B. J. Ravoo, *Chem. Soc. Rev.* **2009**, *38,* 495–505.
[23] S. Akare, J. D. Martinez, *Biochim. Biophys. Acta* **2005**, *1735,* 59–67.
[24] D. Kessel, J. A. Caruso, J. J. Reiners, *Cancer Res.* **2000**, *60,* 6985–6988.
[25] D. M. Heuman, *Ital. J. Gastroenterol.* **1995**, *27,* 372–375.
[26] K. K. W. Lo, *Struct. Bonding* **2007**, *123,* 205–245.
[27] H. C. Kolb, M. G. Finn, K. B. Sharpless, *Angew. Chem. Int. Ed.* **2001**, *40,* 2004–2021.
[28] O. David, S. Maisonneuve, J. Xie, *Tetrahedron Lett.* **2007**, *48,* 6527–6530.
[29] M. Obata, A. Kitamura, A. Mori, C. Kameyama, J. A. Czaplewska, R. Tanaka, I. Kinoshita, T. Kusumoto, H. Hashimoto, M. Harada, Y. Mikata, T. Funabiki, S. Yano, *Dalton Trans.* **2008**, 3292–3300.
[30] M. Felici, P. Contreras-Carballada, J. M. M. Smits, R. J. M. Nolte, R. M. Williams, L. De Cola, M. C. Feiters, *Molecules* **2010**, *15,* 2039–2059.
[31] M. Nonoyama, *Bull. Chem. Soc. Jpn.* **1974**, *47,* 767–768.
[32] K. A. McGee, K. R. Mann, *Inorg. Chem.* **2007**, *46,* 7800–7809.
[33] K. Kalyanasundaram, *Photochemistry of Polypyridine and Porphyrin Complexes,* Academic Press, New York, **1992**.
[34] A. Guerrero-Martínez, Y. Vida, D. Domínguez-Gutiérrez, R. Q. Albuquerque, L. De Cola, *Inorg. Chem.* **2008**, *47,* 9131–9133.
[35] D. Domínguez-Gutiérrez, G. De Paoli, A. Guerrero-Martínez, G. Ginocchietti, D. Ebeling, E. Eiser, L. De Cola, C. J. Elsevier, *J. Mater. Chem.* **2008**, *18,* 2762–2768.
[36] C. S. K. Mak, A. Hayer, S. I. Pascu, S. E. Watkins, A. B. Holmes, A. Köhler, R. H. Friend, *Chem. Commun.* **2005**, 4708–4710.
[37] G. M. Sheldrick, *SHELXL-97, Program for the Refinement of Crystal Structures,* University of Göttingen, Germany, **1997**.
[38] R. de Gelder, R. A. G. de Graaff, H. Schenk, *Acta Cryst.* **1993**, *A49,* 287–293.
[39] ***CAUTION!*** *In the first step of this synthesis methyl azide was formed, but never isolated. In fact, it is known that organic azides, especially low-molecular-weight ones, can be highly explosive. For organic azides, the "rule of six" is very useful: six carbon atoms (or other atoms of about the same size) per energetic functional group (azide, diazo, nitro, etc.) provides sufficient dilution to render the compound relatively safe. Sodium azide is relatively safe, unless acidified to form* HN_3*, which is volatile and highly toxic. For these reasons, azides should not be distilled or treated in a careless fashion. We have never experienced a safety problem with these materials. For more information, see H. C. Kolb, M. G. Finn, K. B. Sharpless, Angew. Chem. Int. Ed.* ***2001****, 40, 2004–2021.*
[40] G. M. Sheldrick, *SADABS, Program for Empirical Absorption Correction,* University of Göttingen, Germany, **1996**.

7

β-Cyclodextrin-Appended Giant Amphiphile: Aggregation to Vesicle Polymersomes and Immobilisation of Enzymes

Abstract

A giant amphiphile consisting of polystyrene end-capped with permethylated β-cyclodextrin was synthesised and found to form vesicular structures when injected as a solution in THF into water. The ability of the cyclodextrins on the surface of the polymersomes to form inclusion complexes with hydrophobic compounds was tested by carrying out a competition experiment with a fluorescent probe sensitive to the polarity of the surrounding medium. It was found that 1-hydroxyadamantane can displace the fluorescent probe from the cavities of the cyclodextrin moieties of the polymersomes. The recognition of molecules by cell membranes in nature is often based on interactions with specific membrane receptors. To mimic this behaviour, the enzyme horseradish peroxidase was modified with adamantane groups through a poly(ethylene glycol) spacer and its interaction with the polymersomes was investigated. It was established that the presence of adamantane moieties on the enzyme allowed a host–guest interaction with the multifunctional surface of the polymersomes.

This work has been published as: M. Felici, M. Marzá-Pérez, N. S. Hatzakis, R. J. M. Nolte, M. C. Feiters, Chem. Eur. J. ***2008****, 14, 9914–9920.*

7.1 Introduction

There is increasing interest in self-assembled nanostructures of well-defined size and specific properties. β-Cyclodextrin is a water-soluble receptor molecule with a hydrophobic interior,[1] which forms aggregates when appended with conventional (polymethylene) hydrophobic alkyl tails.[2,3] It occurred to us that β-cyclodextrin (diameter 1.53 nm) might have the proper dimension to serve as a polar head group in functional amphiphiles based on polystyrene (PS),[4] which nowadays can easily be prepared by atom transfer radical polymerisation (ATRP).[5,6] In our group the copper(I)-catalysed [3+2] cycloaddition of acetylene and azide ("click" or Huisgen reaction)[7–11] has been used to prepare conjugates of polymers and bio-molecules and other types of compounds.[12–14] In previous studies we have also used β-cyclodextrin-azide derivatives as intermediates for the preparation of β-cyclodextrin dimers which are excellent host molecules for different types of guests.[15,16] This click reaction, therefore, was our method of choice for the preparation of the target molecule, PS-appended permethylated β-cyclodextrin (βCD) (**1**), from acetylene-endcapped PS (**2**)[12,13] and the mono-azide βCD (**3**; Scheme 7.1).[17,18]

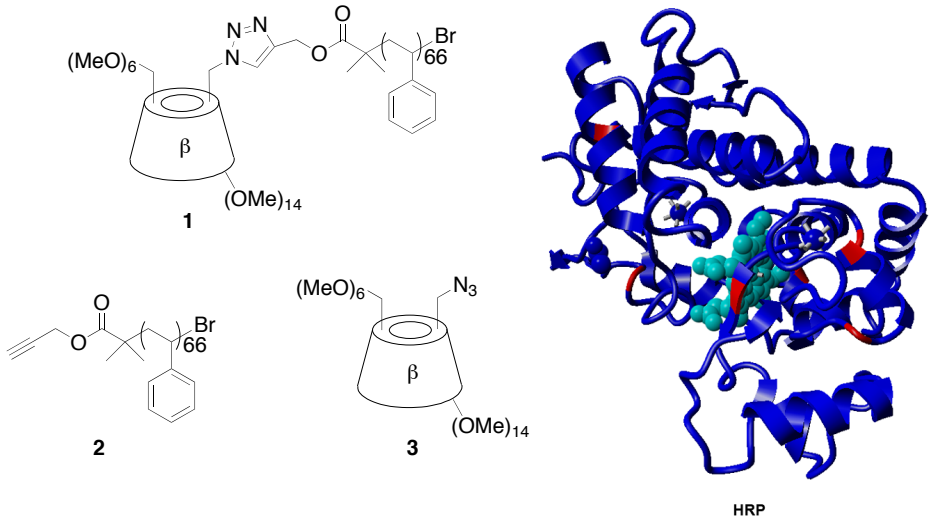

Scheme 7.1 *Structures of **1**, **2**, **3** and the enzyme HRP. Red: lysines, light blue: haem group, dark blue: HRP tertiary structure.*

Vesicles of compound **1** can be used to mimic the process of recognition of biomolecules by the biological cell membrane, which is of interest to understand this phenomenon better and to be able to prepare vesicles decorated with functionalities that are specific for a certain target. As the outer and inner surfaces of these vesicles are covered with βCD receptors, they can also be used for the study of multivalent interactions, that is, the simultaneous binding of

multiple ligands to one entity, which enhances binding affinity and selectivity.[19,20] We have previously found that polymersomes without additional functionalisation can bind enzyme molecules by non-specific, non-covalent interactions[21,22] or covalent bonds;[23] this allowed them to be used for the preparation of nanoreactors, in which cascade reactions are performed by different enzymes. In this chapter we report on the non-covalent interaction of a chemically modified enzyme with the surface of polymersomes of **1**. The enzyme horseradish peroxidase (HRP; see Scheme 7.1 for a graphical representation) was functionalised with adamantane groups, which are good guests for βCD, via a poly(ethylene glycol) (PEG) spacer. We find that HRP shows enhanced affinity for the polymersomes of **1** compared with non-functionalised HRP, and that it retains its catalytic activity when bound to the polymersome surface.

7.2 Results and discussion

7.2.1 Synthesis and physical properties

Compound **2**[12,13] was prepared from propargyl alcohol (**4**) and bromide **5**, which were reacted to give **6**, which was subsequently subjected to an ATRP with styrene (Scheme 7.2). βCD derivative **3** was synthesised by a sequence of reactions involving mono-tosylation of native β-cyclodextrin **7** on its primary side to give **8**, azide substitution to give **9**, and finally a permethylation reaction.[17,18]

The product of the CuPMDTA-catalysed (PMDTA = *N*,*N*,*N*′,*N*′,*N*-pentamethyldiethylene-triamine) click reaction between **2** and **3** was characterised by a variety of techniques. Infrared spectroscopy showed the disappearance of the vibrations characteristic of the azide and acetylene functional groups.

Mass spectrometry (Figure 7.1) and gel permeation chromatography (GPC; Figure 7.2) indicated that the molecular weight of the polymer had increased after the click reaction. It can be clearly observed that the molecular weight distribution of the functionalised polymer (Figure 7.1a) had shifted upwards with respect to starting material (Figure 7.1b). The average mass of **1** corresponds to the expected mass of 8450 g mol^{-1} [*M*+H] and the difference with the average mass of **2** (M_r = 7009) corresponds to the mass of **3** (M_r = 1441), which is the attached βCD.

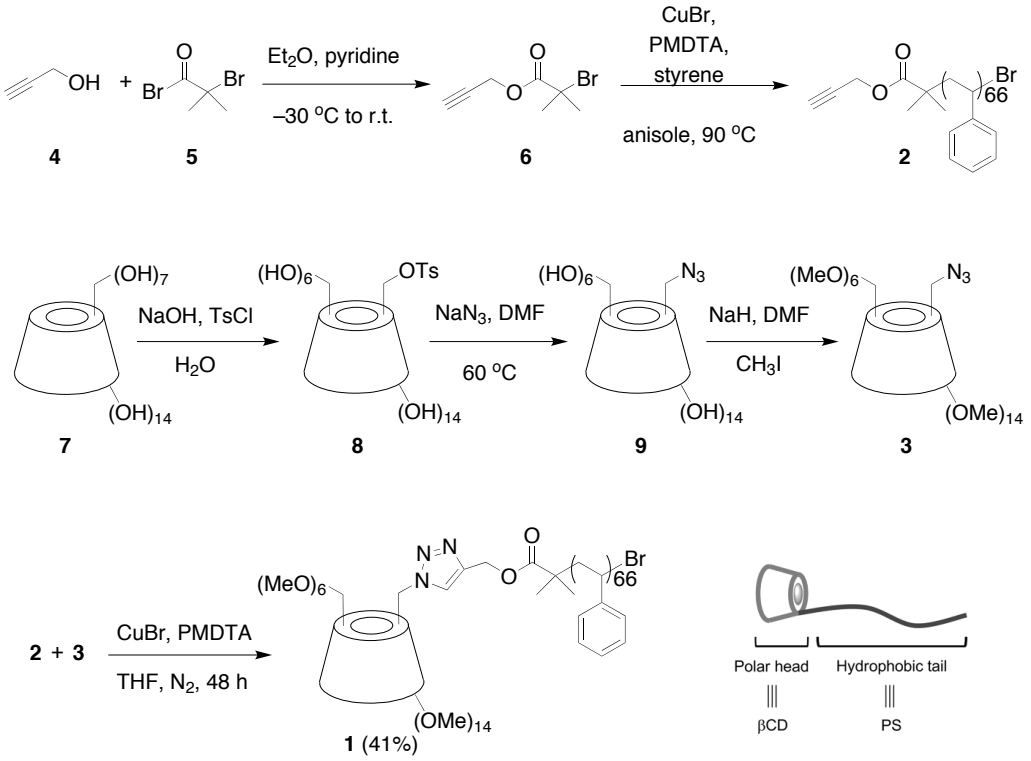

Scheme 7.2 *Preparation of **1** and its precursors **2** and **3**. Bottom right: schematic representation of **1**.*

In Figure 7.2, the GPC traces of PS-acetylene **2** and PS-βCD **1** are presented. For the latter polymer, the peak was narrower and slightly shifted to a higher molecular weight than **2**. This difference can be due in part to different interactions of the two polymers with the column, but it is consistent with the proposed formation of **1**.

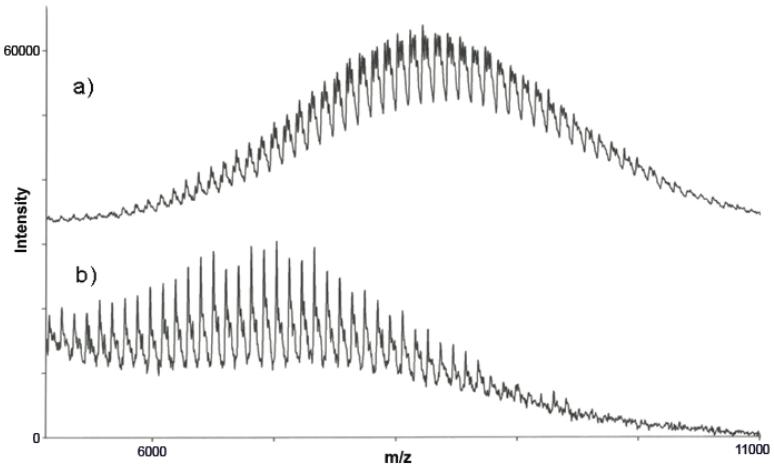

Figure 7.1 *MALDI-TOF spectra of a) **1** and b) **2**.*

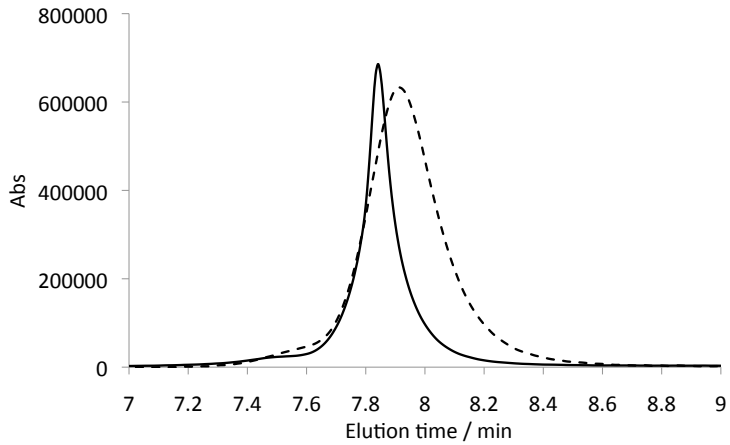

Figure 7.2 *GPC traces of **1** (solid line) and **2** (dashed line) in THF at λ = 254 nm.*

7.2.2 Aggregation studies

Injection of **1**, dissolved in THF, into water gave large vesicular structures (polymersomes) with a diameter of up to 10 μm. TEM micrographs (Figure 7.3A,B) revealed the presence of large circular structures with diameters ranging from 100 nm to 10 μm. SEM images (Figure 7.3C) confirmed the spherical nature of the structures.

To establish if these spherical structures were eventually completely closed or contained holes or defects, Cryo-SEM pictures were taken after 6 d (Figure 7. 3D).

When the polymersomes were prepared at high temperature, some of the structures were partly opened and found to be hollow; this allowed the thickness of the outer layer to be determined (Figure 7.3E). This thickness (34 nm) was found to be approximately twice the length of a single extended molecule of **1** (17 nm), which suggested that the objects observed were polymersomes consisting of bilayers of molecules of **1**, presumably oriented with the apolar PS tails pointing towards each other and the polar βCD head groups facing the outer and the inner aqueous compartments (Figure 7.3F). The polymersomes were similar in appearance to the aggregates prepared previously by us from PS-appended porphyrins,[6] but much larger than those formed from the conventional βCD amphiphiles reported to date.[2,3]

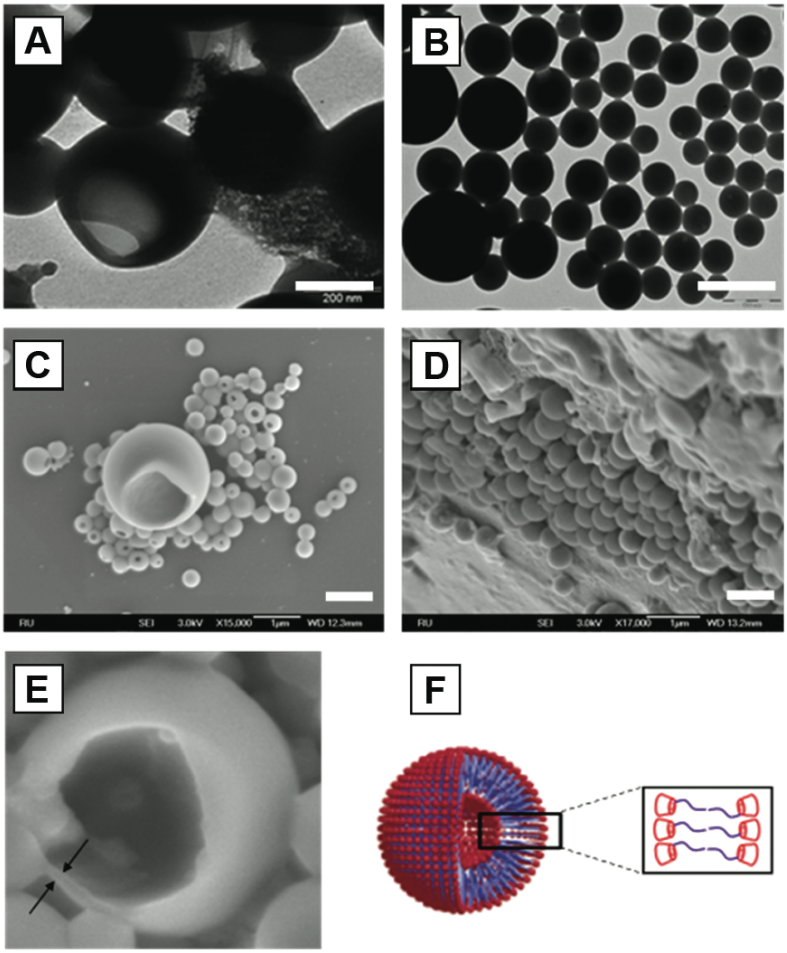

Figure 7.3 *Electron microscopy images of the aggregates formed after injecting a solution of* ***1*** *in THF into water. A, B) TEM images taken directly after injection (scale bars represent 200 and 500 nm for A and B, respectively). C) SEM image directly taken after injection. D) Cryo-SEM image taken 6 d after injection (scale bars represent 1 μm for both C and D). E) Electron micrograph indicating the thickness of the polymersomes (T_{water} = 100 °C). F) Schematic representation of the bilayer polymersomes prepared from* ***1****.*

To verify that the βCDs are accessible for guest molecules we performed an inclusion experiment. We added prop-2-yn-1-yl-5-(dimethylamino)naphthalene-1-sulfonate (**10**), which is known to shift its fluorescence spectrum towards lower wavelengths when interacting with a hydrophobic environment such as the interior of the βCD, to a solution of polymersomes of **1**.[24] The shift, shown in Figure 7.4, demonstrates that the βCDs are accessible for guests. This result furthermore demonstrates that the polystyrene chains are not included in the βCD cavity.

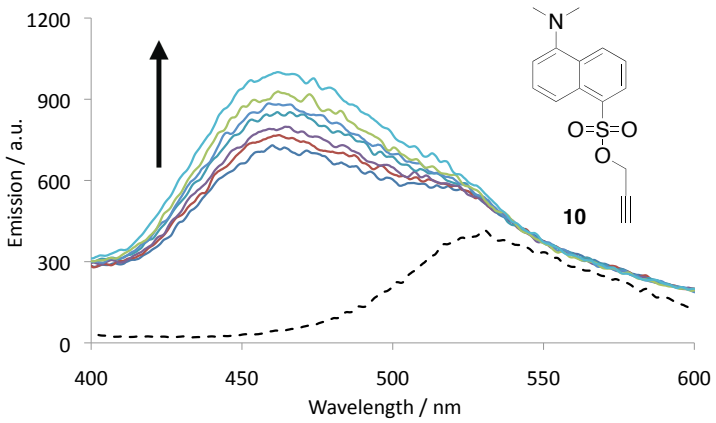

Figure 7.4 *Fluorescence data of the inclusion of **10** in the βCD cavities of the polymersomes. λ_{exc} = 305 nm, emission range 400–600 nm. Dashed line: emission of free **10** in water (40 μM). Other traces: emission of the suspension of the polymersomes after adding different aliquots (from 1 to 10 μL) of **10**.*

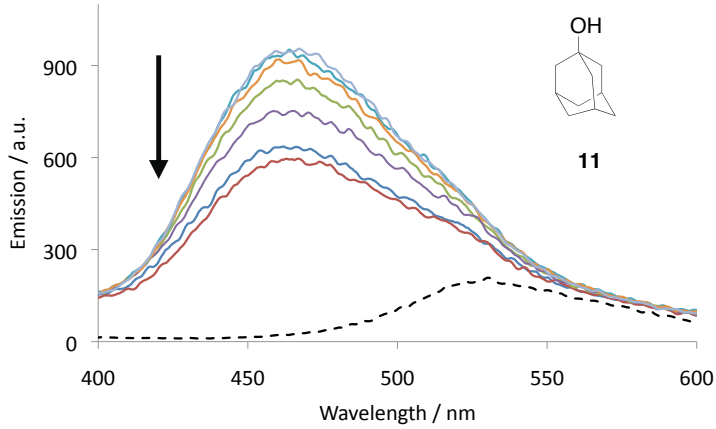

Figure 7.5 *Fluorescence data for the exclusion of **10** with **11**. λ_{exc} = 305 nm, emission range 400–600 nm. Dashed line: emission of free **10** in water (20 μM). Other traces: emission of the suspension containing polymersomes and **10** after adding different aliquots (from 1 to 15 μL) of **11**.*

We realised that the observed shift could be due not only to inclusion of **10** in the βCD cavities, but also to the non-specific absorption of **10** in the hydrophobic region of the PS tails in the inner part of the bilayer. To exclude this possibility we performed a competition experiment. We added a solution of 1-hydroxyadamantane (**11**), which is known to have a higher affinity for the cavity of βCD (4000 M^{-1}) than **10**,[25] to the polymersomes containing **10**. As shown in Figure 7.5, this addition was found to restore the original fluorescence of **10**

to a large extent, illustrating the formation of an inclusion complex of the βCDs of the polymersomes with **10**, which can be displaced by **11**.

7.2.3 Functionalisation of HRP with adamantane-PEG spacer

The enzyme peroxidase from horseradish type VI (HRP) has a molecular mass of around 44.000 and catalyses the oxidation of substrates with H_2O_2 as the oxidant, for example, the oxidation of 2,2'-azino-bis(3-ethylbenzothiazoline-6-sulfonate) (ABTS) to a compound absorbing at 420 nm. The enzyme is extensively used in molecular biology, especially for its ability to amplify a weak signal and increase the detectability of a target molecule. It is ideal, in many respects, for these applications because it is smaller, more stable, and less expensive than other popular enzyme alternatives such as alkaline phosphatase, and it has a characteristic absorption due to the presence of the haem group.

In the primary structure of HRP, six lysines are present (illustrated in Scheme 7.1). By analysing the protein crystal structure,[26] we found that two of the lysines are buried in the protein interior, but four are solvent accessible, and therefore, can be used to couple functional groups to the enzyme surface. In our case, we decided to modify HRP with adamantane moieties, which are good guests for βCD. Since the four lysines on the enzyme surface are not located in close proximity, it is necessary to have a long spacer between the enzyme and the adamantane moieties to allow the simultaneous interaction of the adamantanes with the vesicle surface. We decided to use a PEG spacer because it is very flexible and water soluble.

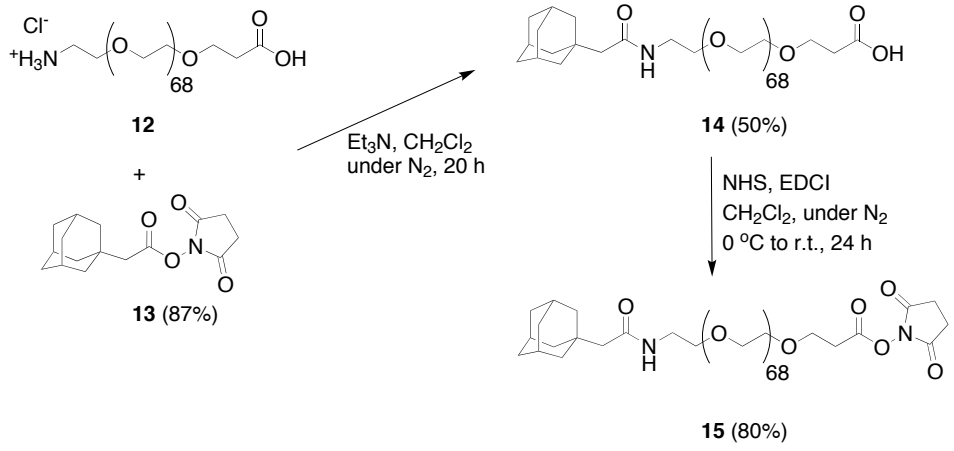

Scheme 7.3 *Synthesis of adamantyl compound **15**.*

For the synthesis of this spacer, a commercially available poly(ethylene glycol) with a terminal carboxylic acid moiety (M_r = 3000; **12**) was coupled with **13**, followed by the activation of the carboxylic acid of PEG as an *N*-hydroxysuccinimide ester (Scheme 7.3).

For the functionalisation of HRP with **15** (Scheme 7.4), the enzyme was dissolved in acetate buffer (50 mM, pH 5.5) and a solution of **15** (25 equiv.) was added in distilled THF. The reaction was gently stirred at 4 °C. After approximately 48 h, the mixture was dialysed against acetate buffer (50 mM, pH 5.5) to remove the unreacted PEG. The resulting solution was analysed by size-exclusion fast protein liquid chromatography (FPLC), using UV detection at 280 and at 403 nm (absorption of the haem group of the HRP) (Figure 7.6, left).

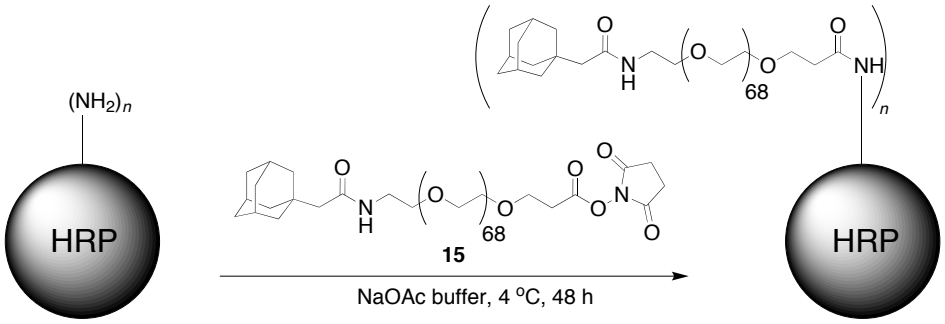

Scheme 7.4 *Functionalisation of HRP (for detailed structure see Scheme 7.1) with compound **15** in acetate buffer.*

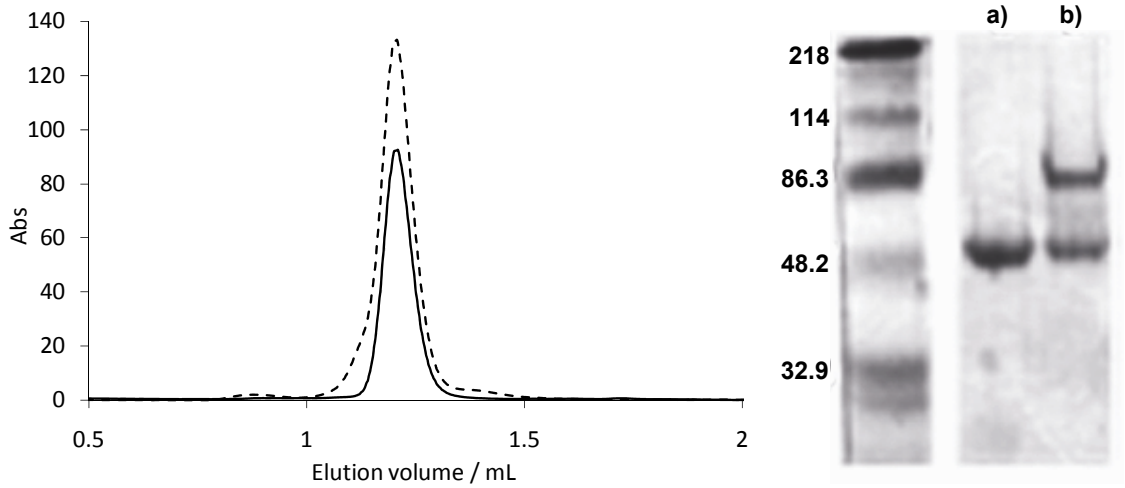

Figure 7.6 *Left: FPLC of HRP (solid line) and HRP modified with compound **15** (dashed line) at λ = 403 nm. Right: SDS-PAGE of a) HRP native (non-modified); b) HRP modified with compound **15** after dialysis.*

It was not possible to separate the modified and native proteins by size-exclusion FPLC, probably due to the small differences in their masses and the unfavourable interaction of the PEG-adamantane tail with the column (Figure 7.6, left). However, sodium dodecylsulfate-polyacrylamide gel electrophoresis (SDS-PAGE; Figure 7.6, right), clearly confirmed the formation of a new conjugate with a higher molecular weight than the native HRP. The presence of a single new band on the gel, in addition to a band due to non-modified enzyme, suggested that an equal number of PEG-adamantane tails were attached to the surface of each enzyme molecule. However, the different nature of the PEG tail interaction with the gel did not allow us to precisely quantify the molecular weight of the conjugate, and thus, the number of adamantanes attached to the HRP protein.

7.2.4 Interaction of modified HRP with polymersomes of 1

To investigate the presence of specific interactions of the modified HRP with the polymersomes of **1**, the following experiment was carried out: a suspension of the polymersomes in phosphate buffer was mixed with a solution of HRP functionalised with adamantane (1×10^{-5} M). In a control experiment the polymersomes were mixed with the non-modified HRP under otherwise identical conditions. After incubating for 2 h, the two suspensions were purified with several rinsing steps by using eppendorf micro test tubes equipped with filter units.

The control experiment was set up to establish when the non-functionalised HRP would be completely removed from the surface of the polymersomes, since some weak, non-specific interactions between the enzyme and the polymersomes were expected to be present. Because of the absence of adamantanes on the enzyme in the control experiment, fewer washing steps should be required to completely remove the enzyme molecules from the surface of the polymersomes.

In Figure 7.7 the catalytic activity of the polymersomes functionalised with the modified enzymes after 25 rinsing steps (solid line) is reported. The HRP-polymersomes were catalytically active, whereas the absence of activity in the control shows that no enzyme molecules are present in the polymersomes unless they are bound to them.

Due to the reversibility of the binding, the bound HRP can still be removed by centrifugation, but it requires a higher number of washing steps than the control experiment. During the washing process, after a certain number of rinsing steps (5, 10, 17, 20, 25), the enzyme activity in the eluates of both the control experiment and the sample was tested. In Figure 7.7 the enzymatic activity of the eluate of the experiment (dashed line) and the control

(dotted line) after the same number of filtrations (17) are presented. It can be observed that enzymatic activity is still present when using the modified HRP, whereas there are no enzyme molecules present in the control experiment. The stronger interaction of modified enzyme with polymersomes of **1** is due to the interaction of the adamantane moieties with the βCD cavities on the surface of the polymersomes.

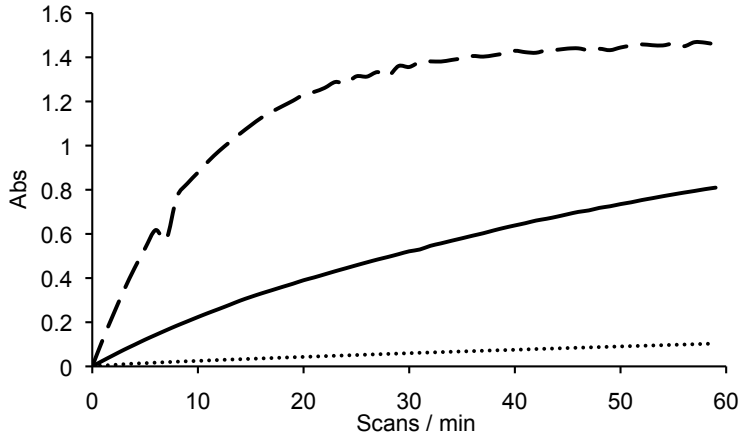

Figure 7.7 *Activity measurements of HRP-PEG at λ = 420 nm: blank eluate after 17 rinsing steps (dotted line); experiment eluate after 17 rinsing steps (dashed line); activity retained in polymersomes after 25 rinsing steps (solid line).*

Both samples from the experiment and the control were analysed by TEM to confirm that the vesicular structure was retained after the numerous centrifugation steps.

7.3 Conclusion

We have shown that PS-appended βCDs can form well-defined vesicular structures. The accessibility of the βCDs was proven by binding and unbinding experiments with dansyl (**10**) and 1-hydroxyadamantane (**11**) derivatives. We subsequently utilised the host-guest interaction of βCD with adamantane to decorate the polymersomes with PEG-adamantane-functionalised HRP. Activity studies confirmed that HRP remained catalytically active and was successfully bound to the polymersomes. This opens new routes for the construction of polymersomes decorated with multiple enzymes that can act in concert.

7.4 Acknowledgements

I wish to thank to Dr. N. Hatzakis for the fruitful discussions and suggestions, and M. Marzá-Pérez for great experimental help. Dr. A. J. Dirks is acknowledged for the generous gift of compound **2**.

7.5 Experimental

7.5.1 Methods and materials

General. THF was purified by distillation under nitrogen from sodium/benzophenone; dichloromethane was distilled under nitrogen from calcium hydride. Compounds **2**[12,13] and **3**[17,18] were prepared according to literature procedures. All other chemicals were purchased from Aldrich, Fluka, or Acros and used as received. Analytical thin-layer chromatography (TLC) was performed on Merck precoated silica gel 60 F-254 plates (layer thickness 0.25 mm) and the compounds were visualised by UV irradiation at λ = 254 and/or 366 nm and/or staining with phosphomolybdic acid reagent or $KMnO_4$. Silica gel chromatography was performed by using Acros (0.035–0.070 mm, pore diameter ca. 6 nm) silica gel. Ultra pure water ($R > 18 \times 106$ Ω) was used for the aggregation studies in aqueous solutions. Dialysis membranes were purchased from Spectrum Laboratories and Dialyser Tubes (Maxi, Midi or Mini) were purchased from Novagem. Peroxidase from horseradish type VI (E.C. 1.11.1.7) was purchased from Sigma.

NMR spectroscopy. ^{1}H NMR spectra were recorded at 25 °C on Varian Inova 400 or Bruker DMX-300 spectrometers operating at 400 and 300 MHz, respectively. ^{13}C NMR spectra were recorded on a Bruker DMX-300 spectrometer operating at 75 MHz. ^{1}H NMR chemical shifts (δ) are reported in parts per million (ppm) relative to the proton signal of tetramethylsilane (δ = 0.00 ppm) as an internal standard, otherwise to the residual proton signal of the solvent, δ = 7.26 ppm for $CDCl_3$. Multiplicities are reported as follows: s (singlet), d (doublet), t (triplet), or m (multiplet). Broad peaks are indicated by b. Coupling constants are reported as a J value in Hertz (Hz). The number of protons (n) for a given resonance is indicated as nH, and is based on spectral integration values. ^{13}C NMR chemical shifts (δ) are reported in ppm relative to $CDCl_3$ (δ = 77.0). Succ refers to the succinimide group.

Mass spectrometry (MS). Electrospray LC-MS analysis was performed by using a Shimadzu LC-MS 2010A system. Matrix-assisted laser desorption/ionisation time-of-flight (MALDI-TOF) spectra were measured on a Bruker Biflex III spectrometer and samples were prepared from solutions in MeOH by using 3-indoleacrylic acid (IAA) (20 mg mL^{-1}) as a matrix.

Infrared spectroscopy. IR spectra were recorded on an ATI Matson Genesis Series FTIR spectrometer with a fitted ATR cell. Frequencies (ν) are given in cm^{-1}.

UV-vis spectroscopy. UV-vis spectra were recorded on a Varian Cary 50 spectrophotometer by using a quartz cuvette. For catalysis experiments, the UV-vis spectra were recorded on an Elisa Ryder spectrophotometer.

Fluorescence spectroscopy. Fluorescence spectra were measured on a PerkinElmer LS 55 fluorescence spectrophotometer by using a 50 µL quartz cuvette.

Transmission electron microscopy (TEM). TEM images were obtained by using a JEOL JEM 1010 microscope (60 kV) equipped with a CCD camera. Samples were prepared by pouring a drop of the aggregate suspension onto a carbon-coated copper grid, which was allowed to dry in air. The structures were visualised without further treatment. The aggregate solution was prepared by dissolving amphiphile **1** (1 mg) in distilled THF (1 mL). The resulting solution was then slowly injected into ultrapure (Millipore) water (1 mL). The sample was shaken by hand to obtain a homogeneous mixture. Measurements of the sealed sample were done after 5 min, 1 d, 3 d and 6 d.

Scanning electron microscopy (SEM). SEM was performed on a JEOL JSM-6330F instrument by using the same samples as prepared for TEM. Before measurement, a 1.5 nm layer of Pd/Au was sputtered on the grids with a Cressington 208 HR sputter coater fitted with a Cressington layer-thickness controller.

Gel permeation chromatography (GPC). Molecular weight distributions were measured with a Shimadzu size-exclusion column equipped with a guard column and a PL gel 5 μm mixed D column (Polymer Laboratories) with differential refractive index and UV (λ = 254 and 330 nm) detection using THF as an eluent (1 ml min^{-1} at 35 °C). PS standards were used for calibration.

Fast protein liquid chromatography (FPLC). Protein mixtures were analysed with a Pharmacia Smart high-performance liquid chromatography (HPLC) system, equipped with a Superdex 75 PC 3.2/30 column (optimal separation 3–70 kDa) (Pharmacia) or Superose 12 PC 3.2/30 column (optimal separation 1–300 kDa) (Pharmacia) using phosphate buffer (20 mM, pH 7.2) as an eluent (50 μl min^{-1} at room temperature) in combination with UV detection (λ = 254 and 280 nm).

7.5.2 Synthesis and characterisation

Compound 1. Nitrogen was bubbled through distilled THF for 1 h prior to use. Compound **2** (0.05 g, 0.03 mmol) and **3** (0.24 g, 0.03 mmol) were dissolved in THF (3 mL) under nitrogen. A solution of CuBr (0.005 g, 0.03 mmol) and PMDTA (0.007 mL, 0.03 mmol) in THF (2 mL) was made free of oxygen by bubbling nitrogen through it for 30 min and this solution was added to the solution of the **2** and **3**. The mixture was stirred under a nitrogen atmosphere for 48 h. The solvent was removed by evaporation and the solid obtained was purified by column chromatography (chloroform→chloroform/methanol 4/1 v/v). Product **1** was obtained as a white solid (0.12 g, 41%). ^{1}H NMR (400 MHz, $CDCl_3$): δ ppm 7.09 (m, aromatic protons of the PS tail), 3.15–4.00 (m, 118H), ppm 1.25–2.10 (m, aliphatic protons of the PS tail); IR: ν = 3023, 3053, 3088 (CH_2); 2841, 2919 (CH); 1938, 1873, 1804, 1739 (C=O); 1600 (C=C); 1160 (O-Me); 693, 771 cm^{-1} (mono-substituted benzenes). The vibration of the N_3 group of compound **3** had disappeared in compound **1**.

2,5-dioxopyrrolidin-1-yl 2-(adamantan-1-yl)acetate (13). 1-Adamantylacetic acid (0.30 g, 1.5 mmol) and *N*-hydroxysuccinimide (0.19 g, 1.6 mmol) were dissolved in distilled dichloromethane under a nitrogen atmosphere. The mixture was cooled to 0 °C and EDCI (0.33 g, 1.7 mmol) was added. The mixture was stirred under a nitrogen atmosphere for 20 h. The solvent was removed and the solid was redissolved in ethyl acetate and extracted with ammonium chloride (2×), dried over anhydrous sodium sulfate, filtered and evaporated to dryness. Product **13** was obtained as a white solid (0.38 g, 87%). M.p. 134 °C; ^{1}H NMR (400 MHz, $CDCl_3$): δ ppm 2.82 (s, 4H), 2.33 (s, 2H), 2.01 (s, 3H), 1.67–1.74 (m, 12H); ^{13}C NMR (75 MHz, $CDCl_3$): δ ppm 169.19 (CO succ.), 166.22 (CO), 45.26 (adamantane-CH_2-CO), 41.93, 36.45 (CH_2 from adamantane), 33.14 (quaternary C), 28.49 (CH from adamantane), 25.55 (CH_2 succ.).

3-{2-[2-(1-Adamantyl)acetamido]ethyl[octahexaconta(oxyethylene)]}propanoic acid (14). Compound **12** (0.20 g, 0.06 mmol) was dissolved in distilled dichloromethane (20 mL) under a nitrogen atmosphere followed by the addition of triethylamine (19 μL, 0.13 mmol). The mixture was stirred for 10 min and compound **13** (0.03 g, 0.10 mmol) was added. The reaction was stirred for 20 h and the resulting mixture extracted with a saturated aqueous solution of $NaHCO_3$ (2×) and HCl (1 M), dried over anhydrous sodium sulfate, filtered and evaporated to dryness. The product was precipitated in ethyl ether and filtered. The solid was dissolved in chloroform. The solvent was removed *in vacuo* and the product was dried under high vacuum to give compound **14** as a white powder (0.18 g, 50%). ^{1}H NMR (300 MHz, $CDCl_3$): δ ppm 3.35–3.85 (m, 276 H), 2.58 (t, 2H), 1.95 (s, 3H), 1.92 (s, 2H), 1.57–1.70 (m, 12H); ^{13}C NMR (75 MHz, $CDCl_3$): δ ppm 172.4 (CO), 170.5 (CO), 70.0 (CH_2 repeating unit), 66.2, 65.3 (CH_2), 51.0 (adamantane-CH_2-CO), 42.1, 36.3 (CH_2 from adamantane), 28.1 (CH from adamantane), 38.5 (O-CH_2), 36.3 (CH_2-COOH), 32.2 (quaternary C).

1-(3-{2-[2-(1-Adamantyl)acetamido]ethyl[octahexaconta(oxyethylene)]}-propoxy) succinimide (15). Compound **14** (0.18 g, 0.06 mmol) and *N*-hydroxysuccinimide (0.008 g, 0.07 mmol) were dissolved in distilled dichloromethane (15 mL) under a nitrogen atmosphere. The mixture was cooled to 0 °C and EDCI (0.02 g, 0.12 mmol) was added. The reaction was stirred for 24 h with the temperature slowly reaching r.t., and the resulting mixture was extracted with HCl (0.5 M), dried over anhydrous sodium sulfate, filtered and evaporated to dryness. The product was precipitated in ethyl ether and the solid was dissolved in chloroform. The solvent was removed *in vacuo* and the product was dried under high vacuum to give compound **15** as a white powder (0.15 g, 80%). ^{1}H NMR (300 MHz, $CDCl_3$): δ ppm 3.38–3.87 (m, 276 H), 2.89 (t, 2H), 2.83 (s, 4H), 1.98 (s, 3 H), 1.92 (s, 2 H), 1.57–1.70 (m, 12H); ^{13}C NMR (75 MHz, $CDCl_3$): δ ppm 170.9 (CO), 168.8 (CO succ.), 166.6 (CO), 70.4 (CH_2 repeating unit), 65.7, 65.6 (CH_2), 51.5 (adamantane-CH_2-CO), 42.5, 36.7 (CH_2 from adamantane), 29.5 (CH from adamantane), 38.8, 32.0 (CH_2), 32.6 (quaternary C), 25.5 (CH_2 succ).

Binding of 10 in polymersomes of 1. A suspension of the polymersomes of **1** (0.5 mg mL^{-1}) was prepared as described above and kept for 6 d in a sealed tube to allow them to close completely. Before any fluorescence measurements were recorded, the vesicles were dialysed against ultrapure water for one night to remove THF. In the inclusion experiment, different aliquots of a stock solution of **10** (1 mM in THF) were added until a final concentration of 40 μM was reached. The mixture was followed in time by fluorescence spectroscopy. The competition experiment was carried out after 18 h by using the suspension containing polymersomes and **10** mentioned before. Since the measured emission was off the scale, the suspension was diluted to half the concentration and then different aliquots of a stock solution of **11** (2 mM in tetrahydrofuran/water 1/1 v/v) were added. Fluorescence measurements were then performed.

Functionalisation of HRP with the adamantane–PEG derivative. HRP (1 mg) was dissolved in sodium acetate buffer (160 mL, 50 mM, pH 5.5) followed by the addition of a solution of **15** (1 mg) in distilled THF (30 μL). The reaction was stirred for 48 h at 4 °C and dialysed by using dialysis tubes (MWCO 12–14 kDa) against sodium acetate buffer (50 mM, pH 5.5) for 24 h, changing the buffer three times to remove the unreacted PEG. The solution obtained from dialysis (0.14 mM) was analysed and purified by FPLC. Injections of aliquots (20 μL) of the samples in the FPLC column (Superdex 200) at room temperature were monitored by UV detection at 280 and 403 nm. Fractions (60 μL) were collected in well plates. SDS-PAGE was performed by using a 10% polyacrylamide gel containing 1% SDS. The samples were neither heated nor treated with β-mercaptoethanol before loading onto the gel. The concentration of the samples was 0.09 mM both for native HRP and for HRP modified with the adamantane–PEG derivative.

Reaction between HRP modified with 15 and polymersomes of 1. A suspension of the polymersomes of **1** (0.5 mg mL^{-1}) was prepared as described above and kept for 6 d in a sealed tube to allow them to close

completely. A volume (500 μL) of this suspension was dialysed against phosphate buffer (20 mM, 100 mM NaCl, pH 7.2) by using dialysis bags (MWCO 12–14 kDa). Only 300 μL of the resulting suspension were mixed for 2 h at room temperature with a solution of HRP functionalised with compound **15** (200 μL, 1×10^{-5} M).

A control experiment was performed using the non-modified HRP, under the same reaction conditions.

Free enzyme molecules were removed from the reaction mixture by filtration using an eppendorf micro test tube fitted with a filter unit with pores of 0.1 μm. The eppendorf micro test tube was centrifuged at 3000 rpm for 5 min and fresh buffer solution was added before the tube was again subjected to centrifugation. This sequence was repeated 15–25 times after which time the eluate of the control experiment no longer showed any enzymatic activity. The sample remaining on the filter was redispersed in buffer solution (300 μL) and catalysis experiments were performed. A sample (10 μL) prepared by the procedure described above was added to a well plate (250 μL) followed by the subsequent addition of phosphate buffer (220 μL, 20 mM, pH 7.2), an aqueous solution of ABTS (10 mL, 0.05 M), and an aqueous solution of hydrogen peroxide (10 μL, 7%). The sample was mixed thoroughly by using a pipette and the progress of the reaction was monitored by UV-vis spectroscopy, measuring the absorption at 420 nm.

7.6 References

[1] J. Szejtli, T. Osa, *Comprehensive Supramolecular Chemistry, Vol. 3: Cyclodextrins,* (Eds.: J. M. Lehn, J. L. Atwood, J. E. D. Davies, D. D. MacNicol, F. Vögtle, J. Szejtli, T. Osa), Pergamon, Oxford, **1996**.

[2] B. J. Ravoo, R. Darcy, *Angew. Chem.* **2000**, *112,* 4494–4496.

[3] B. J. Ravoo, R. Darcy, *Angew. Chem. Int. Ed. Engl.* **2000**, *39,* 4324–4326.

[4] J. N. Israelachvili, D. J. Mitchell, B. W. Ninham, *J. Chem. Soc., Faraday Trans. 2* **1976**, *72,* 1525–1568.

[5] J. C. M. van Hest, D. A. P. Delnoye, M. W. P. L. Baars, M. H. P. van Genderen, E. W. Meijer, *Science* **1995**, *268,* 1592–1595.

[6] F. de Loos, I. C. Reynhout, J. J. L. M. Cornelissen, A. E. Rowan, R. J. M. Nolte, *Chem. Commun.* **2005**, 60–62.

[7] H. C. Kolb, M. G. Finn, K. B. Sharpless, *Angew. Chem.* **2001**, *113,* 2056–2075.

[8] H. C. Kolb, M. G. Finn, K. B. Sharpless, *Angew. Chem. Int. Ed.* **2001**, *40,* 2004–2021.

[9] J. F. Lutz, *Angew. Chem. Int. Ed.* **2007**, *46,* 1018–1025.

[10] J. F. Lutz, *Angew. Chem.* **2007**, *119,* 1036–1043.

[11] P. Wu, V. V. Fokin, *Aldrichim. Acta* **2007**, *40,* 7–17.

[12] J. A. Opsteen, J. C. M. van Hest, *J. Polym. Sci. Part A: Polym. Chem.* **2007**, *45,* 2913–2924.

[13] J. A. Opsteen, J. C. M. van Hest, *Chem. Commun.* **2005**, 57–59.

[14] A. J. Dirks, J. J. L. M. Cornelissen, F. L. van Delft, J. C. M. van Hest, R. J. M. Nolte, A. E. Rowan, F. P. J. T. Rutjes, *QSAR Comb. Sci.* **2007**, *26,* 1200–1210.

[15] F. Venema, C. M. Baselier, E. van Dienst, B. H. M. Ruel, M. C. Feiters, J. F. J. Engbersen, D. N. Reinhoudt, R. J. M. Nolte, *Tetrahedron Lett.* **1994**, *35,* 1773–1776.

[16] E. van Dienst, B. H. M. Snellink, I. von Piekartz, M. H. B. Grote Gansey, F. Venema, M. C. Feiters, R. J. M. Nolte, J. F. J. Engbersen, D. N. Reinhoudt, *J. Org. Chem.* **1995**, *60,* 6537–6545.

[17] R. C. Petter, J. S. Salek, C. T. Sikorski, G. Kumaravel, F. T. Lin, *J. Am. Chem. Soc.* **1990**, *112,* 3860–3868.

[18] Z. Chen, J. S. Bradshaw, M. L. Lee, *Tetrahedron Lett.* **1996**, *37,* 6831–6834.

[19] M. Mammen, S. K. Choi, G. M. Whitesides, *Angew. Chem.* **1998**, *110,* 2908–2953.

[20] M. Mammen, S. K. Choi, G. M. Whitesides, *Angew. Chem. Int. Ed. Engl.* **1998**, *37,* 2754–2794.

[21] D. M. Vriezema, P. M. L. Garcia, N. Sancho Oltra, N. S. Hatzakis, S. M. Kuiper, R. J. M. Nolte, A. E. Rowan, J. C. M. van Hest, *Angew. Chem. Int. Ed.* **2007**, *46,* 7378–7382.

[22] D. M. Vriezema, P. M. L. Garcia, N. Sancho Oltra, N. S. Hatzakis, S. M. Kuiper, R. J. M. Nolte, A. E. Rowan, J. C. M. van Hest, *Angew. Chem.* **2007**, *119,* 7522–7526.

[23] S. F. M. van Dongen, M. Nallani, S. Schoffelen, J. J. L. M. Cornelissen, R. J. M. Nolte, J. C. M. van Hest, *Macromol. Rapid Commun.* **2008**, *29,* 321–325.

[24] H. F. M. Nelissen, F. Venema, R. M. Uittenbogaard, M. C. Feiters, R. J. M. Nolte, *J. Chem. Soc., Perkin Trans. 2* **1997**, *1997,* 2045–2053.

[25] M. V. Rekharsky, Y. Inoue, *Chem. Rev.* **1998**, *98,* 1875–1918.

[26] G. I. Berglund, G. H. Carlsson, A. T. Smith, H. Szöke, A. Henriksen, J. Hajdu, *Nature* **2002**, *417,* 463–468.

Summary

Light is an important source of energy and the interaction of light and matter plays an essential role in our lives. The absorption of light activates processes such as photosynthesis, which are crucial for many living organisms. Much of our technology is also based on light and its properties. The synthesis of molecules able to capture light is the first step toward the exploitation of this energy source in artificial systems for the production of clean fuels as well as in optical devices, for example.

In this thesis, I aimed to describe the preparation of new inorganic luminescent compounds functionalised with permethylated β-cyclodextrin (βCD) or its guests that are water soluble and absorb and transfer energy efficiently. The functionalisation of these coordination complexes with βCD results in luminescent labels that have the ability to self-assemble in a designed manner, enhancing their luminescence efficiency at the same time. Our major interest is focused on the preparation of a hydrogen evolution system in which a photosensitiser, an electron relay, and a metal nanoparticle self-organise into a linear structure, allowing an electron transfer process to be triggered by the absorption of light.

The work described in this thesis comprises i) the exploitation of "click chemistry" as a tool for the functionalisation of βCD and its guests (Chapters 2 and 6), ii) the characterisation of the interaction between βCD and coordinating ligands (Chapter 3), and iii) the application of the resulting βCD-containing molecules in different fields (Chapters 4, 5, and 7). The results have been published (or are in the process of being published) in leading scientific journals.

In **Chapter 1** an overview of the two major topics discussed in this thesis is given: i) cyclodextrins and their ability to form inclusion complexes, and ii) light-induced electronic transitions in coordination compounds. At the end of this chapter, the aims and an outline of this thesis are summarised.

Chapter 2 describes the synthesis and characterisation of novel 2-(1-substituted-1*H*-1,2,3-triazol-4-yl)pyridine (pytl) ligands prepared by click chemistry. They have been used in the synthesis of heteroleptic complexes of ruthenium(II) and iridium(III) with 2,2'-bipyridine (bpy) and 2-phenylpyridine (ppy), respectively, resulting in $[Ru(bpy)_2(pytl\text{-}R)]Cl_2$ and $[Ir(ppy)_2(pytl\text{-}R)]Cl$ (R = adamantyl, methyl, βCD). All of the ruthenium(II) complexes have

lower lifetimes and quantum yields than other polypyridine complexes. In contrast, cyclometalated Ir complexes display rather long lifetimes and very high emission quantum yields. Surprisingly, the emission quantum yield and lifetime are enhanced in the case of [Ir(ppy)$_2$(pytl-βCD)]Cl (Φ = 0.54, τ = 2800 ns). βCD, which is covalently attached to pytl, plays an important role by acting as a second-sphere ligand and by shielding the coordination complex from quenching of its luminescence by dynamic collision or oxygen energy transfer, for example. The complex [Ir(ppy)$_2$(pytl-βCD)]Cl exists in two diastereoisomeric forms, Δ and Λ, which have significant differences between their quantum yields (0.49 vs. 0.70). Such behaviour is attributed to different interactions of the chiral βCD substituent with the Δ and Λ isomers of the metal complex.

In **Chapter 3** a detailed analysis of the structure of the diastereoisomer Δ-[Ir(ppy)$_2$(pytl-βCD)]Cl in D_2O by high-resolution liquid NMR spectroscopy is reported. The results confirmed an interaction between the iridium complex and the covalently attached βCD cavity. In particular, one of the ppy ligands is located inside the βCD cavity, while the other ligands, ppy and pytl, are located above and outside the cavity, respectively. The emissive excited state is mostly located on the ppy ligands; (partial) self-inclusion in the βCD cavity increases the rigidity of the iridium complex and protects the emissive excited state from quenching by water molecules as well as from dioxygen quenching.

Chapter 4 deals with the application of five ionic iridium(III) complexes of the general formulas [Ir(ppy)$_2$(pytl-R)]Cl (R = methyl, βCD, propylamine) and [Ir(F$_2$ppy)$_2$(pytl-R)]Cl (F$_2$ppy = 2-(2,4-bisfluorophenyl)-pyridine, R = adamantyl, propylamine) as luminophores in electrochemiluminescence (ECL). Emissive excited states of the metal complexes are generated by electron transfer reactions between electro-generated species. Pytl ligands appended with various functional groups were used in the synthesis of the iridium(III) complexes. The complexes of the general formulas [Ir(ppy)$_2$(pytl-R)]Cl and [Ir(F$_2$ppy)$_2$(pytl-R)]Cl are shown to give bright green and blue ECL signals, respectively, in air-equilibrated aqueous media. A straightforward route towards the functionalised pytl ligand by click chemistry allowed the attachment of a βCD as a solubilising group, which resulted in enhanced ECL emission of the iridium complex in water. With the prospect of applying such luminophores in ECL-based biological assays, the pytl ligand was appended with a propylamino group. The presence of such a group provides the complex with a potential link for the covalent labelling of biomolecules and immobilisation on solid substrates. Under the operating conditions used, the free amino terminus underwent irreversible oxidation, resulting

in electrode fouling. The functionalised amino group is, however, expected to be stable under oxidative conditions when the iridium label is covalently linked to substrates; therefore, its reactivity should not interfere with ECL.

In **Chapter 5** our efforts to exploit the photophysical properties of iridium(III) complexes functionalised with pytl in a self-assembled system for the photocatalytic production of hydrogen are reported. The activity of linear, light-driven, catalytic, three-component systems for the reduction of protons comprised of a metal complex as a photosensitiser, a viologen-based electron relay, cyclodextrin-modified platinum nanoparticles as the catalyst, and a sacrificial donor was investigated in a home-made setup. The photosensitiser, electron relay, and catalyst were appended with host and guest molecules, such as βCD, adamantane, and ursodeoxycholic acid, which were used to assemble the components of the photocatalytic system in a supramolecular manner. The modular approach introduced in this study allows the generation of several functional photo-active systems by self-assembly from a limited number of building blocks. We established that the polypyridine iridium complexes of general formula $[Ir(ppy)_2(pytl\text{-}R)]Cl$ (R = adamantyl, methyl, βCD) were active in the production of H_2, with yields that, under our conditions, were 2.5–450 times higher than the classical three-component system Ru-bpy/Me-V-Me/Pt-βCD/EDTA (Ru-bpy = $[Ru(bpy)_3]Cl_2$, Me-V-Me = methyl viologen, Pt-βCD = non-methylated β-cyclodextrin-functionalised platinum nanoparticles, EDTA = ethylenediaminetetraacetic acid). By investigating different photocatalytic systems, it was found that the electron relay played an essential role and was necessary to guarantee an efficient electron transfer process, and the amount of hydrogen produced was directly proportional to the quantum yield of the photosensitiser. An attempt to increase the efficiency of our systems by using viologens appended with guest molecules for βCD led us to unexpected observations. The presence of adamantane or bile acid groups induced aggregation and increased the stabilisation of the viologen radical cations, which was disadvantageous for hydrogen formation.

Chapter 6 describes the preparation of a class of bidentate 1-substituted-4-phenyl-1*H*-1,2,3-triazole cyclometalating ligands (phtl) bearing different substituents on the triazole moiety by means of click chemistry. By using various ligands (phtl-R^1 and pytl-R^2; R^1 = adamantyl, methyl and R^2 = adamantyl, methyl, βCD, ursodeoxycholic acid), we prepared a small library of new luminescent heteroleptic ionic iridium complexes $[Ir(phtl\text{-}R^1)_2(pytl\text{-}R^2)]Cl$ and investigated their photophysical properties.

Chapter 7 deals with the synthesis of a giant amphiphile consisting of polystyrene end-capped with βCD. This compound forms vesicular structures when injected as a solution in THF into water. The ability of the βCDs on the surface of the polymersomes to form inclusion complexes was tested by carrying out a competition experiment with a fluorescent probe sensitive to the polarity of its surroundings. We used this system to mimic the recognition of molecules by cell membranes, which in nature is often based on interactions with specific membrane receptors. The enzyme horseradish peroxidase was modified with adamantane groups on a poly(ethylene glycol) spacer and its interaction with the polymersomes was investigated. It was established that the presence of adamantane moieties on the enzyme allowed host-guest interactions with the multifunctional surface of the polymersomes.

Samenvatting

Licht is een belangrijke bron van energie en de interactie van licht en materie speelt een belangrijke rol in ons leven. De absorptie van licht activeert processen, zoals de fotosynthese, die van crucial belang zijn voor vele levende organismen. Veel van onze technologie is ook gebaseerd op licht en zijn eigenschappen. De synthese van moleculen die licht kunnen invangen is de eerste stap naar de benutting van deze energiebron in kunstmatige systemen voor bv. de productie van schone brandstoffen, en in optische instrumenten.

In dit proefschrift had ik als doel de bereiding van nieuwe anorganische luminescente verbindingen die met volledig gemethyleerd β-cyclodextrine (βCD) of zijn gastmoleculen zijn gefunctionaliseerd, en die daarbij wateroplosbaar zijn, en efficient energie absorberen en overdragen. De functionalisering van deze coördinatiecomplexen met βCD resulteert in luminescente labels die in staat zijn om op een ontworpen manier te aggregeren, en daarbij hun luminescentie-efficiëntie te verhogen. Ons belangrijkste interesse is gefocusseerd op de bereiding van een systeem voor de ontwikkeling van waterstof, waarin een fotosensitiser, een elektronendrager, en een metaal nanodeeltje zichzelf organiseren in een lineaire structuur, waarbinnen een elektronoverdrachtsproces in gang kan worden gezet door de absorptie van licht.

Het werk dat in dit proefschrift wordt beschreven omvat i) de toepassing van "click chemie" als een hulpmiddel voor de functionalisering van βCD en zijn gasten (hoofdstuk 2 en 6), ii) de karakterisering van βCD en de coördinerende liganden (hoofdstuk 3), en iii) de toepassing van de resulterende βCD-bevattende moleculen in verschillende gebieden (hoofdstuk 4, 5, en 7). De resultaten zijn gepubliceerd (of worden gepubliceerd) in toonaangevende wetenschappelijke tijdschriften.

In **Hoofdstuk 1** wordt een overzicht gegeven van de twee belangrijke onderwerpen die in dit proefschrift besproken worden: i) cyclodextrines en hun vermogen om insluitingscomplexen te vormen, en ii) licht-geïnduceerde elektron-overgangen in coördinatiecomplexen. Aan het eind van dit hoofdstuk worden doel en hoofdlijnen van dit proefschrift samengevat.

Hoofdstuk 2 beschrijft de synthese en karakterisering van nieuwe 2-(1-gesubstitueerde-1*H*-1,2,3-triazol-4-yl)pyridine (pytl) liganden die met click chemie zijn

bereid. Ze zijn gebruikt in de bereiding van heteroleptische complexen van ruthenium(II) en iridium(III) met respectievelijk 2,2'-bipyridine (bpy) en 2-fenylpyridine (ppy), met $[Ru(bpy)_2(pytl\text{-}R)]Cl_2$ en $[Ir(ppy)_2(pytl\text{-}R)]Cl$ (R = methyl, adamantyl, βCD) als product. Alle nieuwe rutheniumcomplexen hebben een kortere levensduur en lagere quantumopbrengsten dan andere polypyridine complexen. Daarentegen hebben de cyclogemetalleerde iridium complexen langere levensduur en zeer hoge emissiequantumopbrengsten. De emissiequantumopbrengst en levensduur zijn verrassend hoog in het geval van $[Ir(ppy)_2(pytl\text{-}\beta CD)]Cl$ (Φ = 0.54, τ = 2800 ns). Het βCD, dat covalent aan de pytl is gebonden, speelt een belangrijke rol door als een second-sphere ligand op te treden en het coördinatiecomplex af te schermen voor uitdoving van de luminescentie door zgn. "dynamic quenching" of energieoverdracht aan zuurstof. Het complex $[Ir(ppy)_2(pytl\text{-}\beta CD)]Cl$ bestaat in twee diastereomere vormen, Δ and Λ, die significant verschillen in hun quantumopbrengst (0.49 vs. 0.70). Dit wordt toegeschreven aan verschillende interacties van de chirale βCD-substituent met de Δ en Λ isomeren van het metaalcomplex.

In **Hoofdstuk 3** wordt een gedetailleerde analyse van de struktuur van het Δ diastereomeer van $[Ir(ppy)_2(pytl\text{-}\beta CD)]Cl$ in D_2O met hoge-resolutie NMR-spectroscopie gerapporteerd. De resultaten bevestigen een interactie tussen het iridium complex en de holte van het covalent gebonden βCD. In bijzonder een van de ppy liganden is gelocaliseerd in de holte van het βCD, terwijl de andere liganden, ppy en pytl, zich respectievelijk boven en onder de holte bevinden. De licht-uitzendende aangeslagen toestand is grotendeels gelocaliseerd op de ppy liganden; de (gedeeltelijke) zelfinsluiting in de holte van het βCD verhoogt de starheid van het iridiumcomplex, en beschermt de licht-uitzendende aangeslagen toestand tegen uitdoving door watermoleculen en tegen zuurstof.

Hoofdstuk 4 behandelt de toepassing van vijf ionische iridium(III)-complexen met de algemene formules $[Ir(ppy)_2(pytl\text{-}R)]Cl$ (R = methyl, βCD, propylamine) en $[Ir(F_2ppy)_2(pytl\text{-}R)]Cl$ (F_2ppy = 2-(2,4-bisfluorofenyl)-pyridine, R = adamantyl, propylamine) als oplichtende verbindingen in elektrochemiluminescentie (ECL). De licht-uitzendende aangeslagen toestanden van de metaal-complexen worden gevormd door elektronoverdrachtsreakties tussen elektrochemisch gegenereerde verbindingen. Pytl liganden met diverse functionele groepen werden gebruikt in de synthese van de iridium(III) complexen. De complexen met de algemene formules $[Ir(ppy)_2(pytl\text{-}R)]Cl$ en $[Ir(F_2ppy)_2(pytl\text{-}R)]Cl$ geven respectievelijk helder groene en blauwe ECL signalen in lucht-geëquilibreerde waterige media. Door de directe route naar gefunctionaliseerde pytl-liganden met click chemie was het mogelijk om er een

βCD als een solubiliserende groep aan vast te maken, wat resulteerde in een toegenomen ECL emissie in water voor het iridium complex. In de verwachting zulke oplichtende verbindingen in op ECL gebaseerde biologische assays toe te kunnen passen, werd aan pytl een propylamino-groep gebonden. Door de aanwezigheid van zo'n groep is het complex voorzien van een mogelijk aanknopingspunt voor het covalent labelen van biomoleculen en het immobiliseren op vaste substraten. Onder werkcondities onderging de vrije amine-eind groep onomkeerbare oxidatie, met als resultaat dat de elektrode onklaar raakt. Verwacht wordt echter dat de gefunctionaliseerde amino-groep stabiel is als het iridium-label covalent is gebonden aan een substraat, en dat zijn reactiviteit de ECL niet belemmert.

In **Hoofdstuk 5** worden onze inspanningen om de fotofysische eigenschappen van gefunctionaliseerde iridium(III) complexen uit te buiten in een zelf-geassembleerd system voor de fotokatalytische productie van waterstof gerapporteerd. De activiteit van een lineair licht-gedreven katalytisch drie-componentensysteem bestaande uit een metaal-complex als photosensitiser, een viologeen als elektronendrager, platina-nanodeeltjes met cyclodextrine als de katalysator, en een elektrondonor werd onderzocht in een zelfgebouwde opstelling. Aan de fotosensitiser, de elektronendrager en de katalysator werden gastheer- en gast-moleculen vastgemaakt, zoals βCD, adamantaan, en ursodeoxycholzuur, die werden gebruikt om langs supramoleculaire weg het fotokatalytische systeem in elkaar te zetten. De in dit werk geïntroduceerde benadering om het systeem uit modules samen te stellen maakt het mogelijk om uit een beperkt aantal bouwstenen verscheidene functionele fotoactieve systemen te vormen. We vonden dat de polypyridine iridium complexen met de algemene formule $[Ir(ppy)_2(pytl\text{-}R)]Cl$ actief zijn in de productie van H_2, met opbrengsten die onder onze omstandigheden 2.5–450 keer hoger zijn dan die van het klassieke drie-componentensysteem Ru-bpy/Me-V-Me/Pt-βCD/EDTA (Ru-bpy = $[Ru(bpy)_3]Cl_2$, Me-V-Me = methylviologeen, Pt-βCD = platina nanodeeltjes gefunctionaliseerd met ongemethyleerd βCD, EDTA = ethyleendiaminetetra-azijnzuur). Door verschillende fotokatalytische systemen te onderzoeken werd gevonden dat de elektrondrager een essentiele rol speelt, dat het noodzakelijk is om een efficiënte elektronenoverdracht te garanderen, en dat de hoeveelheid waterstof die geproduceerd wordt direct evenredig is met de quantumopbrengst van de sensitiser. De poging om de efficiëntie van onze systemen te verhogen door viologenen te gebruiken waar gastmoleculen voor cyclodextrine covalent aan gebonden waren leidde ons tot onverwachte waarnemingen. De aanwezigheid van adamantaan- of galzuur-groepen gaf aggregatie en stabilisatie van de viologeen radicaal-kationen, wat niet voordelig is voor waterstofvorming.

Hoofdstuk 6 beschrijft de bereiding, middels click chemie, van een groep bidentate 1-gesubstitueerde-4-fenyl-1*H*-1,2,3-triazool-cyclometallerende liganden (phtl) met verschillenden substituenten op de triazool-groep. Door diverse liganden (phtl-R^1 en pytl-R^2) (R^1 = adamantaan, methyl and R^2 = adamantyl, methyl, βCD, ursodeoxycholzuur) te gebruiken verkregen we een kleine bibliotheek van nieuwe heteroleptische ionische iridium complexen [Ir(phtr-R^1)$_2$(pytl-R^2)]Cl, waarvan we de fotofysische eigenschappen onderzocht hebben.

Hoofdstuk 7 behandelt de synthese van een reuzenamfifiel dat bestaat uit polystyreen dat aan het einde gebonden is aan βCD. Deze verbinding vormt blaasjes wanneer zij wordt opgelost in THF en geïnjecteerd in water. Het vermogen van de βCDs op het oppervlak van de polymersomen om insluitingsverbindingen te vormen werd getest door een competitie-experiment uit te voeren met een fluorescente probe die gevoelig is voor de polariteit van de omgeving. Wij gebruikten dit systeem om de herkenning na te bootsen van moleculen door celmembranen, die in de natuur vaak gebaseerd is op interacties met specifieke membraanreceptoren. Het enzym mierikswortel peroxidase werd gemodificeerd met adamantaan-groepen aan een poly(ethylene glycol) spacer, en zijn interactie met de polymersomen onderzocht. Vastgesteld werd dat de aanwezigheid van adamantaan groepen op het enzym een gast-gastheer interactie met het multifunctionele oppervlak van de polymersomes mogelijk maakte.

Acknowledgements

I would like to thank my promotor, Roeland Nolte, for the unique experience of working in his group, for believing in me, and for his support. Coming to The Netherlands was the beginning of a great story for me that still continues.

A special thank you goes to Martin Feiters, my co-promotor, for his support, patience, and suggestions any time I needed it. I am still not sure how, considering the level of my English at the beginning, I managed to convince you and Roeland at the job interview that I was a good candidate for this position. I am glad that you believed in me and helped me until the end.

I would like to thank my Master's degree supervisor, Rinaldo Marini Bettolo, the tallest Italian organic chemistry professor I have ever met. It is also because of you that I am here today. Thanks for helping me take this path; hard but full of satisfaction (and for all the walks and coffees that we had in Rome).

I would like to thank the people in the department who make our work possible each day. My thanks go to Désirée, Jacky, Paula, Peter v.D. (always smiling and super helpful), Theo, Pieter v.d.M. (thanks for rescuing my computer more than once), Jan D., René A., Hans A., and Helene. Peter v.G., Ad, and Paul S. I am still annoying you with all kinds of questions about MS and NMR spectroscopy. Geert-Jan and Liesbeth from the department of General Instruments for their help with microscopy. René d.G. and Jan S, for solving all the crystal structures.

Research always requires financial support and this work would have not been possible without the support of the EU through the Marie Curie Research and Training Network (RTN) UNI-NANOCUPS. It was a wonderful experience and I would like to thank everybody that was part of the network. Guys, I have enjoyed the UNI-NANOCUPS meetings, the discussions, the ideas (and the beers) that we had. They have been (also the beers) a great opportunity for professional and personal growth. I would like to thank Nikos M., Pablo, Luisa, René, and Yolanda, with whom I had a great collaboration.

Alan, Paul K., and Michal, thanks a lot for the short but very fruitful collaboration that ended with a nice publication (Paul, it was my opportunity to enjoy one of your barbecues!).

A very special thank goes to my Erasmus and Master's student María. I had just arrived in Nijmegen when Martin told me I would have a student for six months. I just did not know where to begin, but you survived the cyclodextrin test and came back for more (I am glad you did!). My first publication (and Chapter 7 of this thesis) was also possible because of your very hard work: muchas gracias guapa!!

On my first day in Nijmegen, I found a Greek post-doc sitting at the desk next to the one that I was given. I did not know it then, but that was the beginning of a very long and deep friendship. Since that moment, we shared the lab, a successful project (described in Chapter 7), many passions, friends, and many many moments of our lives. Thank you Nikos.

One year later a new greek post-doc came working with me on cyclodextrins. His name is also Nikos and we had a great time, working, discussing, or simply enjoying our times together. Working with greek people has always brought me good luck; the project with Nikos was very successful (Chapter 5 and two publications) and more important, a friendship that goes on. Thank you Nikos.

Much of the work described in this thesis is the result of intense and fruitful collaborations with many people already mentioned. In addition, I would like to thank Dr. M. Tessari for the NMR measurements on samples so dilute they were almost undetectable and Dr. S. Zanarini and Prof. F. Paolucci for the electrochemiluminescence measurements.

I would like to thank the people that worked in lab HG.03.118, Nikos (Don) H., Nikos M., Joost C., Mark D. (great playing with you), Maria B., Joe, Friso, Marta C., Eva, Raquel, Ribera, Gloria, Núria, Anna, Stijn v.D., Guillaume (I'll never walk even one day of 4-daagse again), Edgar, Linda, Inge, Reneé the "pink girl", and Martijn. The time in the lab would have not been so "crazy" and funny without you.

I would like to thank all the other colleagues and friends with whom I shared an office, time, parties, barbecues, cakes, Lunterens, and much more. Many of you were much more than just colleagues. Thanks Suzanne, Femke, Bram, Onno, Hans-Peter, Edward, Hans Elemans, Hans Engelkamp, Bas v.d.B., Jasper K., Kaspar, Pieter, and Maaike (great volleyball player!); Joost O., Sjef, Sjors, Gerald, Waqar, Anup, Silvie, Pjotr, Oliviér, Richard v.H., Paul T., Jaap, Paul v.G., Richard and Hester; Johan H., Petra, Mwakaboko, Jorge and Bas R. (first-aid and fireman course buddies); Madhavan, Dennis and Roy Lensen; Dennis Löwik, Niels and

Zaskia; Ruud, Bram, Britta, Egle, and Luiz C.; and everybody from the Rowan, Rutjes, and van Hest groups.

Starting a new life in a foreign country and finding your way is never easy, but good friends help a lot. You have all crossed my path, in and outside the lab, and all of you have left a mark on me. I would like to thank you all for this. Grazie mille a Pieter d.W., Dani and Maria, Erik, Alexander, Aurélie, David, Lee and Hefziba, Dennis and Paula (thanks a lot!!), Daniel, Ghislaine and Speedy, Valeria and Ellert (there are no words to thank you two), Henar and Ozan, Nico, Rosalyne (thank you for reading my thesis in record time and answering all my peculiar questions), Alex (never lose your smile!), Michalito (pronto pronto!), Johny and Dagmara, Heather (my honorary paranimf), Arend, Victor and TuHa, Matthieu (I loved when you played accordion for us), Andrés, Paco and Dingena, Candice, Cyrille, Stephane, Joris (the inventor of the "Joris movement"), Vincent and Christine, Ton, Marta J., Laura, Lisa, Isa, Alberto, Irene, Silvia, Carol, Luis, Elena, Mònica, Sandra, Gemma, Ismael, Tomeu, Jelle, Jill and Maarten, Morten and Sanne, Mauri and Elina, Jelena (next summer motorbyke trip!) and Michiel, Iria, Adolfo, Tahoora, Stijn G., Matthijs O., Irene R., Joost C., Stan and Manon, Saskia, Valentina, Ire, Andrea T.S., Sander, Marloes, Sander H., Svetlana, Alfred (meeting you was a great pleasure and I will miss you, goodbye my friend!) and Anny (for enormous patience in explaining to me the details of the Dutch belastingdienst). Menno, Niels and Simone, Rosa and Bas, Bas v.d.L (the volleyball king), Kasper (ciao bello), Carolina, Pili, Bea, my "little" italian (and non) community Laura (mommy always comes first!) and Mauro (chicco), Giuseppe (marmottone) and Anastasia, Cosimo (accio), Maddalena and Renaud (the best cooks ever!), Sara (ciao Koala) and Hoeke, Angela, Antoine, Ganesh, Matteo and Laura, Eugenio, Riccardo, Antonio, Giorgio, Giorgia and Claudio (I am trying the mozzarella again).

I would like to thank the people that I met during my stay in Vossenveld: Audrie, Fawzy, Menna, and Rita, who together with Daniel, Dani, Johny and Dagmara, and Nikos H. made it so nice.

Whenever I go back home (to Italy) I know that there are people who are always ready to pick me up from the airport, organise dinners, visit me, or just talk to me when I need it. A big hug to my friends Tina, Federica, Oscar, Priscilla and Raffaele, Alessandro and Chiara, Marcos and Sara.

The people with whom I shared great times and headaches discussing NMR spectroscopy:

Geerten, Nadia, Vincent, Wouter, Ezgi and Geokmei. All my colleagues at Lead Pharma and especially Ad (thanks for letting me be part of the Lead Pharma team). Thank you guys (and girls, of course).

The list of people that I would like to remember is surely longer than what my memory allows me to remember. I apologise if I have forgotten anybody. Even if your name is not in these pages, you will always be in my heart.

Un grazie particolare a tutta la mia famiglia che mi ha appoggiato in questo lungo percorso, ed in particolare alle persone senza le quali oggi non sarei qui, mia madre, mio padre e mio fratello.

A special thank you to my "paranimfen": Guillaume and Daniel. It was a privilege working next to you, sharing laughs and everyday moments, even the more difficult ones. I have no words to thank you, but I am happy to have you here again. I know I can always count on you. Thank you sweeties!

Dora, my last words are for you. You are the biggest achievement of my life. Thank you for your support and patience, especially when I was writing until late in the night or my reply to your questions "what do we do tonight?" was always "I have to finish the thesis". A bright, new future together is out there waiting for us. Σ 'αγαπώ πολύ αγάπη μου!

Marco

Nijmegen, January 2013

List of Publications

β-Cyclodextrin-Appended Giant Amphiphile: Aggregation to Vesicle Polymersomes and Immobilisation of Enzymes
M. Felici, M. Marzá-Pérez, N. S. Hatzakis, R. J. M. Nolte, M. C. Feiters*, Chem. Eur. J.* **2008***, 14,* 9914–9920.

Ir(III) and Ru(II) Complexes Containing Triazole-Pyridine Ligands: Luminescence Enhancement upon Substitution with β-Cyclodextrin
M. Felici, P. Contreras-Carballada, Y. Vida, J. M. M. Smits, R. J. M. Nolte, L. De Cola, R. M. Williams, M. C. Feiters*, Chem. Eur. J.* **2009***, 15,* 13124–13134.

Cationic Heteroleptic Cyclometalated Iridium(III) Complexes Containing Phenyl-Triazole and Triazole-Pyridine Clicked Ligands
M. Felici, P. Contreras-Carballada, J. M. M. Smits, R. J. M. Nolte, R. M. Williams, L. De Cola, M. C. Feiters*, Molecules* **2010***, 15,* 2039–2059.

Green and Blue Electrochemically Generated Chemiluminescence from Click Chemistry-Customisable Iridium Complexes
S. Zanarini, M. Felici, G. Valenti, M. Marcaccio, L. Prodi, S. Bonacchi, P. Contreras-Carballada, R. M. Williams, M. C. Feiters, R. J. M. Nolte, L. De Cola, F. Paolucci*, Chem. Eur. J.* **2011***, 17,* 4640–4647.

Triazole-Pyridine Ligands: a Novel Approach to Chromophoric Iridium Arrays
M. Juricek, M. Felici, P. Contreras-Carballada, J. Lauko, S. Rodriguez Bou, P. H. J. Kouwer, A. M. Brouwer, A. E. Rowan*, J. Mater. Chem.* **2011***, 21,* 2104–2111.

Cyclodextrin-Based Systems for Photoinduced Hydrogen Evolution
N. Mourtzis, P. Contreras-Carballada, M. Felici, R. J. M. Nolte, R. M. Williams, L. De Cola, M. C. Feiters*, Phys. Chem. Chem. Phys.* **2011***, 13,* 7903–7909.

Variation of the Viologen Electron Relay in Cyclodextrin-based Self-Assembled Systems for Photoinduced Hydrogen Evolution from Water
Contreras-Carballada, N. Mourtzis, M. Felici, S. Bonnet, R. J. M. Nolte, R. M. Williams, L. De Cola, M. C. Feiters, *Eur. J. Org. Chem.* **2012***,* 6729–6736.

Curriculum Vitae

Marco Felici was born on the 24th April, 1975, in Colleferro, Italy. From when he was a small child, he has always loved animals and wanted to become a veterinary surgeon. However, the chemistry course that he took at the high school was enough to make him realise that this was even more fun. In December 2002 he completed his Master's degree at the University of Rome "La Sapienza" under the supervision of Prof. Rinaldo Marini Bettolo. He graduated *cum laude* with the thesis "Synthesis of Analogues of Patchouli Alcohol". Shortly before defending his Master's thesis, he joined the Italian National Firemen Corps to perform military service. Twelve months later his duty was accomplished, and he went back to the university with a junior researcher fellowship supported by the pharmaceutical company EUTICALS S.p.A. to work on the synthesis and characterisation of new non-steroidal anti-inflammatory drugs (NSAID) under his former Master's thesis supervisor. Meanwhile, he was granted a Ph.D. position in physical organic chemistry in the group of Prof. Roeland Nolte at the Radboud University in Nijmegen and in October 2004 he moved to The Netherlands. His project, which was directly supervised by Dr. Martin Feiters and is described in this Ph.D. thesis, was funded by a Marie Curie Fellowship and has been developed within the framework of the Marie Curie Research and Training Network (RTN) UNI-NANOCUPS. After the period of his practical Ph.D. work, in 2009, he joined the group of Prof. Alan Rowan in Nijmegen for six months, during which he worked on chromophoric iridium arrays. Since February 2010, he has been part of the team at the company Lead Pharma in Nijmegen where he has strengthened his knowledge and expertise in NMR spectroscopy techniques applied to peptides as well as small molecules. Within Lead Pharma he works both as a physical and an organic chemist. He will defend his Ph.D. thesis on the 28th January, 2013.